ORNL-6088/V3
(Third volume of
ORNL-6086)

Contract No. DE-AC05-84OR21400

Physics Division

ATOMIC DATA FOR CONTROLLED FUSION RESEARCH
VOLUME III
"PARTICLE INTERACTIONS WITH SURFACES"

E. W. Thomas
Georgia Institute of Technology

Published and Edited by
Controlled Fusion Atomic Data Center

Date Published - February 1985

OAK RIDGE NATIONAL LABORATORY
Oak Ridge, Tennessee 37831
operated by
MARTIN MARIETTA ENERGY SYSTEMS, INC.
for the
U.S. DEPARTMENT OF ENERGY

Printed in the United States of America. Available from
National Technical Information Service
U.S. Department of Commerce
5285 Port Royal Road, Springfield, Virginia 22161
NTIS price codes—Printed Copy: A09 Microfiche A01

SERIES PREFACE

The primary objective of the Controlled-Fusion Atomic Data Center at Oak Ridge National Laboratory is to publish handbooks containing numerical and graphical cross sections and other physical data relevant to fusion energy research. In 1977, a two-volume compilation was published as ORNL reports ORNL-5206 and ORNL-5207. Since that time, a large volume of pertinent data has become available, necessitating an update of the previous compilation. Plans are to include both cross sections and rate coefficients for collisional processes, and to publish the revised series in handbook form. The specific volumes which are in preparation are listed below, with their expected completion dates.

Vol. 1, "Collisions of H, H_2, He, and Li Atoms and Ions with Atoms and Molecules," C. F. Barnett, ORNL (January 1986).

Vol. 2, "Collisions of Electrons with Atoms and Molecules," J. W. Gallagher, Joint Institute for Laboratory Astrophysics; and C. F. Barnett, ORNL (October 1985).

Vol. 3, "Particle Interactions with Surfaces," E. W. Thomas, Georgia Institute of Technology (January 1985).

Vol. 4, "Spectroscopic Data for Iron," W. L. Wiese, National Bureau of Standards (March 1985).

Vol. 5, Collisions of Carbon and Oxygen Ions with Electrons, H, H_2, and He," R. A. Phaneuf, ORNL; R. K. Janev, Institute of Physics, Yugoslavia; and M. S. Pindzola, Auburn University (March 1986).

C. F. Barnett
H. T. Hunter
M. I. Kirkpatrick
R. A. Phaneuf

TABLE OF CONTENTS

Abstract

This report provides a handbook of data concerning particle solid interactions that are relevant to plasma-wall interactions in fusion devices. Published data have been collected, assessed, and represented by a single functional relationship which is presented in both tabular and graphical form. Mechanisms reviewed here include sputtering, secondary electron emission, particle reflection, and trapping.

Introduction

This volume provides a compendium of data concerning processes which occur at the first wall of fusion plasma devices. Included are sputtering, ejection of electrons by impact of electrons and heavy particles, heavy particle reflection, as well as hydrogen trapping and re-emission. Plasma wall interactions are of substantial importance to device operation. Most impurities have their origin at the wall and most of the fuel recycles from the wall during a discharge; potentials in the plasma edge are much influenced by electrons ejected from the wall.

In assembling data for inclusion I have restricted myself largely to projectile-target combinations of direct importance to the fusion program. Thus projectiles are generally hydrogen, helium, common impurities, ions of these species, as well as electrons. Targets are materials commonly employed for walls, limiters and coatings. Generally I include only data for polycrystalline targets of possible technical ability. Thus I do not include here the voluminous data for single crystal surfaces and for rare gas projectiles that are of such importance for fundamental research.

A potential difficulty in the use of these data for modelling purposes is that the surface used for the measured data presented here is generally not the same as one would find in a practical fusion device. A device wall will initially carry a macroscopic layer of dirt and oxides with a topography related to the metal working processes employed in its fabrication. With cleaning (e.g., by glow discharges) and repetitive use, these surfaces change. On the one hand the surface may become cleaner and flatter due to erosion. On the other hand certain surfaces may become coated with foreign materials due to re-deposition from eroded surfaces or from subsidiary sources such as getter pumps. Thus in general the nature of the surface of the wall, limiter or other component is unknown. By contrast the data presented here is (unless otherwise indicated) for atomically clean, homogeneous, pure materials. In using these data for modelling purposes the reader will inevitably first choose a data set appropriate to the material of nominal construction. We would urge the reader also to try using data that may be appropriate to a contaminated surface and then determine whether the predicted device behavior will be significantly altered. For example, with a steel walled device operating with titanium getter pumps one should certainly compare predictions using data for a titanium surface with predictions for a steel surface. If differences are found to be critical then clearly the composition of the device wall should be monitored in situ and data appropriate to actual wall composition should be obtained by laboratory experiments. It is to be expected that processes involving electron ejection (i.e., secondary electron ejection coefficients) and electron transfer (excited and ionized states of reflected and sputtered species) will be very sensitive to surface contamination. Processes governed by kinematic effects (total sputtering and total projectile reflection) are likely to be fairly independent of minor surface contamination.

In choosing data for inclusion here we have concentrated on the experimental work of research groups that have an extended record of studying a specific class of processes and where one might reasonably expect that systematic errors have been elminated. In general, we have avoided theoretical predictions. We have omitted data that appears to be inaccurate, inconsistent with the work of other well established groups or where data was extracted by use of assumptions that were not separately tested. Many sections of this volume have an introduction which includes a note giving references to other major data compendia. Frequently those other compendia include all available data even when there are serious inconsistencies; those compendia also sometimes include semi-empirical theoretical formulations that describe much of the data by simple algebraic formulations.

The compendium has many serious gaps. Data on processes induced by impurity ion impact are generally sparse. Secondary electron emission has received little recent attention and the data presented were often acquired with antiquated and inferior technology. Synergistic effects occuring when two or more species are simultaneously (or sequentially) incident on a surface have not yet been systematically studied. It is to be hoped that the present compendium will prompt further work on areas that are now inadequately covered.

E. W. Thomas
Atlanta, GA
1 October 1984

A. SPUTTERING

Sputtering

Introductory Notes

A. Cautionary Notes

Light ion sputtering has been the subject of many accurate experimental studies. Algebraic representation of data are available to permit extrapolation and interpolation of data. To maintain a consistent picture we have chosen to present data drawn primarily from the group of Roth, Bohdansky and Ottenberger at MPI Garching.

Sputtering yields of alloys may be roughly estimated as a sum of the yields for the components each weighted by the proportion of the component present. However it must be recognized that sputtering will remove components at different rates so that surface composition is different from that in bulk.

Sputtering is basically a kinematic effect involving energy transfer from projectile to target. Such processes are known as physical sputtering. For certain conditions the projectiles may form volatile compounds with target atoms resulting in a chemical erosion process. This is known as chemical sputtering and can have sputtering yields some orders of magnitude higher than physical sputtering. The best known case of chemical sputtering is for H^+ and D^+ on C where CH_4 (or CD_4) is formed giving very high erosion rates for targets at elevated temperatures (300 to 500°C).

B. Definitions

Sputtering Yield is defined as the ratio between the number of target atoms ejected to the number of projectile ions incident. Most of the data presented here were determined by weight loss from the bombarded target.

C. Algebraic Representation

1. Total Yield

The total yield S of sputtered atoms due to light ion impact can be frequently represented by the following equation.

$$S = 6.4 \times 10^{-3} M_2 \left[\frac{4 M_1 M_2}{(M_1+M_2)^2}\right]^{5/3} E'^{1/4} \left(1 - \frac{1}{E'}\right)^{7/2} \qquad (1)$$

Where M_1 = projectile mass (a.m.u.)

M_2 = target mass (a.m.u.)

$E' = \frac{E}{E_{th}}$

E = Projectile energy

E_{th} = Threshold energy for sputtering

The threshold energy E_{th} is obtained by fitting to experimental data. Typical values are as follows.

Threshold energy E_{th} in eV

Target \ Ion	H	D	He^3	He^4
Al	53	34		20.5
Au	184	94	60	44
Be	27.5	24		33
C	9.9	11		16
Fe	64	40		35
Mo	164	86	45	39
Ni	47	32.5		20
Si	24.5	17.5		14
Ta	460	235		100
Ti	43.5			22
V	76			27
W	400	175		100
Zr				60

For cases where there are no experimental data equation 1 can be used to provide a reliable prediction. In this case threshold energy E_{th} must be predicted from the equation

$$E_{th} = \frac{E_B}{\gamma(1-\gamma)}$$

$$\gamma = \frac{4\, M_1 M_2}{(M_1+M_2)^2}$$

E_B = surface binding energy (can be obtained from sublimation energies as in JANAF - Thermo-Chemical Tables, Ed. D. R. Stull, H. Prophet, NSRDS-NBS 37).

This equation is valid only for $M_1/M_2 < 0.4$ and generally overestimates E_{th}.

2. Dependence on Incidence Angle

The sputtering yield $S(\theta)$ for projectiles incident at an angle of θ^o to the normal is related to that for incidence at 0^o to the normal, S, by the relation

$$S(\theta) = S \cos^{-f} \theta \quad .$$

where $1 \leq f \leq 2$. This relationship is valid only to an angle θ of about 60^o. The value to be assigned to f is not clear but unity has been satisfactory in the few cases where experiments have been performed.

3. Impact of Molecules

Studies have been made of the sputtering yield S_m for impact of different molecular ions H_m^+ (m = 1, 2, 3) at various energies E_m. It is found that $S_m \div$ m plotted against $E_m \div m$ is the same for all species. Thus each constituent nucleon acts as a separate particle. [See E. Hintz et al., J. Nucl. Mater. 93 & 94, 656 (1980)].

D. Principal Compendia

Two major data compendia are available.

1). J. Roth, J. Bohdansky, W. Ottenberger. "Data on Low Energy Light Ion Sputtering," Report No. IPP 9/26 (May 1979), Max-Planck-Institut fur Plasmaphysik, Garching.

2). N. Matsunami et al., "Energy Dependence of Sputtering Yields at Monatomic Solids", Report No. IPPJ-AM-14 (June 1980), Institute of Plasma Physics, Nagoya University.

This page left blank intentionally.

Sputtering of C by H^+, D^+ and $^4He^+$

(normal incidence, room temperature)

Energy (keV)	Sputtering Coefficient S (atoms/ion) H^+	D^+	$^4He^+$
2.0E-02	6.00E-04	8.50E-04	3.30E-04
3.0E-02	1.80E-03	3.10E-03	2.20E-03
4.0E-02	3.00E-03	5.70E-03	7.20E-03
6.0E-02	4.90E-03	9.70E-03	1.80E-02
1.0E-01	7.40E-03	1.60E-02	3.60E-02
2.0E-01	9.00E-03	2.30E-02	6.40E-02
3.0E-01	9.00E-03	2.55E-02	7.80E-02
4.0E-01	8.60E-03	2.60E-02	8.30E-02
6.0E-01	7.80E-03	2.30E-02	8.90E-02
1.0E+00	6.40E-03	1.80E-02	8.80E-02
2.0E+00	4.70E-03	1.20E-02	8.20E-02
3.0E+00	3.80E-03	8.80E-03	7.80E-02
4.0E+00	3.30E-03	7.20E-03	7.45E-02

<u>References</u>:

J. Roth, J. Bohdansky, and W. Ottenberger, Report IPP 9/26 (May 1979) from Max-Planck-Institut fur Plasmaphysik, Garching. This report is a compendium of data from various sources.

<u>Accuracy</u>: ± 10%.

<u>Notes</u>: (1) The data shown here is largely derived from a semi-empirical expression [Eq. 1 in the introduction] fitted to experimental data in the region 0.05 to 0.3 keV and extrapolated to lower energies. At higher energies it is simply a fit to experimental data. Experimental data agrees with this presentation to better than ± 10%.

(2) The sputtering yield for carbon varies by as much as a factor of two depending on the type and manufacturer. [See R. Behrisch *et al*., J. Nucl. Mater. **60**, 321 (1976) and J. A. Borders *et al*., J. Nucl Mater. **76** & **77**, 168 (1978)]. These data are appropriate to pyrolytic carbon (Union Graphite).

(3) The sputtering yield of C by H and D increases by orders of magnitude at elevated temperatures due to chemical effects. [See J. Roth *et al*., J. Nucl. Mater. **63**, 222 (1976)].

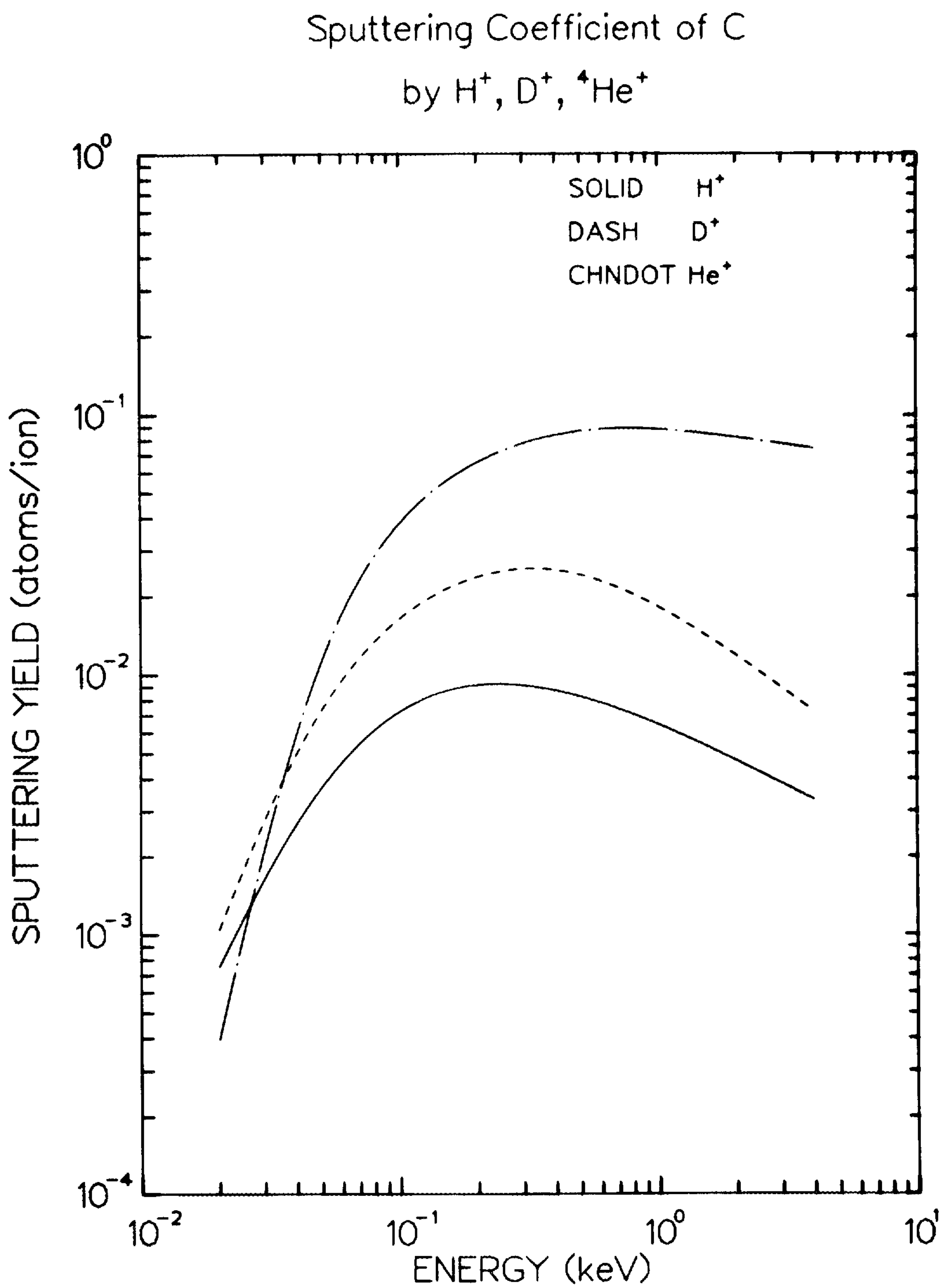

Sputtering Coefficient of C
by H+, D+, 4He+
SOLID H+
DASH D+
CHNDOT He+
SPUTTERING YIELD (atoms/ion)
ENERGY (keV)
10^0
10^-1
10^-2
10^-3
10^-4
10^-2
10^-1
10^0
10^1

Sputtering of Al by H^+, D^+ and $^4He^+$

(normal incidence, room temperature)

Energy (keV)	Sputtering Coefficient S (atoms/ion) H^+	D^+	$^4He^+$
4.0E-02		2.00E-04	8.20E-03
6.0E-02		1.30E-03	2.90E-02
1.0E-01	5.00E-04	6.80E-03	7.00E-02
2.0E-01	2.80E-03	2.00E-02	1.50E-01
3.0E-01	5.00E-03	2.80E-02	1.80E-01
4.0E-01	6.70E-03	3.20E-02	2.00E-01
6.0E-01	9.00E-03	3.80E-02	2.20E-01
1.0E+00	1.20E-02	4.10E-02	2.10E-01
2.0E+00	1.22E-02	3.30E-02	1.73E-01
3.0E+00	1.05E-02	2.50E-02	1.50E-01
4.0E+00	9.00E-03	2.00E-02	1.20E-01
6.0E+00	6.70E-03	1.30E-02	9.20E-02

References:

J. Roth, J. Bohdansky, and W. Ottenberger, Report IPP 9/26 (May 1979) from Max-Planck-Institut fur Plasmaphysik, Garching. This report is a compendium of data from various sources.

Accuracy: ± 10%.

Notes: (1) The data shown here is largely derived from a semi-empirical expression [Eq. 1 in the introduction] fitted to experimental data in the region 0.07 to 1.0 keV and extrapolated to lower energies. At higher energies it is simply a fit to experimental data. Experimental data agrees with this presentation to better than ± 10%.

(2) For H^+ and D^+ impact the data is very similar to that for Al_2O_3 suggesting perhaps that oxide was present during the experimental measurements.

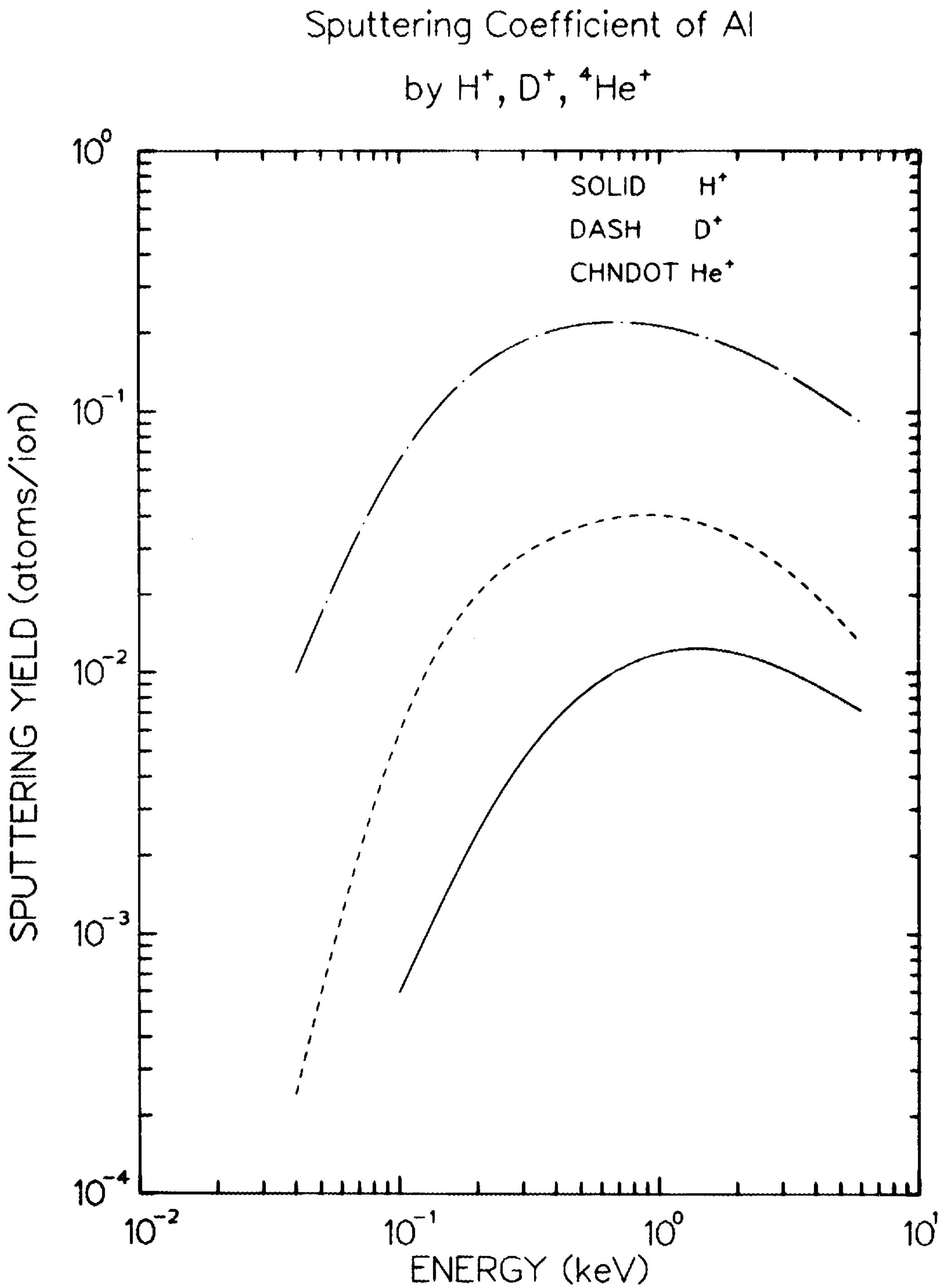
Sputtering Coefficient of Al
by H⁺, D⁺, ⁴He⁺
SOLID H⁺
DASH D⁺
CHNDOT He⁺
SPUTTERING YIELD (atoms/ion)
ENERGY (keV)
10⁰
10⁻¹
10⁻²
10⁻³
10⁻⁴
10⁻²
10⁻¹
10⁰
10¹

Sputtering of Ti by H^+, D^+ and $^4He^+$

(normal incidence, room temperature)

Energy (keV)	Sputtering Coefficient S (atoms/ion) H^+	D^+	$^4He^+$
4.0E-02			5.20E-04
6.0E-02		2.80E-04	2.90E-03
1.0E-01	1.00E-04	1.70E-03	9.20E-03
2.0E-01	8.00E-04	5.10E-03	2.10E-02
3.0E-01	1.70E-03	7.40E-03	2.90E-02
4.0E-01	2.20E-03	9.30E-03	3.40E-02
6.0E-01	3.00E-03	1.20E-02	4.00E-02
1.0E+00	3.50E-03	1.30E-02	4.90E-02
2.0E+00	3.40E-03	1.20E-02	5.55E-02
3.0E+00	2.80E-03	1.04E-02	5.30E-02
4.0E+00	2.30E-03	9.20E-03	5.00E-02
6.0E+00	1.70E-03	7.90E-03	4.30E-02

References:

J. Roth, J. Bohdansky, and W. Ottenberger, Report IPP 9/26 (May 1979) from Max-Planck-Institut fur Plasmaphysik, Garching. This report is a compendium of data from various sources.

Accuracy: ± 20%.

Notes: (1) The data shown here is largely derived from a semi-empirical expression [~Eq. 1 in the introduction] fitted to experimental data in the region 0.1 to 6.0 keV and extrapolated to lower energies. Experimental data for H^+ and He^+ agrees with this presentation to better than ± 20%.

(2) The data for D^+ impact are interpolated by Eq. 1 in the introduction and have not been confirmed experimentally.

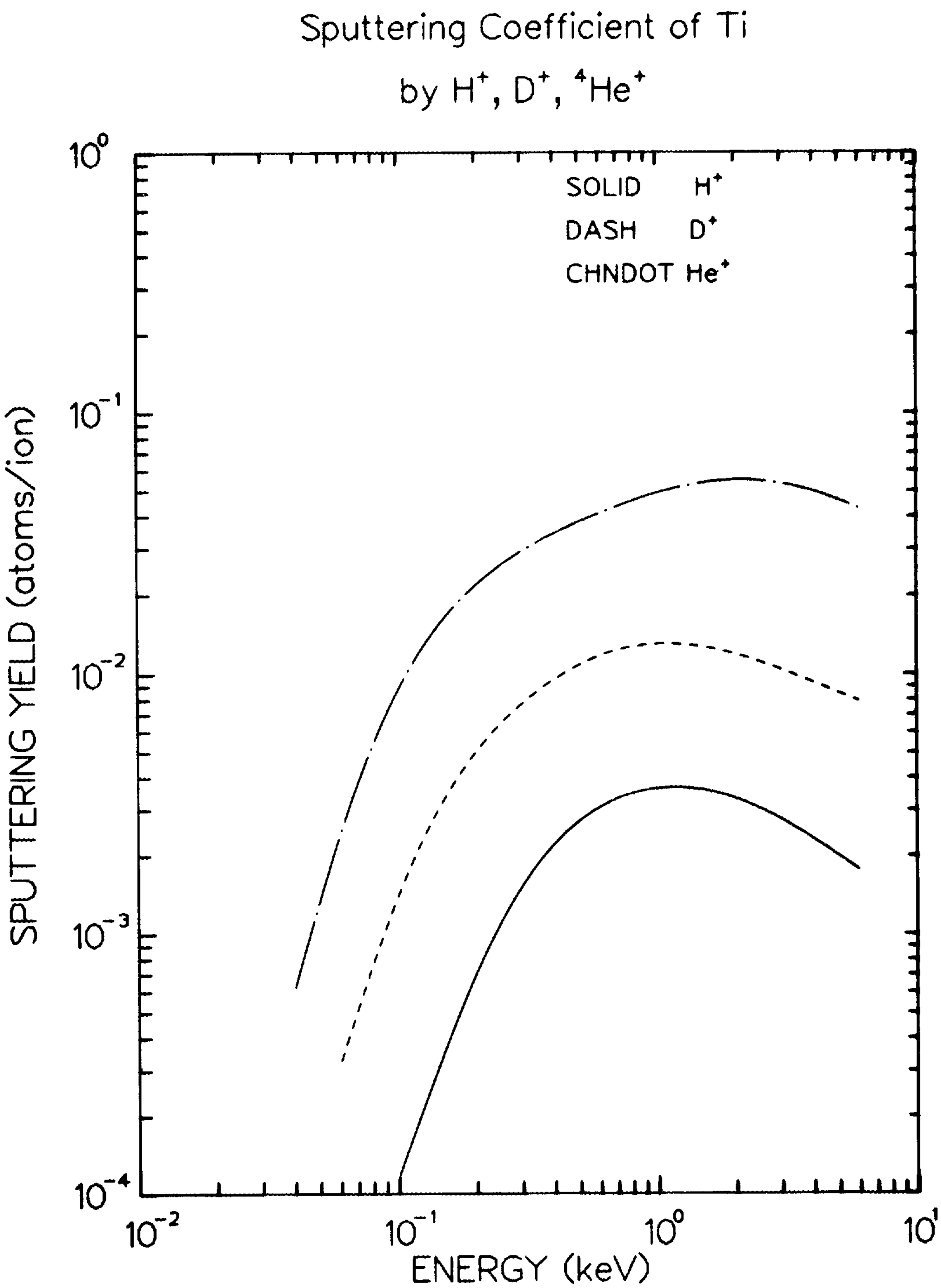
Sputtering Coefficient of Ti
by H⁺, D⁺, ⁴He⁺
SOLID H⁺
DASH D⁺
CHNDOT He⁺
SPUTTERING YIELD (atoms/ion)
ENERGY (keV)
10⁰
10⁻¹
10⁻²
10⁻³
10⁻⁴
10⁻²
10⁻¹
10⁰
10¹

Sputtering of Mo by H^+, D^+, and $^4He^+$

(normal incidence, room temperature)

Energy (keV)	Sputtering Coefficient S (atoms/ion) H^+	D^+	$^4He^+$
6.0 E-02			9.5 E-04
1.0 E-01		3.0 E-05	4.8 E-03
2.2 E-01	1.0 E-05	9.0 E-04	1.8 E-02
3.0 E-01	6.3 E-05	1.7 E-03	2.4 E-02
4.0 E-01	2.0 E-04	2.6 E-03	2.8 E-02
6.0 E-01	5.0 E-04	4.1 E-03	3.8 E-02
1.0 E+00	1.1 E-03	6.0 E-03	4.8 E-02
2.0 E+00	2.0 E-03	7.9 E-03	5.1 E-02
3.0 E+00	2.1 E-03	7.9 E-03	5.1 E-02
4.0 E+00	2.0 E-03	7.7 E-03	5.0 E-02
6.0 E+00	1.8 E-03	7.4 E-03	4.7 E-02
9.0 E+00	1.5 E-03	5.0 E-03	4.2 E-02

References: J. Roth, J. Bohdansky, and W. Ottenberber, Report IPP 9/26 (May 1979) from Max-Planck-Institut für Plasmaphysik, Garching. This report is a compendium of data from various sources.

Accuracy: ±10%.

Notes: (1) The data shown here are largely derived from a semi-empirical expression [Eq. 1 in the introduction] fitted to experimental data in the region 0.15 to 8.0 keV and extrapolated to lower energies. Experimental data agree with this presentation to better than ±10%.

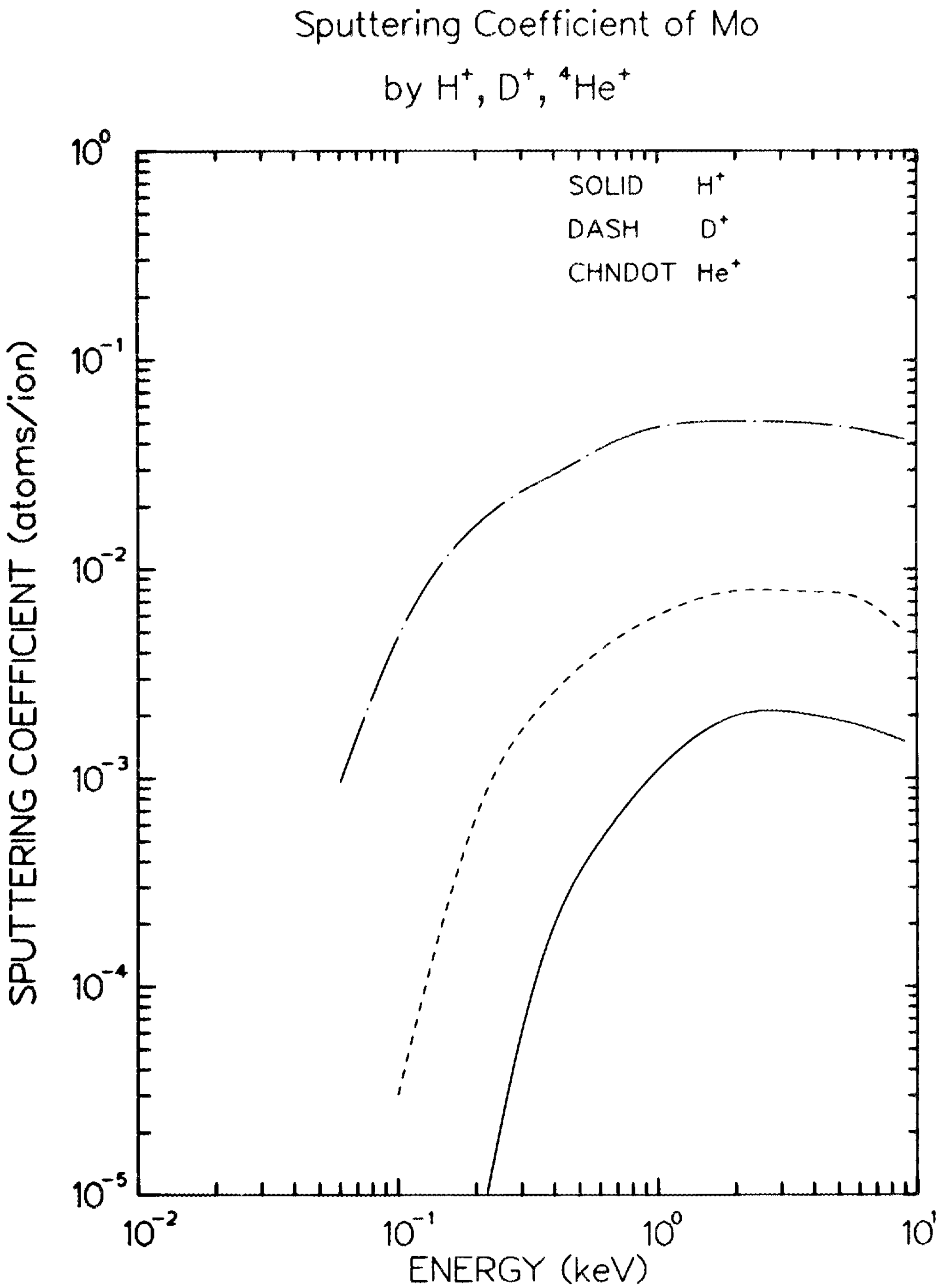
Sputtering Coefficient of Mo
by H+, D+, 4He+
SOLID H+
DASH D+
CHNDOT He+
SPUTTERING COEFFICIENT (atoms/ion)
10^0
10^-1
10^-2
10^-3
10^-4
10^-5
10^-2
10^-1
10^0
10^1
ENERGY (keV)

Sputtering of Stainless Steel by H^+, D^+ and $^4He^+$

(normal incidence, room temperature)

Energy (keV)	Sputtering Coefficient S (atoms/ion) H^+	D^+	$^4He^+$
4.0E-02		1.00E-04	3.80E-03
6.0E-02		5.30E-04	1.40E-02
1.0E-01	4.90E-04	3.60E-03	3.50E-02
2.0E-01	2.60E-03	1.20E-02	6.50E-02
3.0E-01	4.30E-03	1.70E-02	7.90E-02
4.0E-01	5.80E-03	2.10E-02	9.10E-02
6.0E-01	7.80E-03	2.50E-02	1.10E-01
1.0E+00	9.60E-03	2.90E-02	1.30E-01
2.0E+00	9.00E-03	2.70E-02	1.40E-01
3.0E+00	8.00E-03	2.20E-02	1.40E-01
4.0E+00	6.80E-03	1.90E-02	1.30E-01
6.0E+00	4.80E-03	1.60E-02	1.17E-01

References:

J. Roth, J. Bohdansky, and W. Ottenberger, Report IPP 9/26 (May 1979) from Max-Planck-Institut fur Plasmaphysik, Garching. This report is a compendium of data from various sources.

Accuracy: ± 20%.

Notes: (1) The data shown here is largely derived from a semi-empirical expression [Eq. 1 in the introduction] fitted to experimental data in the region 0.1 to 1.0 keV and extrapolated to lower energies. At higher energies it is simply a fit to experimental data. Experimental data agrees with this presentation to better than ± 20%.

(2) The stainless steel was types 316 and 304.

Sputtering Coefficient of Stainless Steel

by H^+, D^+, $^4He^+$

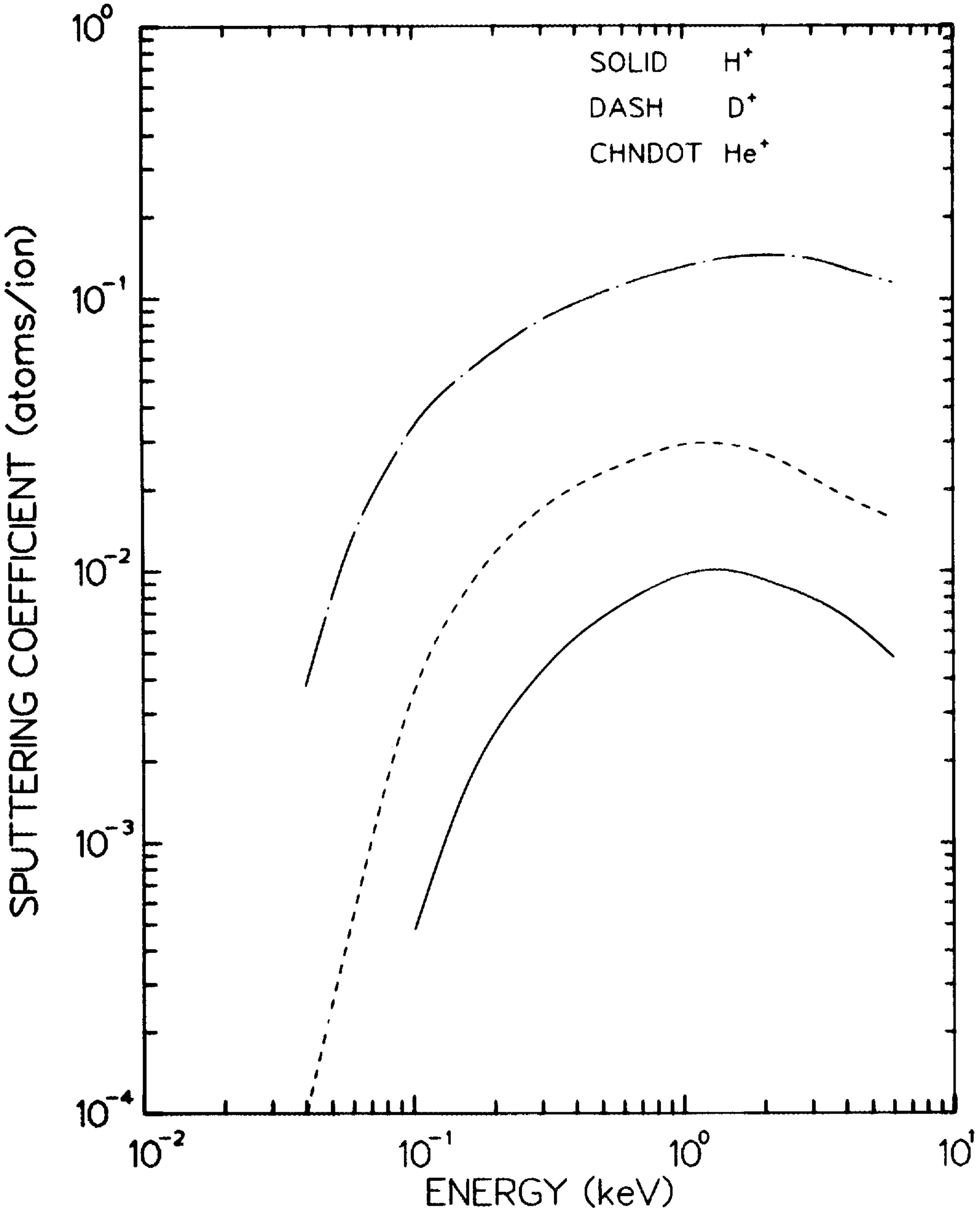

Sputtering of TiC by H^+, D^+ and $^4He^+$

(normal incidence, room temperature)

Energy (keV)	Sputtering Coefficient S (atoms/ion) H^+	D^+	$^4He^+$
4.0E-02			3.20E-04
6.0E-02		1.00E-04	2.70E-03
1.0E-01	1.10E-04	1.50E-03	1.30E-02
2.0E-01	1.30E-03	7.10E-03	3.10E-02
3.0E-01	2.80E-03	1.20E-02	4.40E-02
4.0E-01	4.00E-03	1.50E-02	5.50E-02
6.0E-01	5.80E-03	1.80E-02	6.30E-02
1.0E+00	7.20E-03	2.00E-02	7.60E-02
2.0E+00	7.20E-03	1.90E-02	8.50E-02
3.0E+00	6.80E-03	1.80E-02	8.30E-02
4.0E+00	6.10E-03	1.70E-02	8.40E-02
6.0E+00	4.50E-03	1.50E-02	7.90E-02

References:

J. Roth, J. Bohdansky, and W. Ottenberger, Report IPP 9/26 (May 1979) from Max-Planck-Institut fur Plasmaphysik, Garching. This report is a compendium of data from various sources.

Accuracy: ± 10%.

Notes: (1) The data shown here is largely derived from a semi-empirical expression [Eq. 1 in the introduction] fitted to experimental data in the region 0.1 to 1.0 keV and extrapolated to lower energies. At higher energies it is simply a fit to experimental data. Experimental data agrees with this presentation to better than ± 10%.

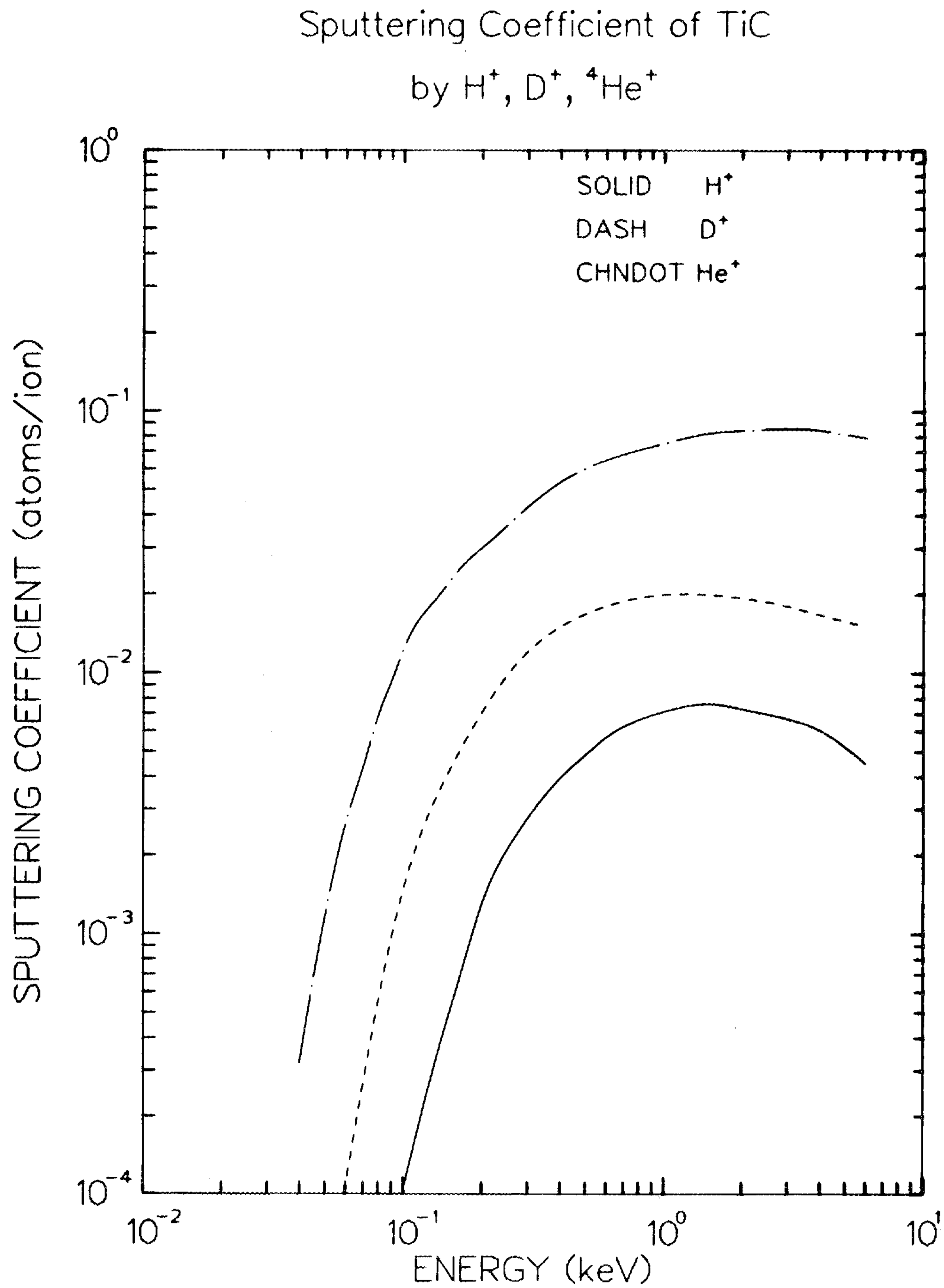

Sputtering Coefficient of TiC
by H+, D+, 4He+
SOLID H+
DASH D+
CHNDOT He+
SPUTTERING COEFFICIENT (atoms/ion)
ENERGY (keV)
10^0
10^-1
10^-2
10^-3
10^-4
10^-2
10^-1
10^0
10^1

Self-Sputtering Coefficients for

Al, Cr, Ni, Cu, and Zn

(normal incidence, room temperature)

	Self-Sputtering Coefficients, S (atoms/ion)				
Energy (keV)	Al	Cr	Ni	Cu	Zn
2.0E-02	1.6E-02				
3.0E-02	2.5E-02	2.4E-02			1.7E-01
4.0E-02	3.7E-02	4.0E-02			3.0E-01
6.0E-02	7.1E-02	7.4E-02		2.1E-01	5.0E-01
1.0E-01	1.7E-01	2.0E-01	1.8E-01	5.3E-01	6.4E-01
2.0E-01	4.7E-01	4.6E-01	4.6E-01	1.1E+00	7.2E-01
3.0E-01	7.0E-01	7.0E-01	7.2E-01	1.7E+00	
4.0E-01	8.9E-01	9.1E-01	9.5E-01	2.0E+00	
6.0E-01	1.1E+00		1.4E+00	2.5E+00	
1.0E+00	1.3E+00		1.8E+00	3.5E+00	
2.0E+00	1.2E+00		2.5E+00	4.4E+00	
3.0E+00	1.1E+00		3.0E+00	5.0E+00	
4.0E+00	1.0E+00			5.2E+00	
6.0E+00	8.6E-01			6.0E+00	
1.0E+01	7.0E-01			6.9E+00	
2.0E+01	5.5E-01			7.8E+00	
3.0E+01	4.8E-01			8.1E+00	
4.0E+01	4.2E-01			8.2E+01	

References:

Al^+ + Al: W. W. Hayward and A. R. Wolter, J. Appl. Phys. 40, 2911 (1969); O. Almen and G. Bruce, Nucl. Instrum. Meth. 11, 279 (1961).

Cr^+ + Cr: W. W. Hayward and A. R. Wolter, J. Appl. Phys. 40, 2911 (1969).

Ni^+ + Ni: E. Hechtl, H. L. Bay, and J. Bohdansky, Appl. Phys. (Germany) 16, 147 (1978).

Cu^+ + Cu: W. H. Hayward and A. R. Wolter, J. Appl. Phys. 40, 2911 (1969); O. Almen and G. Bruce, Nucl. Instrum. Meth. 11, 279 (1961).

Zn^+ + Zn: A. Fontell and E. Arminen, Can. J. Phys. 47, 2405 (1969).

Accuracy: Unknown.

Note: The data for Al involve a liberal interpolation from 5.0E-01 to 4.0E01 keV energy.

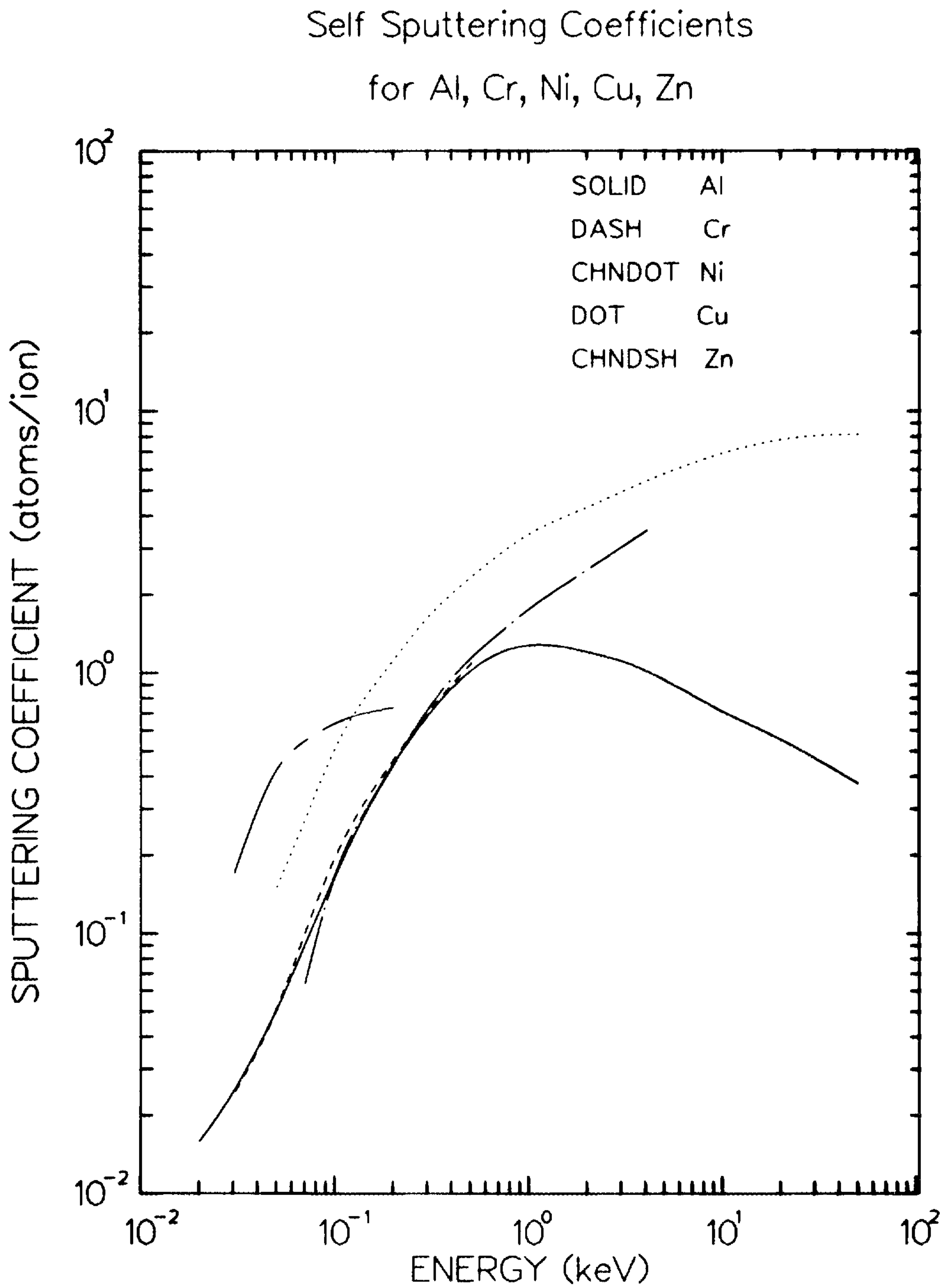
Self Sputtering Coefficients
for Al, Cr, Ni, Cu, Zn
SOLID Al
DASH Cr
CHNDOT Ni
DOT Cu
CHNDSH Zn
SPUTTERING COEFFICIENT (atoms/ion)
ENERGY (keV)
10^{2}
10^{1}
10^{0}
10^{-1}
10^{-2}

Self-Sputtering Coefficients for

Ag, Au, Mo, Nb, and W

(normal incidence, room temperature)

	Self-Sputtering Coefficients (atoms/ion)				
Energy (keV)	Ag	Au	Mo	Nb	W
3.0E-02	1.3E-01	3.3E-02			
4.0E-02	2.7E-01	1.0E-01			
6.0E-02	5.5E-01	2.5E-01			
1.0E-01	9.7E-01	6.0E-01	4.0E-02		1.1E-01
2.0E-01	1.8E+00	1.4E+00	1.2E-01		1.9E-01
3.0E-01	2.4E+00	2.0E+00	1.9E-01		2.7E-01
4.0E-01	2.9E+00	2.5E+00	2.5E-01		3.5E-01
6.0E-01	3.9E+00	3.3E+00	3.7E-01		4.7E-01
1.0E+00	5.3E+00	4.7E+00	5.6E-01		6.9E-01
2.0E+00	7.3E+00	7.0E+00	8.3E-01		1.1E+00
3.0E+00	8.9E+00	9.0E+00	1.1E+00		1.5E+00
4.0E+00	1.0E+01	1.1E+01	1.3E+00		2.0E+00
6.0E+00	1.2E+01	1.3E+01	1.6E+00		2.5E+00
1.0E+01	1.5E+01	1.8E+01	2.1E+00	2.6E+00	3.8E+00
2.0E+01	2.0E+01	2.6E+01		2.5E+00	
3.0E+01	2.3E+01	3.3E+01		3.0E+00	
4.0E+01	2.6E+01			3.3E+00	
6.0E+01	3.1E+01			3.8E+00	
1.0E+02	3.7E+01				

References:

Ag^+ + Ag: H. Andersen and H. L. Bay, Radiat. Eff. 19, 139 (1973); W. H. Hayward and A. R. Wolter, J. Appl. Phys. 40, 2911 (1969).

Au^+ + Au: W. H. Hayward and A. R. Wolter, J. Appl. Phys. 40, 2911 (1969); E. P. Eernisse, Appl. Phys. Lett. 29, 14 (1976).

Nb^+ + Nb: A. J. Summers, N. J. Freeman, and N. R. Daly, J. Appl. Phys. 42, 4774 (1971).

Mo^+ + Mo: M. Saidoh and K. Sone, Jap. J. Appl. Phys. 22, 1361 (1983).

W^+ + W: M. Saidoh and K. Sone, Jap. J. Appl. Phys. 22, 1361 (1983).

Accuracy: Unknown.

Note: The data for Au involve a liberal interpolation from 4.0E-01 to 4.0E01 keV energy.

Self Sputtering Coefficients
for Ag, Au, Mo, Nb, W

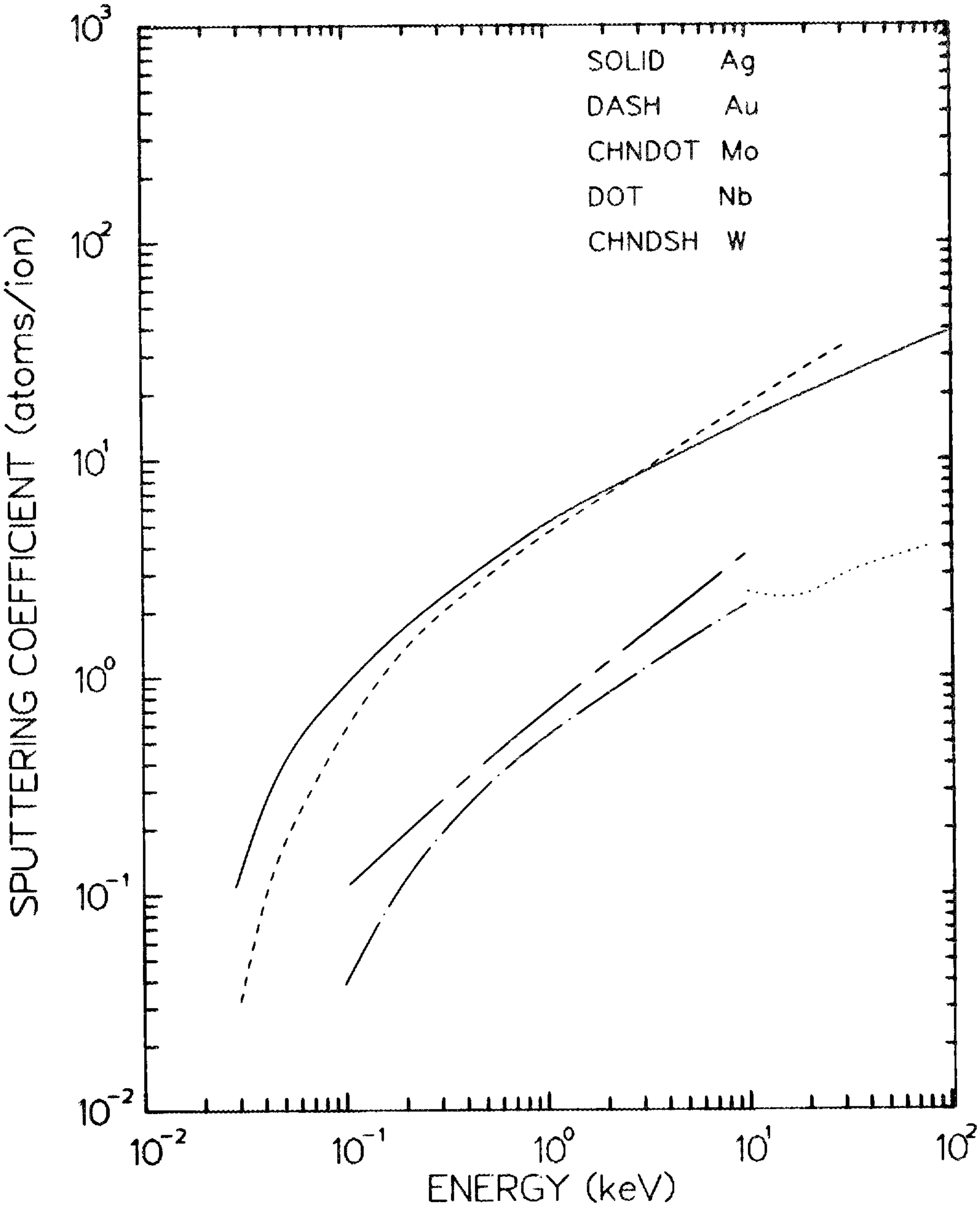

Example of Energy Distribution of Sputtered Atoms

Gold Atoms Sputtered from Au by H^+ Impact

(normal incidence, room temperature)

Energy of Sputtered Particles (eV)	Flux of Sputtered Particles (arbitrary units)	
	H^+ (15-keV Impact)	H^+ (30-keV Impact)
5.0E-01	8.0	6.5
1.0E 00	13.0	9.5
2.0E 00	14.0	10.0
3.0E 00	13.0	9.0
5.0E 00	10.0	6.5
1.0E 01	5.0	3.4
2.0E 01	2.0	1.3
3.0E 01	1.0	0.6
5.0E 01	0.4	0.25

Reference:

P. Hucks et al., J. Nucl. Mater. 76 & 77, 136 (1978).

Accuracy: ± 5%.

Note: (1) The fluxes are in arbitrary units; the numbers for 15-keV and 30-keV impact have no relative significance.

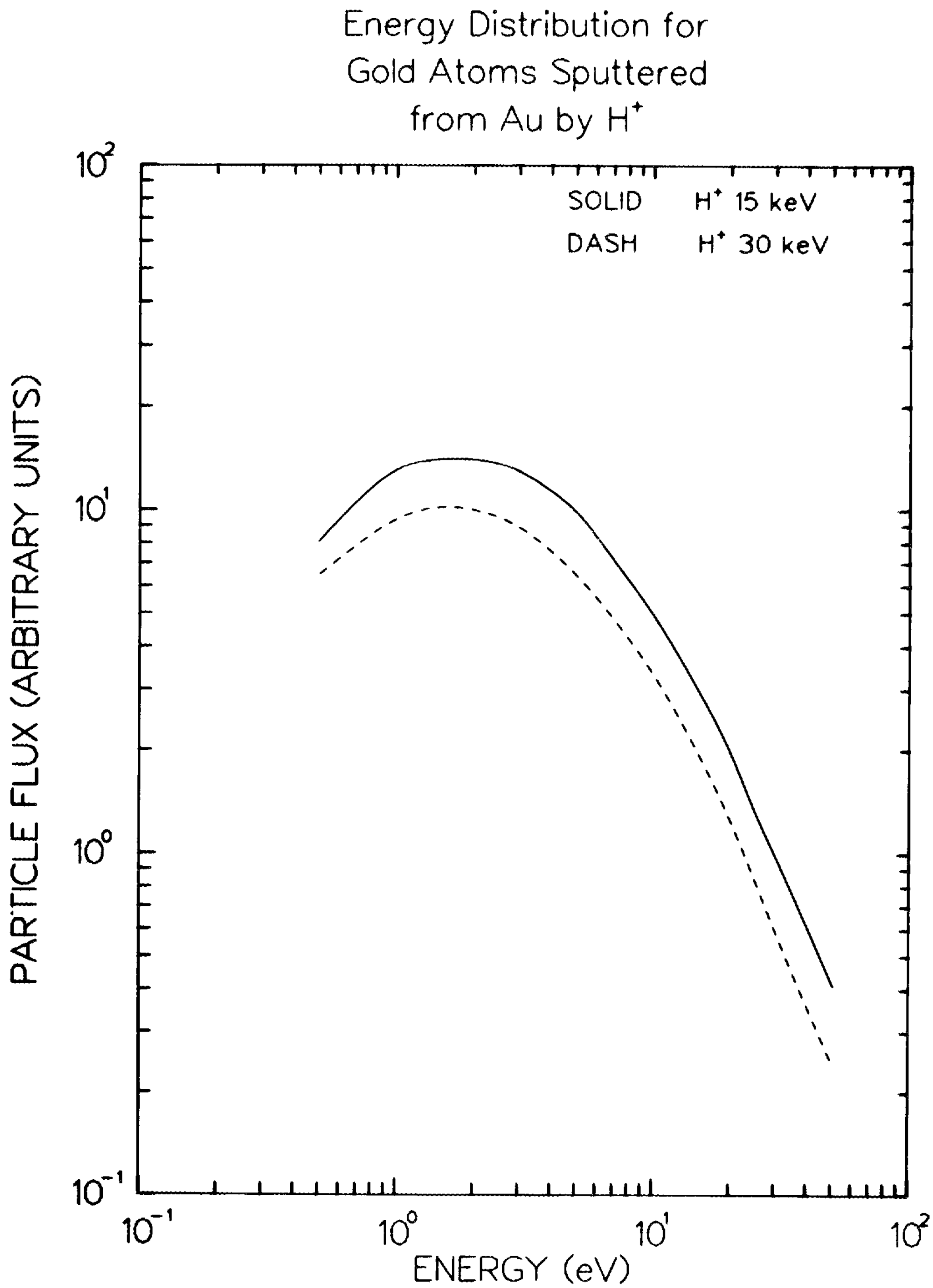

Energy Distribution for
Gold Atoms Sputtered
from Au by H+
SOLID H+ 15 keV
DASH H+ 30 keV
PARTICLE FLUX (ARBITRARY UNITS)
10^2
10^1
10^0
10^-1
10^-1
10^0
10^1
10^2
ENERGY (eV)

Example of Chemical Sputtering

Sputtering of C (Graphite) by H^+ and He^+ as a Function of Temperature (normal incidence)

Temperature (°C)	Sputtering Coefficients, S (atoms/ion)				
	H^+ (0.67 keV)	H^+ (1.0 keV)	H^+ (2.0 keV)	H^+ (3.0 keV)	He^+ (6.0 keV)
2.0E 01					9.1E-02
2.0E 02		2.0E-03	4.0E-03	2.0E-03	
3.0E 02		2.5E-03	6.0E-03	3.0E-03	
4.0E 02	1.3E-02	8.0E-03	7.0E-03	5.0E-03	
4.5E 02	2.7E-02	1.6E-02	9.0E-03	8.0E-03	
5.0E 02	4.3E-02	3.0E-02	1.3E-02	1.2E-02	
5.5E 02	6.8E-02	5.1E-02	2.0E-02	1.9E-02	
6.0E 02	8.0E-02	7.0E-02	3.2E-02	3.0E-02	9.9E-02
6.5E 02	8.1E-02	7.8E-02	6.0E-02	3.0E-02	
7.0E 02	6.7E-02	5.5E-02	5.0E-02	2.0E-02	
7.5E 02		4.0E-02	3.5E-02	1.2E-02	

Reference:

J. Roth *et al.*, J. Nucl. Mater. 63, 222 (1976).

Accuracy: ± 20%.

Notes: (1) The sample material is pyrolytic graphite from Union Carbide with the surface cut parallel to the c-axis. It is well known that sputtering coefficients of carbon vary greatly depending on manufacturer, form of material, and orientation of the surface; variations of at least a factor of two are to be expected - see reference cited.

(2) Many other measurements of sputtering are available, generally for incident energies of 1 eV or less. For a complete listing see B. M. U. Scherzer *et al.*, in *Proc. Int. Symposium on Plasma Wall Interaction, Julich, 1976* (Pergammon Press, Oxford, 1977), p. 353.

(3) The data were taken using H_2^+ and H_3^+ projectiles; they are shown here as though they were for protons of the same velocity with S given as atoms ejected per nucleon incident.

(4) It is noted that the values of S at low temperatures are inconsistent with those presented in D.1.4 and D.1.5. These differences may simply be due to different forms of carbon.

(5) Chemical sputtering may be dependent on projectile flux (see J. N. Smith and R. H. Meyer, J. Nucl. Mater. 76 & 77, 193 (1978)).

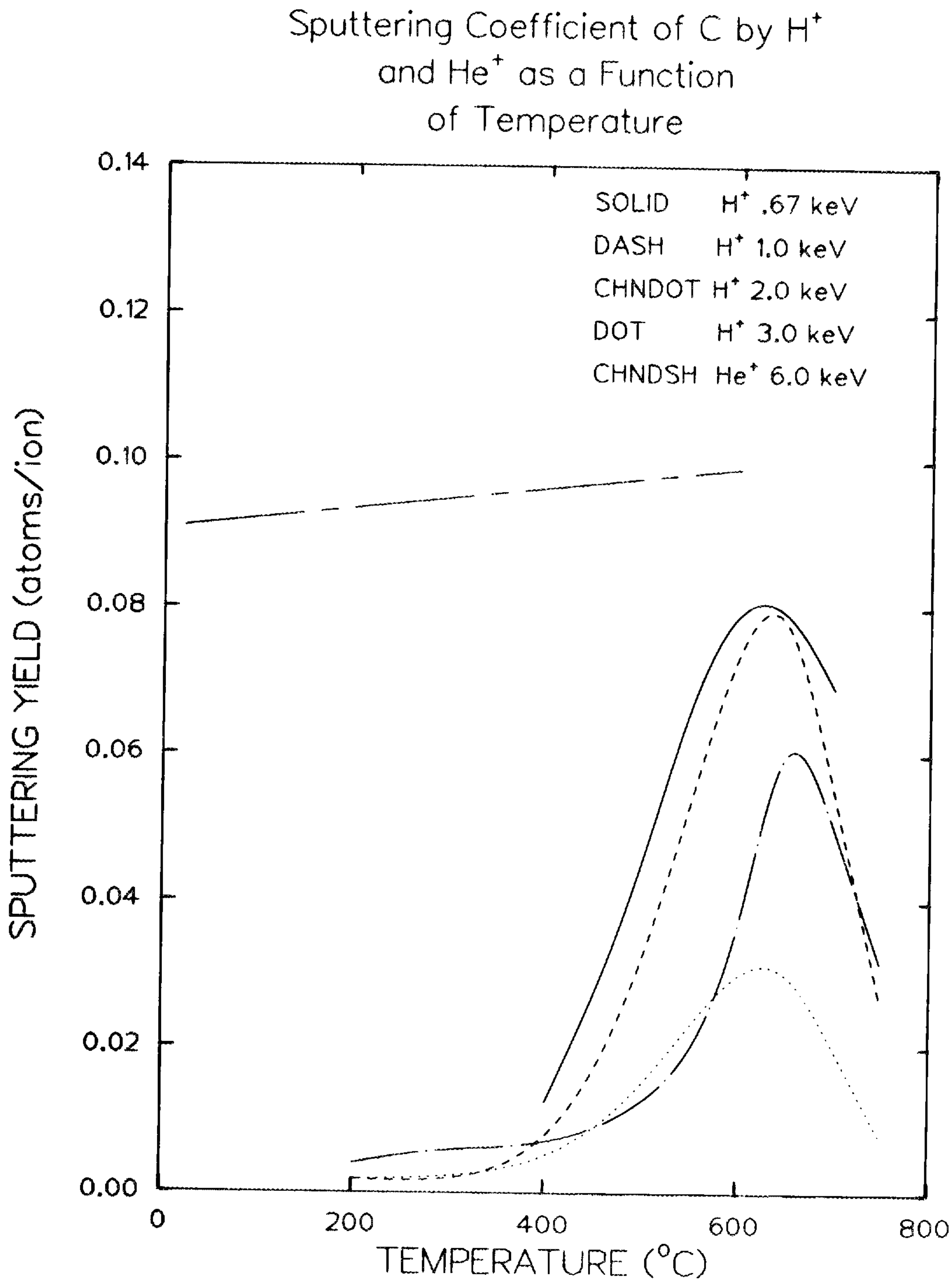
Sputtering Coefficient of C by H+
and He+ as a Function
of Temperature
SOLID H+ .67 keV
DASH H+ 1.0 keV
CHNDOT H+ 2.0 keV
DOT H+ 3.0 keV
CHNDSH He+ 6.0 keV
SPUTTERING YIELD (atoms/ion)
0.14
0.12
0.10
0.08
0.06
0.04
0.02
0.00
0
200
400
600
800
TEMPERATURE (°C)

Sputtering Coefficient of

Ni and W by O^+

(normal incidence, room temperature)

Energy (keV)	Sputtering Coefficients, S (atoms/ion) Ni	W
1.0E-01	2.46E-02	
2.0E-01	1.01E-01	1.16E-02
3.0E-01	1.62E-01	1.56E-02
4.0E-01	2.05E-01	2.23E-02
6.0E-01	2.69E-01	6.41E-02
1.0E+00	3.51E-01	1.95E-01
2.0E+00	4.81E-01	3.47E-01
3.0E+00	5.60E-01	4.06E-01

Reference: J. Roth, J. Bohdansky, and W. Ottenberger, Report IPP 9/26 (May 1979) from Max-Planck-Institut fur Plasmaphysik, Garching. This report is a compendium of data from various sources.

Accuracy: Unknown.

Note: Original data points deviate from the curve shown here by up to 40% in limited energy regions.

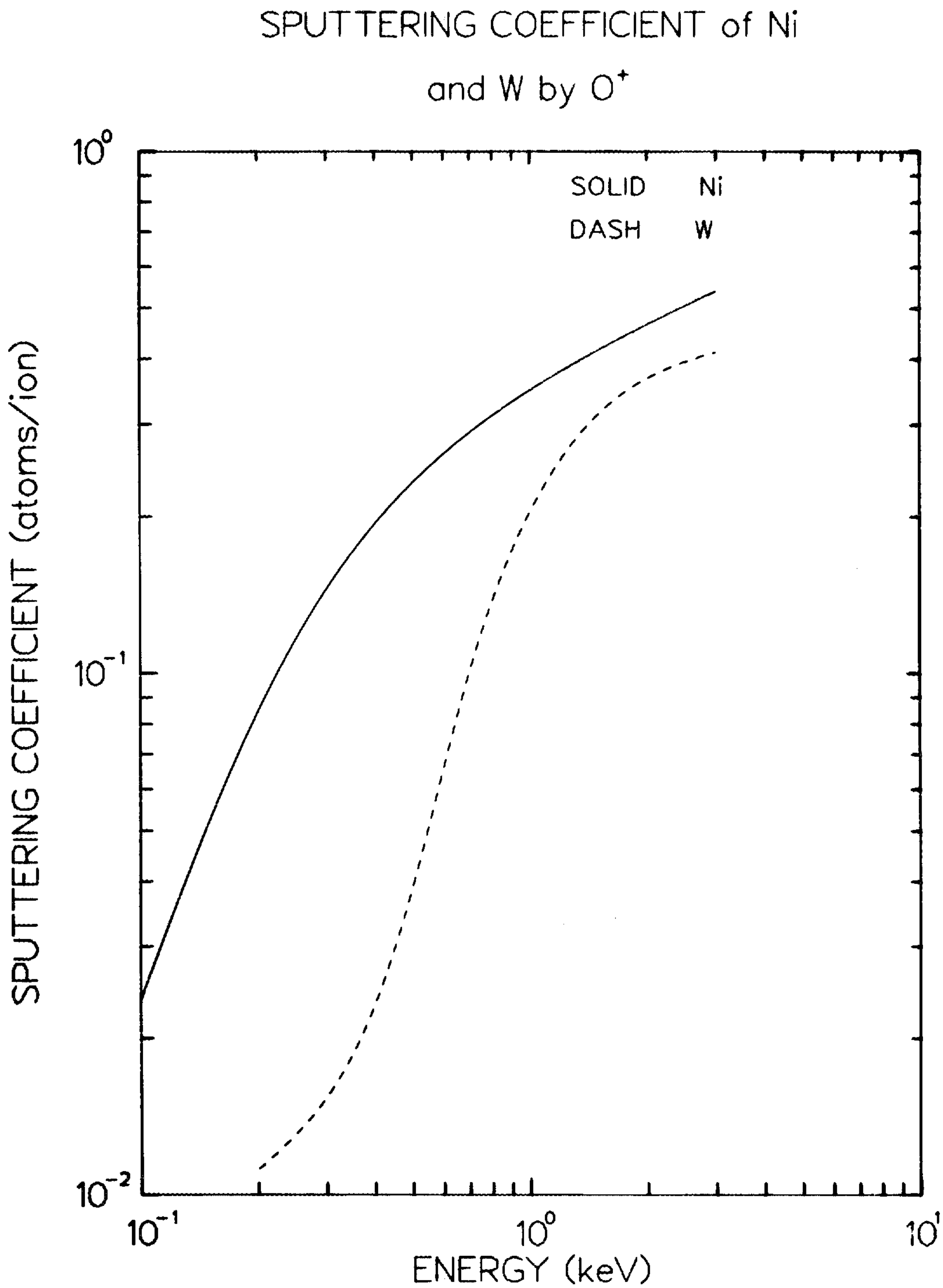
SPUTTERING COEFFICIENT of Ni
and W by O⁺
SOLID Ni
DASH W
SPUTTERING COEFFICIENT (atoms/ion)
ENERGY (keV)
10^0
10^-1
10^-2
10^-1
10^0
10^1

Neutron Sputtering of V, Co, Nb, and Au

(Materials are polycrystalline.

Temperatures are room temperature.)

Material	Neutron Energy (MeV)	Upper Bound to Sputtering Coefficients (atoms/neutron)	Principal Reference
V	14.8	$< 5 \times 10^{-5}$	5
Co	16 (avg)	$< 2 \times 10^{-5}$	1
Nb	14.8	$< 10^{-4}$ "certain"	2,3
		$< 5 \times 10^{-5}$ "most likely"	2,3
Au	14.8	$< 4 \times 10^{-5}$	1,4

References:

(1) L. H. Jenkins et al., J. Nucl. Mater. 63, 438 (1976).
(2) R. Behrisch et al., J. Appl. Phys. 48, 3914 (1977).
(3) O. K. Harling et al., J. Appl. Phys. 48, 4315 (1977).
(4) O. K. Harling et al., J. Nucl. Mater. 63, 422 (1976).
(5) M. Kaminsky and S. K. Das, J. Nucl. Mater. 66, 333 (1977).

Accuracy: Unknown.

Notes: (1) In most neutron sputtering measurements the quoted results are an upper bound set by the limits of detectability. Numerous earlier measurements exist (not quoted here but largely cited in references 2, 3, and 4) giving larger upper bounds reflecting poorer detection sensitivity.

(2) All quoted measurements involve removal of less than one monolayer of a surface covered with an unknown amount of oxide; consequently, the data may not be representative of bulk metal.

(3) Early reports of "chunk" ejection appear to be related to the method of target preparation and are not reported by most workers; see reference 2.

(4) For a theoretical estimate see R. Behrisch, Nucl. Instrum. Meth. 132, 293 (1976) and also H. Uecher et al., J. Nucl. Mater. 93 & 94, 670 (1980).

B. SECONDARY ELECTRON EMISSION BY ELECTRON IMPACT

Secondary Electron Emission Coefficients for Electron Impact on Clean Surfaces of C, Al, and Ti

Energy (keV)	Secondary Electron Emission Coefficient (electrons/electron)		
	C	Al	Ti
1.0 E-02		8.01 E-02	
2.0 E-02		1.99 E-01	
4.0 E-02	3.73 E-01	4.22 E-01	
7.0 E-02	5.22 E-01	6.15 E-01	4.80 E-01
1.0 E-01	6.32 E-01	7.23 E-01	5.42 E-01
2.0 E-01	8.92 E-01	9.06 E-01	7.72 E-01
4.0 E-01	9.24 E-01	9.75 E-01	8.41 E-01
7.0 E-01	7.46 E-01	9.11 E-01	7.54 E-01
1.0 E 00	6.08 E-01	8.32 E-01	6.79 E-01
1.5 E 00	4.77 E-01	7.25 E-01	6.05 E-01
2.0 E 00	3.79 E-01	6.56 E-01	
4.0 E 00	2.28 E-01		
5.0 E 00	1.87 E-01		

References: e + C - H. Bruining, Philips Tech. Rev. 3, 80 (1938); J. Hölzl and K. Jacobi, Surface Sci. 14, 351 (1969); D. Ruzic, R. Moore, D. Manos, and S. Cohen, J. Vac. Sci. Technol., 20, 1313 (1982).

e + Al - I. M. Bronshtein and V. V. Roshchin, Sov. Phys. Tech. Phys. 3, 2271 (1958); S. Thomas and E. B. Pattinson, J. Phys. D 3, 349 (1969).

e + Ti - D. Ruzic, R. Moore, D. Manos, and S. Cohen, J. Vac. Sci. Technol. 20, 1313 (1982).

Accuracy: Random error <5% (estimated).

Note: The relative variation of the secondary emission coefficient may be reliable. The absolute data from different sources may differ up to 30% in some cases.

Secondary Electron Emission Coefficient for Electron Impact on Clean Surfaces of C, Al, and Ti

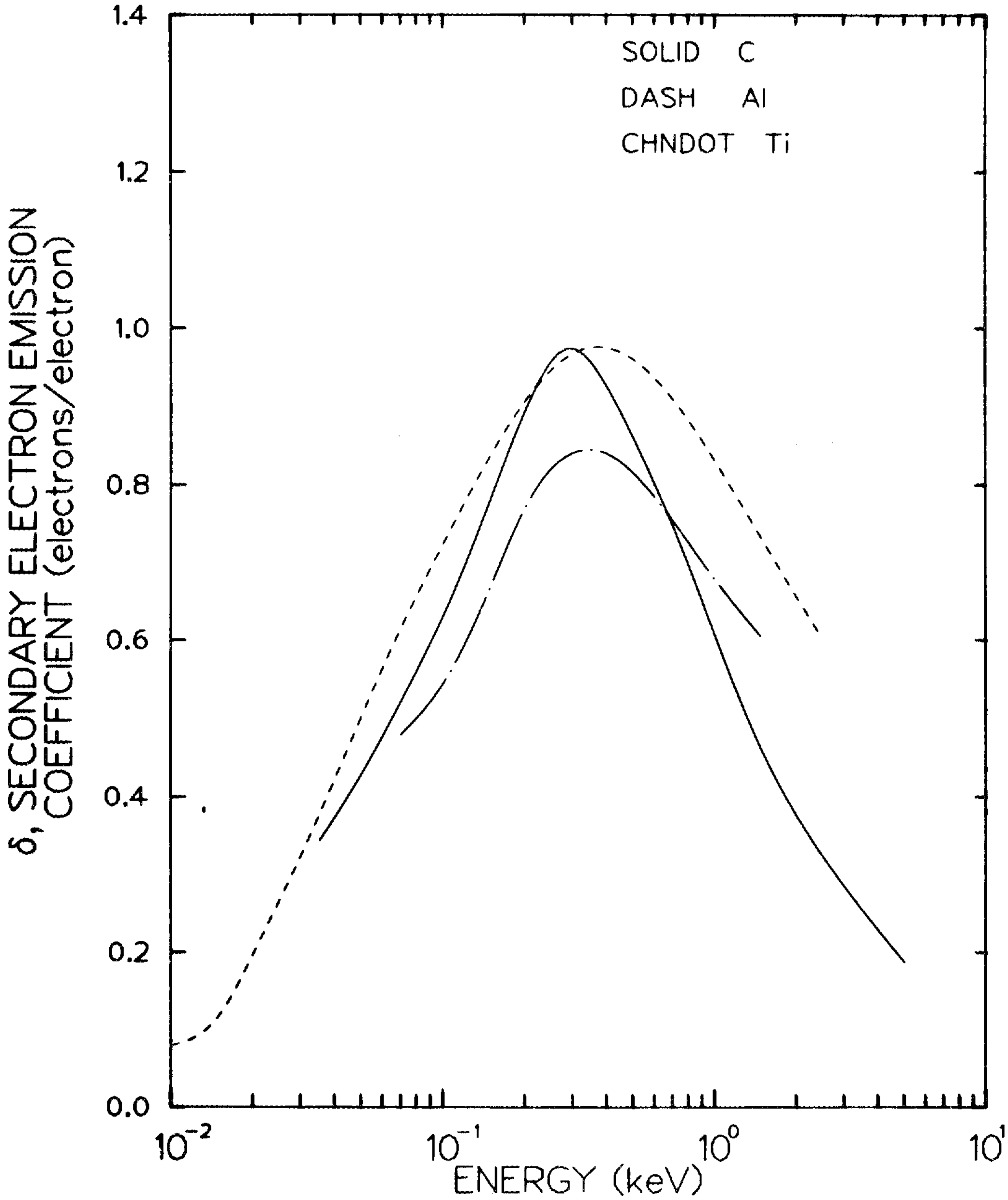

Secondary Electron Emission Coefficients for Electrons at Normal Incidence on Clean SS, Ni, Mo, and Au

Energy (eV)	Secondary Electron Emission Coefficient (electrons/electron) SS	Ni	Mo	Au
3.4 E-03			6.16 E-03	
7.0 E-03			8.89 E-02	
1.0 E-02			1.43 E-01	2.04 E-01
2.0 E-02			2.66 E-01	3.64 E-01
4.0 E-02			4.18 E-01	6.97 E-01
7.0 E-02	5.22 E-01	6.08 E-01	5.71 E-01	9.38 E-01
1.0 E-01	6.77 E-01	8.36 E-01	6.96 E-01	1.09 E 00
2.0 E-01	1.00 E 00	1.16 E 00	1.01 E 00	1.37 E 00
4.0 E-01	1.24 E 00	1.34 E 00	1.25 E 00	1.63 E 00
7.0 E-01	1.14 E 00	1.29 E 00	1.18 E 00	1.80 E 00
1.0 E 00	1.03 E 00	1.18 E 00	1.05 E 00	1.77 E 00
2.0 E 00			7.82 E-01	1.59 E 00
4.0 E 00			4.72 E-01	
7.0 E 00			3.29 E-01	

References: E + SS - D. Ruzic, R. Moore, D. Manos, and S. Cohen, J. Vac. Sci. Technol. 20, 1313 (1982).

e + Ni - S. Thomas and E. B. Pattinson, J. Phys. D 3, 349 (1969).

e + Mo - Von G. Blankenfeld, Ann. der Physik 9, 48 (1951); I. M. Bronshtein, Bull. Acad. Sci. USSR 22, 442 (1958); D. Ruzic, R. Moore, D. Manos, and S. Cohen, J. Vac. Sci. Technol. 20, 1313 (1982).

e + Au - I. M. Bronshtein and V. V. Roshchin, Sov. Phys. Tech. Phys. 3, 2271 (1958); S. Thomas and E. B. Pattinson, J. Phys. D 3, 349 (1969).

Accuracy: Random error ≤5% (estimated).

Notes: (1) Errors for the four elements are estimated.
(2) For secondary emission from steel in the energy range 40-200 keV, see J. G. Trump and R. J. Van de Graff, Phys. Rev. 75, 44 (1948).
(3) The relative variation of the secondary emission coefficient may be reliable. The absolute data from different sources may differ up to 30% in some cases.

Emission of Secondary Electrons by Electron Impact on Clean Surfaces of Stainless Steel, Ni, Mo, and Au

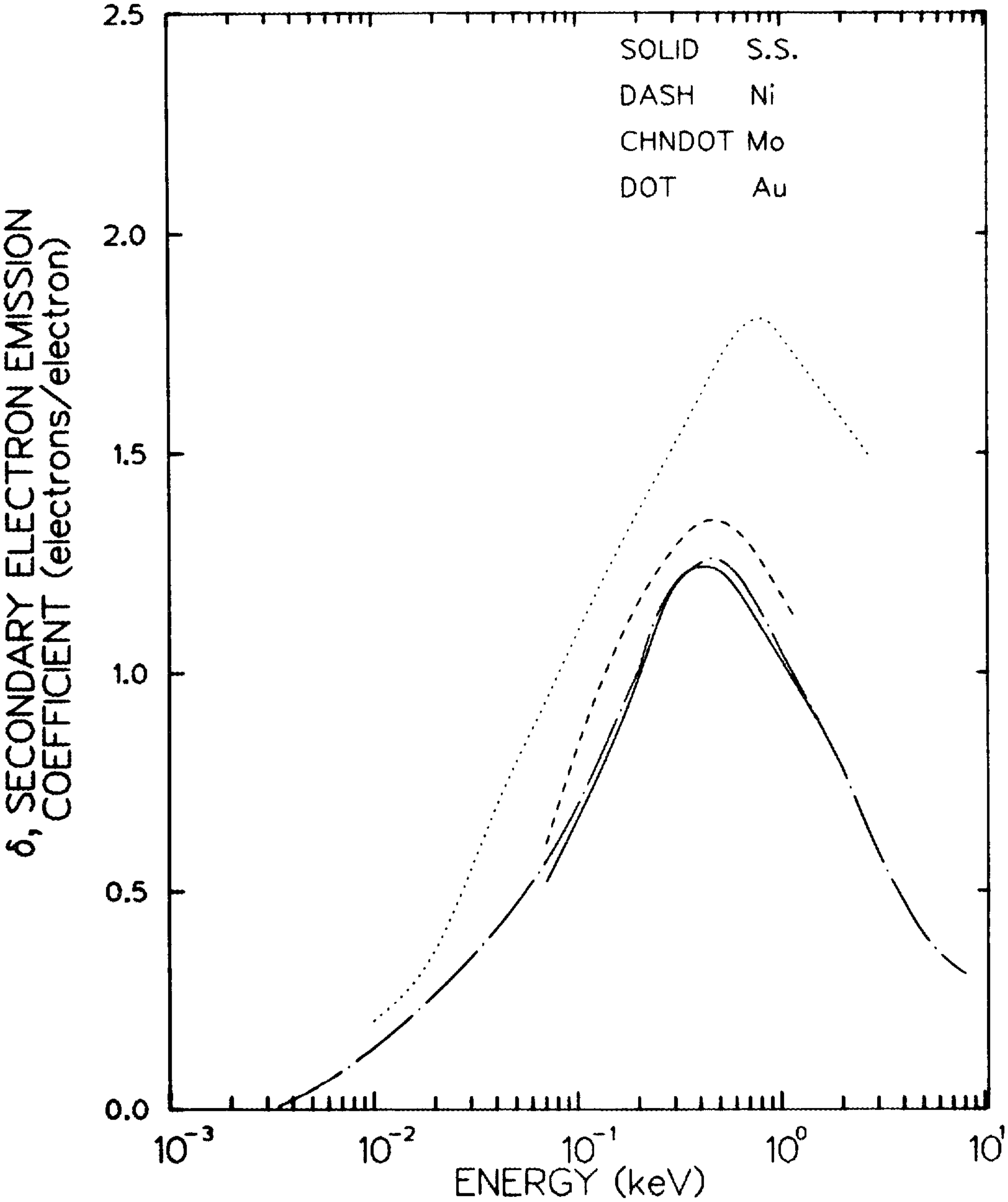

Secondary Electron Emission Coefficients for Electrons

at Normal Incidence on Clean and Gas Covered Ti

Energy (eV)	Secondary Electron Emission Coefficient (electrons/electron) Before Cleaning	200 Å Removed	Air Exposure
200	9.31 E-01	1.44 E 00	1.25 E 00
400	9.13 E-01	1.31 E 00	1.15 E 00
600	8.75 E-01	1.17 E 00	1.07 E 00
800	8.31 E-01	1.07 E 00	9.96 E-01
1000	7.83 E-01	9.93 E-01	9.25 E-01
1200	7.46 E-01	9.31 E-01	8.67 E-01
1400	7.11 E-01	8.80 E-01	8.15 E-01
1600		8.27 E-01	

Reference: H. Padamsee and A. Joshi, J. Appl. Phys. 50, 1112 (1979).

Accuracy: Systematic error, uncertain; random error, ≤5% (estimated).

Notes: (1) The column, before cleaning, refers to the Ti as received; clean Ti refers to Ti after a 200 Å layer was removed from the surface; after exposure refers to exposing the Ti surface to air after the 200 Å layer was removed.
(2) The Ti data after the 200 Å layer was removed do not agree with "clean Ti" of other authors and other graphs.

Secondary Electron Emission Coefficient

for Clean and Gassy Ti

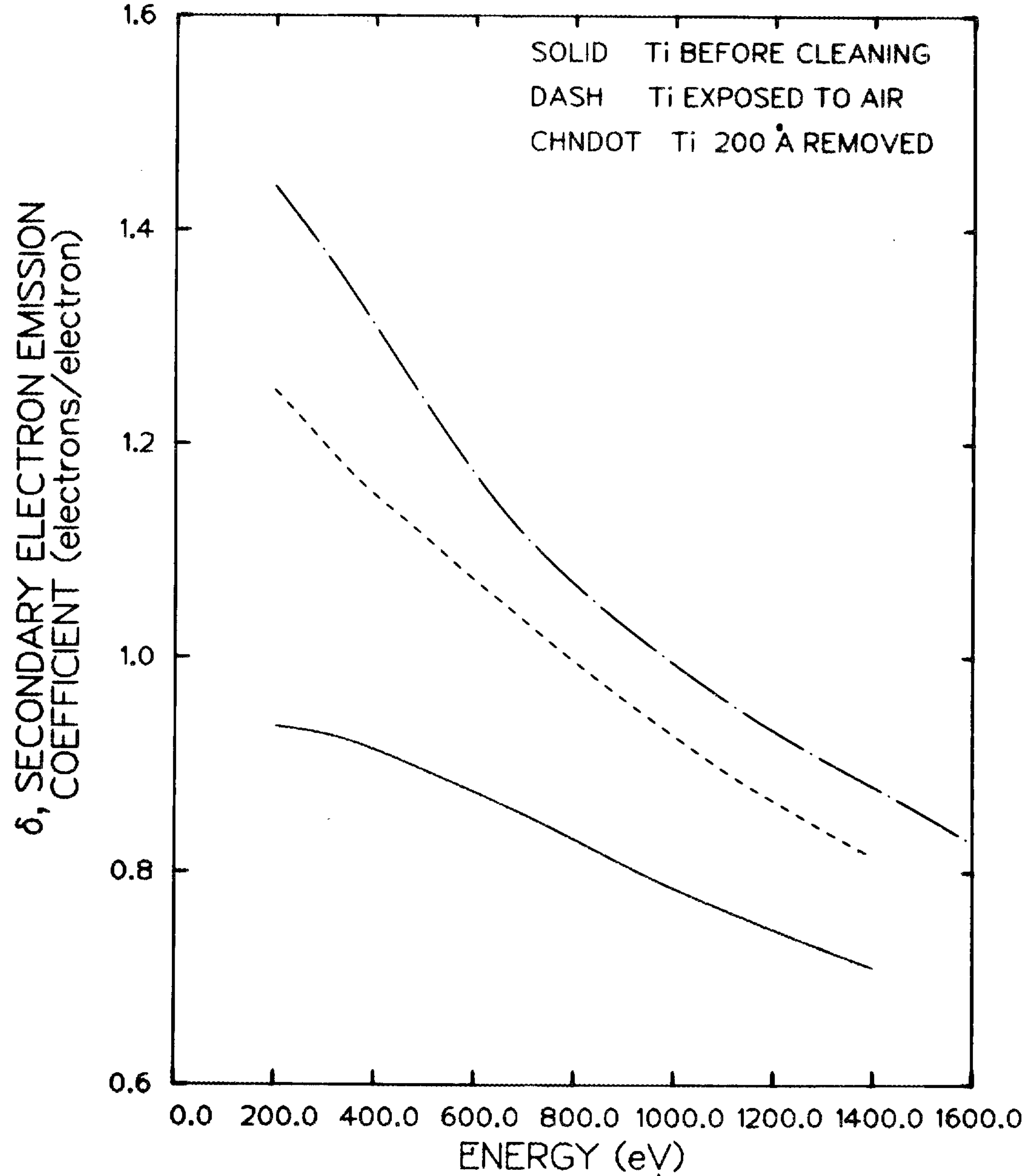

Secondary Electron Emission Coefficients for Electrons

at Normal Incidence on Clean and Gas Covered TiC

Energy (eV)	Secondary Electron Emission Coefficient	
	Clean	Gassy
75		1.01 E 00
90	5.73 E-01	1.12 E 00
100	6.25 E-01	1.16 E 00
200	8.48 E-01	1.43 E 00
300	9.70 E-01	1.47 E 00
400	1.02 E 00	1.42 E 00
600	9.96 E-01	1.26 E 00
800	9.35 E-01	1.12 E 00
1000	8.33 E-01	1.00 E 00
1200	8.08 E-01	9.41 E-01

Reference: S. Thomas and E. B. Pattinson, J. Phys. D 2, 1539 (1969).

Accuracy: Systematic error, uncertain; random error <5.

Notes: (1) TiC was deposited on a Cu substrate. The clean TiC refers to the surface after heating at 800°C for 6 hours. Gassy refers to the surface as received from the supplier.

Secondary Electron Emission Coefficient
for Clean and Gassy TiC

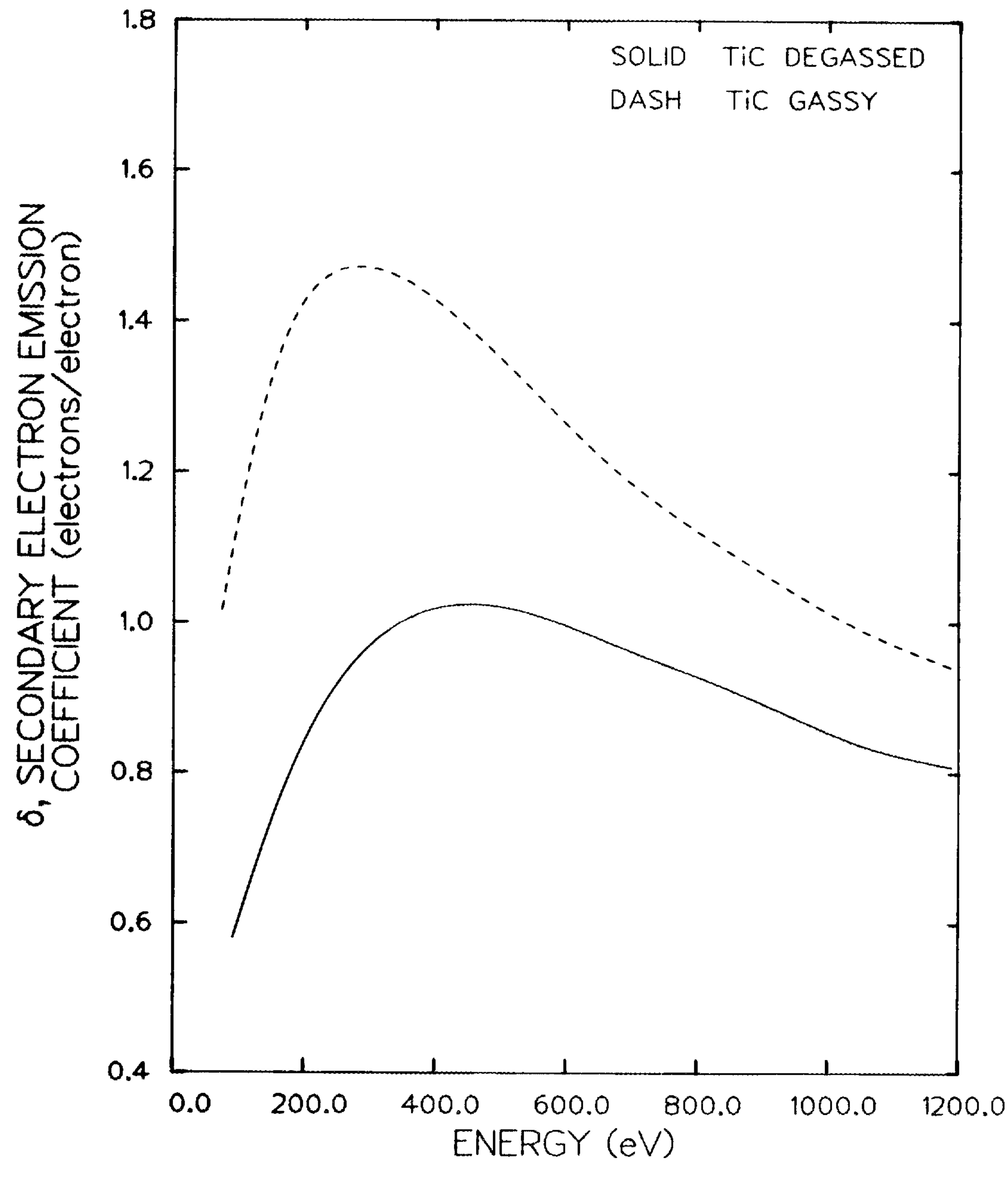

Secondary Electron Emission Coefficients for Electrons

on Ti for 0°, 30°, 45°, and 60° Incident Angle.

0° is Normal to the Surface

Energy (keV)	Secondary Electron Emission Coefficient (electrons/electron) 0°	30°	45°	60°
7.0 E-02	4.80 E-01	4.61 E-01	4.60 E-01	5.15 E-01
1.0 E-01	5.37 E-01	5.48 E-01	5.43 E-01	5.83 E-01
2.0 E-01	7.73 E-01	7.36 E-01	7.41 E-01	7.94 E-01
4.0 E-01	8.39 E-01	7.97 E-01	8.47 E-01	9.09 E-01
7.0 E-01	7.52 E-01	7.40 E-01	8.07 E-01	9.11 E-01
1.0 E-01	6.78 E-01	6.93 E-01	7.65 E-01	8.71 E-01
1.5 E-01	6.06 E-01	6.27 E-01	7.05 E-01	8.20 E-01

<u>Reference</u>: D. Ruzic, R. Moore, D. Manos, and S. Cohen, J. Vac. Sci. Technol. <u>20</u>, 1313 (1982).

<u>Accuracy</u>: Systematic error, uncertain; random error ≤5%.

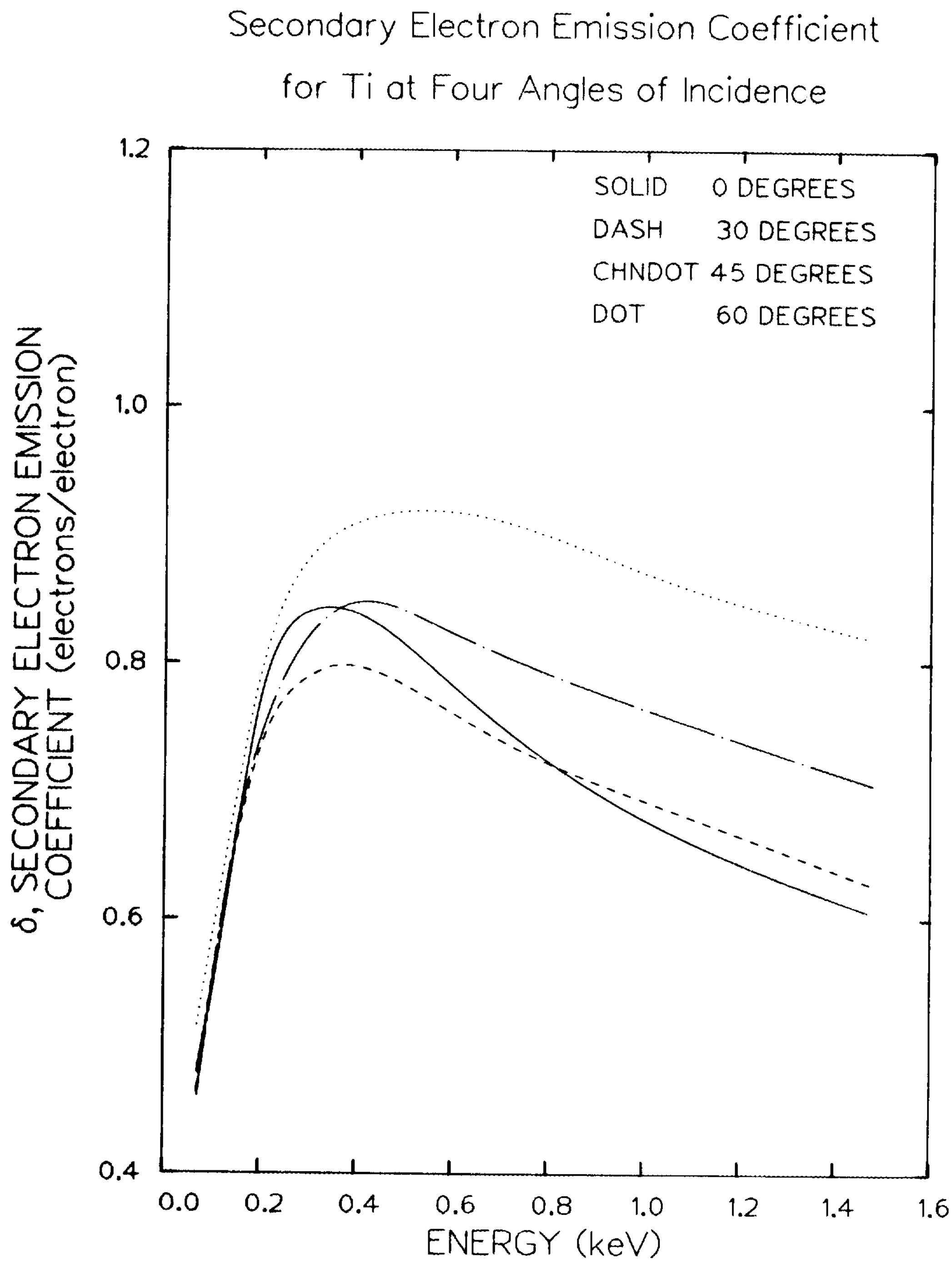
Secondary Electron Emission Coefficient
for Ti at Four Angles of Incidence
SOLID 0 DEGREES
DASH 30 DEGREES
CHNDOT 45 DEGREES
DOT 60 DEGREES
δ, SECONDARY ELECTRON EMISSION COEFFICIENT (electrons/electron)
ENERGY (keV)
1.2
1.0
0.8
0.6
0.4
0.0
0.2
0.4
0.6
0.8
1.0
1.2
1.4
1.6

Secondary Electron Emission Coefficients for Electrons at Normal Incidence on Different Textured Pyrolytic Graphite (PG) Surfaces

Energy (keV)	Secondary Electron Emission Coefficient (electrons/electron) Smooth PG	Textured PG	Soot
3.0 E-01	1.02 E 00	2.81 E-01	3.81 E-01
4.0 E-01	9.33 E-01	3.37 E-01	3.97 E-01
6.0 E-01	7.84 E-01	3.20 E-01	3.75 E-01
8.0 E-01	6.49 E-01	2.95 E-01	3.62 E-01
1.0 E 00	5.32 E-01	2.86 E-01	3.54 E-01
1.2 E 00	4.69 E-01	2.76 E-01	3.54 E-01
1.4 E 00	4.30 E-01	2.68 E-01	3.54 E-01
1.6 E 00	3.93 E-01	2.63 E-01	3.54 E-01
1.8 E 00	3.70 E-01	2.52 E-01	3.55 E-01
2.0 E 00	3.55 E-01	2.49 E-01	3.57 E-01

Reference: E. G. Wintucky, A. N. Curren, and J. S. Sovey, Thin Sol. Films 84, 161 (1981).

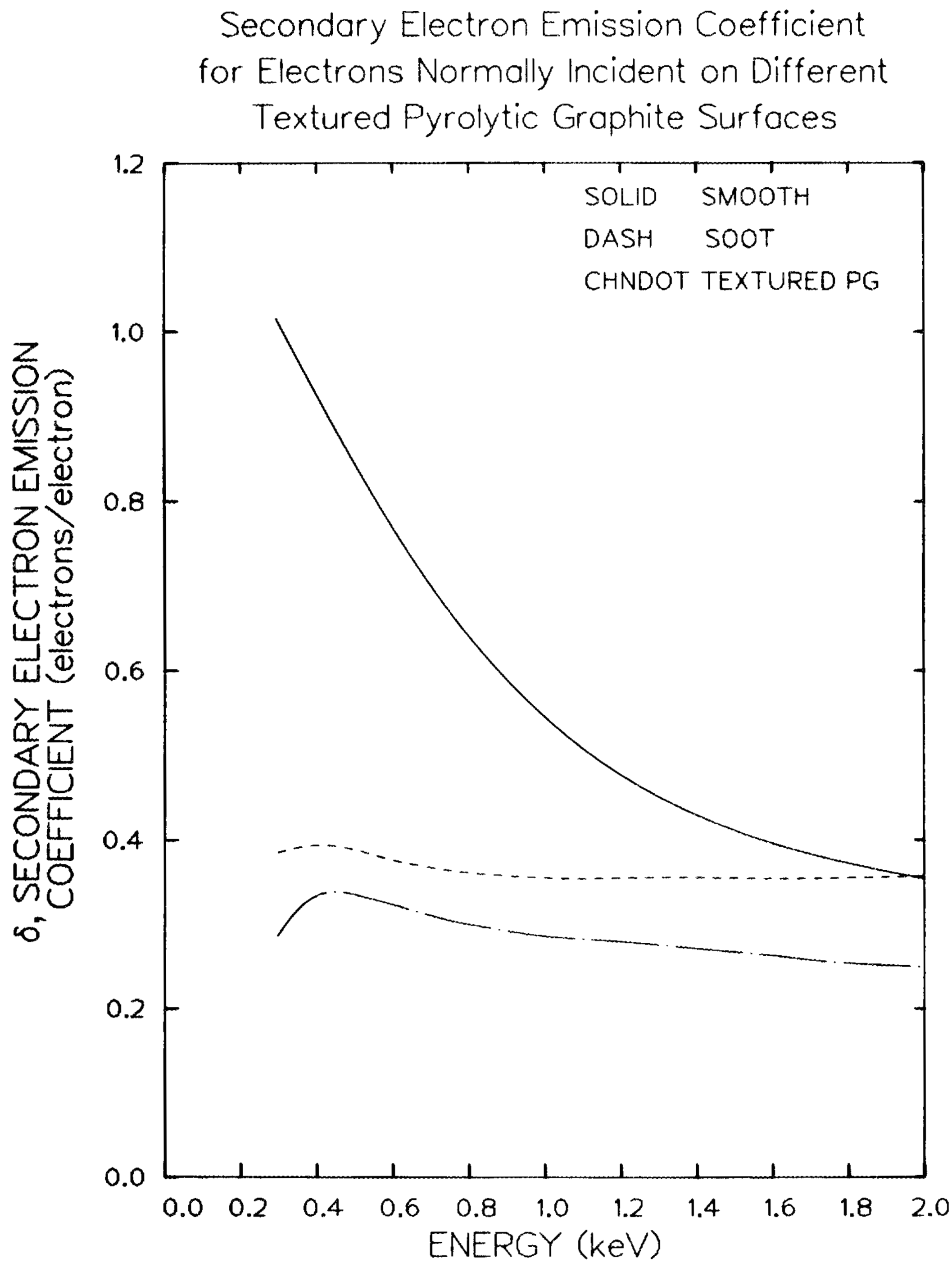
Secondary Electron Emission Coefficient
for Electrons Normally Incident on Different
Textured Pyrolytic Graphite Surfaces
SOLID SMOOTH
DASH SOOT
CHNDOT TEXTURED PG
δ, SECONDARY ELECTRON EMISSION
COEFFICIENT (electrons/electron)
0.0
0.2
0.4
0.6
0.8
1.0
1.2
0.0 0.2 0.4 0.6 0.8 1.0 1.2 1.4 1.6 1.8 2.0
ENERGY (keV)

C. SECONDARY ELECTRON EMISSION BY HEAVY PARTICLE IMPACT

Secondary Electron Emission Coefficients by Impact

of Normally Incident H^+, H_2^+ Ions on C

Energy (keV)	Secondary Emission Coefficient Electrons/Ion H^+	H_2^+
2.0 E+01	1.68 E 00	2.40 E 00
3.0 E+01	1.90 E 00	2.70 E 00
5.0 E+01	2.25 E 00	3.40 E 00
7.0 E+01	2.50 E 00	3.90 E 00
1.0 E+02	2.55 E 00	4.55 E 00

References: L. N. Large and W. S. Whitlock, Proc. Phys. Soc. (London) 79, 148 (1962).

Accuracy: ± 10%.

Notes: (1) There is substantial evidence that coefficients for H^+ and D^+ are the same at equal velocities suggesting that this is true also for T^+.

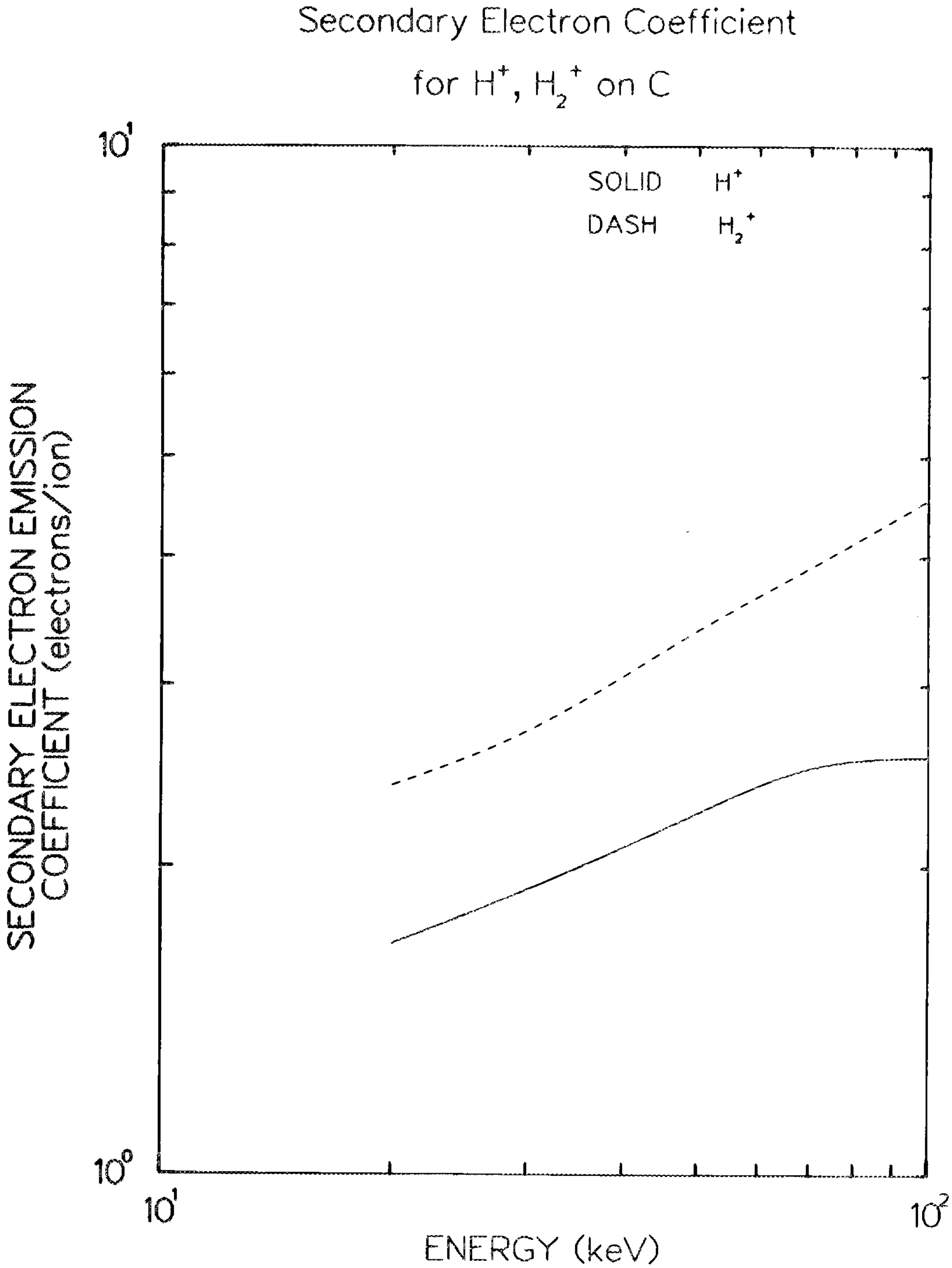
Secondary Electron Coefficient
for H+, H2+ on C
SOLID H+
DASH H2+
SECONDARY ELECTRON EMISSION COEFFICIENT (electrons/ion)
10^1
10^0
10^1
10^2
ENERGY (keV)

Secondary Electron Emission Coefficients by Impact

of Normally Incident H^+, H_2^+, He^+, C^+, and O^+ Ions on Al

Energy (keV)	Secondary Emission Coefficient Electrons/Ion				
	H^+	H_2^+	$^4He^+$	C^+	O^+
2.0 E 00	2.25 E-01	1.74 E-01	2.80 E-01		
4.0 E 00	3.80 E-01	3.12 E-01	3.80 E-01	2.40 E-01	4.50 E-01
7.0 E 00	5.60 E-01	4.60 E-01	5.10 E-01	4.40 E-01	6.80 E-01
1.0 E+01	7.00 E-01	6.20 E-01	6.20 E-01	6.50 E-01	8.80 E-01
2.0 E+01	1.01 E 00	1.11 E 00	8.85 E-01	1.06 E 00	1.32 E 00
3.0 E+01	1.23 E 00	1.50 E 00	1.10 E 00	1.38 E 00	1.58 E 00
4.0 E+01	1.34 E 00	1.77 E 00	1.31 E 00	1.65 E 00	1.72 E 00
5.0 E+01	1.38 E 00	1.91 E 00		1.90 E 00	1.80 E 00

<u>References</u>: R. A. Baragiola, E. V. Alonso, and A. Olivia-Florio, Phys. Rev. B <u>19</u>, 121 (1979). E. V. Alonso, R. A. Baragiola, J. Ferron, M. M. Jakas, and A. Olivia-Florio, Phys. Rev. A <u>22</u>, 80 (1980).

<u>Accuracy</u>: ±10%.

<u>Notes</u>: (1) There is substantial evidence that coefficients for H^+ and D^+ are the same at equal velocities suggesting that this is true also for T^+.
(2) Data for He^+ are by Baragiola et al. Data for H^+ and H_2^+ come from both Baragiola and Large. Data for C^+ and O^+ are from Alonso.

Secondary Electron Coefficient

for H^+, H_2^+, He^+, C^+, O^+ on Al

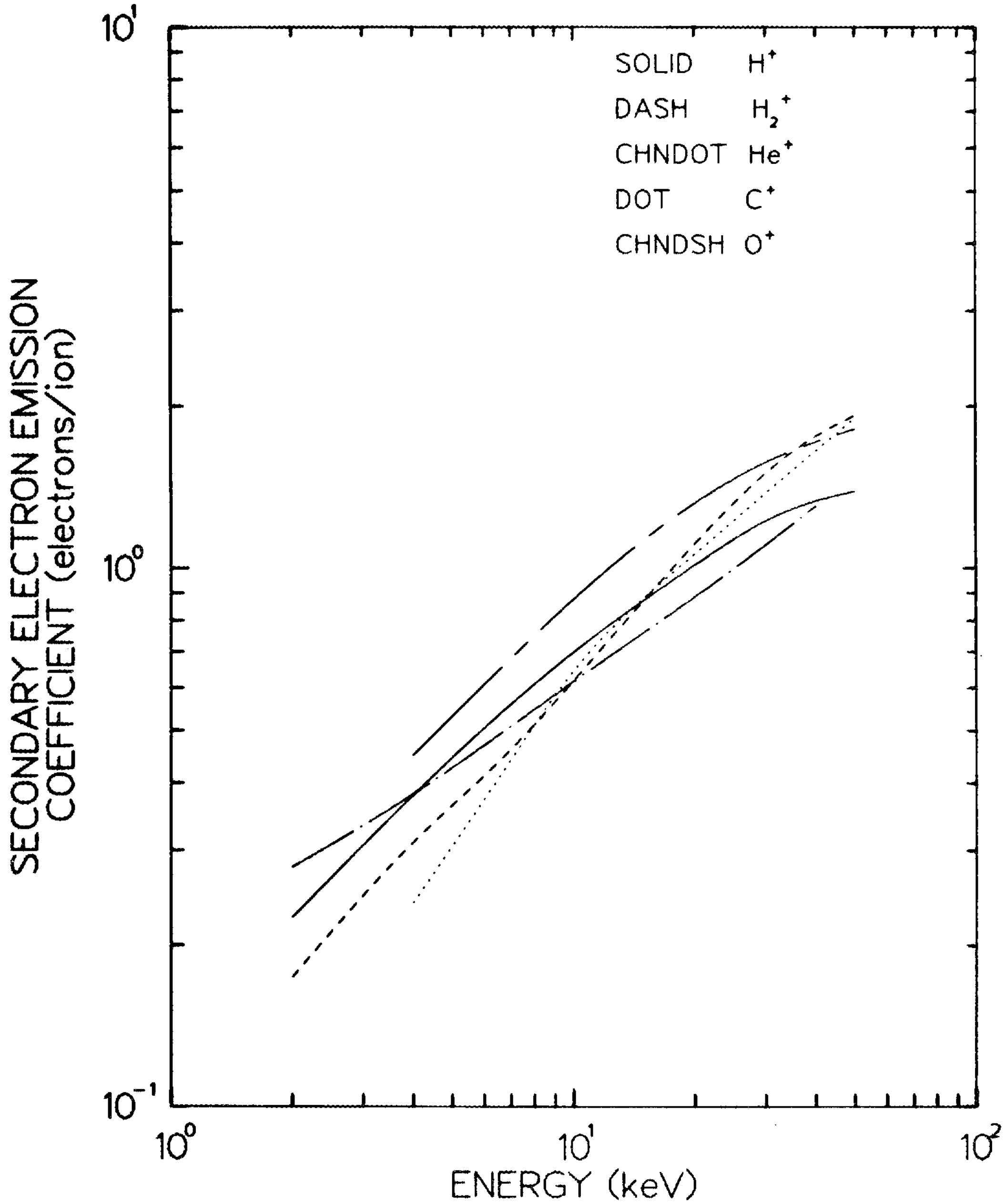

Secondary Electron Emission Coefficients by Impact of Normally Incident H^+ and H_2^+ Ions on Ti

Energy (keV)	Secondary Emission Coefficient Electrons/Ion	
	H^+	H_2^+
2.0 E+01	8.50 E-01	1.25 E 00
4.0 E+01	1.07 E 00	1.60 E 00
5.0 E+01	1.12 E 00	1.74 E 00
7.0 E+01	1.18 E 00	1.95 E 00
1.0 E+02	1.20 E 00	2.23 E 00
1.5 E+02	1.20 E 00	2.57 E 00

References: L. N. Large and W. S. Whitlock, Proc. Phys. Soc. (London) 79, 148 (1962).

Accuracy: ±10%.

Notes: (1) There is substantial evidence that coefficients for H^+ and D^+ are the same at equal velocities suggesting that this is true also for T^+.

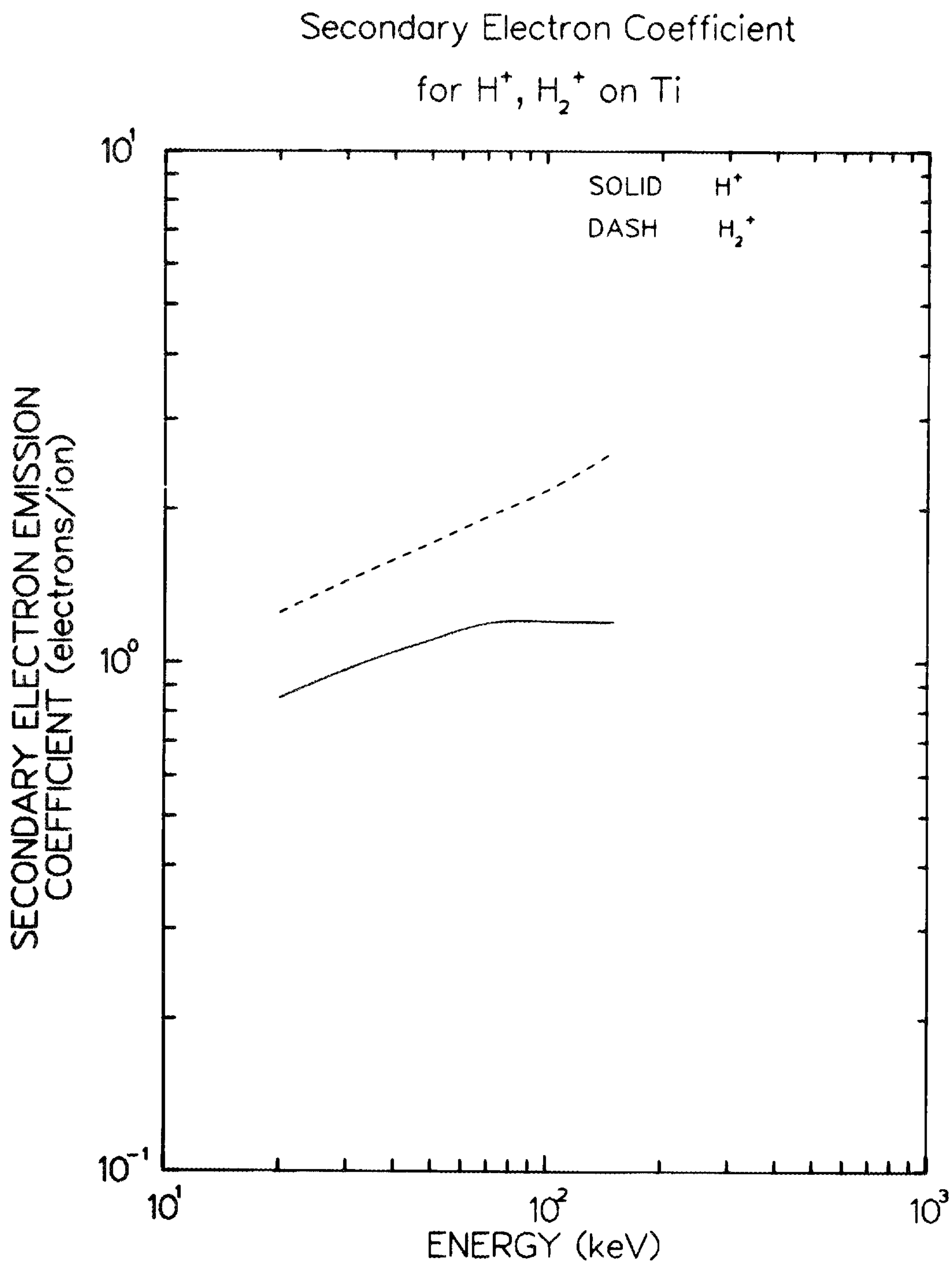
Secondary Electron Coefficient
for H^+, H_2^+ on Ti
SOLID H^+
DASH H_2^+
SECONDARY ELECTRON EMISSION
COEFFICIENT (electrons/ion)
10^1
10^0
10^{-1}
10^1
10^2
10^3
ENERGY (keV)

Secondary Electron Emission Coefficients by Impact

of Normally Incident H^+, H_2^+, and He^+ Ions on Ni

Energy (keV)	Secondary Emission Coefficient Electrons/Ion H^+	H_2^+	He^+
1.0 E 00			1.80 E-01
2.0 E 00			2.40 E-01
3.0 E 00			3.00 E-01
5.0 E 00			4.30 E-01
7.0 E 00			5.20 E-01
1.0 E+01			6.30 E-01
2.0 E+01	9.50 E-01	1.18 E-01	9.30 E-01
3.0 E+01	1.15 E 00	1.41 E 00	1.13 E 00
5.0 E+01	1.39 E 00	1.77 E 00	1.45 E 00
7.0 E+01	1.50 E 00	2.18 E 00	
1.0 E+02	1.58 E 00	2.60 E 00	
1.3 E+02	1.60 E 00	2.92 E 00	

References: H^+, H_2^+, H_3^+ on Ni: L. N. Large and W. S. Whitlock, Proc. Phys. Soc. 79, 148 (1962).
He^+ on Ni: V. A. Arifov, R. R. Rakhimov, and O. V. Khozinskii, Bull. Acad. Sci. USSR, Phys. Ser. 26, 1422 (1962) [Izv. Akad. Nauk SSR, Ser. Fiz, 26, 1398) (1962)].

Accuracy: ±10%.

Notes: (1) There is substantial evidence that coefficients for H^+ and D^+ are the same at equal velocities suggesting that this is true also for T^+.

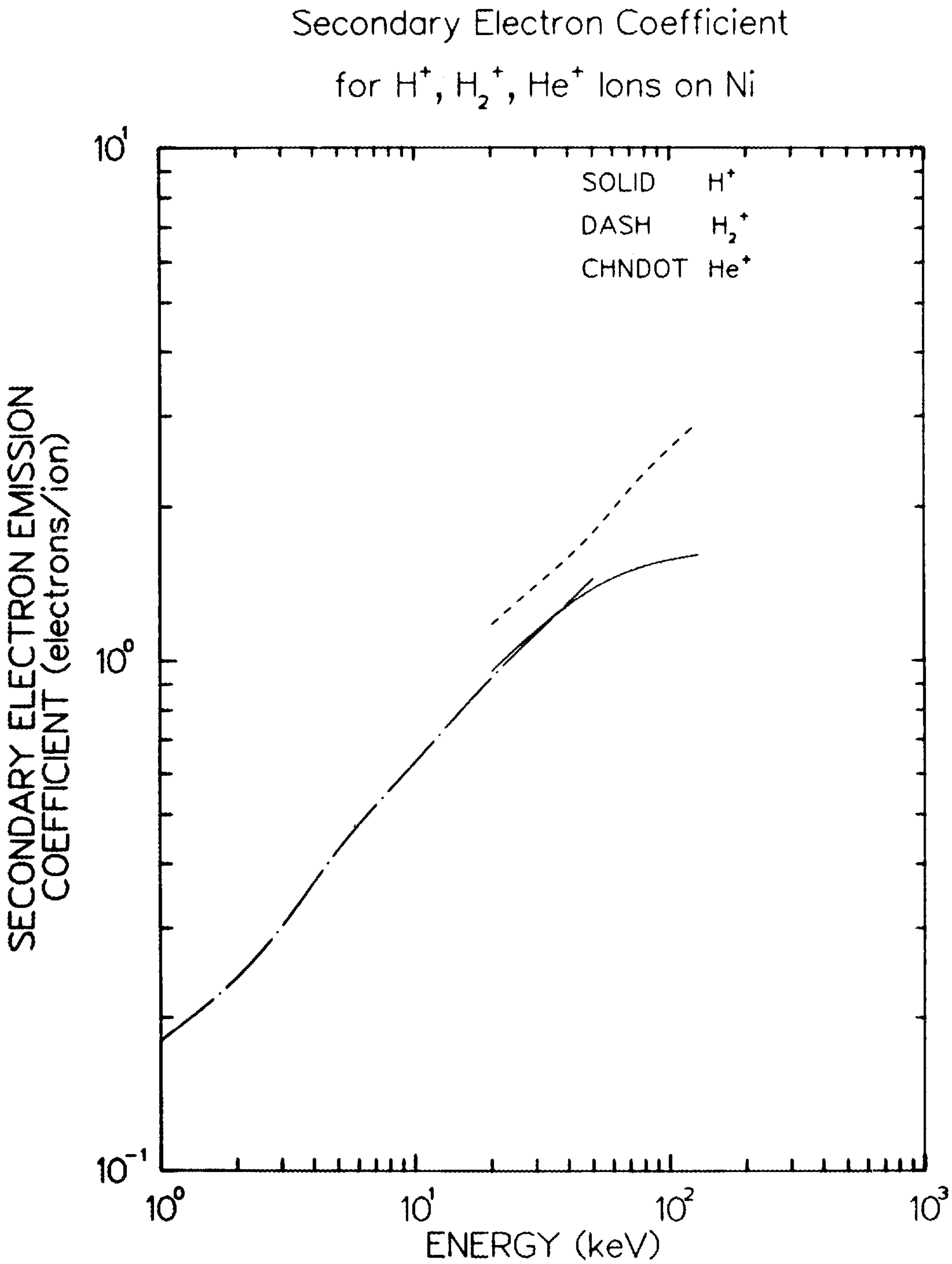
Secondary Electron Coefficient
for H+, H2+, He+ Ions on Ni
SOLID H+
DASH H2+
CHNDOT He+
SECONDARY ELECTRON EMISSION
COEFFICIENT (electrons/ion)
ENERGY (keV)
10^1
10^0
10^-1
10^0
10^1
10^2
10^3

Secondary Electron Emission Coefficients by Impact of Normally Incident H^+, H_2^+, He^+ Ions on Cu

Energy (keV)	Secondary Emission Coefficient Electrons/Ion H^+	H_2^+	He^+
2.0 E 00	3.80 E-01	3.24 E-01	
4.0 E 00	4.80 E-01	5.30 E-01	4.55 E-01
7.0 E 00	6.50 E-01	7.60 E-01	6.20 E-01
1.0 E+01	7.80 E-01	8.90 E-01	8.00 E-01
2.0 E+01	1.08 E 00	1.20 E 00	1.18 E 00
3.0 E+01	1.15 E 00	1.50 E 00	1.44 E 00
4.0 E+01	1.23 E 00	1.70 E 00	1.70 E 00
7.0 E+01	1.32 E 00	2.14 E 00	
1.0 E+02	1.32 E 00	2.60 E 00	
1.5 E+02	1.32 E 00	2.90 E 00	

References: L. N. Large and W. S. Whitlock, Proc. Phys. Soc. (London) 79, 148 (1962). R. A. Baragiola, E. V. Alonso, and A. Olivia-Florio, Phys. Rev. B 19, 121 (1979).

Accuracy: ±10%.

Notes: (1) There is substantial evidence that coefficients for H^+ and D^+ are the same at equal velocities suggesting that this is true also for T^+.

(2) Data for He^+ are by Baragiola *et al.* Data for H^+ and H_2^+ come from both sources cited.

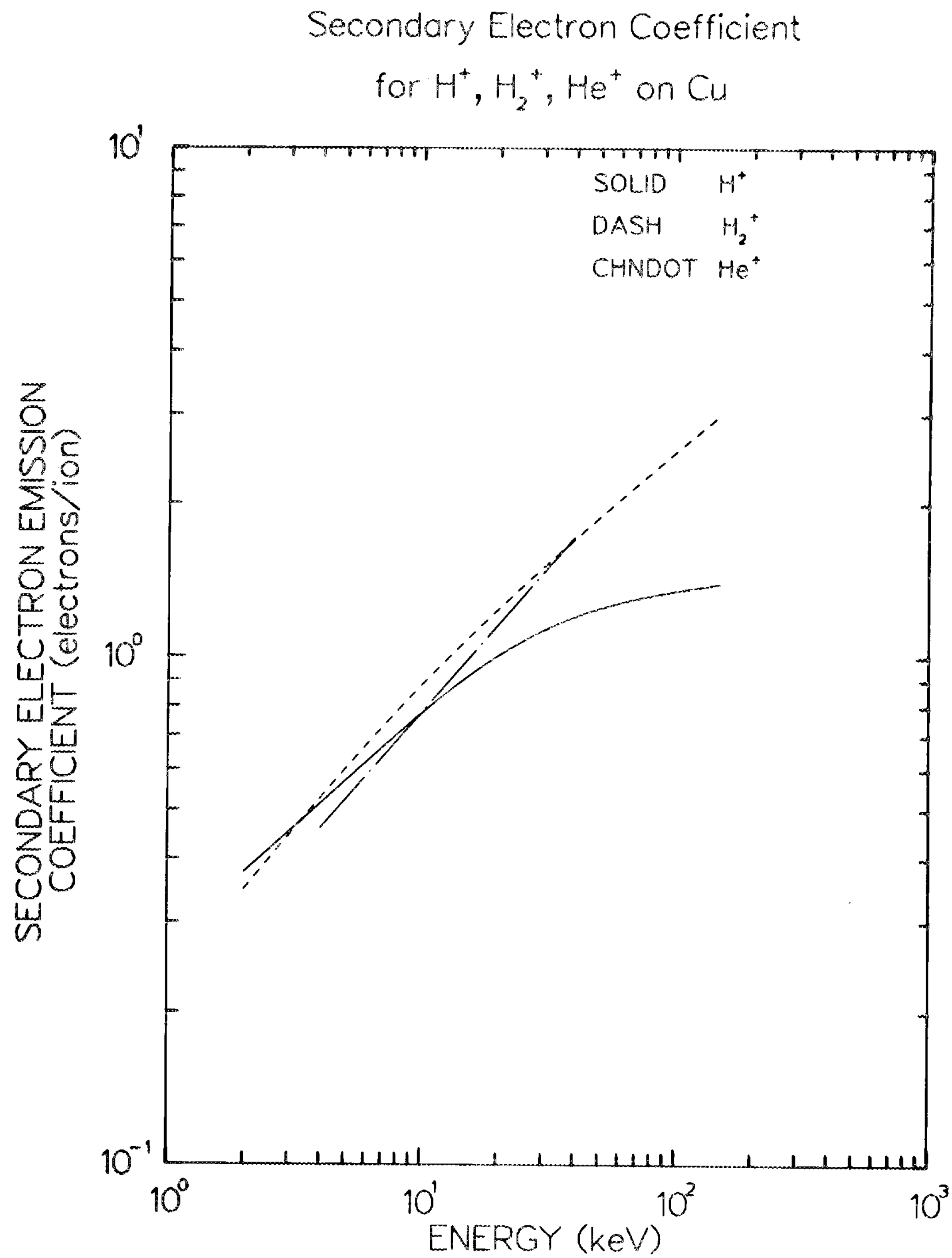

Secondary Electron Coefficient
for H^+, H_2^+, He^+ on Cu
SOLID H^+
DASH H_2^+
CHNDOT He^+
SECONDARY ELECTRON EMISSION COEFFICIENT (electrons/ion)
ENERGY (keV)
10^1
10^0
10^{-1}
10^0
10^1
10^2
10^3

Secondary Electron Emission Coefficients by Impact of Normally Incident H^+, H_2^+, He^+, and O^+ Ions on Mo

Energy (keV)	Secondary Emission Coefficient (electrons/ion)			
	H^+	H_2^+	$^4He^+$	O^+
3.0 E-02		3.3 E-02	2.9 E-01	
5.0 E-02	6.3 E-02	3.4 E-02	2.8 E-01	4.0 E-02
7.0 E-02	7.2 E-02	3.5 E-02	2.7 E-01	4.2 E-02
1.0 E-01	8.3 E-02	3.8 E-02	2.6 E-01	4.3 E-02
2.0 E-01	1.1 E-01	5.2 E-02	2.5 E-01	5.4 E-02
4.0 E-01	1.6 E-01	9.8 E-02	2.5 E-01	8.0 E-02
7.0 E-01	2.1 E-01	1.7 E-01	2.6 E-01	1.3 E-01
1.0 E 00	2.5 E-01	2.4 E-01	2.8 E-01	1.8 E-01
2.0 E 00	3.9 E-01	4.5 E-01	4.0 E-01	3.3 E-01
4.0 E 00	6.2 E-01	7.6 E-01	6.0 E-01	5.7 E-01
7.0 E 00	8.4 E-01	1.05 E 00	8.5 E-01	8.7 E-01
1.0 E+01	9.8 E-01	1.25 E 00	1.0 E 00	1.1 E 00
2.0 E+01	1.2 E 00	1.7 E 00	1.5 E 00	1.7 E 00
4.0 E+01	1.4 E 00	2.4 E 00	2.1 E 00	2.2 E 00
7.0 E+01	1.5 E 00	3.0 E 00		
1.0 E+02	1.5 E 00	3.0 E 00		
1.2 E+02	1.4 E 00	2.8 E 00		

References: U. A. Arifov, R. R. Rakhimov, and O. V. Khozinskii, Bull. Acad. Sci. USSR-Phys. Ser. 26, 1422 (1962); J. Ferrón, E. V. Alonso, R. A. Baragiola, and A. Oliva-Florio, J. Phys. D 14, 1707 (1981); H. D. Hagstrum, Phys. Rev. 104, 672 (1956); L. N. Large and W. S. Whitlock, Proc. Phys. Soc. 79, 148 (1962); W.H.P. Losch, Phys. Stat. Sol. (A) 2, 123 (1970); P. Mahadevan, G. D. Magnuson, J. K. Layton, and C. E. Carlston, Phys. Rev. 140, A1407 (1965); M. Perdix, S. Paletto, R. Goutte, and C. Guilland, Brit. J. Appl. Phys. 2, 441 (1969); D. W. Vance, Phys. Rev. 169, 252 (1968).

Accuracy: ±10%.

Notes: (1) There is substantial evidence that coefficients for H^+ and D^+ are the same at equal velocities suggesting that this is true for T^+.

(2) Data for H^+ taken from Ferrón et al., Large and Whitlock, Losch, Mahadevan et al., and Perdix et al.; data for H_2^+ from Ferrón et al., Large and Whitlock, Losch, Mahadevan et al., and Vance; data for He^+ from Arifov et al., Ferrón et al., Hagstrum, and Vance; and for O^+ Ferrón et al., Mahadevan et al., and Perdix et al.

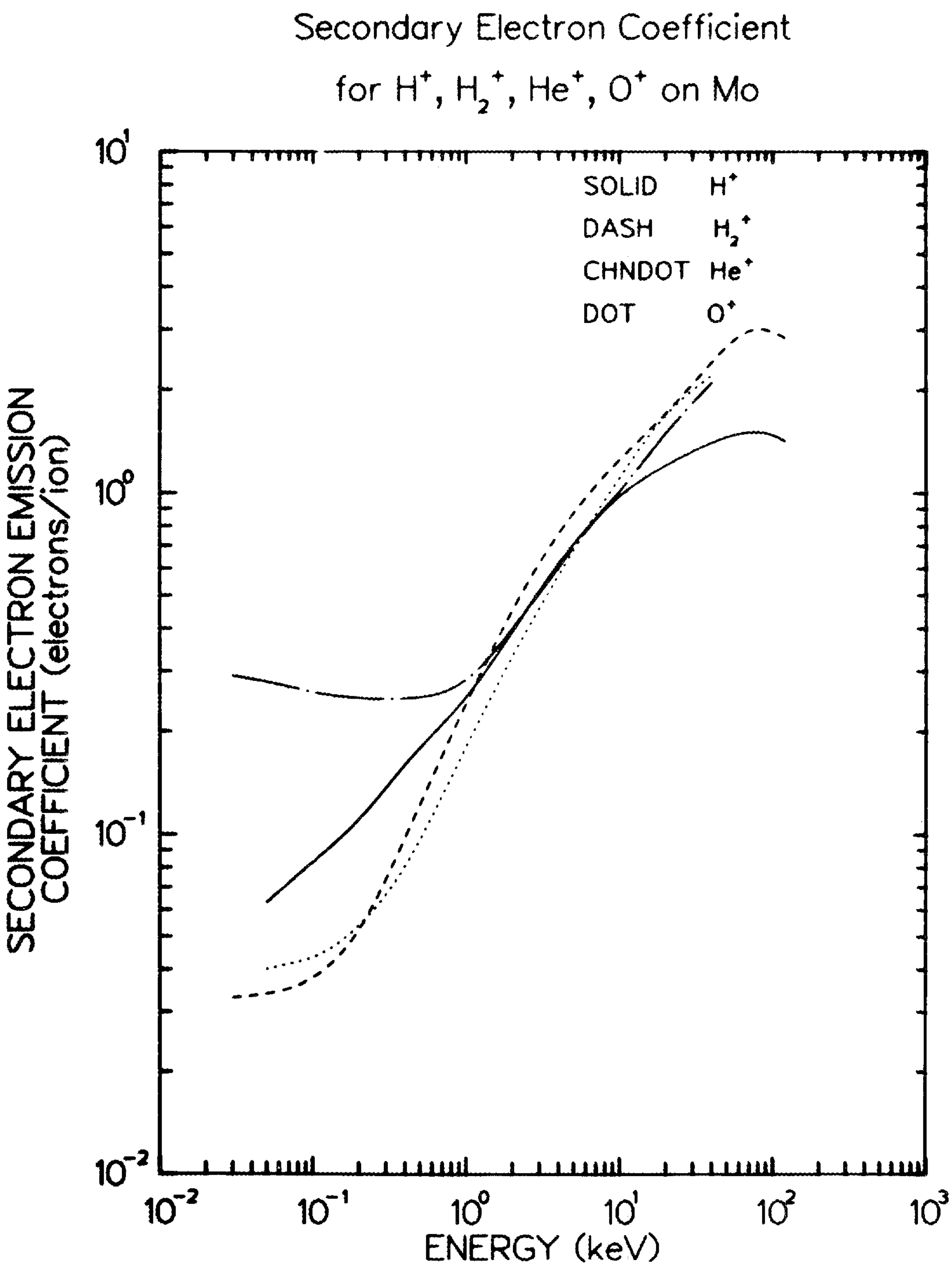
Secondary Electron Coefficient
for H⁺, H₂⁺, He⁺, O⁺ on Mo
SOLID H⁺
DASH H₂⁺
CHNDOT He⁺
DOT O⁺
SECONDARY ELECTRON EMISSION COEFFICIENT (electrons/ion)
ENERGY (keV)
10¹
10⁰
10⁻¹
10⁻²
10⁻²
10⁻¹
10⁰
10¹
10²
10³

The Dependence of the Secondary Electron Emission Coefficients on the Excited States of O_2^+ Bombarding a Clean Mo Surface at Normal Incidence

Energy (eV)	γ_g	γ_i	γ^*
25	0.7 E-02	1.6 E-02	3.2 E-02
50	0.8 E-02	1.7 E-02	3.4 E-02
100	1.1 E-02	2.1 E-02	3.7 E-02
150	1.5 E-02	2.5 E-02	4.3 E-02
200	2.0 E-02	3.1 E-02	4.8 E-02
300	3.0 E-02	4.2 E-02	6.1 E-02
400	4.1 E-02	5.3 E-02	7.3 E-02

References: D. W. Vance, Phys. Rev. 169, 263 (1968).

Accuracy: Unknown.

Notes: Curve labelled γ_g is for incident O_2^+ in the ground electronic state; γ_i is for O_2^+ in a mixture of electronic states; and γ^* is the calculated coefficient for O_2^+ in the $a^4\Pi_u$ state.

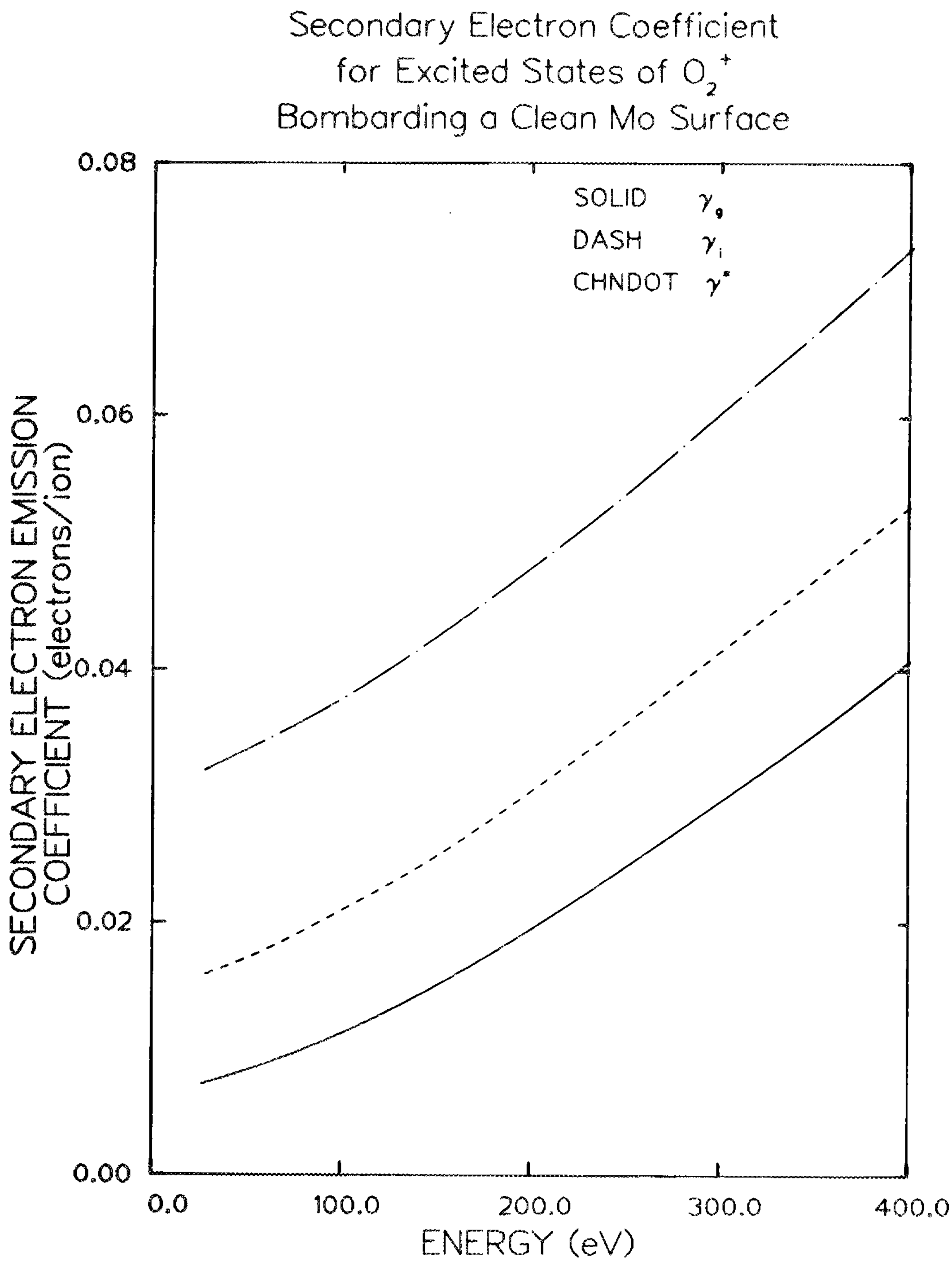
Secondary Electron Coefficient
for Excited States of O_2^+
Bombarding a Clean Mo Surface
SOLID γ_g
DASH γ_i
CHNDOT γ^*
SECONDARY ELECTRON EMISSION
COEFFICIENT (electrons/ion)
0.08
0.06
0.04
0.02
0.00
0.0
100.0
200.0
300.0
400.0
ENERGY (eV)

Typical Energy Distributions of Secondary Electron

Emission Coefficients by He^+ on a Clean Mo Surface at Normal Incidence

Energy (eV)	2 keV	5 keV	10 keV	15 keV
0.2	1.0 E-01	7.0 E-02	6.0 E-02	1.0 E-01
0.4	2.6 E-01	2.0 E-01	2.0 E-01	2.6 E-01
0.6	4.6 E-01	4.0 E-01	3.6 E-01	4.1 E-01
0.8	6.0 E-01	5.5 E-01	5.5 E-01	5.7 E-01
1.0	7.2 E-01	6.8 E-01	6.8 E-01	7.0 E-01
1.2	8.3 E-01	8.0 E-01	8.0 E-01	8.2 E-01
1.4	9.3 E-01	9.9 E-01	9.1 E-01	9.2 E-01
1.6	1.0 E 00	1.0 E 00	9.9 E-01	9.9 E-01
1.8	9.9 E-01	1.0 E 00	1.0 E 00	1.0 E 00
2.0	9.6 E-01	9.9 E-01	9.9 E-01	9.9 E-01
2.5	8.2 E-01	9.1 E-01	9.0 E-01	9.3 E-01
3.0	7.1 E-01	8.1 E-01	8.1 E-01	8.3 E-01
4.0	5.0 E-01	6.3 E-01	6.6 E-01	6.7 E-01
6.0	2.5 E-01	4.2 E-01	4.6 E-01	5.0 E-01
8.0	1.3 E-01	2.7 E-01	3.2 E-01	3.6 E-01
10.0	7.0 E-02	1.8 E-01	2.1 E-01	2.6 E-01
12.0		1.1 E-01	1.5 E-01	1.8 E-01
14.0		7.0 E-02	1.0 E-01	1.3 E-01
16.0		5.0 E-02	8.0 E-02	1.0 E-01
18.0		3.0 E-02	5.0 E-02	7.0 E-02
20.0		2.0 E-02	4.0 E-02	6.0 E-02
22.0		1.0 E-02	3.0 E-02	4.0 E-02

References: G. Wehner, Z. Phys. 193, 439 (1966).

Accuracy: ±10%.

Notes: (1) All distributions normalized to one at the maximum emission.
(2) For metallic surfaces the maximum energy of the electrons ejected from the surface is approximately 25–30 eV.

Typical Energy Distributions of Secondary Emission by Atomic Particles Impact on Metal Surfaces (He^+ on Mo)

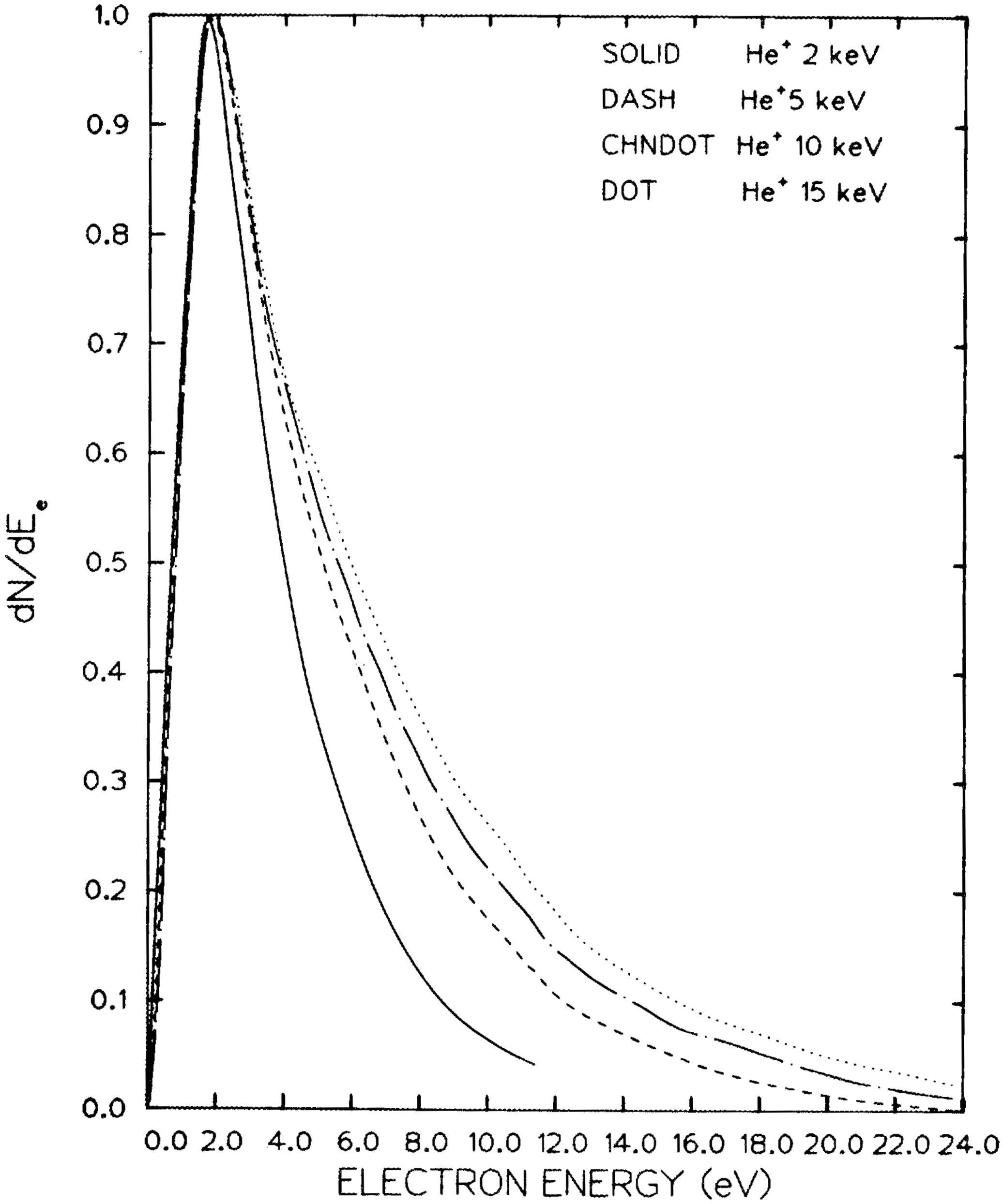

Energy Distributions of Secondary Electrons Ejected by 40, 200, and 1000 eV He^+ Ions Incident on a Clean W Surface

Energy (keV)	Energy Distribution (e/ion/eV) 40 eV	200 eV	1000 eV
0	4.4 E-03	8.0 E-03	7.0 E-03
0.25	6.3 E-03	1.0 E-02	1.9 E-02
0.5	8.0 E-03	1.2 E-02	2.4 E-02
0.75	9.5 E-03	1.3 E-02	2.4 E-02
1.0	1.6 E-02	1.4 E-02	2.5 E-02
1.5	1.3 E-02	1.6 E-02	2.5 E-02
2.0	1.5 E-02	1.8 E-02	2.5 E-02
3.0	1.9 E-02	2.0 E-02	2.3 E-02
4.0	2.3 E-02	2.1 E-02	2.2 E-02
5.0	2.4 E-02	2.3 E-02	2.0 E-02
6.0	2.5 E-02	2.3 E-02	1.9 E-02
8.0	2.5 E-02	2.1 E-02	1.6 E-02
10.0	2.3 E-02	1.8 E-02	1.3 E-02
12.0	1.5 E-02	1.3 E-02	1.0 E-02
14.0	3.4 E-03	5.4 E-03	6.8 E-03
16.0	3.7 E-04	1.4 E-03	3.2 E-03
18.0	2.0 E-04	5.6 E-04	1.2 E-03
20.0		2.3 E-04	6.0 E-04

References: H. D. Hagstrum, Phys. Rev. 96, 325 (1954).

Accuracy: ±10%.

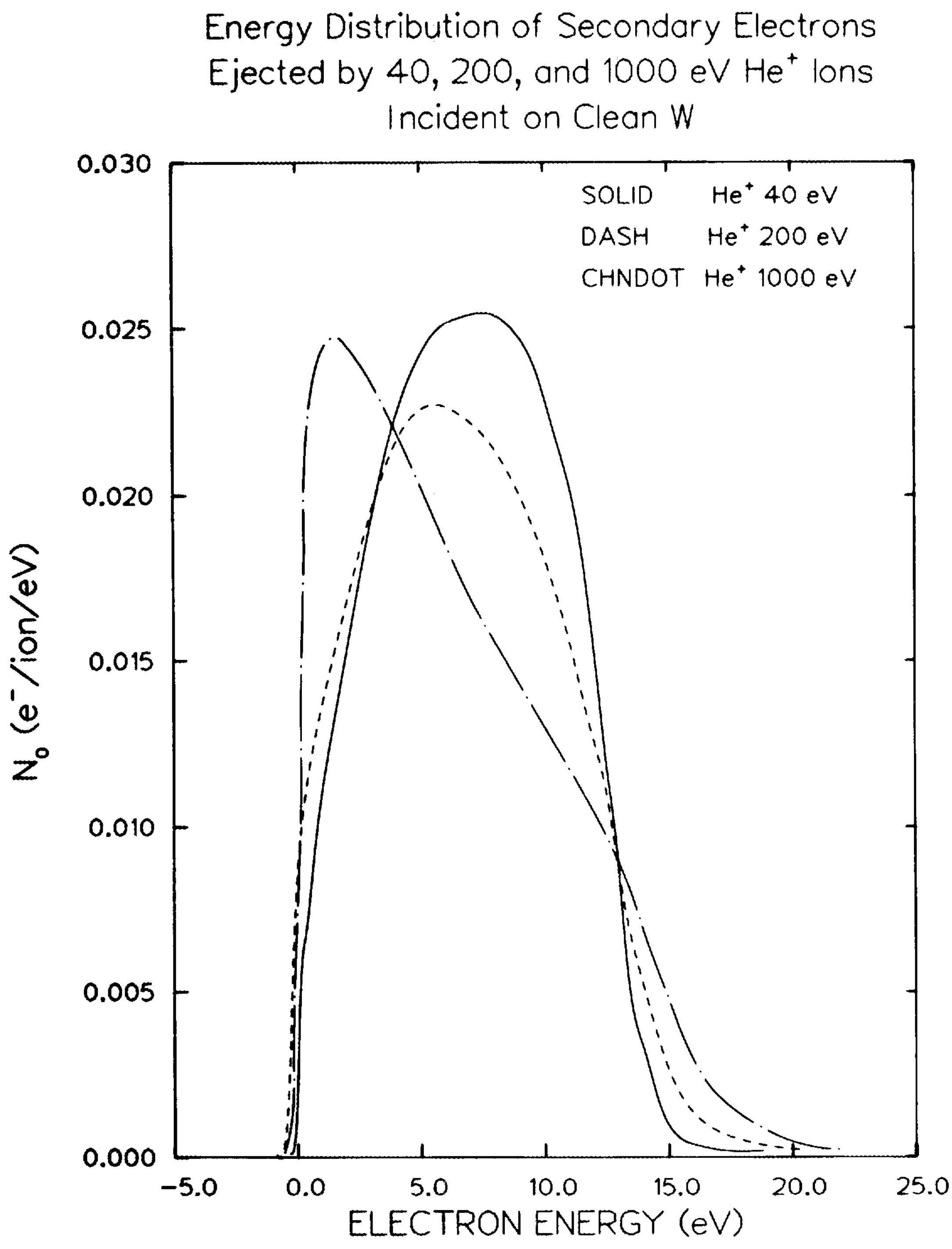
Energy Distribution of Secondary Electrons
Ejected by 40, 200, and 1000 eV He⁺ Ions
Incident on Clean W
SOLID He⁺ 40 eV
DASH He⁺ 200 eV
CHNDOT He⁺ 1000 eV
N₀ (e⁻/ion/eV)
0.030
0.025
0.020
0.015
0.010
0.005
0.000
-5.0
0.0
5.0
10.0
15.0
20.0
25.0
ELECTRON ENERGY (eV)

Secondary Electron Emission Coefficient for 100 keV H^+, H_2^+, and H_3^+ as a Function of the Atomic Number of a Clean Target

Z	H^+	H_2^+	H_3^+
20	1.25	2.24	2.75
30	1.50	2.61	3.35
40	1.72	2.96	3.84
50	1.90	3.36	4.17
60	1.98	3.41	4.28
70	2.05	3.47	4.33
80	2.08	3.48	4.40

References: U. A. Arifov and R. R. Rakhimov, Bull. Acad. Sci. U.S.S.R., Phys. Ser. 24, 266 (1960) [Mo, Ta, and W]; G. D. Magnuson and C. E. Carlston, Phys. Rev. 129, 2403 (1963) [Al, Ni, Cu, Zr, Mo, and Ti]; L. N. Large and W. S. Whitlock, Proc. Phys. Soc. (London) 79, 148 (1962) [Ti, Ni, Cu, Zr, Mo, Ag, Au, and Pt].

Accuracy: ±25%

Secondary Electron Coefficient
for 100 keV H^+, H_2^+, and H_3^+ as a Function of
the Atomic Number of a Clean Target

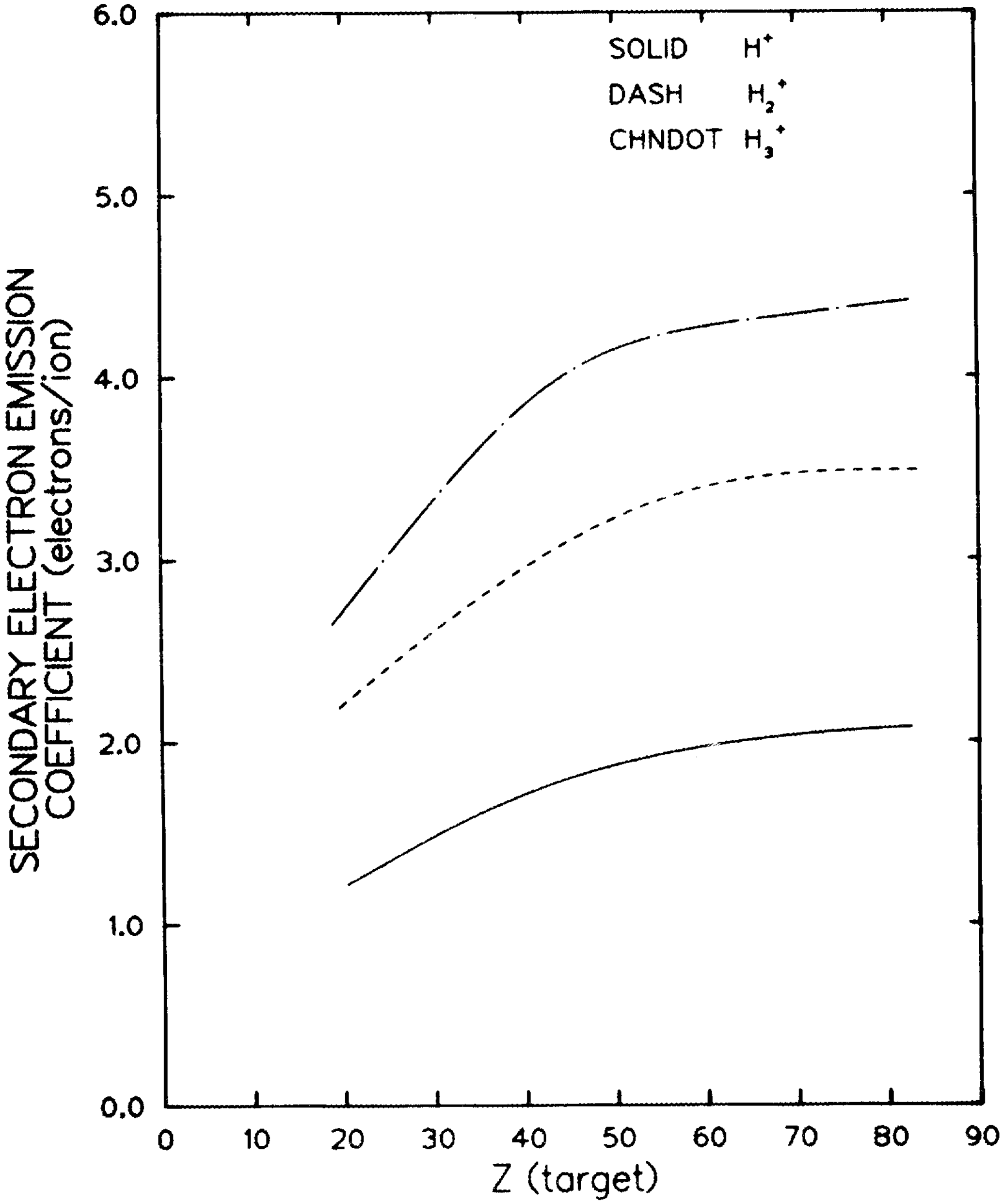

Secondary Electron Emission Coefficients as a Function of the Angle between a 120 keV Proton Beam and a Clean Ni Target

Angle (deg.)	Secondary Emission Coefficient (electrons/ion)
21	4.5
30	3.1
40	2.4
50	2.0
60	1.8
70	1.7
80	1.6
90	1.6

Reference: J. S. Allen, Phys. Rev. 55, 336 (1939).

Accuracy: Unknown

Notes: (1) For all projectile-target combinations the secondary emission coefficient decreases as the angle between projectile and target increases.
(2) Allen's data are normalized at 120 keV to the data given by L. N. Large and W. S. Whitlock, Proc. Phys. Soc. 79, 148 (1962).

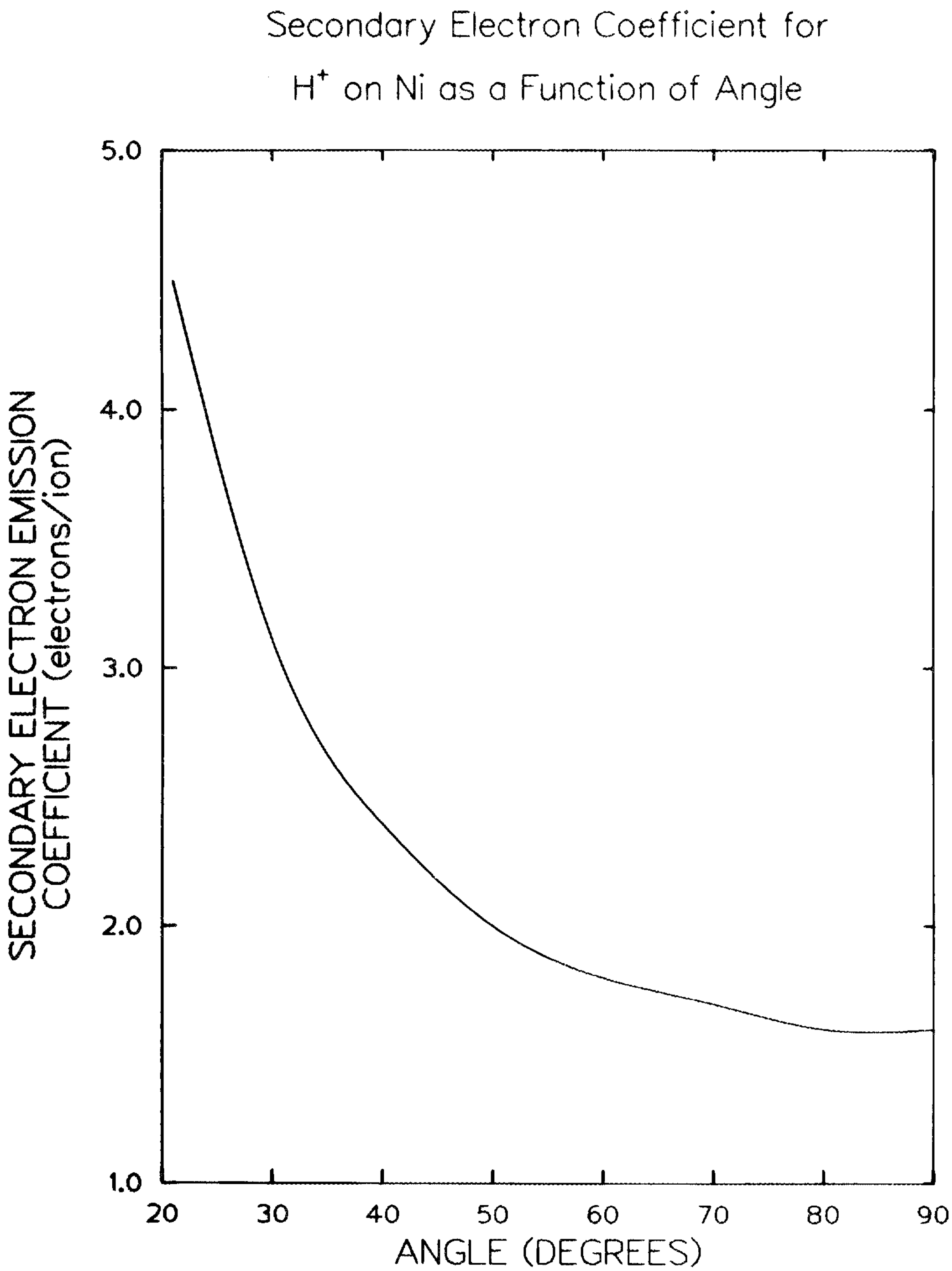
Secondary Electron Coefficient for
H+ on Ni as a Function of Angle
5.0
4.0
3.0
2.0
1.0
20
30
40
50
60
70
80
90
ANGLE (DEGREES)
SECONDARY ELECTRON EMISSION
COEFFICIENT (electrons/ion)

Time to Build Up a N_2 Monolayer on a Previously

Clean Surface at Room Temperature

Pressure (mm Hg)	Time (sec)
1.0 E-12	2.0 E 06
1.0 E-11	2.6 E 05
1.0 E-10	3.5 E 04
1.0 E-09	5.0 E 03
1.0 E-08	6.7 E 02
1.0 E-07	9.3 E 01
1.0 E-06	1.3 E 01
1.0 E-05	1.6 E 00
6.0 E-05	3.8 E-01

Reference: K. H. Krebs, Fortschr. Phys. 16, 419 (1968).

Accuracy: Unknown.

Notes: (1) Values are computed.
(2) The thickness of a monolayer of N_2 is approximately 4 Å which is comparable to the penetration depth of atomic particles in the lower keV region.
(3) Note that at a pressure of 10^{-9} mm Hg the build up time of a monolayer is ~30 minutes.

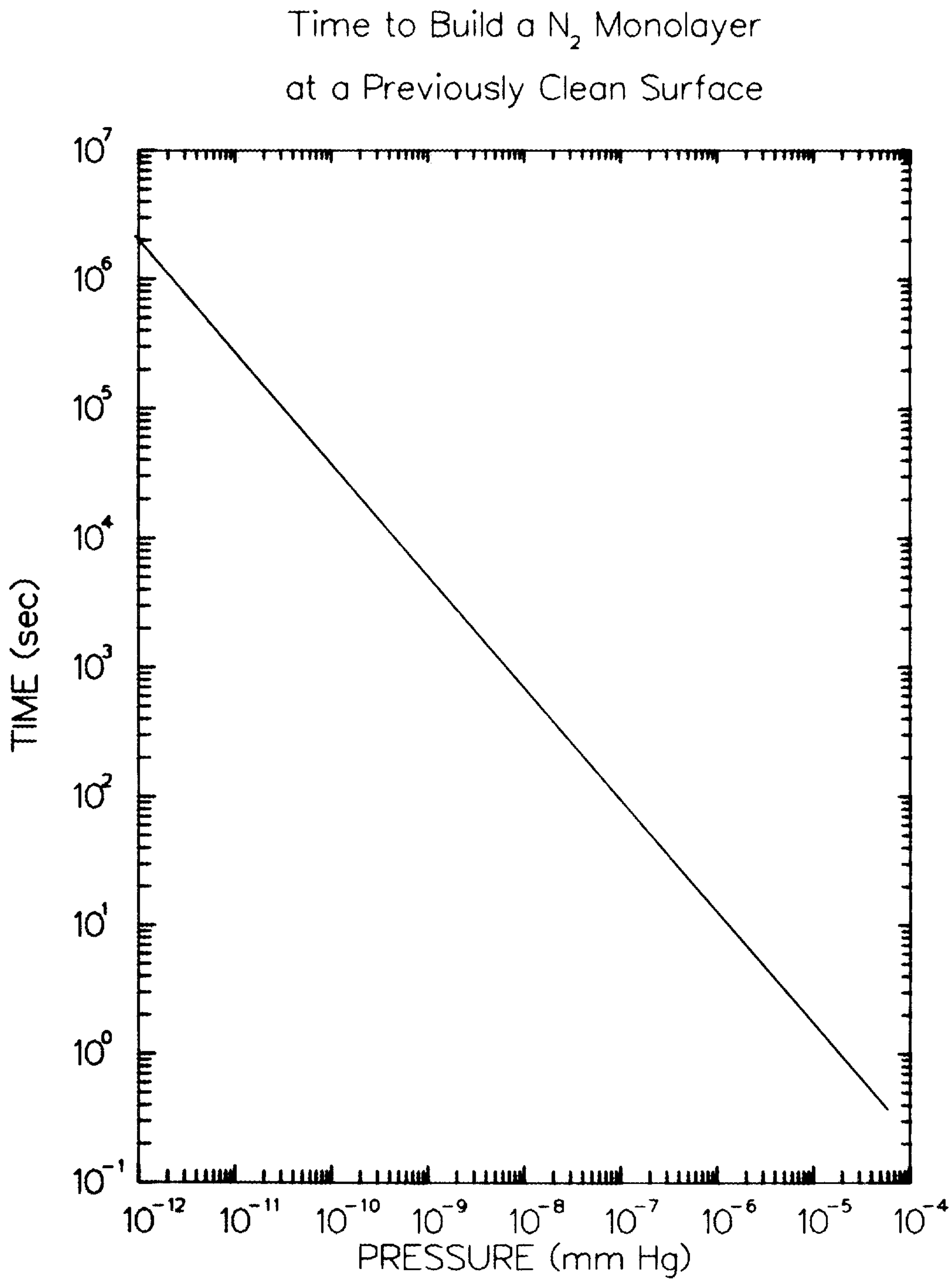

Time to Build a N2 Monolayer
at a Previously Clean Surface
TIME (sec)
PRESSURE (mm Hg)
10^7
10^6
10^5
10^4
10^3
10^2
10^1
10^0
10^-1
10^-12
10^-11
10^-10
10^-9
10^-8
10^-7
10^-6
10^-5
10^-4

Changes in the Secondary Electron Emission When

a Titanium Surface is Completed Outgassed.

H^+ and H_2^+ Normally Incident on Ti

Energy (keV)	Gassy		Degassed	
	H^+	H_2^+	H^+	H_2^+
30	3.62	5.03	0.94	1.32
40	3.72	5.28	1.00	1.58
60	3.90	5.70	1.08	1.86
80	4.01	6.12	1.12	2.13
100	3.98	6.48	1.12	2.30
120	3.86	6.66	1.11	2.41
130	3.75	6.78	1.10	2.48

Reference: L. N. Large, Proc. Phys. Soc. (London) 81, 175 (1963).

Accuracy: Unknown.

Notes: (1) The upper two curves were obtained from a Ti surface after exposure to air at atmospheric pressure for six months.
(2) The two lower curves were obtained after degassing in a background pressure of 10^{-8} mm Hg. The Ti target was cleaned by flashing to 1300°C.

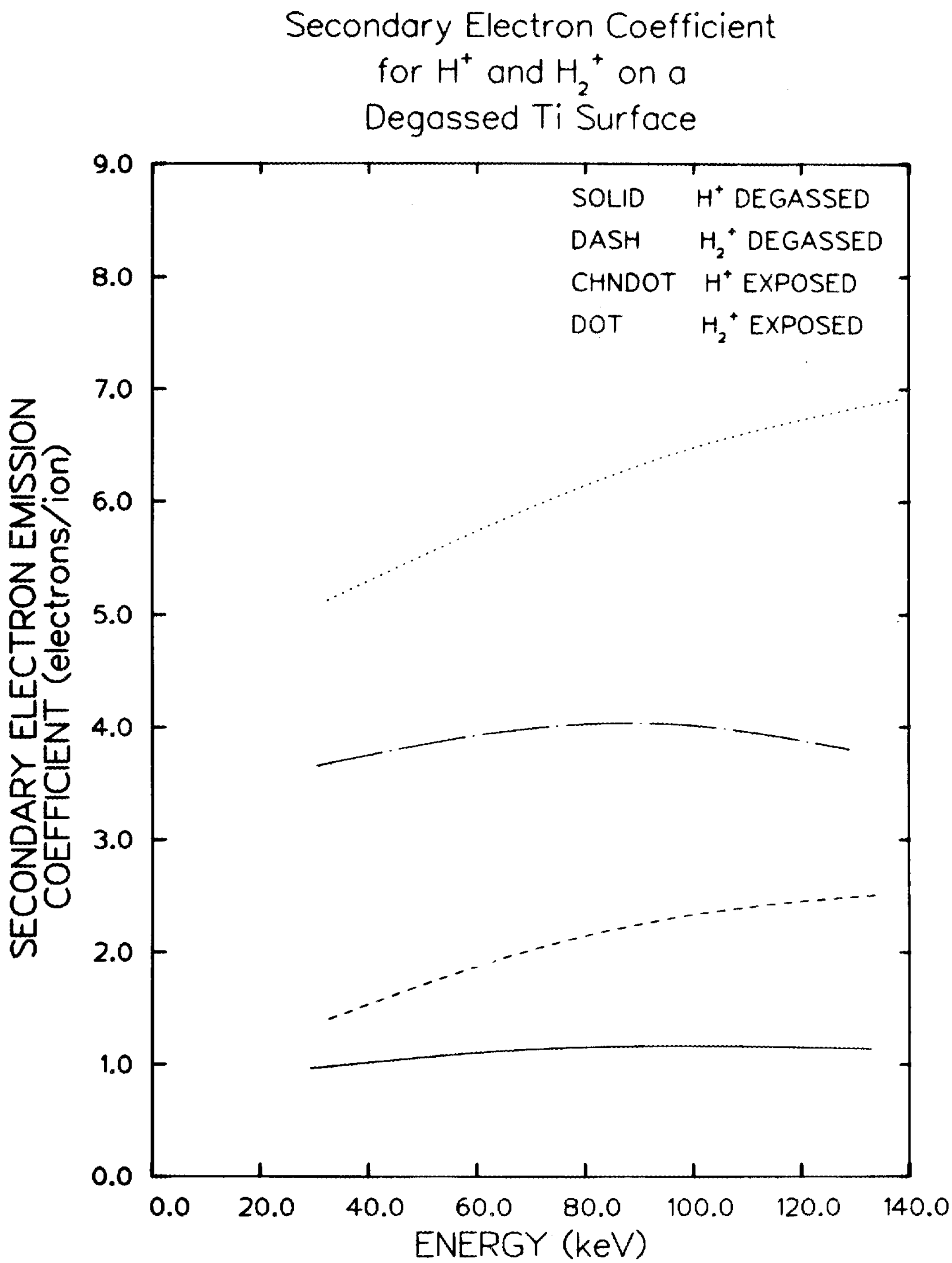

Secondary Electron Coefficient for H+ and H2+ on a Degassed Ti Surface
SOLID H+ DEGASSED
DASH H2+ DEGASSED
CHNDOT H+ EXPOSED
DOT H2+ EXPOSED
SECONDARY ELECTRON EMISSION COEFFICIENT (electrons/ion)
ENERGY (keV)
0.0
1.0
2.0
3.0
4.0
5.0
6.0
7.0
8.0
9.0
0.0
20.0
40.0
60.0
80.0
100.0
120.0
140.0

The Effect of the Secondary Electron Emission Coefficient on the Degassing Technique. H^+ Normally Incident on Mo

Energy (keV)	Chemically Etched	Baked at 400°C	Flashed to 1750°C
15			1.02 E 00
20			1.06 E 00
35	4.55 E 00	2.38 E 00	1.22 E 00
40	4.59 E 00	2.44 E 00	1.28 E 00
60	4.74 E 00	2.69 E 00	1.42 E 00
80	4.80 E 00	2.82 E 00	1.53 E 00
100	4.78 E 00	2.81 E 00	1.56 E 00
120	4.72 E 00	2.71 E 00	1.51 E 00
125	4.69 E 00	2.67 E 00	1.50 E 00

Reference: L. N. Large and W. S. Whitlock, Proc. Phys. Soc. (London) 79, 148 (1962).

Accuracy: Unknown.

Notes: Targets were heated and flashed in a vacuum of approximately 10^{-8} mm Hg.

Secondary Electron Coefficient for H^+ on Mo with Different Degassing Techniques

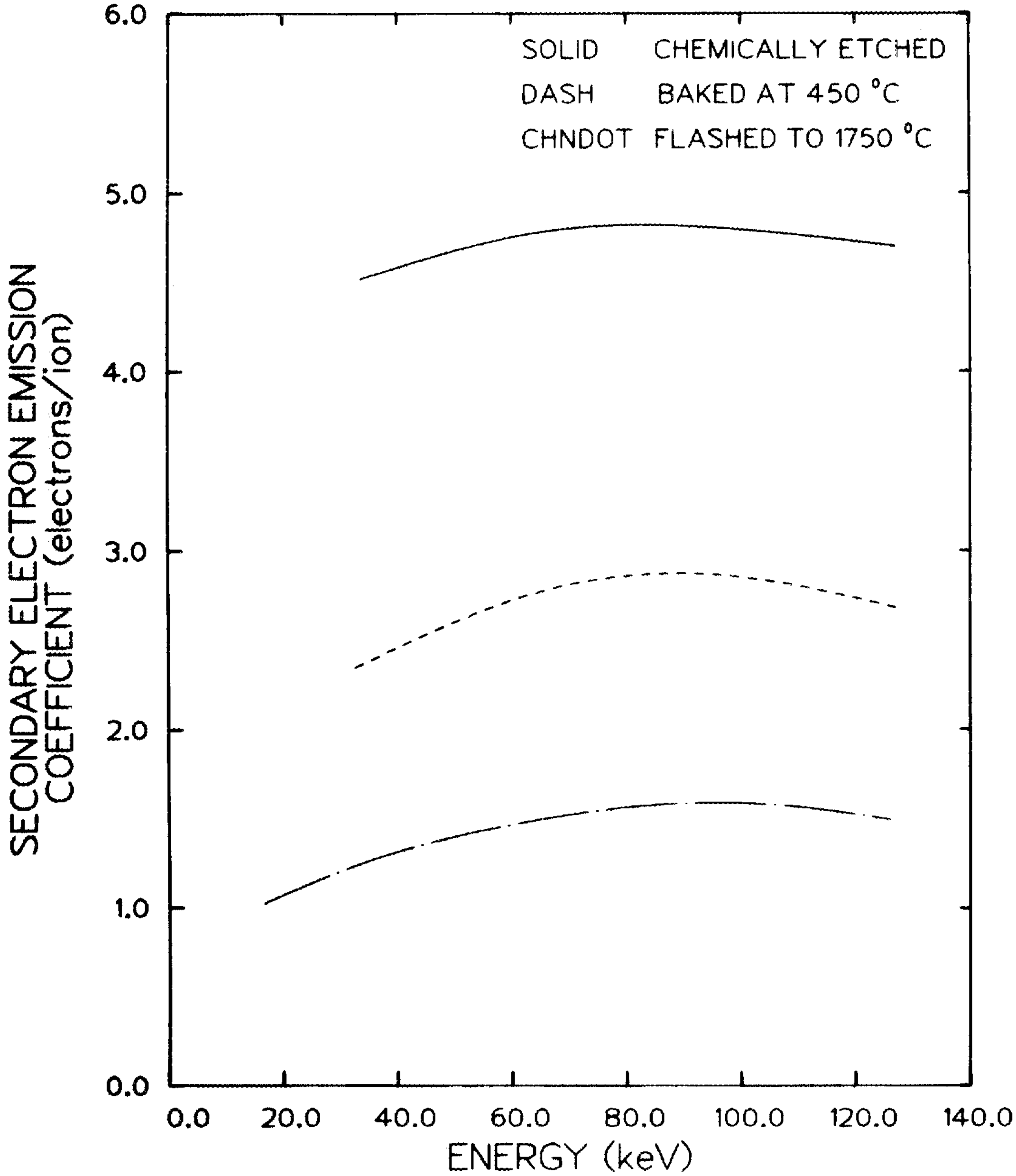

Secondary Electron Emission Coefficient for C^{n+} ($n^+ = 4-6$)

on Gas Covered Cu at High Energies

Energy (keV)	C^{4+}	C^{5+}	C^{6+}
50	5.35		
60	5.50	6.00	
70	5.65	6.15	7.10
100	6.00	6.50	7.52
200	7.08	7.75	8.90
300	7.98	8.80	9.92
385	8.70	9.58	10.55
400		9.70	10.70
470		10.20	11.20
500			11.45
600			12.10

Reference: R. Decoste and B. H. Ripin, J. Appl. Phys. 50, 1503 (1979).

Accuracy: ±10%.

Note: (1) Since the ion kinetic energy is much greater than the multicharged ion potential energy, the kinetic emission dominates the potential emission.

Secondary Electron Coefficient for C^{n+} Ions (n=2–6) on Gassy Cu at High Energies

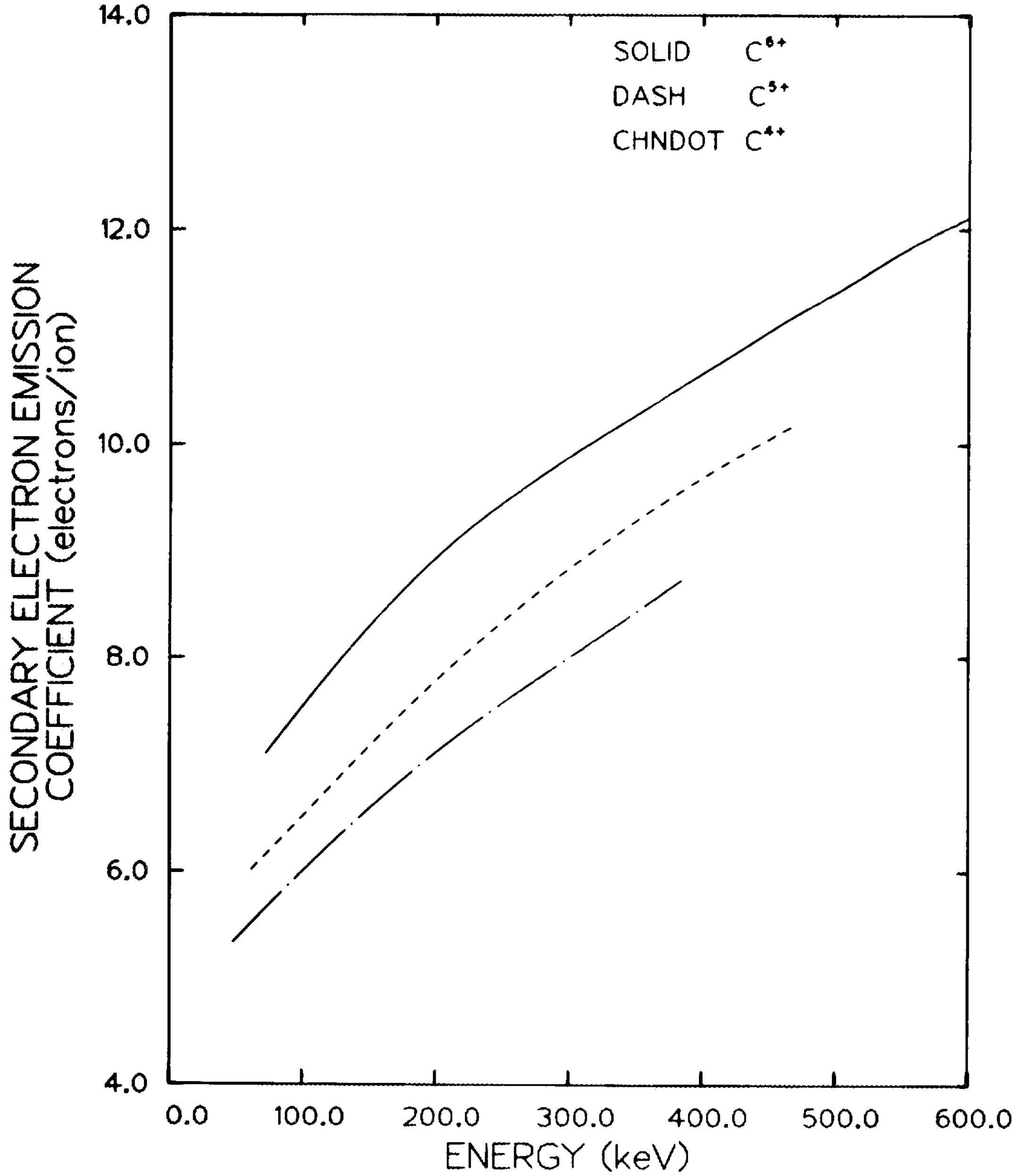

Secondary Electron Emission Coefficients by Impact of Al Multicharged Ions on Gas Covered Au at Low Impact Energies

n	Secondary Emission Coefficient (electrons/ion)
1	0.65
2	1.35
3	2.52
4	4.22
5	6.35
6	8.60
7	11.00
8	13.50
9	16.00

Reference: G. L. Cano, J. Appl. Phys. 44, 5293 (1973).

Accuracy: ±10% (estimated).

Notes: (1) n is the ion charge state.
(2) Data were obtained over the incident 1-6 keV energy range. In this energy region the coefficient is practically independent of the energy. The observed increase in the coefficient with n results from potential emission.

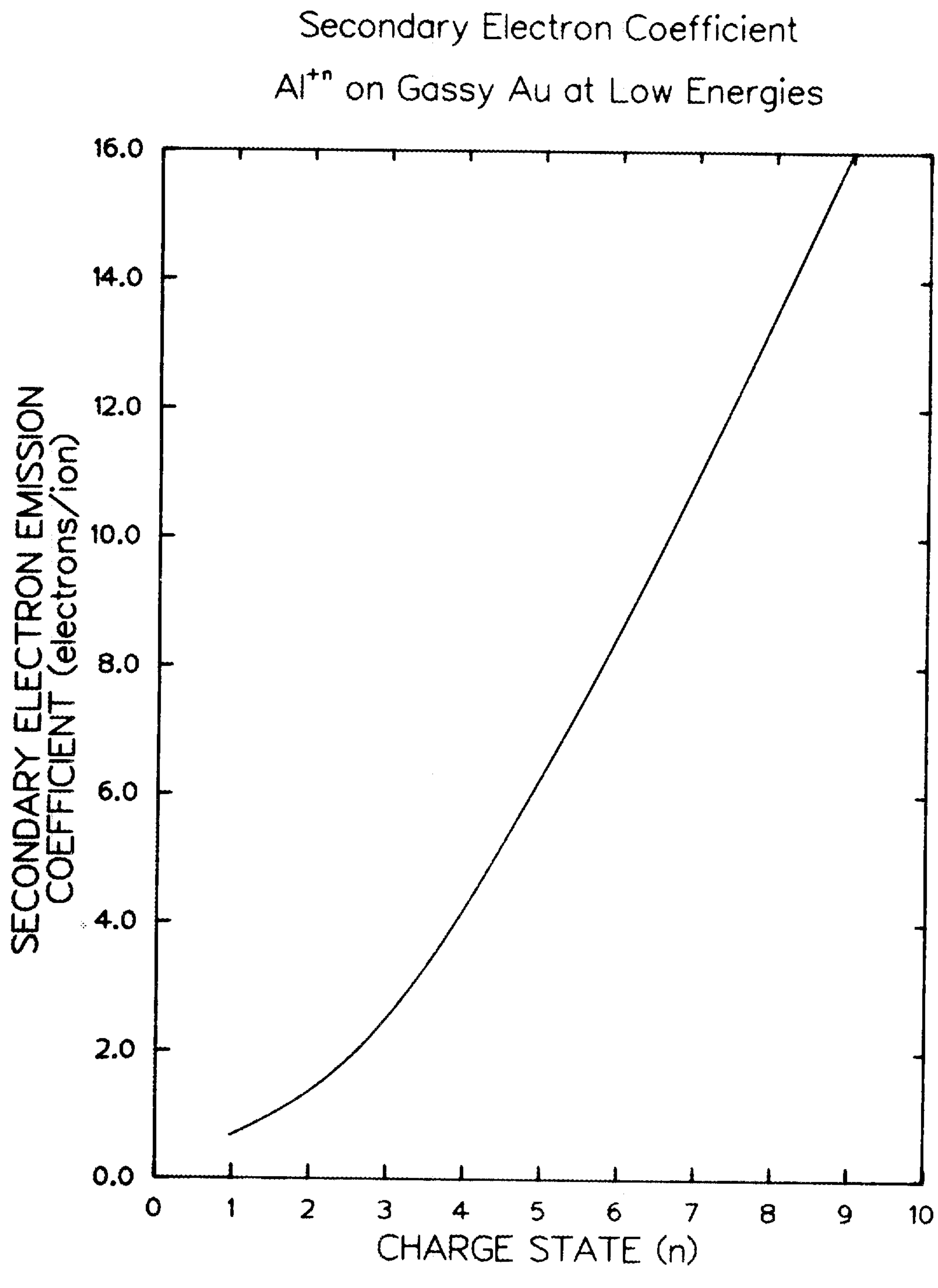
Secondary Electron Coefficient
Al+n on Gassy Au at Low Energies
SECONDARY ELECTRON EMISSION COEFFICIENT (electrons/ion)
0.0
2.0
4.0
6.0
8.0
10.0
12.0
14.0
16.0
0
1
2
3
4
5
6
7
8
9
10
CHARGE STATE (n)

Ratios of the Number of Secondary Electrons from H^o to that of H^+ Impact on Gas Covered and Clean Surfaces at Normal Incidence

Energy (keV)	H^o/H^+ Gassy	H^o/H^+ Clean Ni	H^o/H^+ Clean Al	H^o/H^+ Clean Ag
3.0 E-02	1.18			
6.0 E-02	1.18			
1.0 E-01	1.18			
2.0 E-01	1.18			
4.0 E-01	1.18			
7.0 E-01	1.18			
1.0 E+00	1.18			
2.0 E+00	1.18			
4.0 E+00	1.18			
7.0 E+00	1.18			
1.0 E+01	1.18	0.37	0.29	0.24
2.0 E+01	1.18	0.45	0.38	0.34
4.0 E+01	1.18	0.60	0.55	0.54
7.0 E+01	1.19			
1.0 E+02	1.21			
2.0 E+02	1.33			
4.0 E+02	1.47			
7.0 E+02	1.55			
1.0 E+03	1.65			

References: Gassy - C. F. Barnett and J. A. Ray, Rev. Sci. Instrum. 43, 218 (1972) [Cu]; C. F. Barnett and H. K. Reynolds, Phys. Rev. 109, 355 (1958) [brass]; R. Dagnac, D. Blanc, and D. Molina, J. Phys. B 3, 1239 (1970) [CuO-Be]; R. L. Fitzwilson and E. W. Thomas, Rev. Sci. Instrum. 42, 1864 (1971) [Ni]; M. W. Geis, K. A. Smith, and R. D. Rundel, J. Phys. E, 8, 1011 (1975) [Ag]; A. I. Kislyakov, J. Stöckel and K. Jakubka, Sov. Phys.-Tech. Phys. 20, 986 (1976) [Al, Cu, Mo]; F. W. Meyer, unpublished [SS]; J. A. Ray, C. F. Barnett, and B. Van Zyl, J. Appl. Phys. 50, 6516 (1979) [Cu]; L. E. Sharp, L. S. Holmes, P. E. Stott, and D. A. Aldcroft, Rev. Sci. Instrum. 45, 378 (1974) [Al]; K. A. Smith, M. D. Duncan, M. W. Geis, and R. D. Rundel, J. Geophys. Res. 81, 2231 (1976) [Ag]; P. M. Stier, C. F. Barnett, and G. E. Evans, Phys. Rev. 96, 973 (1954) [Ni].

Clean-Ni - Al, and Ag: K. Morita, H. Akimune, and T. Suita, Jap. J. Appl. Phys. 5, 511 (1966).

Accuracy: ±20%.

Notes: For a "gassy" surface the ratio of the secondary electron emission of H^o to that of H^+ is to within ±20% for all those metallic surfaces indicated in brackets in the reference list. The interpretation of electron emission from a gassy surface is that the gas coverage dominates the emission process.

Ratios of the Number of Secondary Electrons from H^0 to that of H^+ Impact on Gas Covered and Clean Surfaces at Normal Incidence

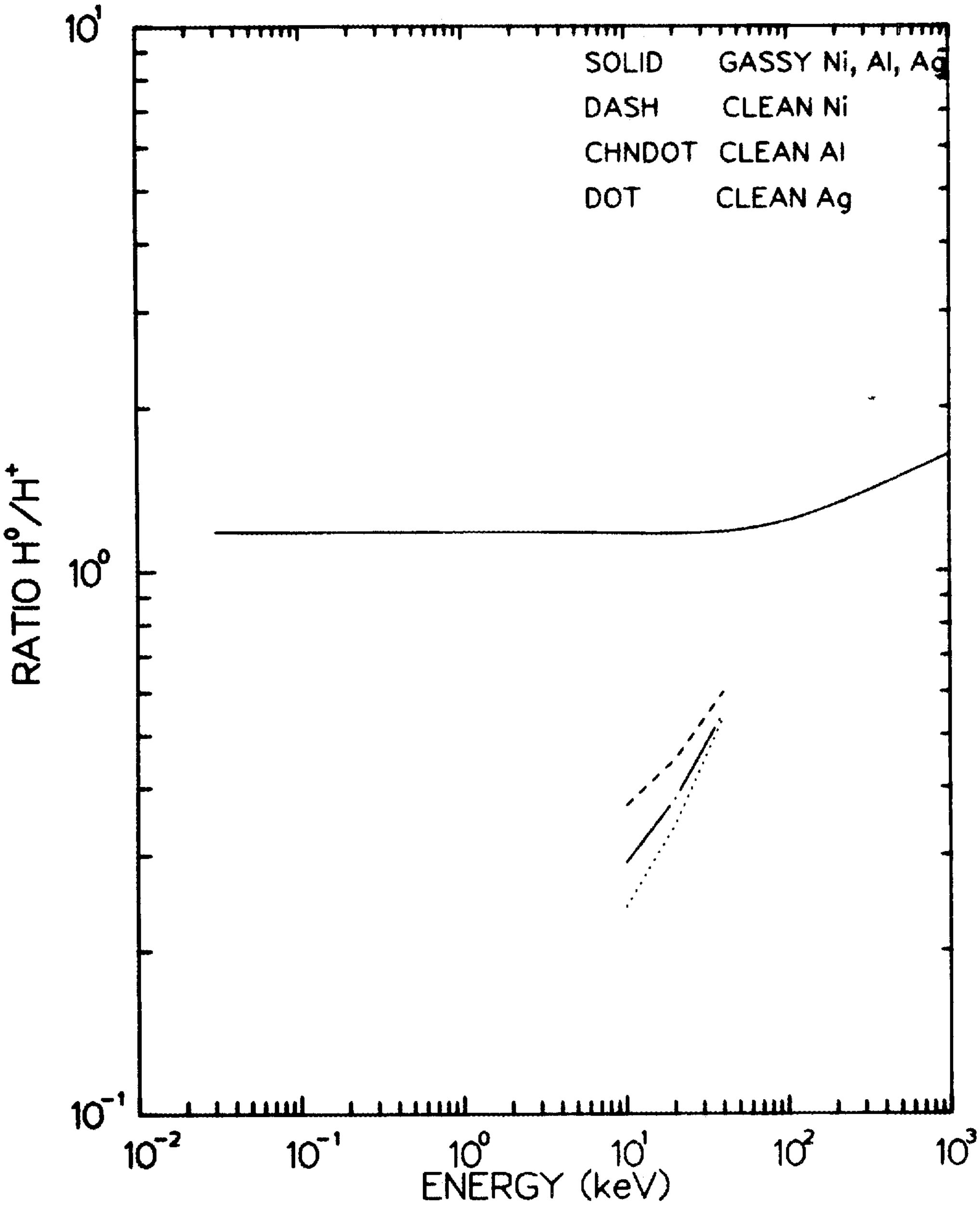

Ratios of the Number of Secondary Electrons from Normally Incident H^- and O^- to that of H^+ and O^+ on Gas Covered and Clean Metallic Surfaces

Energy (keV)	Ratio H^-/H^+ (gassy)	Ratio H^-/H^+ (clean)	Ratio O^-/O^+ (gassy)	Ratio O^-/O^+ (clean)
4.0 E-02	7.3			
5.0 E-02	6.3			
7.0 E-02	5.0			
1.0 E-01	4.0			
2.0 E-01	2.8	0.06		
4.0 E-01	2.2	0.20		0.10
5.0 E-01	2.08	0.26	1.55	0.14
7.0 E-01	1.9	0.39	1.40	0.20
1.0 E+00	1.8	0.55	1.28	0.32
2.0 E+00	1.7	0.84	1.14	0.54
4.0 E+00		1.05		0.74
7.0 E+00		1.10		0.82
1.0 E+01		1.13		0.85
2.0 E+01		1.22		0.90
2.8 E+01		1.27		0.91

References: H^-/H^+ - gassy - J. A. Ray, C. F. Barnett, and B. Van Zyle, J. Appl. Phys. 50, 6516 (1979) [Cu]; F. W. Meyer, unpublished [SS].
H^-/H^+ - clean - M. Perdrix, S. Paletto, R. Goutte, and C. Guilland, J. Phys. D 2, 441 (1969) [W]; P. Mahadevan, G. D. Magnuson, J. K. Layton, and C. E. Carlston, Phys. Rev. 140, A1407 (1965) [Mo].
O^-/O^+ - gassy - P. Mahadevan, G. D. Magnuson, J. K. Layton, and C. E. Carlston, Phys. Rev. 140, A1407 (1965) [Mo].
O^-/O^+ - clean - P. Mahadevan, G. D. Magnuson, J. K. Layton, and C. E. Carlston, Phys. Rev. 140, A1407 (1965) [Mo]; M. Perdrix, S. Paletto, R. Goutte, and C. Guilland, J. Phys. D 2, 441 (1969) [Mo].

Accuracy: ±20% (estimated).

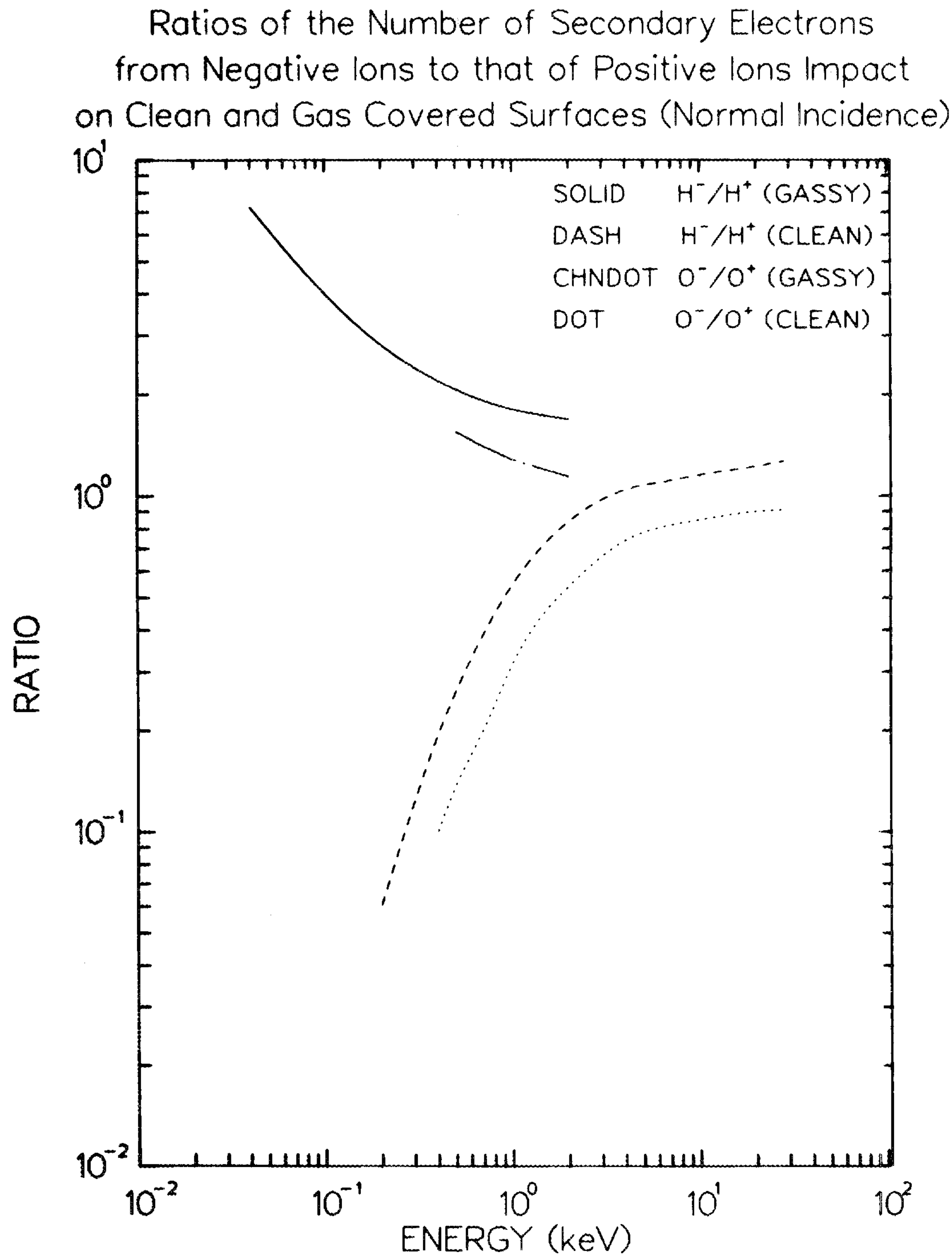

Ratios of the Number of Secondary Electrons from Negative Ions to that of Positive Ions Impact on Clean and Gas Covered Surfaces (Normal Incidence)
SOLID H^-/H^+ (GASSY)
DASH H^-/H^+ (CLEAN)
CHNDOT O^-/O^+ (GASSY)
DOT O^-/O^+ (CLEAN)
RATIO
ENERGY (keV)
10^1
10^0
10^{-1}
10^{-2}
10^{-2}
10^{-1}
10^0
10^1
10^2

Ratios of the Number of Secondary Electrons from Normally Incident Helium Atoms to that of He Ions on Gas Covered and Clean Metallic Surfaces

Energy (keV)	Ratio He^{o}/He^{+} (gassy)	Ratio He^{o}/He^{+} (clean)
5.0 E-02	0.037	
7.0 E-02	0.11	
1.0 E-01	0.28	
2.0 E-01	0.66	
3.0 E-01	0.80	0.06
4.0 E-01	0.87	0.11
7.0 E-01	0.95	0.25
1.0 E+00	0.97	0.36
2.0 E+00	1.02	0.58
4.0 E+00	1.07	0.84
7.0 E+00	1.10	
1.0 E+01	1.10	
2.0 E+01	1.10	
4.0 E+01	1.10	
7.0 E+01	1.09	
1.0 E+02	1.07	
2.0 E+02	1.05	

References: Gassy - H. W. Berry, J. Appl. Phys. 29, 1219 (1958) [W]; M. W. Geis, K. A. Smith, and R. D. Rundel, J. Phys. E 8, 1011 (1975) [Ag]; H. C. Hayden and N. G. Utterback, Phys. Rev. 135, A1575 (1964) [Au]; J. K. Layton, J. Chem. Phys. 59, 5744 (1973); A. Rostagni, Z. Physik 88, 55 (1934) [Cu, Brass]; P. M. Stier, C. F. Barnett, and G. E. Evans, Phys. Rev. 96, 973 (1954) [Ni].
Clean - H. W. Berry, J. Appl. Phys. 29, 1219 (1958) [W].

Accuracy: ±20% (estimated).

Ratios of the Number of Secondary Electrons from Normally Incident Helium Atoms to that of He Ions on Gassy and Clean Metallic Surfaces

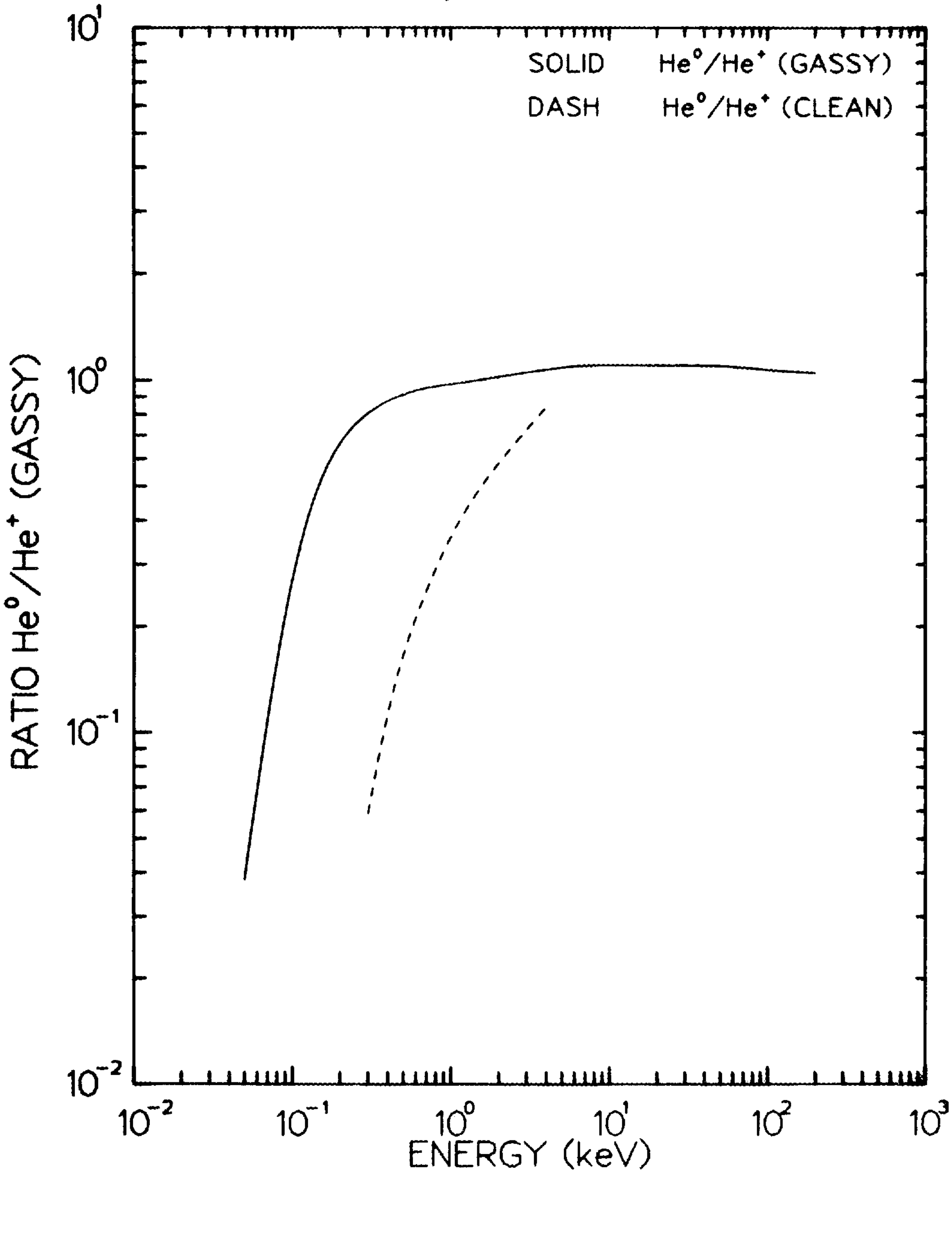

D. ELECTRON REFLECTION

Backscattering Coefficients for Electrons

Incident Normally on C, Al, Ti, and Fe

Energy (keV)	Backscattering Coefficient (electrons/electron) C	Al	Ti	Fe
6.0 E-02		1.20 E-01		
1.0 E-01		1.78 E-01		
2.0 E-01	1.23 E-01	2.22 E-01		
4.0 E-01	1.43 E-01	2.31 E-01		2.11 E-01
7.0 E-01	1.49 E-01	2.31 E-01		2.06 E-01
1.0 E 00	1.45 E-01	2.31 E-01		2.11 E-01
2.0 E 00	1.20 E-01	2.21 E-01		2.54 E-01
4.0 E 00	9.63 E-02	1.96 E-01	2.59 E-01	2.84 E-01
7.0 E 00	8.16 E-02	1.76 E-01	2.62 E-01	2.93 E-01
1.0 E+01	7.49 E-02	1.65 E-01	2.59 E-01	2.86 E-01
2.0 E+01	6.43 E-02	1.50 E-01	2.52 E-01	2.77 E-01
4.0 E+01	5.68 E-02		2.40 E-01	2.66 E-01
6.0 E+01	5.39 E-02			

References: e + C – J. Hölzl and K. Jacobi, Surf. Sci. 14, 351 (1969); H. J. Hunger and L. Kuchler, Phys. Stat. Sol. (a) 56, K45 (1979); G. Neubert and S. Rogaschewski, Phys. Stat. Sol. (a) 59, 35 (1980); H. Sørensen and J. Schou, J. Appl. Phys. 43, 5311 (1978).

e + Al – G. Neubert and S. Rogaschewski, Phys. Stat. Sol. (a) 59, 35 (1980); H. E. Bishop, in "Optique des Rayons X et Microanalyse," IV Congrès International sur l'optique des Rayons X et la Microanalyse," Sept. 1965, p. 153, Herman, Paris; S. Thomas and E. B. Pattinson, J. Phys. D: Appl. Phys. 2, 1539 (1969).

e + Ti – H. J. Hunger and L. Kuchler, Phys. Stat. Sol. (a) 56, K45 (1979).

e + Fe – H. J. Hunger and L. Kuchler, Phys. Stat. Sol. (a) 56, K45 (1979); E. J. Sternglass, Phys. Rev. 95, 345 (1954).

Accuracy: Unknown.

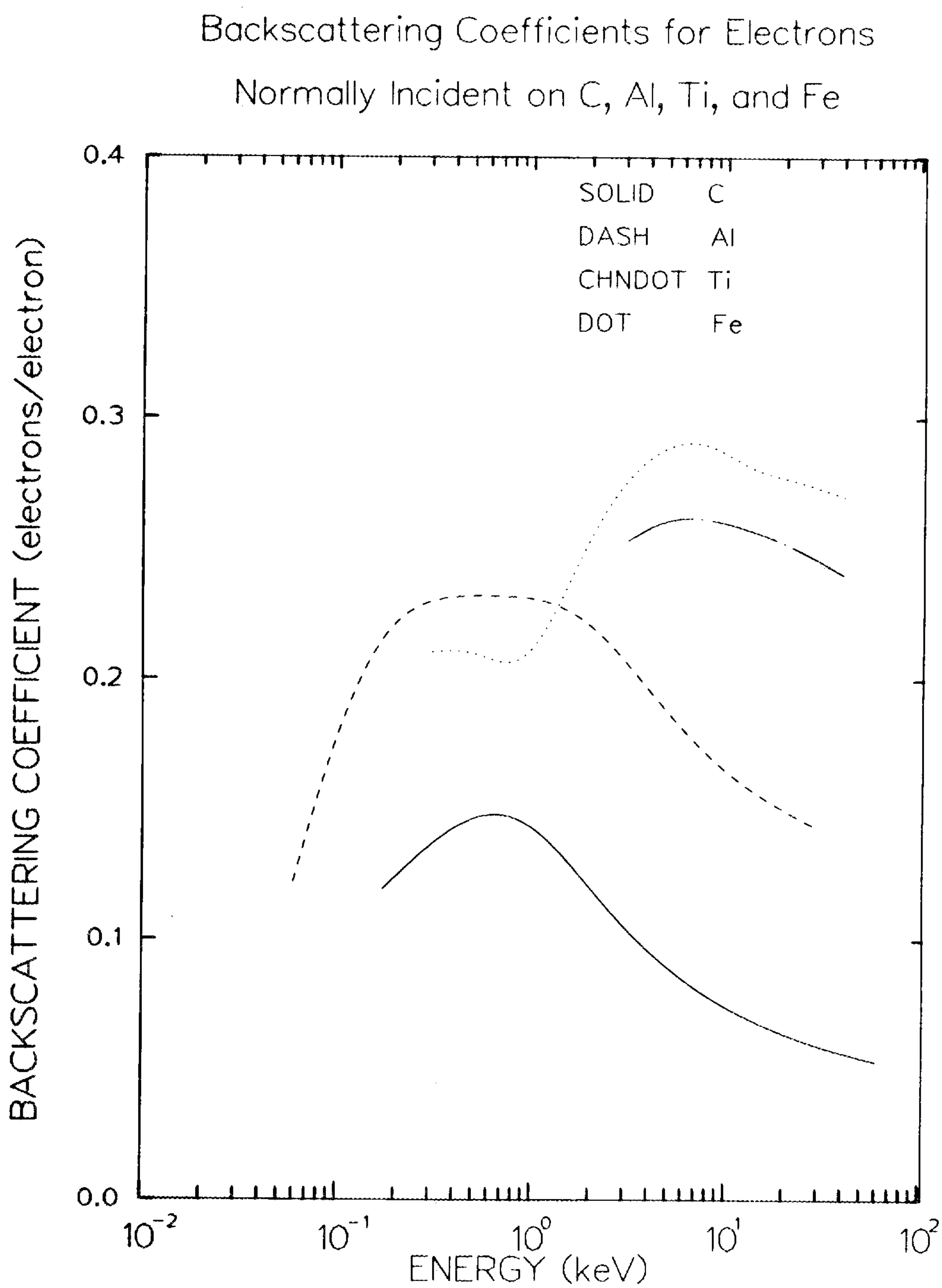
Backscattering Coefficients for Electrons
Normally Incident on C, Al, Ti, and Fe
SOLID C
DASH Al
CHNDOT Ti
DOT Fe
BACKSCATTERING COEFFICIENT (electrons/electron)
0.0
0.1
0.2
0.3
0.4
10^-2
10^-1
10^0
10^1
10^2
ENERGY (keV)

Backscattering Coefficients for Electrons

Incident Normally on Ni, Cu, and Mo

Energy (keV)	Backscattering Coefficient (electrons/electron) Ni	Cu	Mo
2.0 E-01			1.40 E-01
4.0 E-01			1.73 E-01
5.0 E-01		2.62 E-01	1.88 E-01
7.0 E-01		2.62 E-01	2.07 E-01
1.0 E 00		2.66 E-01	2.30 E-01
2.0 E 00		2.82 E-01	2.87 E-01
2.2 E 00	2.91 E-01	2.92 E-01	2.97 E-01
4.0 E 00	2.98 E-01	3.15 E-01	3.36 E-01
7.0 E 00	3.04 E-01	3.22 E-01	3.69 E-01
1.0 E+01	3.06 E-01	3.23 E-01	3.84 E-01
2.0 E+01	3.02 E-01	3.18 E-01	3.94 E-01
4.0 E+01	2.92 E-01	3.09 E-01	
7.0 E+01		2.99 E-01	
1.0 E+02		2.92 E-01	

References: e + Ni - H. J. Hunger and L. Kuchler, Phys. Stat. Sol. (a) 56, K45 (1979); P. Palluel, Comptes Rendus 224, 1492 (1947).

e + Cu - H. J. Hunger and L. Kuchler, Phys. Stat. Sol (a) 56, K45 (1979); P. Palluel, Comptes Rendus 224, 1492 (1947); E. J. Sternglass, Phys. Rev. 95, 345 (1954).

e + Mo - H. E. Bishop, "Optique des Rayons x et Microanalyse," IV Congrès International sur l'optique des Rayons X et la Microanalyse, p. 153, Herman, Paris (1965); P. Palluel, Comptes Rendus 224, 1492 (1947); E. J. Sternglass, Phys. Rev. 95, 345 (1954).

Accuracy: ±5% above 5 keV; ±20% below 5 keV (estimated).

Backscattering Coefficients for Electrons
Incident Normally on Ni, Cu, and Mo

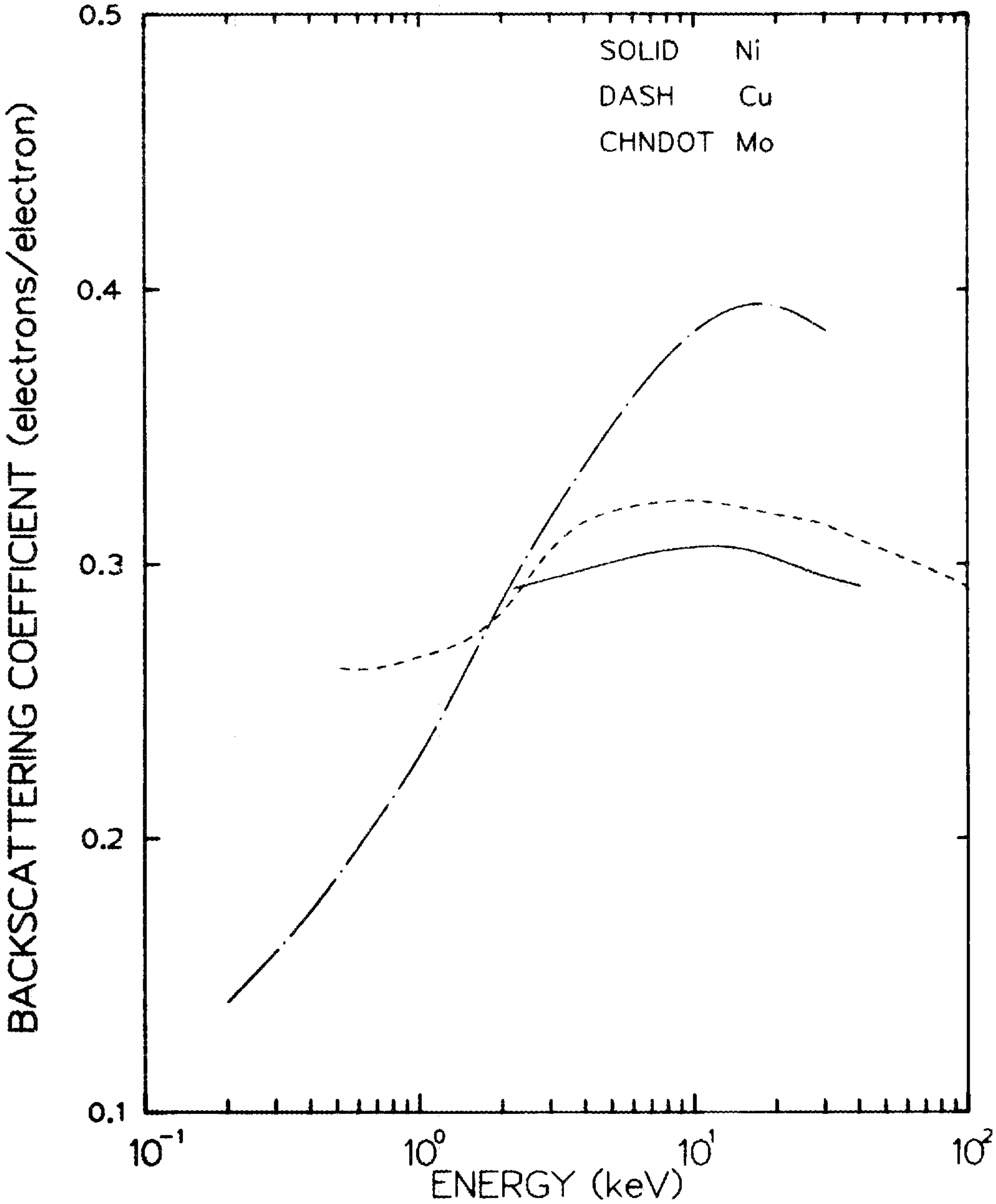

Backscattering Coefficients for Electrons Incident Normally on Ag, W, and Au

Energy (keV)	Backscattering Coefficient (electrons/electrons) Ag	W	Au
7.0 E-02			1.88 E-01
1.0 E-01	1.49 E-01		1.91 E-01
2.0 E-01	2.59 E-01		1.99 E-01
4.0 E-01	3.60 E-01		2.77 E-01
7.0 E-01	4.05 E-01		3.74 E-01
1.0 E 00	4.13 E-01		4.13 E-01
2.0 E 00	4.13 E-01	3.56 E-01	4.50 E-01
4.0 E 00	4.13 E-01	4.15 E-01	4.59 E-01
7.0 E 00	4.12 E-01	4.48 E-01	4.66 E-01
1.0 E+01	4.11 E-01	4.57 E-01	4.72 E-01
2.0 E+01	4.11 E-01	4.76 E-01	4.81 E-01
4.0 E+01	4.10 E-01	4.75 E-01	4.85 E-01
7.0 E+01	4.09 E-01		

References: e + Ag – H. E. Bishop, "Optique des Rayons X et Microanalyse," IV Congrès International sur l'optique des Rayons X et la Microanalyse, p. 153, Herman, Paris (1965); H. J. Hunger and L. Küchler, Phys. Sat. Sol (a) 56, K45 (1979); G. Neubert and S. Rogaschewski, Phys. Stat. Sol. (a) 59, 35 (1980); S. Thomas and E. B. Pattinson, J. Phys. D: Appl. Phys. 3, 349 (1969).

e + Au – H. J. Hunger and L. Küchler, Phys. Sat. Sol. (a) 56, K45 (1979); J. Schou and H. Sørenson, J. Appl. Phys. 49, 816 (1978); S. Thomas and E. B. Pattinson, J. Phys. D: Appl. Phys. 3, 349 (1969).

e + W – H. J. Hunger and L. Küchler, Phys. Sat. Sol. (a) 56, K45 (1979).

Accuracy: Unknown.

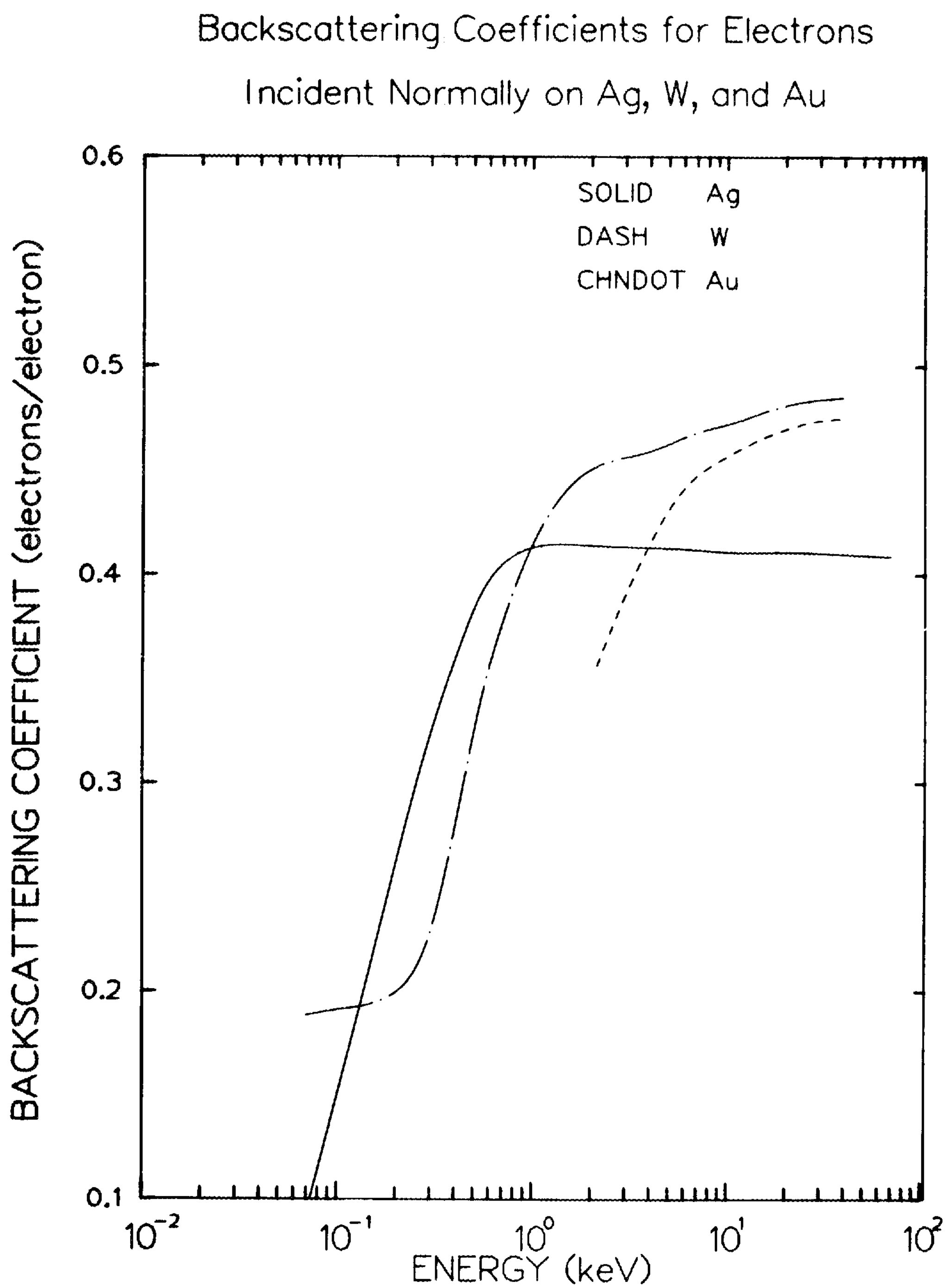
Backscattering Coefficients for Electrons
Incident Normally on Ag, W, and Au
SOLID Ag
DASH W
CHNDOT Au
BACKSCATTERING COEFFICIENT (electrons/electron)
0.6
0.5
0.4
0.3
0.2
0.1
10^-2
10^-1
10^0
10^1
10^2
ENERGY (keV)

Backscattering Coefficients for Electrons Incident

Normally on a "Gassy" and "Degassed" TiC Surface

Energy (keV)	Backscattering Coefficient (electrons/electron)	
	Gassy	Degassed
0.10	2.50 E-01	9.64 E-02
0.15	2.88 E-01	1.58 E-01
0.20	3.00 E-01	1.91 E-01
0.30	2.92 E-01	2.17 E-01
0.40	2.89 E-01	2.38 E-01
0.60	2.92 E-01	2.56 E-01
0.80	2.95 E-01	2.64 E-01
1.00	2.95 E-01	2.64 E-01
1.20	2.96 E-01	2.64 E-01

Reference: S. Thomas and E. B. Pattinson, J. Phys. D 2, 1539 (1969).

Accuracy: Unknown.

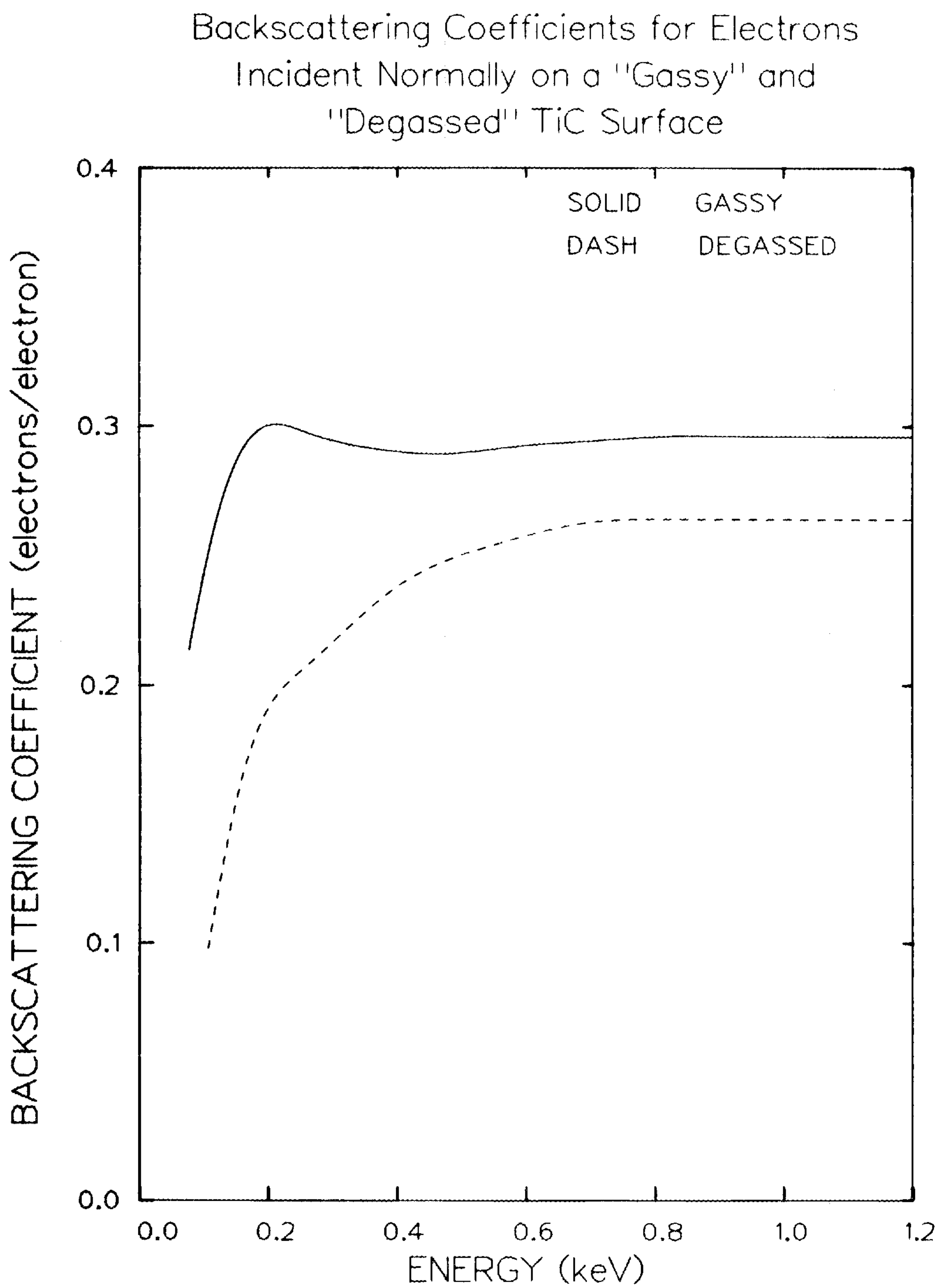
Backscattering Coefficients for Electrons
Incident Normally on a "Gassy" and
"Degassed" TiC Surface
SOLID GASSY
DASH DEGASSED
BACKSCATTERING COEFFICIENT (electrons/electron)
0.0
0.1
0.2
0.3
0.4
0.0
0.2
0.4
0.6
0.8
1.0
1.2
ENERGY (keV)

Backscattering Coefficients for 20, 40, and 60 keV

Electrons Incident on Ti as a Function of Angle

Between the Incident Electrons and the Normal to the Surface

Angle (deg)	Backscattering Coefficient (electrons/electron) 20 keV	40 keV	60 keV
0	2.63 E-01	2.52 E-01	2.46 E-01
10	2.69 E-01	2.58 E-01	2.51 E-01
20	2.87 E-01	2.76 E-01	2.69 E-01
30	3.16 E-01	3.06 E-01	3.00 E-01
40	3.60 E-01	3.51 E-01	3.45 E-01
50	4.19 E-01	4.10 E-01	4.05 E-01
60	4.96 E-01	4.89 E-01	4.83 E-01
70	5.95 E-01	5.87 E-01	5.87 E-01
80	7.29 E-01	7.21 E-01	7.15 E-01

Reference: G. Neubert and S. Rogaschewski, Phys. Stat. Sol. (a) 59, 35 (1980).

Accuracy: Unknown.

Backscattering Coefficients for 20, 40, and 60 keV Electrons Incident on Ti as a Function of the Incident Angle

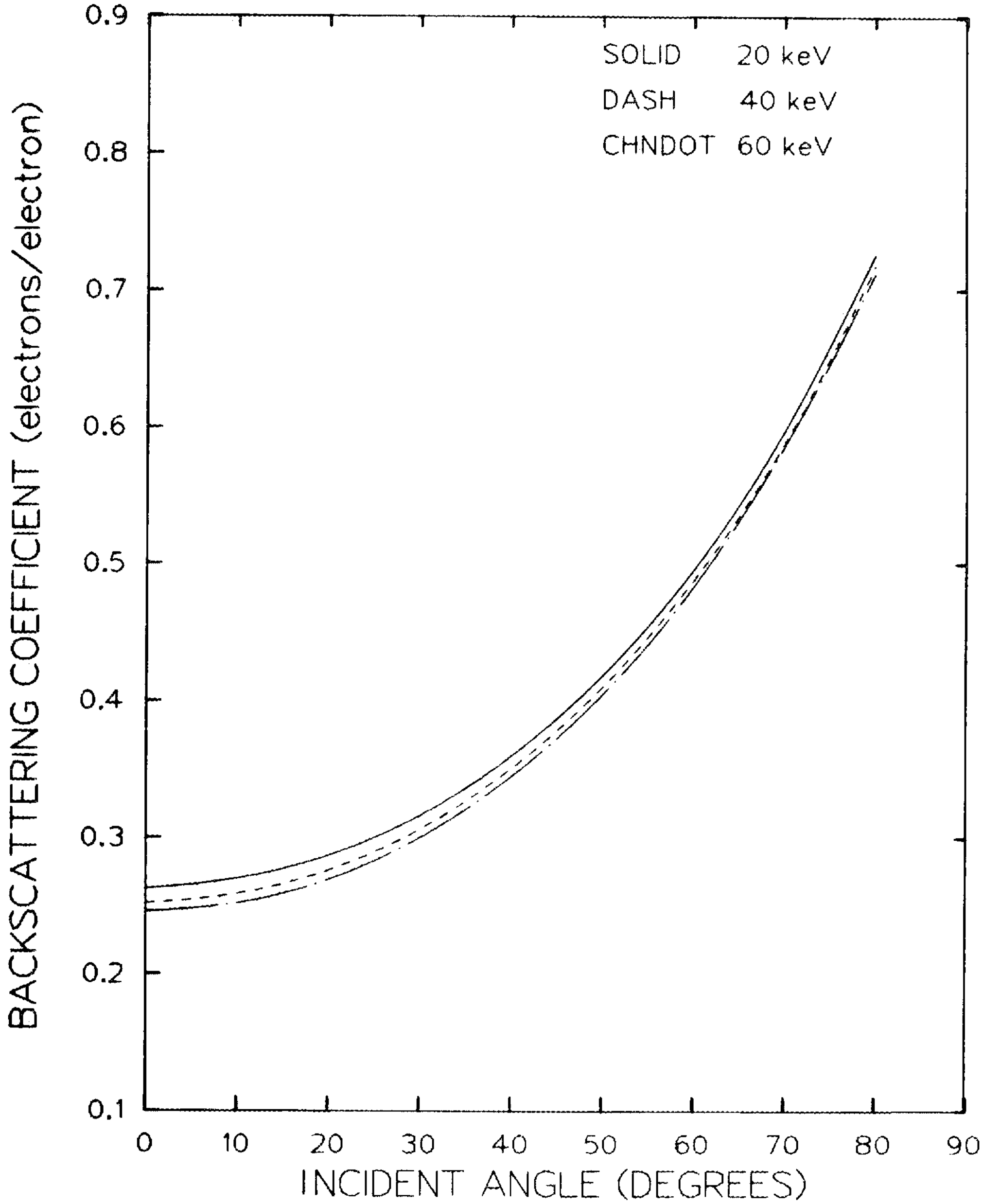

E. HEAVY PARTICLE REFLECTION

Particle Reflection from Surfaces

Introductory Notes

A. Definition of Quantities

1. R_N Particle reflection coefficient

Ratio of total backscattered flux (integrated over all angles and energies) to total incident flux. Specifically if a projectile beam of energy E_o falls on a target, and a fraction $r(E_o,E)dE$ is scattered back with energies in the interval $E \rightarrow E + dE$ (integrated over all emergent angles) then

$$R_N = \int_0^{E_o} r(E_o,E)\cdot dE$$

2. R_E Energy reflection coefficient

Ratio of integrated energy of backscattered particles to energy of incident projectiles.

$$R_E = \frac{1}{E_o}\int_0^{E_o} E\cdot\ r(E_o,E)\,dE$$

3. $\overline{E}$ Mean backscattered energy

Average energy of backscattered particles.

$$\overline{E} = \frac{\int_0^{E_o} E\cdot\ r(E_o,E)\,dE}{\int_0^{E_o} r(E_o,E)\,dE}$$

$$\equiv \frac{R_E}{R_N}\,E_o$$

4. N^i/N^T charge state fraction

For recoils at some energy E the ratio of the flux N^i in charge state i (e.g., i = +, 0 or − for H^+, H^o or H^-) to the total scattered flux N^T at that energy.

B. Scaling Laws

It has generally been found that particle or energy reflection coefficients (R_N and R_E) are the same for most projectile-target combinations when plotted as a function of "reduced energy" ε, where

$$\varepsilon = \frac{32.5\ A_2\ E}{(Z_1^{2/3} + Z_2^{2/3})^{1/2}\ (A_1 + A_2) Z_1\ Z_2}$$

Here Z_1 and Z_2 are the atomic numbers of the projectile and target; A_1 and A_2 are the masses of the projectile and target; and E is the projectile energy (in keV). [See, for example, J. Schou et al., J. Nucl. Mater. 76 and 77, 359 (1978).] This equation may be used to reliably estimate R_N or $\overline{R_E}$ for $\overline{D}$ and T using available data for H or He. It may be used, with some caution to scale between different target material.

A more complete (and more reliable) scaling technique involving the above feature is to be found in work by Tabata [T. Tabata et al., Jap. J. Appl. Phys. 20, 1929 (1981).

C. Major Data Compendia

1. "Data on the Backscattering Coefficients of Light Ions from Solids," T. Tabata et al., IPPJ-AM-18 (Institute of Plasma Physics, Nagoya, Japan). 1981

2. "Data on Light Ion Reflection," W. Eckstein and H. Verbeek, IPP 9/32 (Institute fur Plasmaphysik, Garching, Germany). 1979

D. Data Presentation

In Figs. 5.4 and 5.5 we display a compendium of R_N values for a variety of elements as a function of reduced energy ε. The objective is to illustrate the success of scaling against reduced energy ε.

Subsequent data tables shown particle and energy reflection coefficients R_N and R_E for various projectile target combinations. Samples of data on angular distributions, energy distributions and charge state distributions are shown at the end.

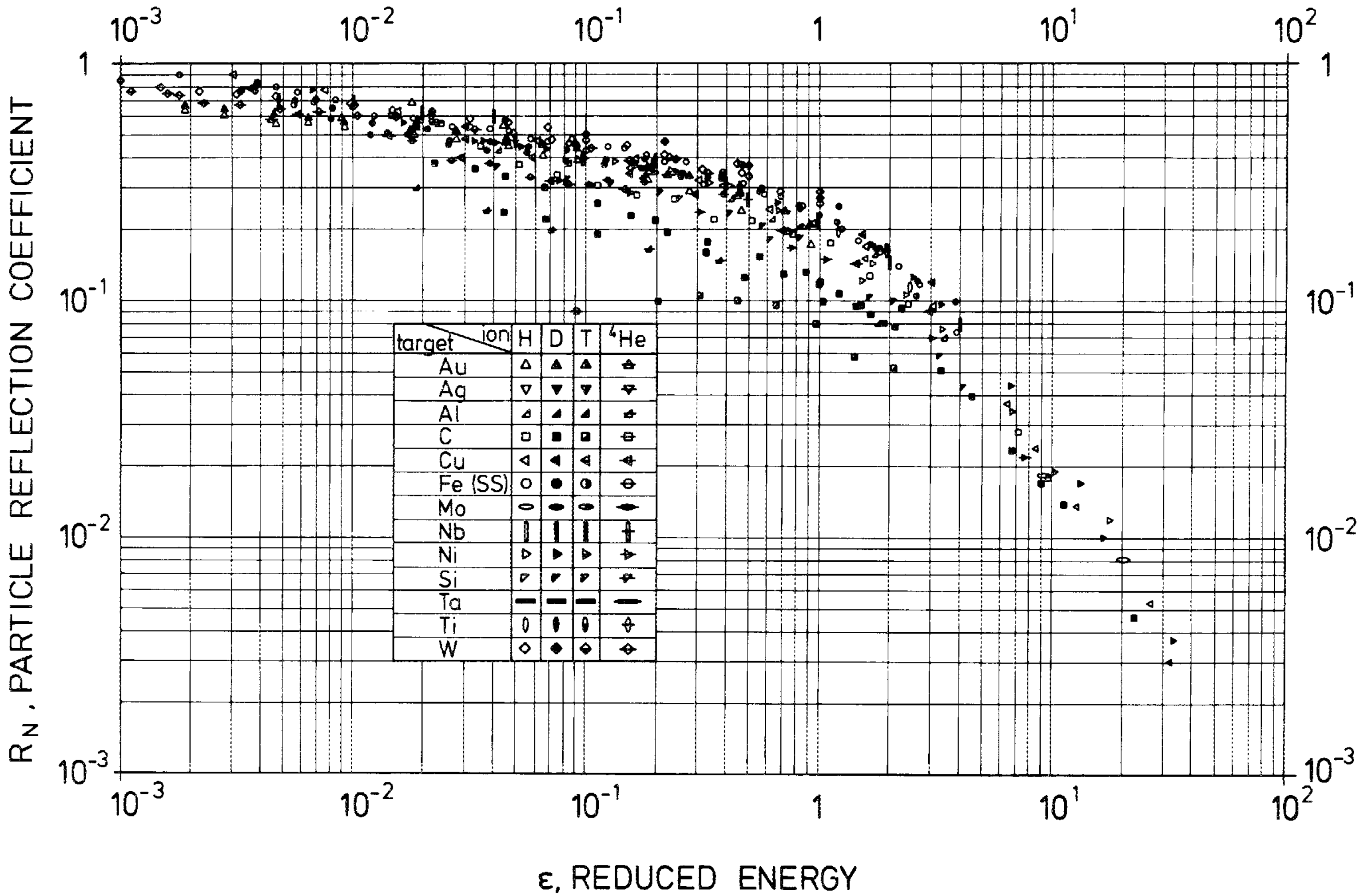

Fig. E-4. Composite Figure Showing Calculated Particle Reflection Coefficients for Several Ion-Target Combinations Versus the Reduced Energy ε (defined on previous pages). Taken from W. Eckstein and H. Verbeek, Report IPP 9/32, MPI Garching, August, 1979.

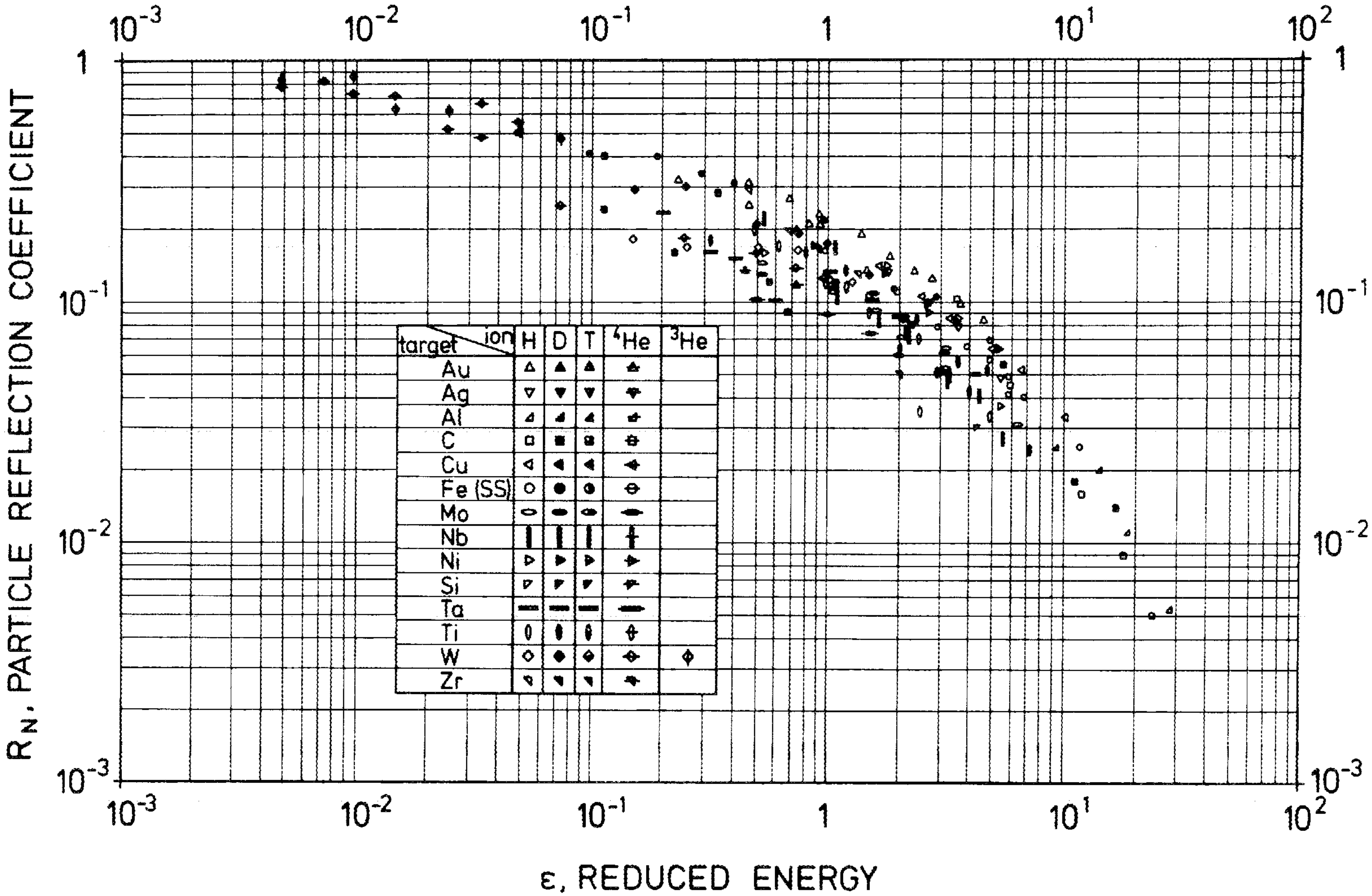

Fig. E-5. Composite Figure Showing Measured Particle Reflection Coefficients for Several Ion-Target Combinations Versus the Reduced Energy ε (defined on previous pages). Taken from W. Eckstein and H. Verbeek, Report IPP 9/32, MPI Garching, August, 1979.

Particle Reflection Coefficients (R_N) for H^+, D^+, and He^+ Incident on C

(normal incidence, room temperature)

Energy (keV)	R_N (H^+ on C)	R_N (D^+ on C)	R_N (He^+ on C)
1.0 E-02	4.56 E-01	3.29 E-01	1.07 E-01
2.0 E-02	4.13 E-01	2.75 E-01	8.71 E-02
4.0 E-02	3.64 E-01	2.36 E-01	7.61 E-02
6.0 E-02	3.31 E-01	2.16 E-01	7.20 E-02
1.0 E-01	2.87 E-01	1.93 E-01	6.83 E-02
2.0 E-01	2.23 E-01	1.59 E-01	6.44 E-02
4.0 E-01	1.59 E-01	1.23 E-01	6.02 E-02
6.0 E-01	1.25 E-01	1.02 E-01	5.71 E-02
1.0 E+00	8.73 E-02	7.60 E-02	5.23 E-02
2.0 E+00	4.83 E-02	4.56 E-02	4.38 E-02
4.0 E+00	2.33 E-02	2.34 E-02	3.36 E-02
6.0 E+00	1.42 E-02	1.46 E-02	2.74 E-02
1.0 E+01	7.01 E-03	7.02 E-03	1.99 E-02
2.0 E+01	2.31 E-03	2.43 E-03	1.14 E-02
4.0 E+01	6.27 E-04	5.84 E-04	5.49 E-03
6.0 E+01			3.29 E-03
1.0 E+02			1.56 E-03

<u>References</u>: <u>H^+ and D^+ Projectiles</u>: W. Eckstein and H. Verbeek, Report IPP 9/32, MPI Garching, August 1979 (10^{-2} to 10 keV); T. Tabata et al., Report IPPJ-AM-18, IPP Nagoya, October 1981 (10-40 keV).

<u>He^+ Projectiles</u>: T. Tabata et al., Report IPPJ-AM-18, IPP Nagoya, October 1981.

<u>Accuracy</u>: Unknown,

<u>Notes</u>: (1) H^+; D^+. These data are based primarily on computer models by the TRIM and MARLOWE codes. Experimental data confirm these codes adequately (±25%) at energies above 1 keV. At lower energies there is recent experimental data [E. W. Thomas and M. Braun, J. Appl. Phys. <u>53</u>, 6446 (1982)] for D^+ that lies above the calculated values by <u>as</u> much as 100% at 30 eV. This discrepancy may be related to the low density form of C used in the experiments (Papyex). It is suggested that the data reproduced here be used for high density forms of C.

(2) For He^+ these values from from a computer simulation and there is no experimental confirmation.

Particle Reflection Coefficient for

H^+, H_2^+, He^+ on C

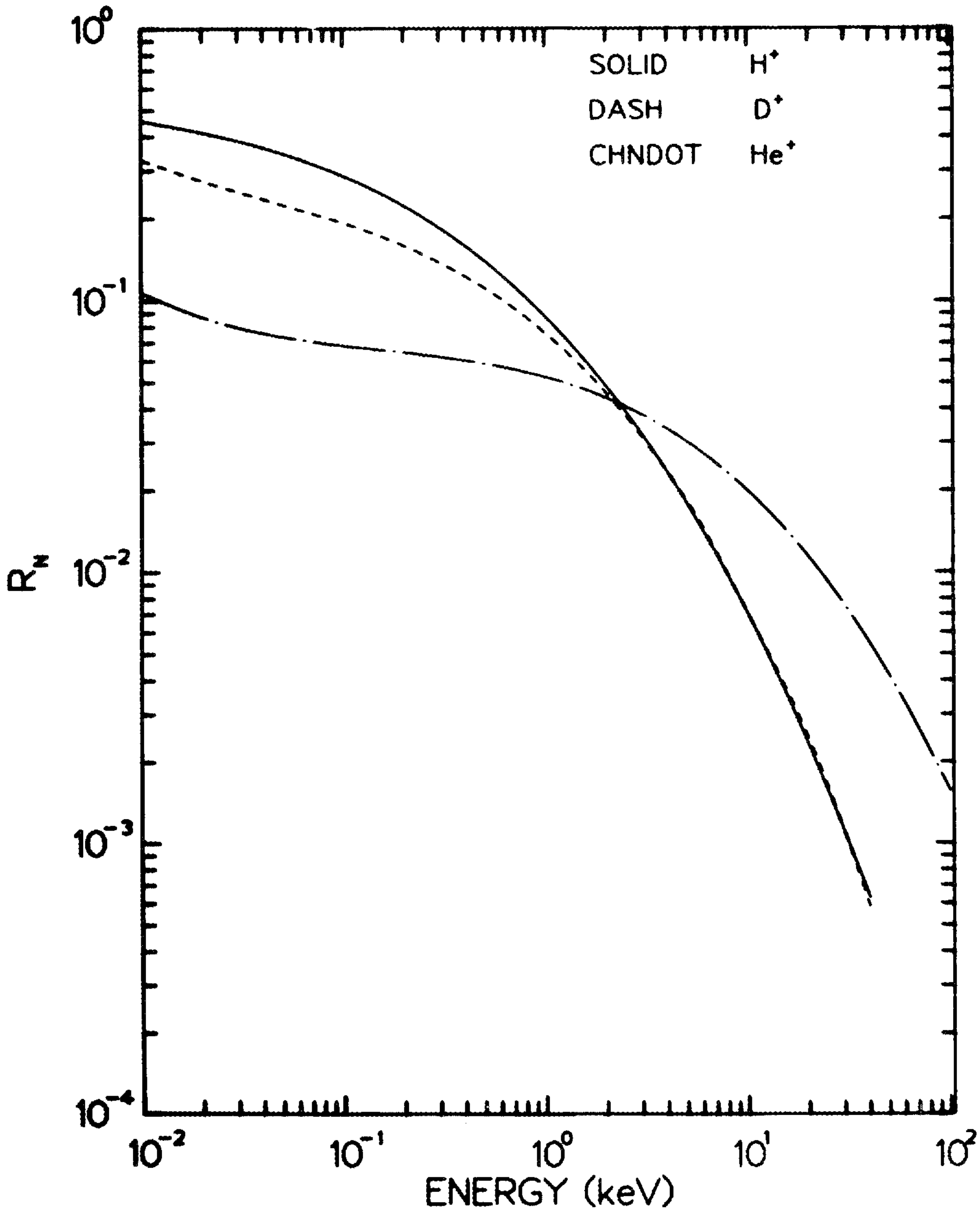

Energy Reflection Coefficients (R_E) for H^+, D^+, and He^+ Incident on C

(normal incidence, room temperature)

Energy (keV)	R_E (H^+ on C)	R_E (D^+ on C)	R_E (He^+ on C)
1.0 E-02	2.65 E-01	1.68 E-01	7.58 E-02
2.0 E-02	2.21 E-01	1.28 E-01	5.66 E-02
4.0 E-02	1.82 E-01	1.01 E-01	4.54 E-02
6.0 E-02	1.59 E-01	8.87 E-02	4.08 E-02
1.0 E-01	1.31 E-01	7.49 E-02	3.63 E-02
2.0 E-01	9.49 E-02	7.59 E-02	3.14 E-02
4.0 E-01	6.29 E-02	4.22 E-02	2.69 E-02
6.0 E-01	4.72 E-02	3.37 E-02	2.43 E-02
1.0 E+00	3.09 E-02	2.41 E-02	2.08 E-02
2.0 E+00	1.54 E-02	1.36 E-02	1.60 E-02
4.0 E+00	6.61 E-03	6.57 E-03	1.13 E-02
6.0 E+00	3.71 E-03	3.94 E-03	8.75 E-03
1.0 E+01	1.63 E-03	1.87 E-03	5.98 E-03
2.0 E+01	4.49 E-04	5.56 E-04	3.14 E-03
4.0 E+01	9.87 E-05	1.28 E-04	1.40 E-03
6.0 E+01			8.01 E-04
1.0 E+02			3.58 E-04

References: H^+ and D^+ Projectiles: W. Eckstein and H. Verbeek, Report IPP 9/32, MPI Garching, August 1979 (10^{-2} to 10 keV); T. Tabata et al., Report IPPJ-AM-18, IPP Nagoya, October 1981 (10-40 keV).

He^+ Projectiles: T. Tabata et al., Report IPPJ-AM-18, IPP Nagoya, October 1981.

Accuracy: Unknown,

Notes: (1) H^+; D^+. These data are based primarily on computer models by the TRIM and MARLOWE codes. Experimental data confirm these codes adequately (±25%) at energies above 1 keV.

(2) For He^+ these values from from a computer simulation and there is no experimental confirmation.

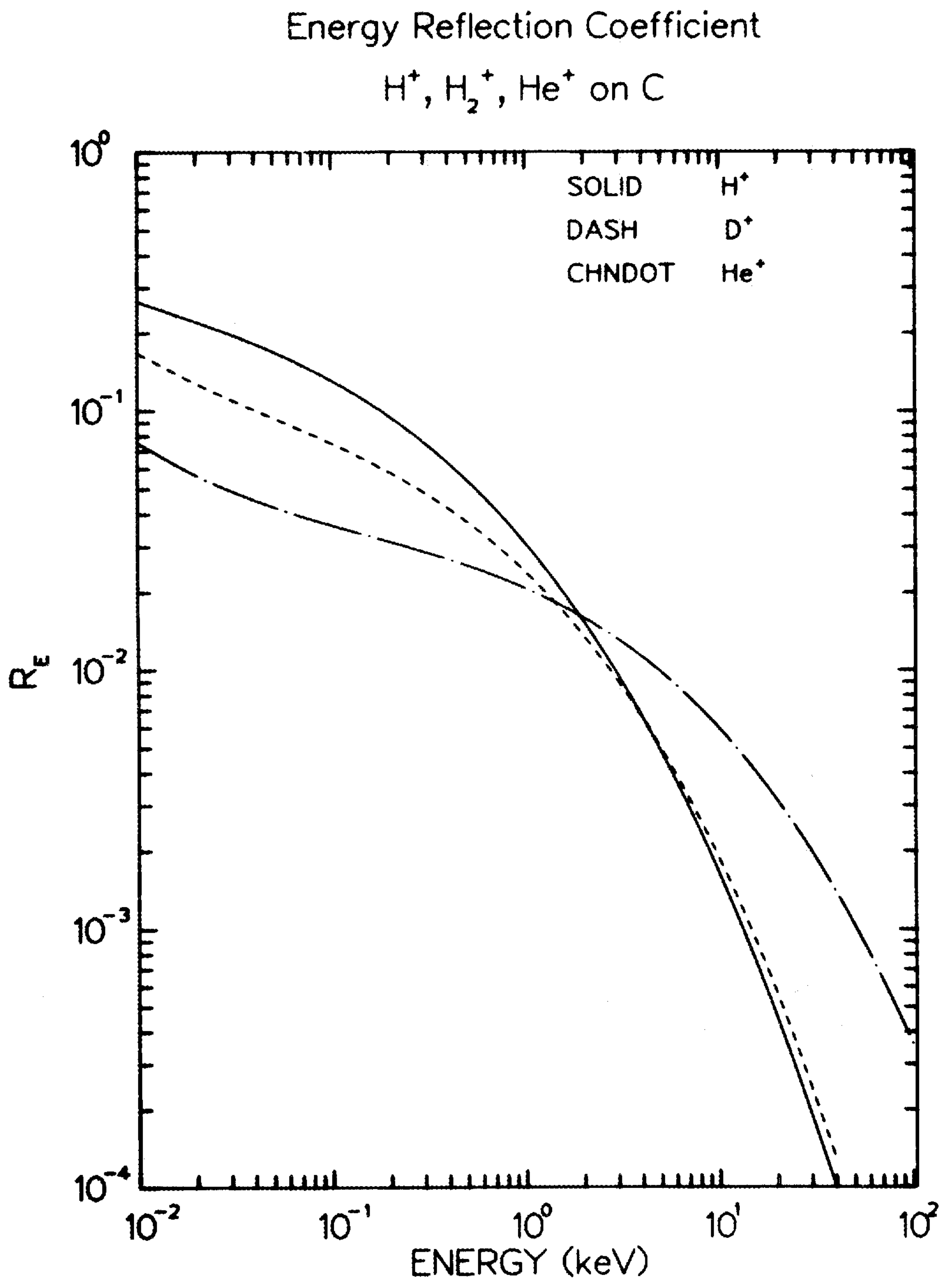

Energy Reflection Coefficient
H⁺, H₂⁺, He⁺ on C
SOLID H⁺
DASH D⁺
CHNDOT He⁺
R_E
10^0
10^-1
10^-2
10^-3
10^-4
10^-2
10^-1
10^0
10^1
10^2
ENERGY (keV)

Particle Reflection Coefficients (R_N)

for H^+ and He^+ Incident on Al

(normal incidence, room temperature)

Energy (keV)	R_N (H^+ on Al)	R_N (He^+ on Al)
1.0 E-02	2.79 E-01	4.42 E-01
2.0 E-02	2.85 E-01	3.13 E-01
4.0 E-02	2.86 E-01	2.47 E-01
6.0 E-02	2.82 E-01	2.22 E-01
1.0 E-01	2.72 E-01	2.01 E-01
2.0 E-01	2.47 E-01	1.81 E-01
4.0 E-01	2.10 E-01	1.65 E-01
6.0 E-01	1.84 E-01	1.55 E-01
1.0 E+00	1.49 E-01	1.41 E-01
2.0 E+00	1.01 E-01	1.18 E-01
4.0 E+00	6.14 E-02	9.02 E-02
6.0 E+00	4.30 E-02	7.34 E-02
1.0 E+01	2.56 E-02	5.31 E-02
2.0 E+01	1.11 E-02	2.99 E-02
4.0 E+01	4.02 E-03	1.41 E-02
6.0 E+01	2.04 E-03	8.25 E-03
1.0 E+02	7.91 E-04	3.67 E-03

Reference: T. Tabata et al., Report IPPJ-AM-18, IPP Nagoya, October 1981.

Accuracy: Unknown.

Notes: These data are largely based on a theoretical interpolation from data for other materials and have been confirmed experimentally only for H^+ at energies above 10 keV.

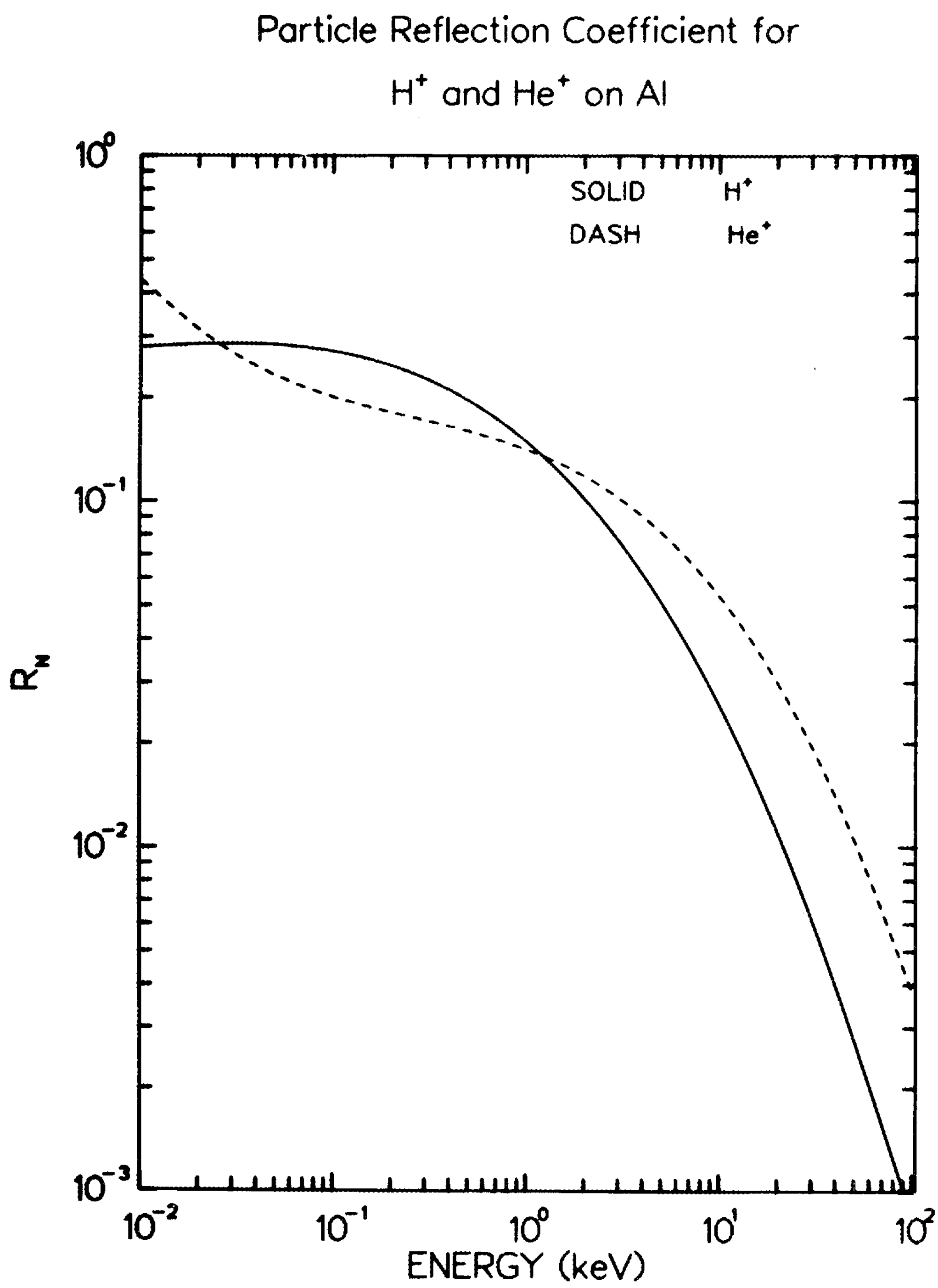

Particle Reflection Coefficient for
H+ and He+ on Al
SOLID H+
DASH He+
R_N
10^0
10^{-1}
10^{-2}
10^{-3}
10^{-2}
10^{-1}
10^0
10^1
10^2
ENERGY (keV)

Energy Reflection Coefficients (R_E)

for H^+ and He^+ Incident on Al

(normal incidence, room temperature)

Energy (keV)	R_E (H^+ on Al)	R_E (He^+ on Al)
1.0 E-02	2.05 E-01	3.23 E-01
2.0 E-02	2.04 E-01	2.10 E-01
4.0 E-02	1.90 E-01	1.54 E-01
6.0 E-02	1.77 E-01	1.33 E-01
1.0 E-01	1.55 E-01	1.15 E-01
2.0 E-01	1.22 E-01	9.72 E-02
4.0 E-01	8.74 E-02	8.33 E-02
6.0 E-01	6.91 E-02	7.56 E-02
1.0 E+00	4.90 E-02	6.57 E-02
2.0 E+00	2.81 E-02	5.13 E-02
4.0 E+00	1.44 E-02	3.67 E-02
6.0 E+00	9.29 E-03	2.85 E-02
1.0 E+01	5.02 E-03	1.94 E-02
2.0 E+01	1.96 E-03	9.95 E-03
4.0 E+01	6.69 E-04	4.20 E-03
6.0 E+01	3.35 E-04	2.29 E-03
1.0 E+02	1.31 E-04	9.49 E-04

Reference: T. Tabata et al., Report IPPJ-AM-18, IPP Nagoya, October 1981.

Accuracy: Unknown.

Notes: These data are largely based on a theoretical interpolation from data for other materials. Experimental tests are confirmed to a few energies at about 10 keV where experiment lies 30% below the data quoted here.

Energy Reflection Coefficient for

H^+ and He^+ on Al

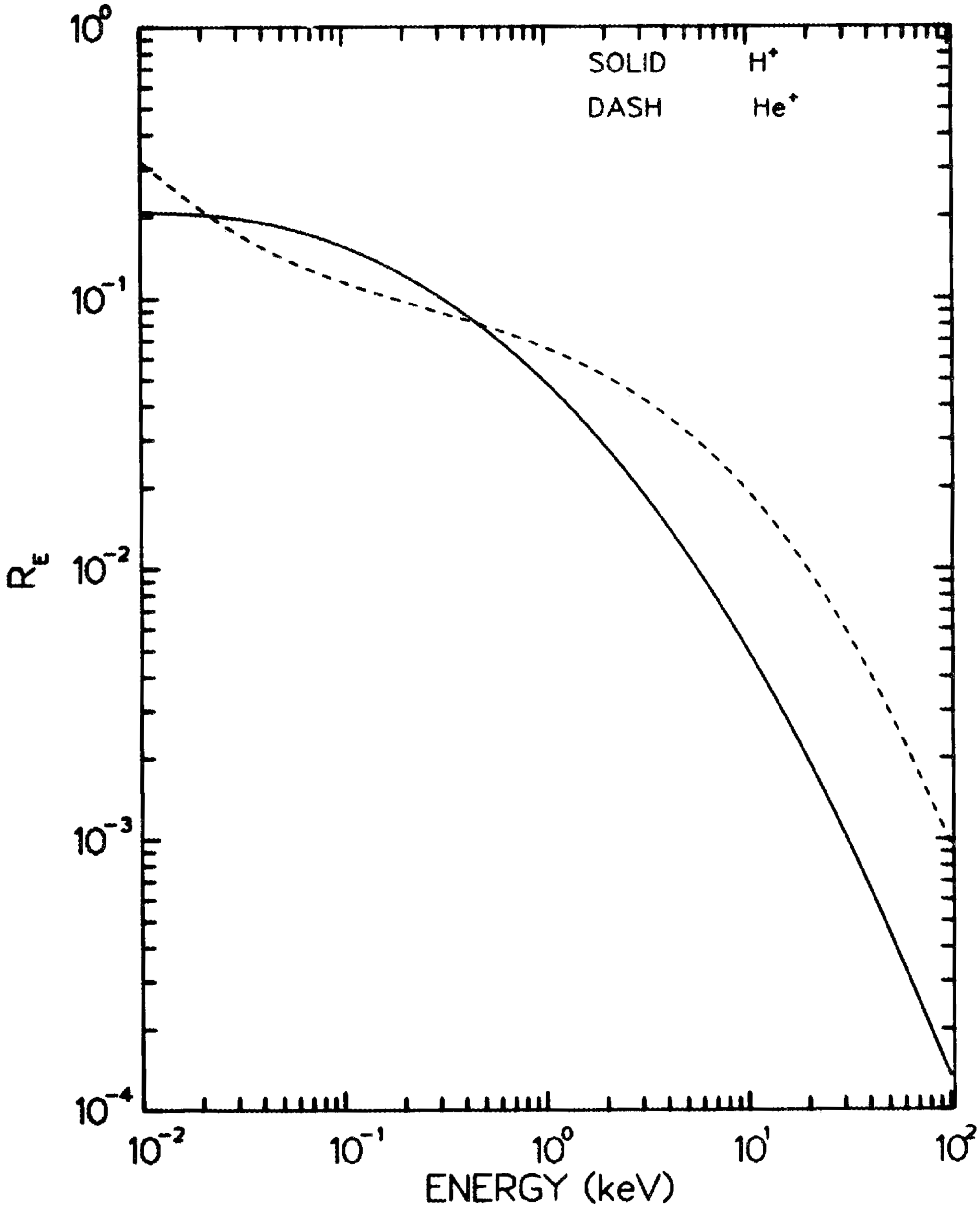

Particle Reflection Coefficients (R_N) for H^+, D^+, and He^+ Incident on Ti

(normal incidence, room temperature)

Energy (keV)	R_N (H^+ on Ti)	R_N (D^+ on Ti)	R_N (He^+ on Ti)
1.0 E-02	3.31 E-01	6.22 E-01	7.93 E-01
2.0 E-02	3.17 E-01	4.67 E-01	5.23 E-01
4.0 E-02	3.07 E-01	3.78 E-01	3.90 E-01
6.0 E-02	3.01 E-01	3.43 E-01	3.36 E-01
1.0 E-01	2.91 E-01	3.08 E-01	2.86 E-01
2.0 E-01	2.71 E-01	2.69 E-01	2.38 E-01
4.0 E-01	2.41 E-01	2.32 E-01	2.02 E-01
6.0 E-01	2.18 E-01	2.09 E-01	1.83 E-01
1.0 E+00	1.86 E-01	1.78 E-01	1.61 E-01
2.0 E+00	1.38 E-01	1.34 E-01	1.31 E-01
4.0 E+00	9.24 E-02	9.06 E-02	1.01 E-01
6.0 E+00	6.91 E-02	6.79 E-02	8.45 E-02
1.0 E+01	4.48 E-02	4.38 E-02	6.44 E-02
2.0 E+01	2.19 E-02	2.08 E-02	4.08 E-02
4.0 E+01	9.10 E-03	8.14 E-03	2.29 E-02
6.0 E+01	5.00 E-03	4.24 E-03	1.53 E-02
1.0 E+02	2.14 E-03	1.66 E-03	8.54 E-03

References: T. Tabata et al., Report IPPJ-AM-18, IPP Nagoya, October 1981.

Accuracy: Unknown.

Notes: (1) These data are based generally on a theoretical formulation. They have been confirmed experimentally at energies between 1 and 10 keV to within 20% for most cases.

(2) It has been shown [Oen and Robinson, J. Nucl. Mat. 76 and 77, 370 (1978)] that as hydrogen builds up in the Ti the reflection coefficient decreases to a value appropriate to TiH_2.

Particle Reflection Coefficient for

H^+, D^+, and He^+ on Ti

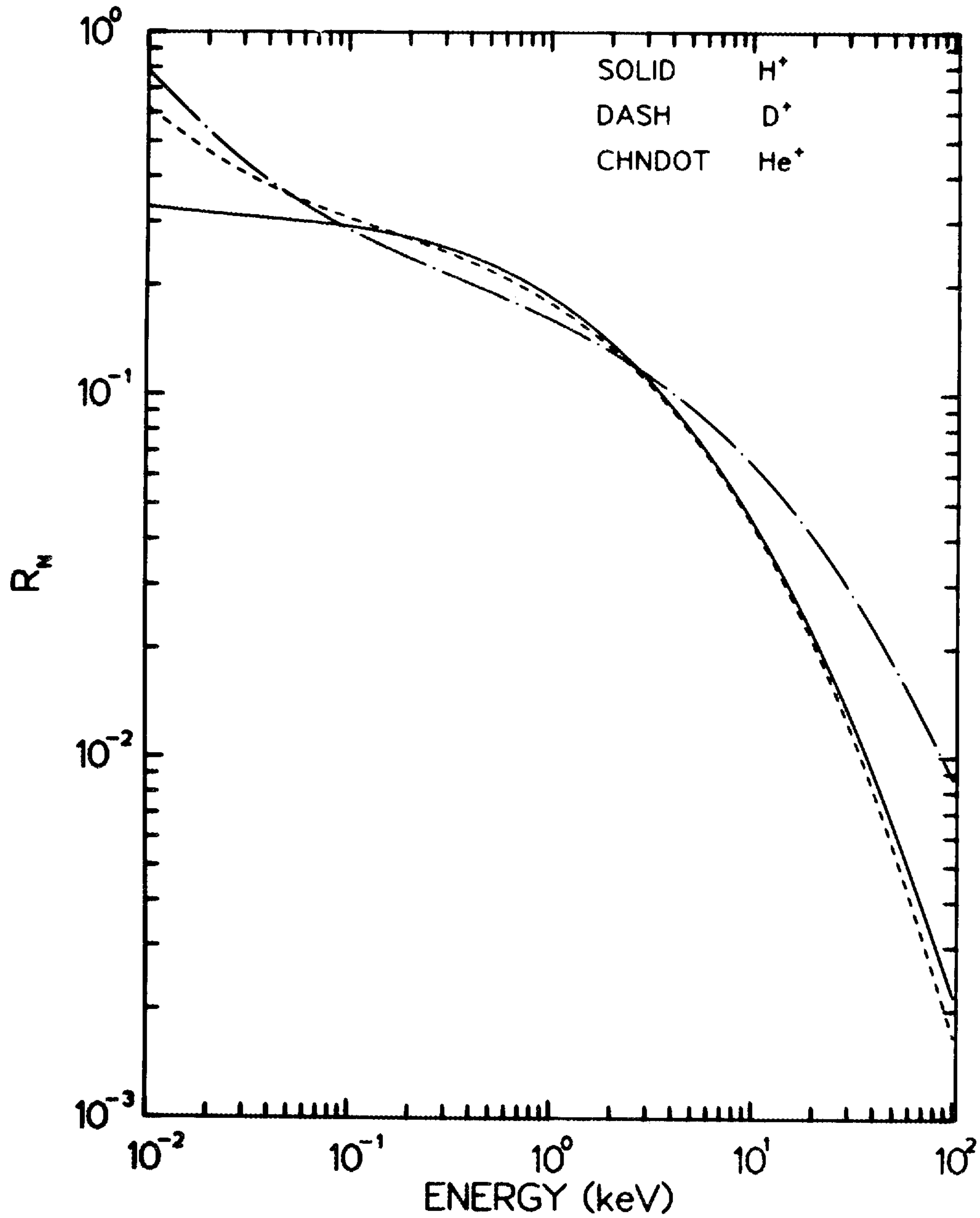

Energy Reflection Coefficients (R_E) for

H^+, D^+, and He^+ Incident on Ti

(normal incidence, room temperature)

Energy (keV)	R_E (H^+ on Ti)	R_E (D^+ on Ti)	R_E (He^+ on Ti)
1.0 E-02	2.80 E-01	4.24 E-01	5.46 E-01
2.0 E-02	2.53 E-01	3.06 E-01	3.57 E-01
4.0 E-02	2.25 E-01	2.36 E-01	2.53 E-01
6.0 E-02	2.08 E-01	2.07 E-01	2.12 E-01
1.0 E-01	1.84 E-01	1.78 E-01	1.74 E-01
2.0 E-01	1.51 E-01	1.46 E-01	1.37 E-01
4.0 E-01	1.16 E-01	1.17 E-01	1.09 E-01
6.0 E-01	9.65 E-02	1.00 E-01	9.46 E-02
1.0 E+00	7.35 E-02	8.06 E-02	7.86 E-02
2.0 E+00	4.68 E-02	5.55 E-02	5.92 E-02
4.0 E+00	2.69 E-02	3.43 E-02	4.22 E-02
6.0 E+00	1.84 E-02	2.43 E-02	3.34 E-02
1.0 E+01	1.07 E-02	1.46 E-02	2.39 E-02
2.0 E+01	4.57 E-03	6.31 E-03	1.38 E-02
4.0 E+01	1.68 E-03	2.23 E-03	7.06 E-03
6.0 E+01	8.65 E-04	1.09 E-03	4.47 E-03
1.0 E+02	3.46 E-04	3.97 E-04	2.33 E-03

References: T. Tabata et al., Report IPPJ-AM-18, IPP Nagoya, October 1981.

Accuracy: Unknown.

Notes: (1) These data are based generally on a theoretical formulation. They have been confirmed experimentally at energies between 1 and 10 keV to within 20% for most cases.

(2) It has been shown [Oen and Robinson, J. Nucl. Mat. 76 and 77, 370 (1978)] that as hydrogen builds up in the Ti the reflection coefficient decreases to a value appropriate to TiH_2.

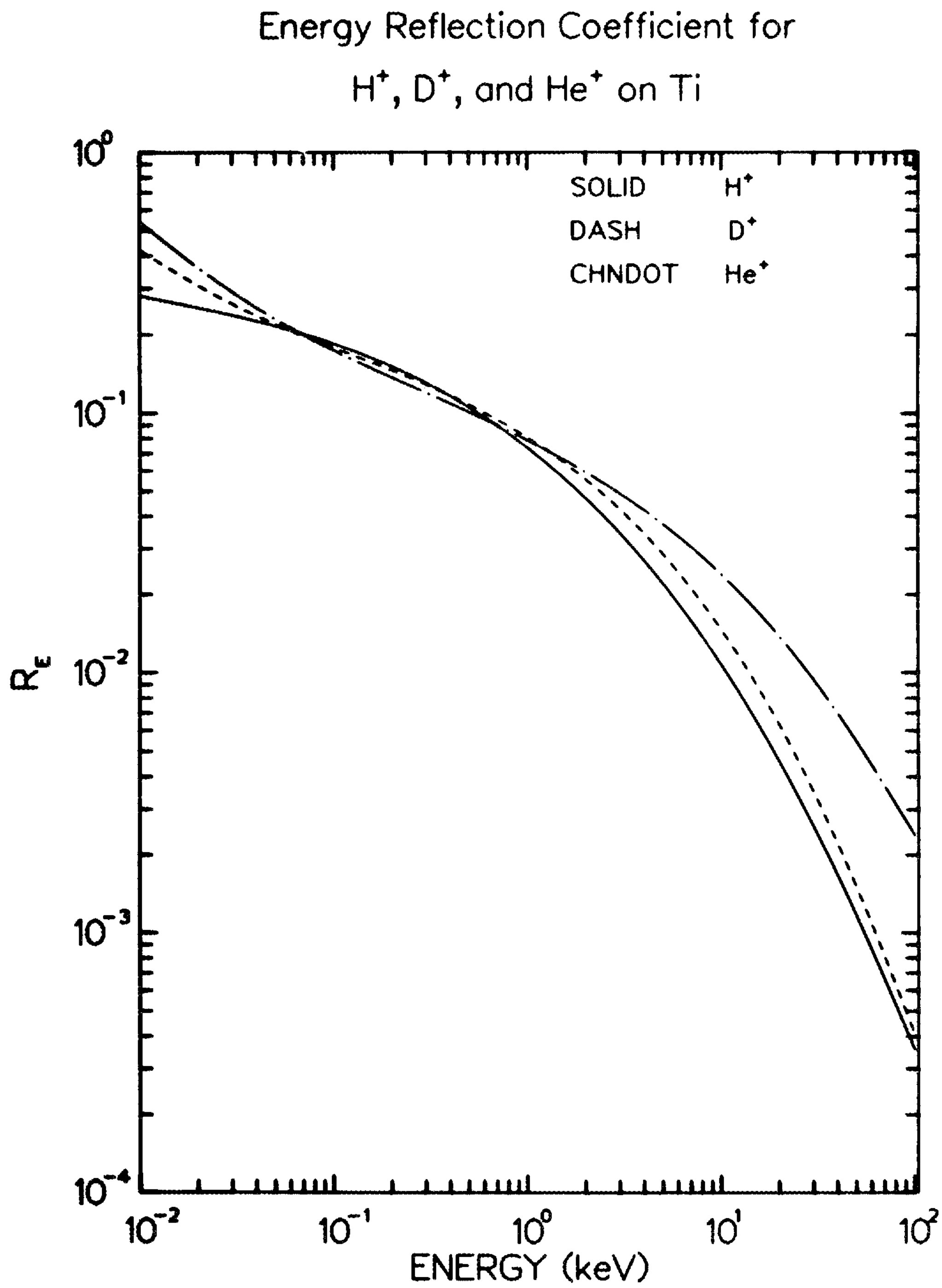
Energy Reflection Coefficient for
H+, D+, and He+ on Ti
SOLID H+
DASH D+
CHNDOT He+
R_E
10^0
10^-1
10^-2
10^-3
10^-4
10^-2
10^-1
10^0
10^1
10^2
ENERGY (keV)

Particle Reflection Coefficients (R_N) for H^+, D^+, and He^+ Incident on Fe and on Stainless Steel

(normal incidence, room temperature)

Energy (keV)	R_N (H^+ on Fe)	R_N (D^+ on Fe)	R_N (He^+ on Fe)
1.0 E-02	8.35 E-01	8.26 E-01	8.42 E-01
2.0 E-02	6.84 E-01	6.38 E-01	5.77 E-01
4.0 E-02	5.98 E-01	5.39 E-01	4.27 E-01
6.0 E-02	5.63 E-01	5.04 E-01	3.69 E-01
1.0 E-01	5.28 E-01	4.72 E-01	3.14 E-01
2.0 E-01	4.81 E-01	4.38 E-01	2.60 E-01
4.0 E-01	4.27 E-01	4.01 E-01	2.20 E-01
6.0 E-01	3.87 E-01	3.74 E-01	2.00 E-01
1.0 E+00	3.31 E-01	3.33 E-01	1.76 E-01
2.0 E+00	2.45 E-01	2.63 E-01	1.46 E-01
4.0 E+00	1.60 E-01	1.85 E-01	1.16 E-01
6.0 E+00	1.18 E-01	1.41 E-01	9.89 E-02
1.0 E+01	7.40 E-02	9.26 E-02	7.84 E-02
2.0 E+01	3.50 E-02	4.43 E-02	5.33 E-02
4.0 E+01	1.47 E-02	1.70 E-02	3.30 E-02
6.0 E+01	8.40 E-03	8.69 E-03	2.36 E-02
1.0 E+02	4.25 E-03	3.26 E-03	1.46 E-02

References: H^+ and D^+ Projectiles: W. Eckstein and H. Verbeek, Report IPP 9/32, MPI Garching, August 1979 (10^{-2} to 10 keV); T. Tabata et al., Report IPPJ-AM-18, IPP Nagoya, October 1981 (10 to 10^2 keV).

He^+ Projectiles: T. Tabata et al., Report IPPJ-AM-18, IPP Nagoya, October 1981.

Accuracy: Unknown.

Notes: (1) The data are largely for Fe but are expected also to be appropriate for stainless steel.

(2) Data for H^+ and D^+ are based primarily on computer models by the TRIM and MARLOWE codes. Experimental data for stainless steel at 2.5 to 15.0 keV agree with the model calculations which are for Fe.

(3) Data for He^+ are from a theoretical calculation that has not been confirmed by experiment.

Particle Reflection Coefficient for

H^+, H_2^+, He^+ on Fe

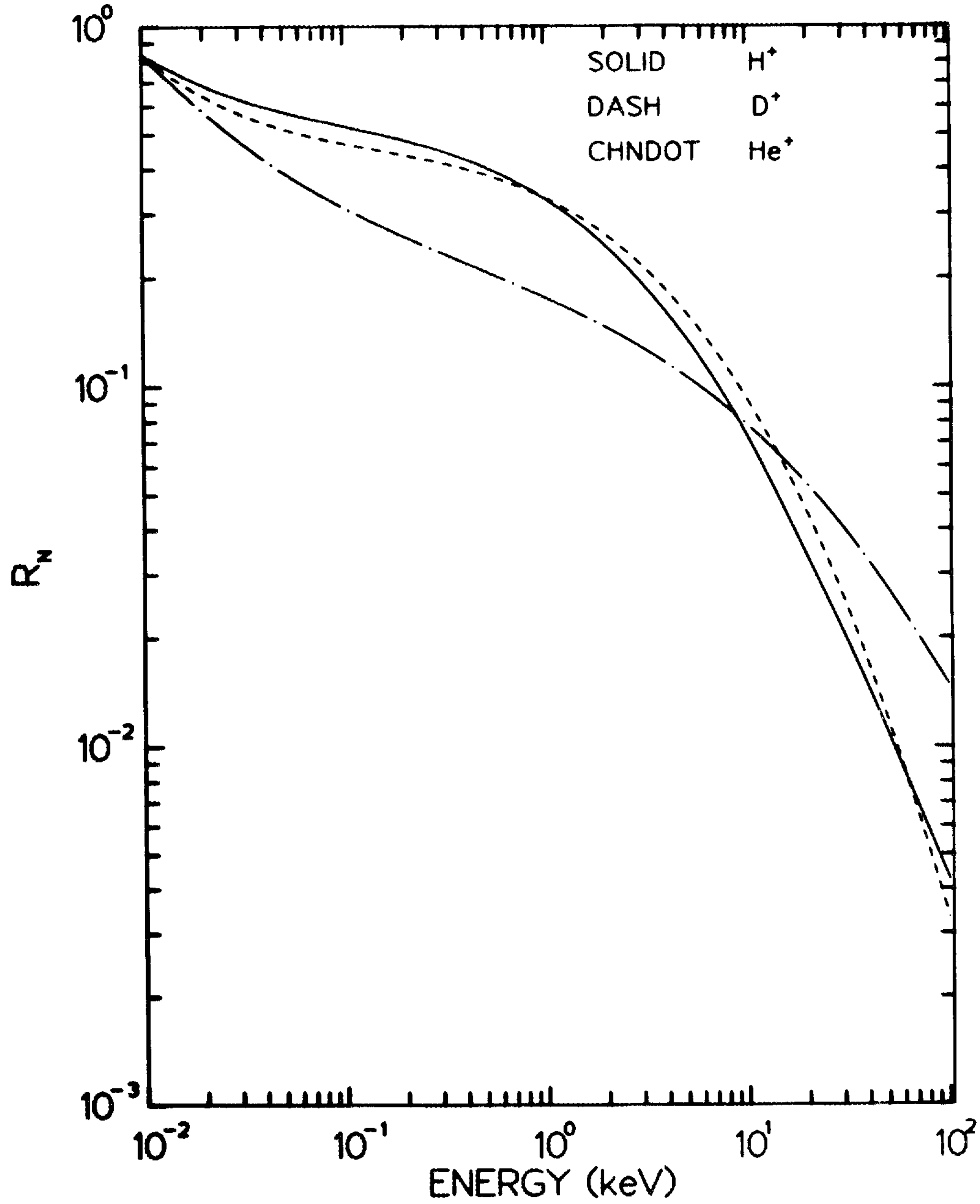

Energy Reflection Coefficients (R_E) for

H^+, D^+, and He^+ Incident on Fe and on Stainless Steel

(normal incidence, room temperature)

Energy (keV)	R_E (H^+ on Fe)	R_E (D^+ on Fe)	R_E (He^+ on Fe)
1.0 E-02	6.26 E-01	5.93 E-01	6.25 E-01
2.0 E-02	4.96 E-01	4.46 E-01	4.21 E-01
4.0 E-02	4.16 E-01	3.64 E-01	3.01 E-01
6.0 E-02	3.81 E-01	3.31 E-01	2.54 E-01
1.0 E-01	3.42 E-01	2.98 E-01	2.08 E-01
2.0 E-01	2.92 E-01	2.61 E-01	1.62 E-01
4.0 E-01	2.39 E-01	2.23 E-01	1.27 E-01
6.0 E-01	2.06 E-01	1.99 E-01	1.10 E-01
1.0 E+00	1.62 E-01	1.66 E-01	9.14 E-01
2.0 E+00	1.07 E-01	1.20 E-01	6.91 E-02
4.0 E+00	6.07 E-02	7.65 E-02	5.00 E-02
6.0 E+00	4.03 E-02	5.48 E-02	4.03 E-02
1.0 E+01	2.20 E-02	3.31 E-02	2.97 E-02
2.0 E+01	8.55 E-03	1.40 E-02	1.83 E-02
4.0 E+01	2.90 E-03	4.75 E-03	1.02 E-02
6.0 E+01	1.52 E-04	2.24 E-03	6.29 E-03
1.0 E+02	6.70 E-04	7.60 E-04	3.98 E-03

References: H^+ and D^+ Projectiles: W. Eckstein and H. Verbeek, Report IPP 9/32, MPI Garching, August 1979 (10^{-2} to 10 keV); T. Tabata et al., Report IPPJ-AM-18, IPP Nagoya, October 1981 (10 to 10^2 keV).

He^+ Projectiles: T. Tabata et al., Report IPPJ-AM-18, IPP Nagoya, October 1981.

Accuracy: Unknown.

Notes: (1) The data are largely for Fe but are expected also to be appropriate for stainless steel.

(2) Data for H^+ and D^+ are based primarily on computer models by the TRIM and MARLOWE codes. Experimental data for stainless steel at 2.5 to 15.0 keV agree to a few percent with the model calculations which are for Fe.

(3) Data for He^+ are from a theoretical calculation that has not been confirmed by experiment only to 15 keV.

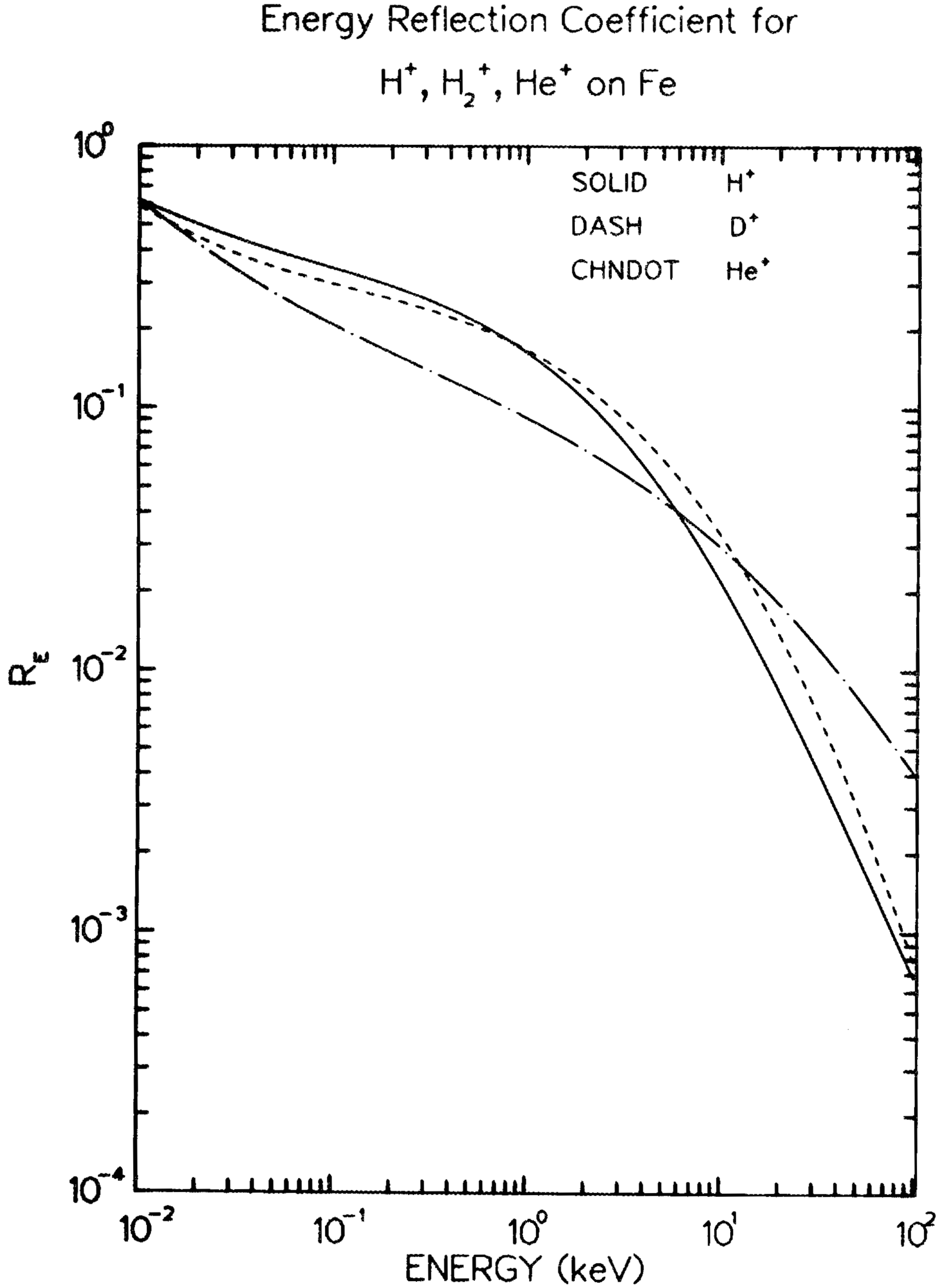
Energy Reflection Coefficient for
H⁺, H₂⁺, He⁺ on Fe
SOLID H⁺
DASH D⁺
CHNDOT He⁺
R_E
10^0
10^-1
10^-2
10^-3
10^-4
10^-2
10^-1
10^0
10^1
10^2
ENERGY (keV)

Particle Reflection Coefficients (R_N)

for H^+, D^+, and He^+ Incident on Mo

(normal incidence, room temperature)

Energy (keV)	R_N (H^+ on Mo)	R_N (D^+ on Mo)	R_N (He^+ on Mo)
1.0 E-02	3.66 E-01	9.22 E-01	7.87 E-01
2.0 E-02	3.28 E-01	6.69 E-01	5.57 E-01
4.0 E-02	3.06 E-01	5.24 E-01	4.18 E-01
6.0 E-02	2.96 E-01	4.65 E-01	3.61 E-01
1.0 E-01	2.85 E-01	4.09 E-01	3.06 E-01
2.0 E-01	2.70 E-01	3.49 E-01	2.49 E-01
4.0 E-01	2.50 E-01	2.99 E-01	2.07 E-01
6.0 E-01	2.34 E-01	2.70 E-01	1.86 E-01
1.0 E+00	2.11 E-01	2.34 E-01	1.62 E-01
2.0 E+00	1.73 E-01	1.84 E-01	1.33 E-01
4.0 E+00	1.30 E-01	1.34 E-01	1.06 E-01
6.0 E+00	1.05 E-01	1.07 E-01	9.18 E-02
1.0 E+01	7.64 E-02	7.62 E-02	7.45 E-02
2.0 E+01	4.43 E-02	4.30 E-02	5.35 E-02
4.0 E+01	2.23 E-02	2.09 E-02	3.60 E-02
6.0 E+01	1.39 E-02	1.27 E-02	2.75 E-02
1.0 E+02	7.01 E-03	6.20 E-03	1.88 E-02

References: T. Tabata et al., Report IPPJ-AM-18, IPP Nagoya, October 1981.

Accuracy: Unknown.

Notes: (1) These data are based generally on a theoretical formulation. They have been confirmed experimentally at energies between 2.5 and 20 keV to within +5%.

Particle Reflection Coefficient for

H^+, H_2^+, He^+ on Mo

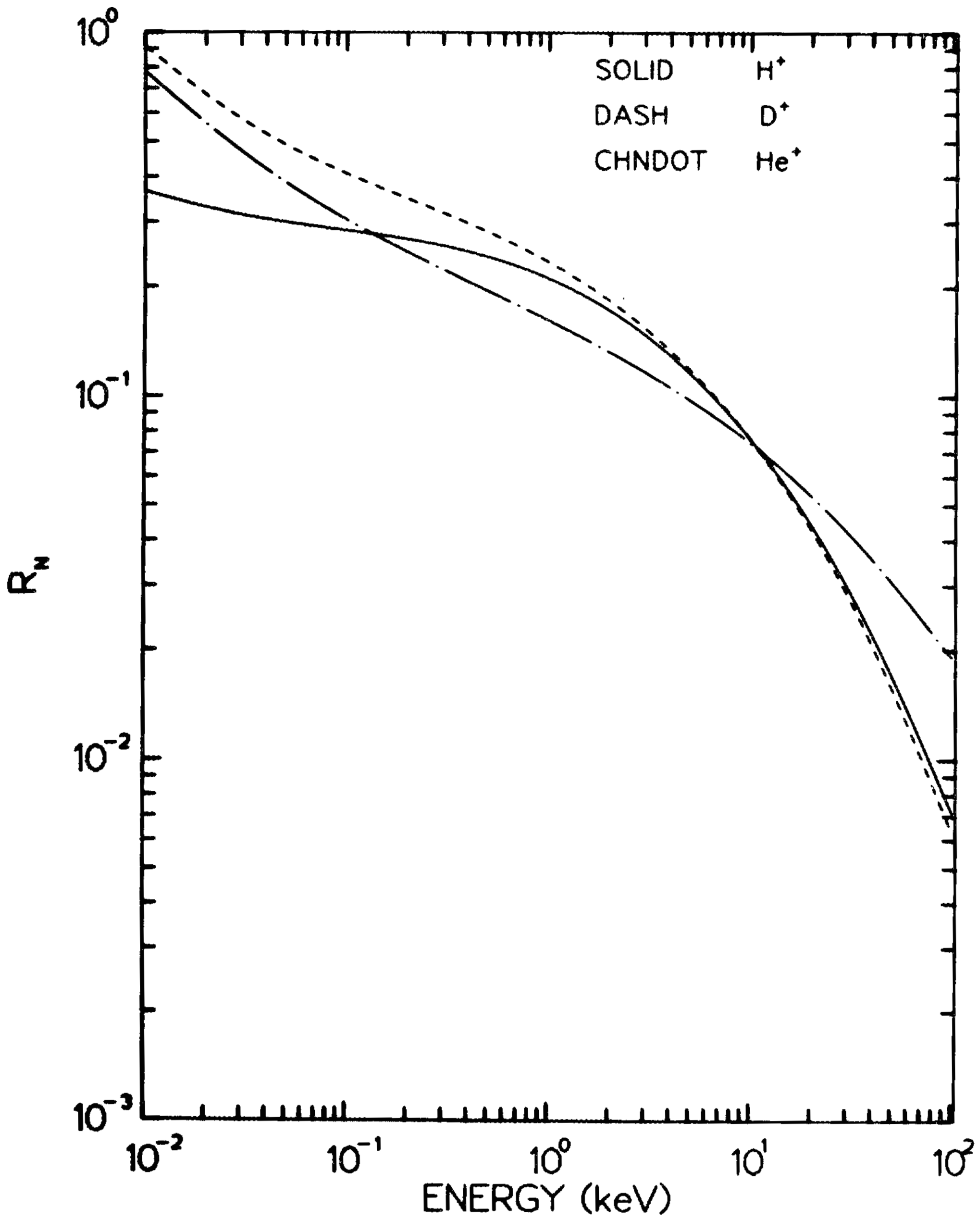

Energy Reflection Coefficients (R_E)

for H^+, D^+, and He^+ Incident on Mo

(normal incidence, room temperature)

Energy (keV)	R_E (H^+ on Mo)	R_E (D^+ on Mo)	R_E (He^+ on Mo)
1.0 E-02	3.18 E-01	6.61 E-01	6.05 E-01
2.0 E-02	2.77 E-01	4.78 E-01	4.24 E-01
4.0 E-02	2.43 E-01	3.64 E-01	3.10 E-01
6.0 E-02	2.24 E-01	3.15 E-01	2.62 E-01
1.0 E-01	2.01 E-01	2.66 E-01	2.14 E-01
2.0 E-01	1.70 E-01	2.12 E-01	1.65 E-01
4.0 E-01	1.38 E-01	1.67 E-01	1.28 E-01
6.0 E-01	1.20 E-01	1.44 E-01	1.10 E-01
1.0 E+00	9.67 E-02	1.16 E-01	9.06 E-02
2.0 E+00	6.81 E-02	8.31 E-02	6.82 E-02
4.0 E+00	4.41 E-02	5.51 E-02	4.98 E-02
6.0 E+00	3.28 E-02	4.15 E-02	4.07 E-02
1.0 E+01	2.14 E-02	2.77 E-02	3.08 E-02
2.0 E+01	1.08 E-02	1.43 E-02	2.01 E-02
4.0 E+01	4.79 E-03	6.49 E-03	1.23 E-02
6.0 E+01	2.79 E-03	3.80 E-03	8.91 E-03
1.0 E+02	1.31 E-03	1.78 E-03	5.69 E-03

References: T. Tabata et al., Report IPPJ-AM-18, IPP Nagoya, October 1981.

Accuracy: Unknown.

Notes: (1) These data are based generally on a theoretical formulation. They have been confirmed experimentally at energies between 2.5 and 20 keV to within ±5%.

Energy Reflection Coefficient for

H^+, H_2^+, He^+ on Mo

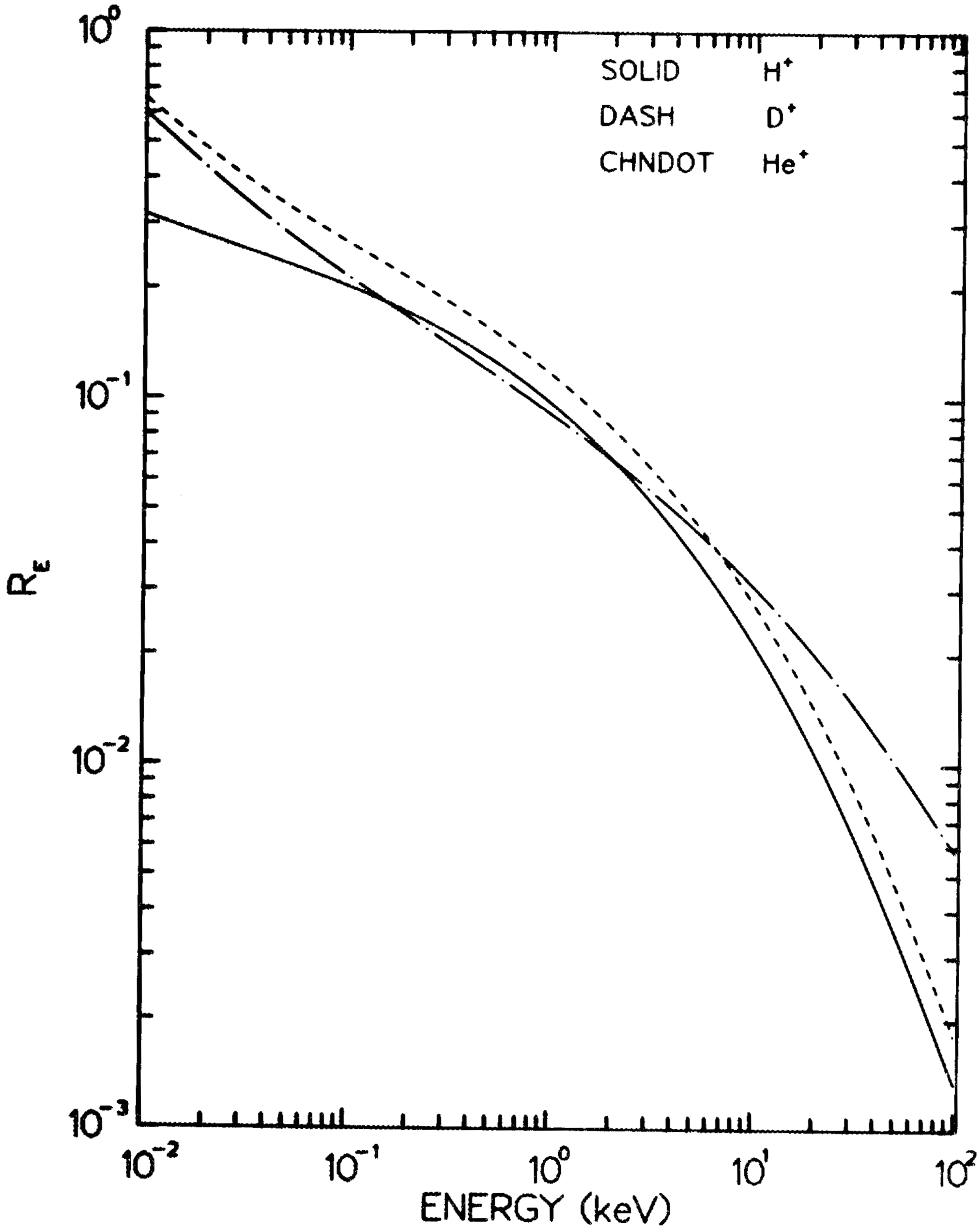

Example of Charge State Distributions of Scattered Particles. Data Show, at a Specific Recoil Energy, the Fraction of Total Recoil Flux which is H, H^+, and H^-. For Stainless Steel Bombarded with 10 keV Protons (normal incidence, room temperature)

	Charge State Fraction (%)		
Recoil Energy (keV)	N^o/N^{tot}	N^+/N^{tot}	N^-/N^{tot}
0.0	100.0	0.0	0.0
1.0 E+00	90.7	5.0	4.5
2.0 E+00	88.5	7.0	5.5
3.0 E+00	87.6	8.0	5.2
4.0 E+00	87.0	8.7	4.8
5.0 E+00	86.5	9.4	4.5
6.0 E+00	85.9	10.2	3.8
7.0 E+00	85.5	11.0	3.5
8.0 E+00	85.1	12.0	2.8
9.0 E+00	84.7	13.0	2.4

Reference:

W. Eckstein, F. E. P. Matschke, and H. Verbeek, J. Nucl. Mat. 63, 199 (1976).

Accuracy: + 1%.

Notes: (1) The data are to be interpreted as follows. For an impact energy E_o a recoil energy interval dE is selected centered on a recoil energy E. The ratios presented are the flux of scattered particles, with the defined charge state, recoiling into the interval dE, divided by the total flux of all particles (i.e., all charge states) into that same interval dE.

(2) It is generally found that these ratios are approximately the same for all target materials and are independent of incident energy, incident angle and exit angle. (See R. Behrisch et al., in Atomic Collisions in Solids, ed. by S. Datz et al., Plenum Publ. Corp., New York, 1975, p. 315).

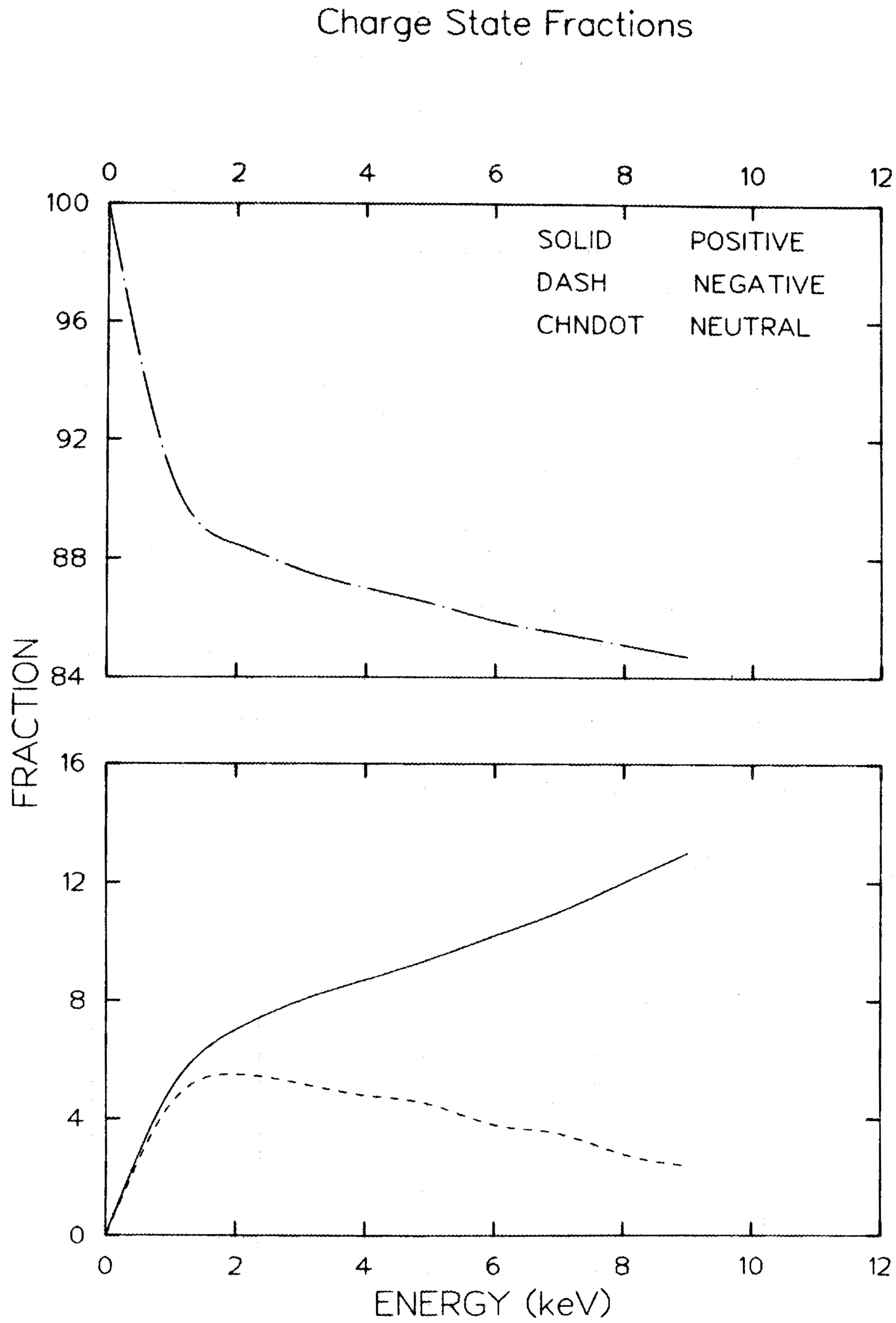
Charge State Fractions
0
2
4
6
8
10
12
100
96
92
88
84
SOLID POSITIVE
DASH NEGATIVE
CHNDOT NEUTRAL
FRACTION
16
12
8
4
0
ENERGY (keV)

Example of Energy Distributions for Different Scattering Angles.

Data for 5 keV H^+ Incident on Stainless Steel at an Angle of 45° to the Surface Normal

(room temperature)

Reflected Flux (defined below) at scattering angle ϕ (defined below)

Recoil Energy (keV)	ϕ = 50°	55°	85°	115°	145°
0	5.30 E-06	0	3.80 E-04	4.82 E-04	1.12 E-03
5.0 E-01	2.57 E-05	4.47 E-05	4.66 E-04	7.27 E-04	7.93 E-04
1.0 E+00	3.83 E-05	9.51 E-04	5.67 E-04	8.22 E-04	6.17 E-04
1.5 E+00	5.23 E-05	1.21 E-04	6.55 E-04	8.11 E-04	5.04 E-04
2.0 E+00	7.21 E-05	1.57 E-04	7.10 E-04	7.35 E-04	4.04 E-04
2.5 E+00	9.77 E-05	2.12 E-04	7.17 E-04	6.23 E-04	3.03 E-04
3.0 E+00	1.24 E-04	2.60 E-04	6.68 E-04	4.97 E-04	2.10 E-04
3.5 E+00	1.43 E-04	2.75 E-04	5.63 E-04	3.72 E-04	1.38 E-04
4.0 E+00	1.41 E-04	2.44 E-04	4.08 E-04	2.53 E-04	9.59 E-05
4.5 E+00	9.83 E-05	1.61 E-04	2.14 E-04	1.38 E-04	6.58 E-05
5.0 E+00	0	0	0	0	0

References: W. Eckstein and H. Verbeek, J. Nucl. Mater. 93 and 94, 518 (1980).

Accuracy: Relative values +10%.

Notes: (1) The data are for a quantity equal to the number of scattered particles per incident particle and per steradian reflected into the energy interval of 64.3 eV.

(2) The incident beam, reflected particles and surface normal are all in the same plane. Incidence angle (45°) is measured from the surface normal. Scattering angle is defined, as in the original publication, as the deviation from the projectile's trajectory. Thus a scattering angle of 50° is a direction 85° (180-45-50) from the surface normal; a scattering angle of 145° in a direction 0° (180-45-145) from the surface normal.

(3) Substantial further information of this type for other energies and materials is to be found in Report IPP 9/32, by W. Eckstein and H. Verbeek, Max-Planck Institute fur Plasmaphysik, Garching, August 1979. See also references cited therein.

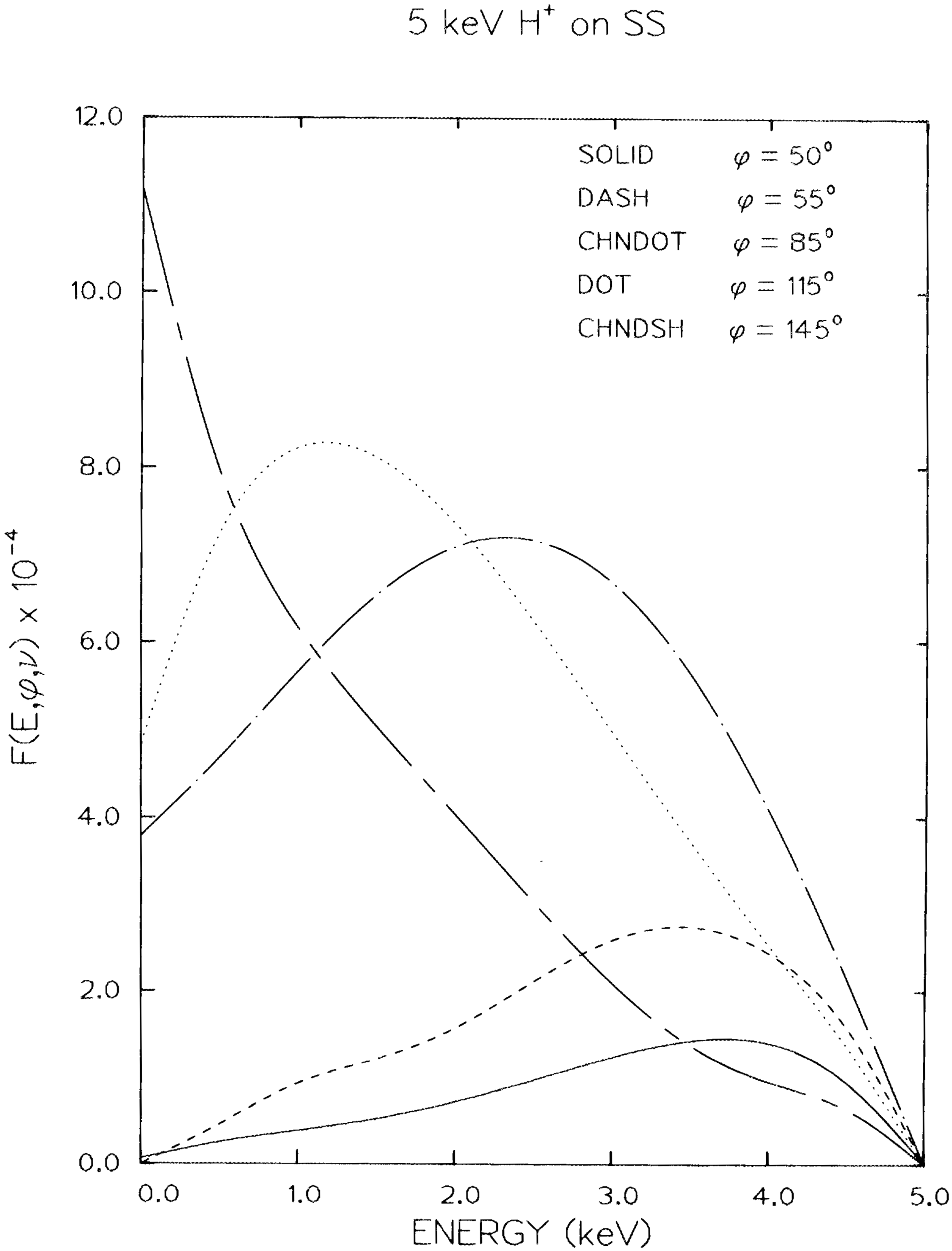
5 keV H+ on SS
SOLID φ = 50°
DASH φ = 55°
CHNDOT φ = 85°
DOT φ = 115°
CHNDSH φ = 145°
F(E,φ,ν) × 10^-4
12.0
10.0
8.0
6.0
4.0
2.0
0.0
0.0
1.0
2.0
3.0
4.0
5.0
ENERGY (keV)

F. TRAPPING AND REEMISSION

Introductory Notes

The subjects of trapping, retention and reemission remain in a confused state. Each is in fact an operationally defined quantity related to the circumstances of an experiment; none can be regarded as a fundamental physical quantity. Two approaches may be used in modelling device operation. One may adopt a model for the thermal energy processes occurring in a candidate wall material and predict behavior using fundamental quantities such as diffusion solubility and recombination. Alternatively one may use an empirical measurement of a specific signal (e.g., reemission rate). Both approaches are discussed below and relevant input data provided on the following pages of tables and graphs.

1. Modelling. In principle the reemission and retention of fuel in a wall material may be represented by a model that uses solubility, diffusion and surface recombination. This may be used to predict the behavior of a device wall for the specific conditions of flux, temperature and time expected in a device; the model may include the important temporal dependence of these quantities. We define below the relevant parameters and list major references for modelling codes. The principal limitation of this approach is that the quoted parameters are for virgin materials and are undoubtedly incorrect for a wall material during device operation. For example the data for diffusion are for undamaged metals; undoubtedly radiation enhanced diffusion in a radiation damaged material will be greatly different.

(a) Diffusivity. Hydrogen migration in a metal is characterized by Diffusivity D that can be written as an Arrhenius equation

$$D = D_o \exp(-E_D/kT) \ . \qquad (1)$$

Here T is material temperature, E_D is the migration energy for diffusion and k is Boltzmann's constant. In the tabular data we quote D_o and E_D from which D may be computed.

(b) Solubility. The solubility S of hydrogen in a metal is given by Sievert's law.

$$S = S_o \sqrt{P} \exp(-E_S/kT) \ . \qquad (2)$$

E_S is the heat of solution, P is gas pressure and again T is temperature. In the tabular data we quote S_o and E_S from which S may be computed.

(c) Recombination. The rate at which hydrogen atoms recombine on a surface to form molecules which desorb is operationally defined by the equation

$$\phi = 2\sigma k_r \ c^2 \ . \qquad (3)$$

Here ϕ is the flux of desorbing molecules (measured in terms of the number of atoms desorbed per cm^2 per sec), c is the near surface volume concentration of hydrogen atoms (atoms/cm^3), σ is a dimensionless surface roughness factor (true surface area/projected area) and the factor 2 is introduced because each molecule contains two atoms. The quantity k_r is a constant of proportionality called the recombination rate. Most measurements of recombination rate provide a value of $2\sigma k_r$ with no specification of σ. It is normally found that $2\sigma k_r$ obeys an Arrhenius expression of the form

$$2\sigma k_r = 2\sigma k_{ro} \exp(-E_r/kT) \tag{4}$$

where E_r is an activation energy for recombination, T is material temperature and k_{ro} is a constant. In the tabular data we quote $2\sigma k_{ro}$ and E_r from which $2\sigma k_r$ can be calculated.

The reader is cautioned that the whole definition of this quantity may be incorrect. The reemission of surface hydrogen must involve first a diffusion of atoms to a recombination site, secondly the recombination itself and thirdly the reemission of a molecule from the surface. The measured recombination rate includes all three factors. It has been suggested (Jin-gor Chang and E. W. Thomas, J. Appl. Phys., to be published) that for a steel surface the recombination rate measured through application of Eq. 3 is in fact not the recombination step at all; for C and O recombination on Pt it has been suggested [J. D. Doll and D. L. Freeman, Surf. Sci. 134, 769 (1983)] that in fact surface diffusion is the rate limiting step.

(d) Models. A variety of modelling codes have been used to interrelate the fundamental quantities. A major limitation is that the quoted values of D, S and $2\sigma k_r$ are for virgin materials exposed to thermal energy particles while in practice wall materials will be radiation damaged and sputter eroded; moreover particle impact is energetic. Principle references to codes: -

DIFFUSE - M. I. Baskes, Sandia National Laboratories, Report SAND80-8201 (1980).

PERI - P. Wienhold, M. Profant, F. Waelbroeck, J. Winter, J. Nucl. Mater. 93 and 94, 866 (1980).

ELM Model - D. K. Brice, B. L. Doyle and W. R. Wampler, J. Nucl. Mater. 111 and 112, 598 (1982).

Gaussian Trapping Model - K. Sone and G. M. McCracken, J. Nucl. Mater. 111 and 112, 606 (1982).

2. Direct Measurement. Data on trapping and reemission are traditionally presented in various forms. Experiments may record what is retained in a surface or what is emitted from a surface as a function of such parameters

as cumulative dose, projectile energy, target temperature, radiation damage and other preliminary treatments. In the data compendium we have generally retained the method of presentation employed in the original publication. The forms of display, their definitions, and relationships are as follows.

(a) Reemission refers to the emission of gas from the target while the target is being bombarded by the projectile ions; the reemission rate is generally measured by the rise in partial pressure of the projectile species as monitored in the vessel which contains the target. If the flux of ions (or atoms) incident on the surface is F_i and the flux of atoms emerging is F_e, then the rate of reemission, expressed as a percentage, is given by:

$$\text{reemission rate } R\ (\%) = \frac{F_e}{F_i} \times 100$$

The general form of reemission rate as a function of dose is shown in Fig. 1; reemission rate is plotted as a function of cumulative areal

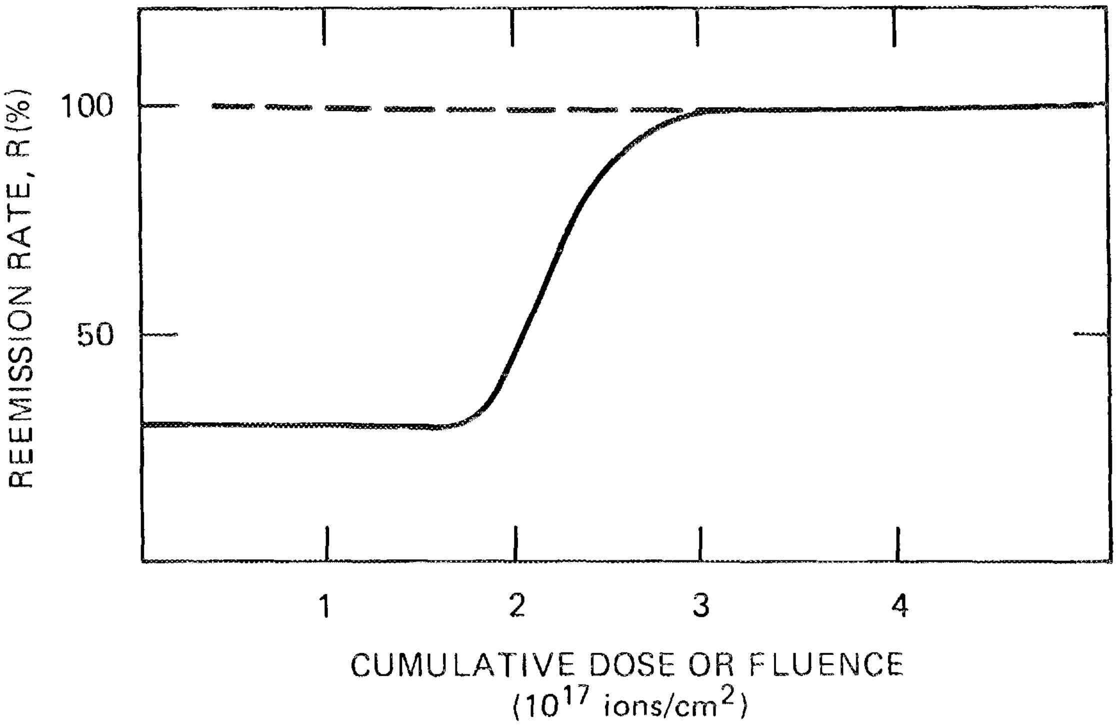

Fig. 1. General form of reemission rate as a function of dose.

dose (ions or atoms/cm^2), otherwise known as Fluence. At low dose the reemission is equal to the backscattered fraction; all ions not backscattered are retained or trapped. As dose increases the reemission rate increases to a saturated value, which is normally 100%; at this value an atom is ejected for every ion or atom incident.

(b) Trapping refers to the fraction of the incident flux which is retained in the target; this is generally determined by a direct measure of the retained projectile density. The measured quantity is the areal density of retained projectiles, or Trapped Fluence (atoms/cm^2), plotted as a function of the incident projectile dose or fluence; a facsimile of such a presentation is shown in Fig. 2. For

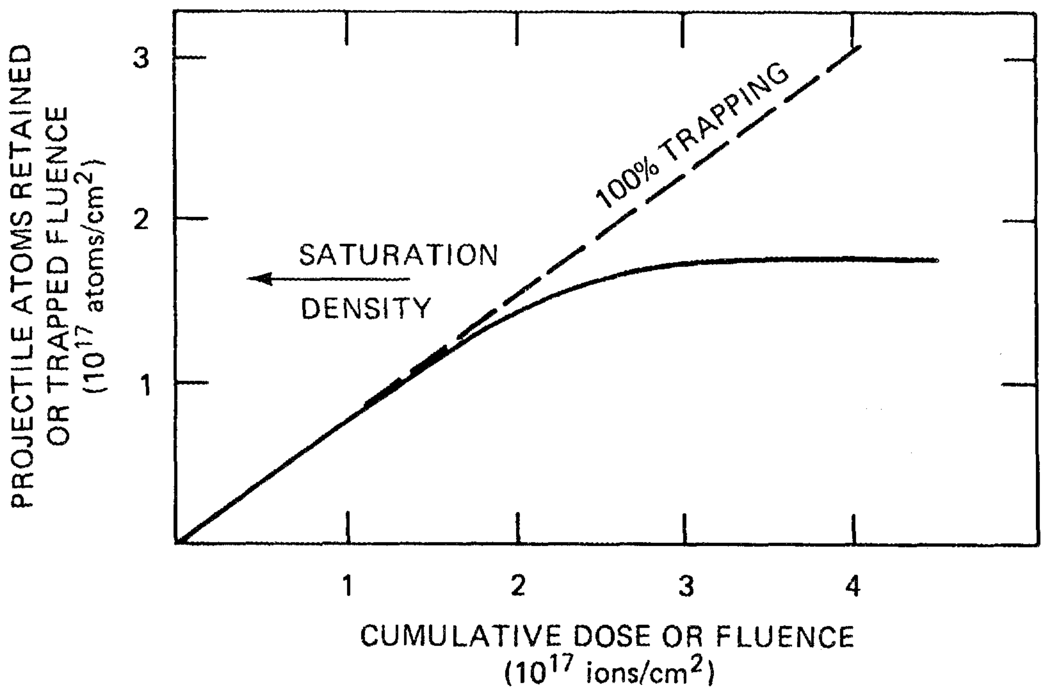

Fig. 2. Retained projectile as a function of dose.

low dose the trapped density increases linearly with fluence; however, the trapped density is less than incident fluence by an amount equal to the fraction backscattered. The dashed line shows the behavior expected if all incident particles not reflected are retained. At high dose the trapped density saturates, corresponding to the 100% reemission in Fig. 1; at this point, for each new ion incident one atom in the target is ejected.

One can relate the presentations of Figs. 1 and 2 as follows: The projectile atoms retained (Fig. 2) is equal to

$$\left(1 - \frac{R}{100}\right) \times \text{Fluence} \ ,$$

where R is the reemission rate (in %) from Fig. 1.

(c) Saturation Density is the areal density of the retained atoms at saturation (i.e., at 100% reemission); in Fig. 1 it is the number of atoms represented by the area between the reemission curve and the 100% reemission line. An alternative terminology is Fluence Trapped at 100% Reemission.

(d) Trapping Coefficient is the probability that an incident ion will be retained. Its maximum value of unity represents the condition where each incident ion is retained. The trapping coefficient will vary with fluence (or dose), eventually dropping to zero when the target saturates and each new ion incident causes one atom to be ejected. Trapping coefficient is equal to

$$1 - \frac{R}{100}$$

where R is the reemission rate (in %) discussed in note 2a above.

(e) It should be noted that the reemission behavior is closely related to Temperature. The behavior shown in Figs. 1 and 2 is appropriate to temperatures where the implanted species has negligible diffusion. At temperatures where diffusion is significant the rising portion of Fig. 1 commences at essentially zero dose; this means also that the retained density of atoms displayed in Fig. 2 always falls below the 100% trapping line.

(f) Replacement Cross Sections refer to the replacement of implanted species (e.g., D) by the arrival of a subsequent atom (such as H). In general, the cross section is evaluated as follows: the target is implanted with one species (e.g., D) to a saturation density (or trapped fluence at saturation) of n_{sat} atoms/cm^2. Subsequently the second species (e.g., H^+) is directed onto the target with a flux density J_o (atoms/cm^{2}s), and the trapped fluence decreases with time t as

$$n = n_{sat} \exp - (J_o \sigma t) \ .$$

Consequently, the rate of removal of the first species (D in our example) is given by

$$\frac{dn}{dt} = n_{sat} \, J_o \sigma \exp - (J_o \sigma t) \ .$$

σ is called the replacement cross section (or sometimes the gas sputtering cross section).

(g) Replacement Efficiency is related to replacement cross section defined in note 2f above. It is the number of primary implanted atoms (in our example, D) removed for every secondary particle (in our example, H) incident; dn_D/dn_H for our example. It is often plotted as a function of the ratio of the fluence of incoming secondary particles (H in our sample) to the saturation density of the primary implant (D in our example), that is to say, as a function of n_H/n_{sat}.

3. Major Reviews. Two major reviews and data compendium are available.

(a) R. A. Langley et al., Nucl. Fusion, Special Edition, "Data Compendium for Plasma — Surface Interactions (1984) - see particularly Chapter 3.

(b) S. Yamaguchi, K. Ozawa, Y. Nakai and Y. Sugizaki, Japan Atomic Energy Research Institute, Report JAERI-M 82-118 (Aug. 1982).

Selected Values of Hydrogen (H) Diffusivity and Solubility for Various Metals and Alloys

$D = D_o \exp - E_d/kT \quad cm^2\ s^{-1}$

$S = S_o\ p^{1/2} \exp - E_s/kT \quad H/cm^3\ (atm)^{1/2}$

Material	D_o $\frac{cm^2}{s}$	E_d eV	S_o $\frac{H}{cm^3 (atm)^{1/2}}$	E_s eV	Ref[1]
Carbon	3.3 E-02	4.3 E 00	9.0 E 15	-1.4 E 00	a
Aluminum	2.1 E-01	4.7 E-01	3.1 E 21	8.4 E-01	b
Titanium	1.8 E-02	5.4 E-01	1.5 E 20	-4.9 E-01	c
304 Stainless	2.0 E-03	5.4 E-01	7.7 E 19	1.1 E-01	d
Nickel	6.9 E-03	4.2 E-01	3.1 E 20	1.6 E-01	e
INC 718	1.0 E-02	5.2 E-01	4.1 E 19	6.0 E-02	f
Copper	1.1 E-02	4.0 E-01	1.3 E 20	3.7 E-01	b
Molybdenum I	4.8 E-03	3.9 E-01	2.7 E 20	5.4 E-01	g
Molybdenum II	2.4 E-04	1.1 E-01	2.3 E 21	6.8 E-01	h
Tungsten	4.1 E-03	3.9 E-01	6.9 E 20	9.8 E-01	i

References: (a) R. A. Causey, T. S. Elleman and K. Verghese, Carbon 17, 323 (1979).

(b) W. Eichenauer and A. Pebler, Z. Metallkd. 48, 373 (1957).

(c) R. J. Wasilewsky and G. M. Kehl, Metallurgical 50, 225 (1954). J. R. Morton and D. S. Stark, Trans. Faraday Soc. 56, 354 (1960).

(d) M. R. Louthan and R. D. Derrick, Corros. Sci. 15, 287 (1965).

(e) J. Volkl and G. Alefeld in *Diffusion in Solids*, edited by A. S. Nowick and J. J. Burton, Academic Press, 231 (1975). W. M. Robertson, Z. Metallkd. 64, 436 (1973).

(f) W. M. Robertson, Metallurgical Trans. 8A, 1709 (1977).

(g) W. G. Perkins, J. Vac. Sci. Technol. 10, 543 (1973). W. A. Oates and R. B. McLellan, Scr. Metall. 6, 349 (1972).

(h) H. Katsuta, R. B. McLellan, K. Furukawa, J. Phys. Chem. Solids 43, 533 (1982).

(i) R. Frayenfelder, J. Vac. Sci. Technol. 6, 388 (1969). R. Frayenfelder, J. Chem. Phys. 48, 3955 (1967).

Notes:

(1) This material is quoted *in toto* from a review by R. A. Langley et al., Nucl. Fusion, Special Edition, "Data Compendium for Plasma-Surface Interactions" (1984).

(2) For explanation of symbols, see introduction.

(3) The data are all for materials that have not been subjected to radiation damage.

(4) Two values are quoted for Molybdenum because there is controversy in the literature.

Selected Values for Deuterium (D) Recombination on Steel and Gold

$$2\sigma k_r = 2\sigma k_{ro} \exp - E_r/kT$$

Material	Condition	$2\sigma k_{ro}$ cm^4/s	E_r (eV)	Ref.
304 Stainless	Electro polished	1.3 E-17	8.1 E-01	(a)
304 Stainless	Sputter cleaned	9.6 E-20	3.4 E-01	(a)
Gold	Polycrystalline - no surface contamination (not dependent on prior bombardment)	2.2 E-23	3.2 E-01	(b)

References: (a) S. M. Myers and W. R. Wampler, J. Nucl. Mater. 111 & 112, 579 (1982).
(b) Jin-gor Chang and E. W. Thomas, (to be published).

Accuracy: The data for steel should be used with great caution. Values are greatly influenced by pre-treatment that changes surface composition. None of the data quoted here is for properly defined surfaces and values ranging from 10^{-29} cm^4 s^{-1} to 10^{-24} cm^4 s^{-1} are reported in the literature for 300 K stainless steel [see review by Langley, Nucl. Fusion, Special Edition, "Data Compendium for Plasma-Surface Interactions," (1984)].

Notes: The data are determined for temperatures in the range 425 K to 575 K for steel and 400 K to 550 K for gold.

Trapped Fluence as a Function of Incident

Fluence for 50-, 150-, and 300-eV D^+ on C

(normal incidence, room temperature, polycrystalline material)

Fluence Incident (D^+ ions/cm^2)	Fluence Trapped (D atoms/cm^2)		
	50 eV	150 eV	300 eV
2.0 E 15	1.2 E 15	1.4 E 15	2.0 E 15
3.0 E 15	1.7 E 15	2.0 E 15	3.0 E 15
5.0 E 15	2.6 E 15	3.3 E 15	5.0 E 15
1.0 E 16	4.4 E 15	6.2 E 15	1.0 E 16
2.0 E 16	6.6 E 15	1.2 E 16	2.0 E 16
3.0 E 16	8.0 E 15	1.6 E 16	2.6 E 16
5.0 E 16	9.8 E 15	2.0 E 16	3.5 E 16
1.0 E 17	1.2 E 16	2.6 E 16	4.7 E 16
2.0 E 17	1.3 E 16	2.9 E 16	5.5 E 16
3.0 E 17	1.4 E 16	3.0 E 16	5.8 E 16
5.0 E 17	1.4 E 16	3.0 E 16	6.0 E 16
1.0 E 18	1.4 E 16	3.0 E 16	6.1 E 16

Reference:

G. Staudenmaier et al., J. Nucl. Mater. 84, 149 (1979).

Accuracy: Unspecified

Note: (1) For a definition of trapping see note 2b at the beginning of this section.

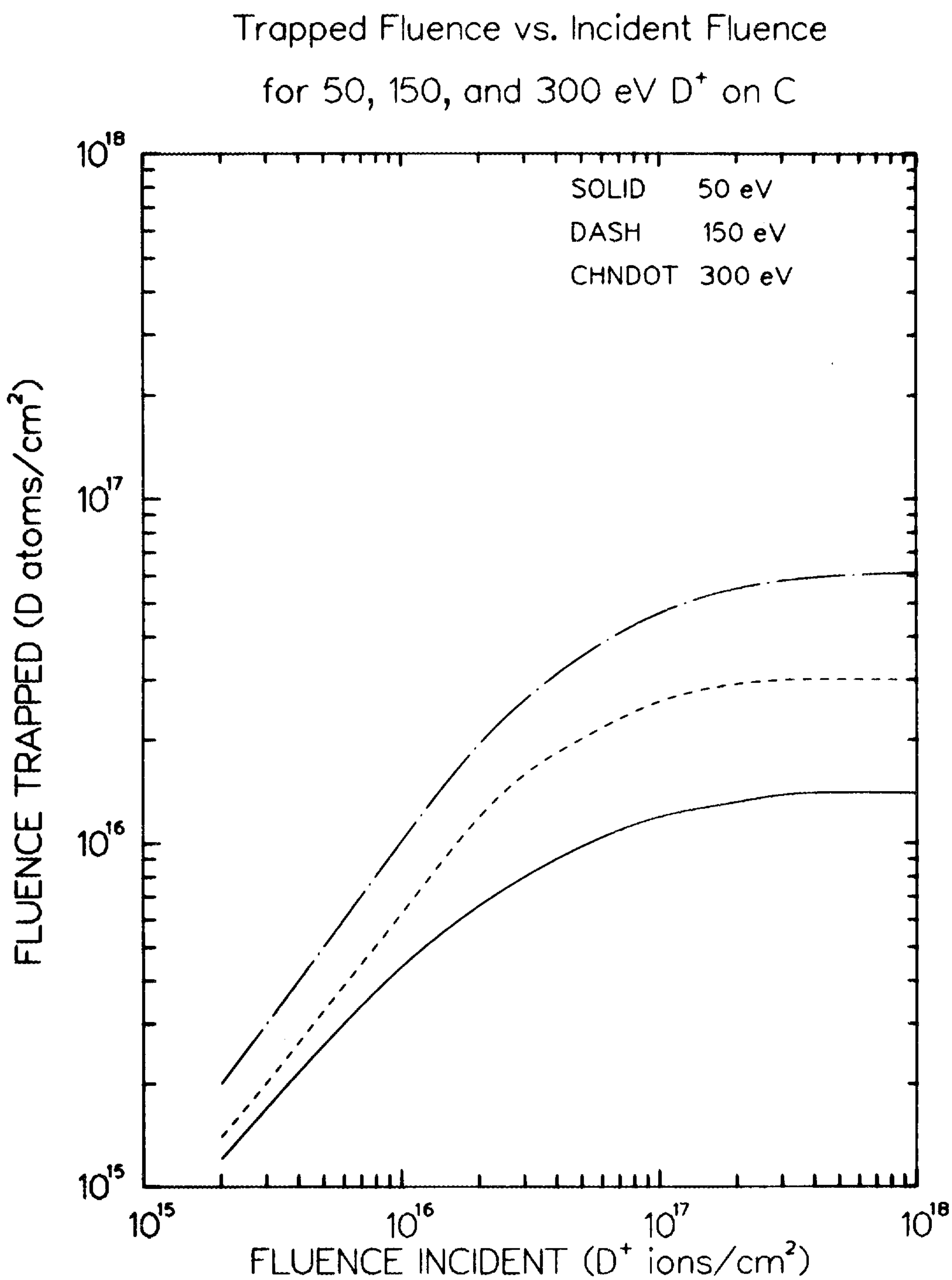
Trapped Fluence vs. Incident Fluence
for 50, 150, and 300 eV D+ on C
SOLID 50 eV
DASH 150 eV
CHNDOT 300 eV
FLUENCE TRAPPED (D atoms/cm2)
FLUENCE INCIDENT (D+ ions/cm2)
10^15
10^16
10^17
10^18

Trapped Fluence as a Function of Incident

Fluence for 500-eV, 700-eV, and 1-keV D^+ on C

(normal incidence, room temperature
polycrystalline material)

Fluence Incident (D^+ ions/cm^2)	Fluence Trapped (D atoms/cm^2)		
	500 eV	700 eV	1 keV
2.0 E 15	2.0 E 15	2.0 E 15	2.0 E 15
3.0 E 15	3.0 E 15	3.0 E 15	3.0 E 15
5.0 E 15	5.0 E 15	5.0 E 15	5.0 E 15
1.0 E 16	1.0 E 16	1.0 E 16	1.0 E 16
2.0 E 16	2.0 E 16	2.0 E 16	2.0 E 16
3.0 E 16	3.0 E 16	3.0 E 16	3.0 E 16
5.0 E 16	5.0 E 16	5.0 E 16	5.0 E 16
1.0 E 17	7.8 E 16	8.7 E 16	9.3 E 16
2.0 E 17	8.8 E 16	1.1 E 17	1.2 E 17
3.0 E 17	9.0 E 16	1.2 E 17	1.3 E 17
5.0 E 17	9.0 E 16	1.2 E 17	1.3 E 17
1.0 E 18	9.0 E 16	1.2 E 17	1.3 E 17

Reference:

G. Staudenmaier et al., J. Nucl. Mater. 84, 149 (1979).

Accuracy: Unspecified

Note: (1) For a definition of trapping see note 2b at the beginning of this section.

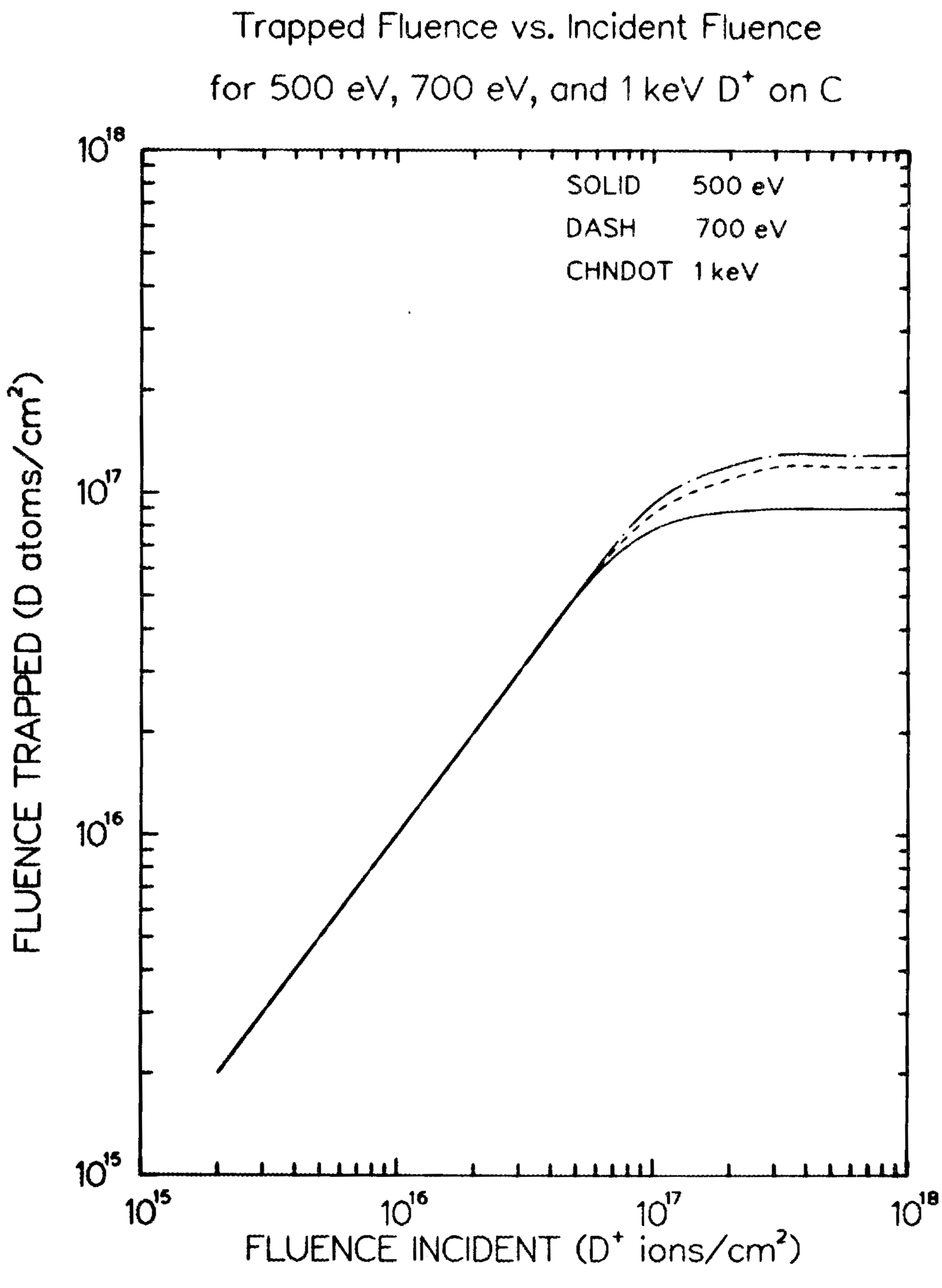

Trapped Fluence vs. Incident Fluence
for 500 eV, 700 eV, and 1 keV D+ on C
SOLID 500 eV
DASH 700 eV
CHNDOT 1 keV
FLUENCE TRAPPED (D atoms/cm2)
FLUENCE INCIDENT (D+ ions/cm2)
10^15
10^16
10^17
10^18

Fluence Trapped at Saturation

for D^+ on C

(normal incidence, room temperature, polycrystalline material)

Energy (keV)	Fluence Trapped at Saturation (D atoms/cm^2)
5.0 E-02	1.3 E 16
7.0 E-02	1.7 E 16
1.0 E-01	2.3 E 16
2.0 E-01	4.1 E 16
3.0 E-01	5.9 E 16
5.0 E-01	9.7 E 16
7.0 E-01	1.3 E 17
1.0 E 00	1.7 E 17
2.0 E 00	3.2 E 17
3.0 E 00	4.6 E 17
5.0 E 00	7.5 E 17
7.0 E 00	1.0 E 18
1.0 E 01	1.4 E 18

Reference:

G. Staudenmaier et al., J. Nucl. Mater. 84, 149 (1979).

Accuracy: ±10%

Notes: (1) For a definition of trapped fluence and its relationship to reemission, see note 2b at the beginning of this section.

(2) The carbon used here is a flexible polycrystalline graphite strip known by the commercial name of "Papyex" (Le Carbonne, France).

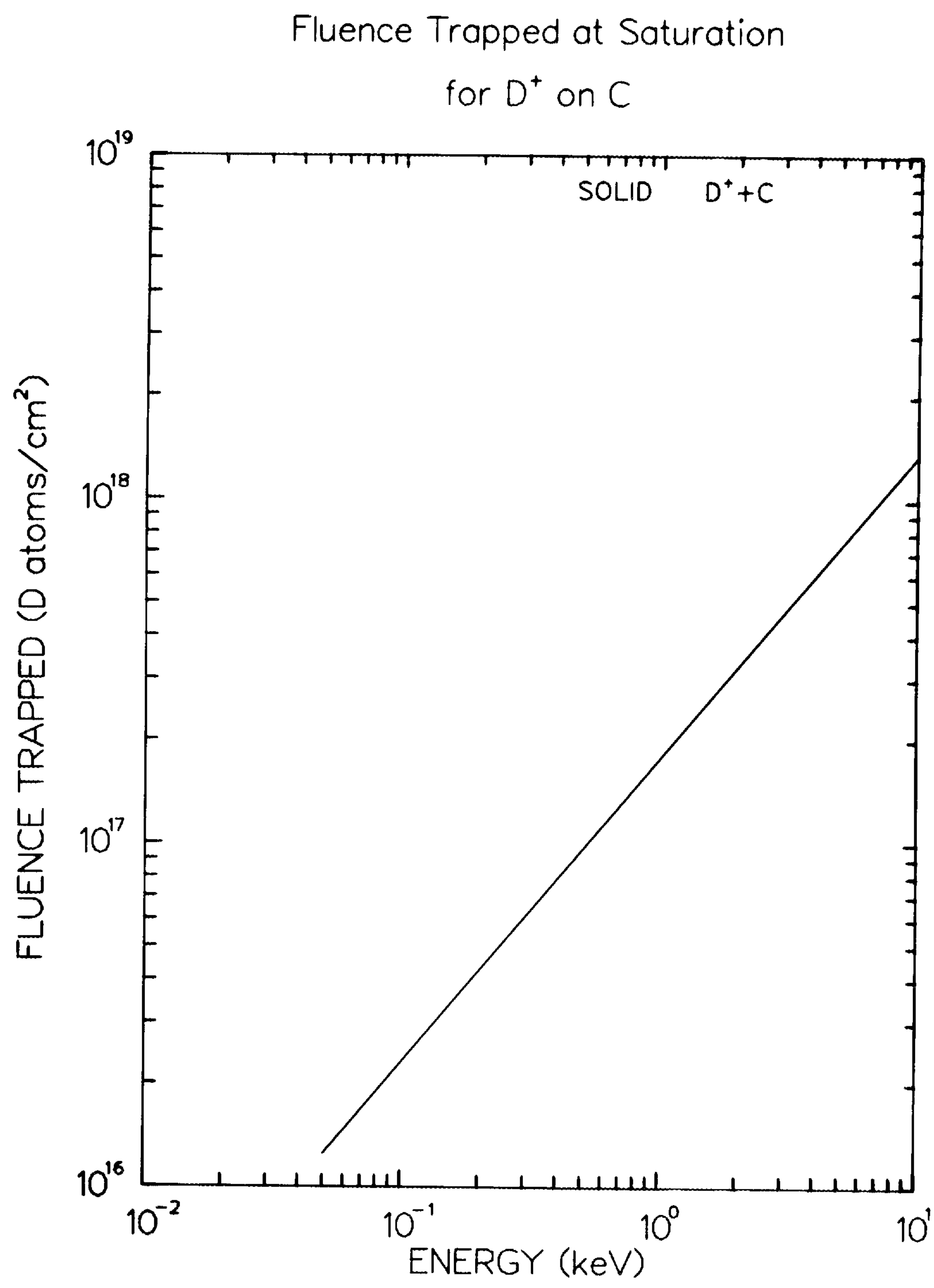
Fluence Trapped at Saturation
for D+ on C
SOLID D+ +C
FLUENCE TRAPPED (D atoms/cm2)
10^19
10^18
10^17
10^16
10^-2
10^-1
10^0
10^1
ENERGY (keV)

Reemission of Deuterium at Various Temperatures for 20-keV D^+ on C

(normal incidence, various temperatures, polycrystalline material)

Fluence Incident (D^+ ions/cm^2)	Reemission Rate (%)			
	293 K	773 K	973 K	1273 K
0.0 E 00	0.0 E 00	0.0 E 00	0.0 E 00	0.0 E 00
2.0 E 16	0.0 E 00	0.0 E 00	0.0 E 00	6.0 E 00
4.0 E 16	0.0 E 00	0.0 E 00	0.0 E 00	1.1 E 01
6.0 E 16	0.0 E 00	0.0 E 00	2.0 E 00	1.4 E 01
8.0 E 16	0.0 E 00	0.0 E 00	7.0 E 00	2.6 E 01
1.0 E 17	0.0 E 00	0.0 E 00	1.0 E 01	3.5 E 01
2.0 E 17	0.0 E 00	0.0 E 00	5.0 E 01	4.6 E 01
4.0 E 17	0.0 E 00	4.0 E 00	7.7 E 01	5.3 E 01
6.0 E 17	0.0 E 00	1.1 E 01	8.4 E 01	5.5 E 01
8.0 E 17	0.0 E 00	2.4 E 01	8.7 E 01	5.6 E 01
1.0 E 18	3.0 E 00	3.5 E 01	9.0 E 01	5.6 E 01
1.2 E 18	1.0 E 01	4.4 E 01	9.1 E 01	
1.4 E 18	2.0 E 01	5.0 E 01		
1.6 E 18	2.7 E 01	5.5 E 01		
1.8 E 18	3.4 E 01	5.8 E 01		
2.0 E 18	3.7 E 01	6.1 E 01		

Reference:

S. K. Erents, Inst. Phys. Conf. Ser. 28, 318 (1976).

Accuracy: Unknown

Notes: (1) For a definition of reemission and how it relates to trapping, see note 2a at the beginning of this section.

(2) The type of carbon used was not specified.

(3) The above data represent the reemission of deuterium in the form of D_2 and HD. In addition, there is some reemission of CD_4 at higher temperatures; this is believed to be less than 5% of the total deuterium emission.

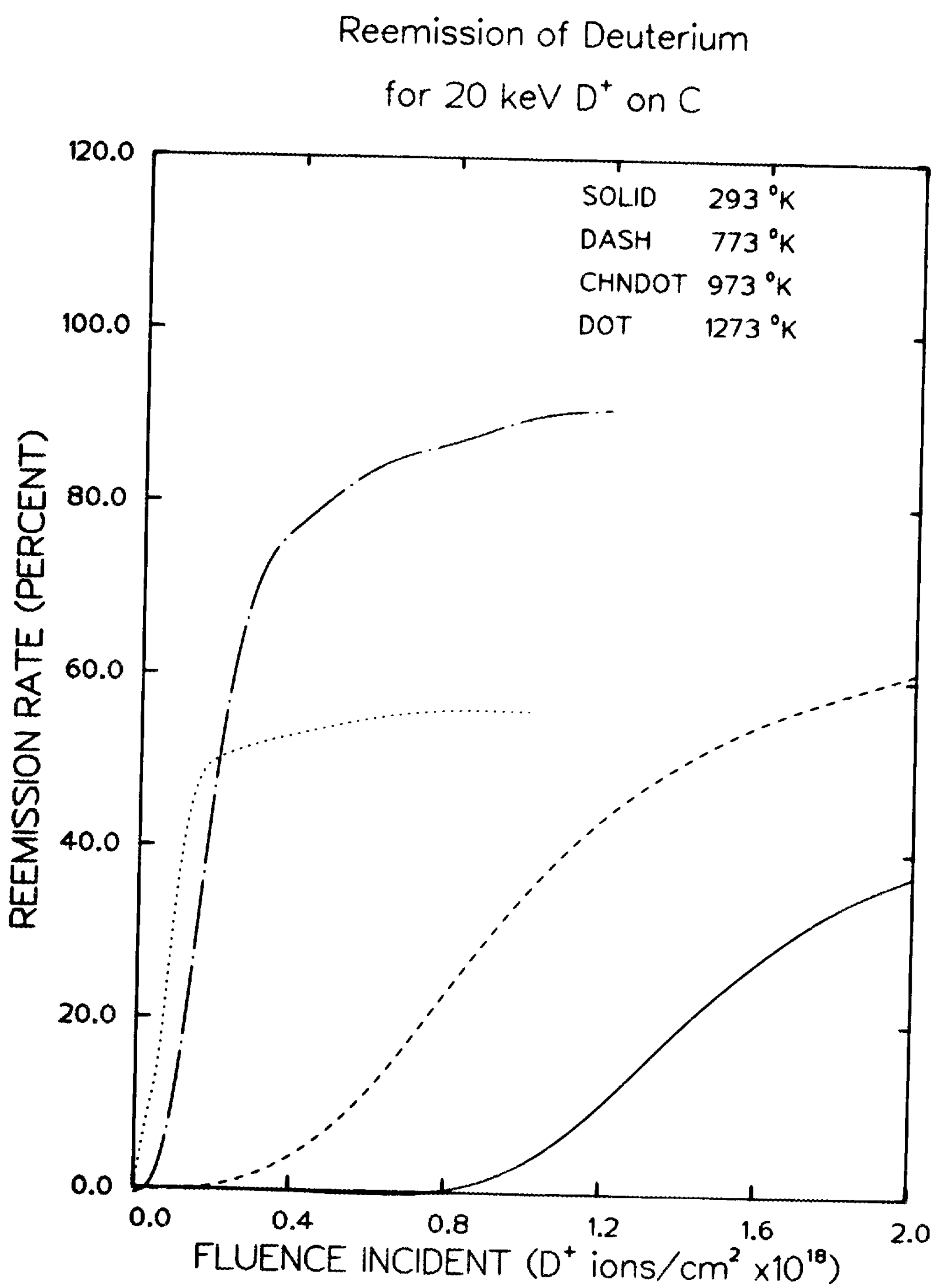
Reemission of Deuterium
for 20 keV D+ on C
SOLID 293 °K
DASH 773 °K
CHNDOT 973 °K
DOT 1273 °K
REEMISSION RATE (PERCENT)
120.0
100.0
80.0
60.0
40.0
20.0
0.0
0.0
0.4
0.8
1.2
1.6
2.0
FLUENCE INCIDENT (D+ ions/cm2 x10^18)

Trapped Fluence at 50, 150, and 300 eV

as a Function of Incident Fluence for D^+ on Si

(normal incidence, room temperature, single crystal)

Fluence Incident (D^+ ions/cm^2)	Fluence Trapped (D atoms/cm^2)		
	50 eV	150 eV	300 eV
1.0 E 15			1.0 E 15
2.0 E 15			2.0 E 15
3.0 E 15	1.0 E 15	1.6 E 15	3.0 E 15
5.0 E 15	1.5 E 15	2.8 E 15	5.0 E 15
1.0 E 16	2.5 E 15	5.5 E 15	9.0 E 15
2.0 E 16	4.1 E 15	9.2 E 15	1.5 E 16
3.0 E 16	5.3 E 15	1.2 E 16	1.8 E 16
5.0 E 16	6.7 E 15	1.5 E 16	2.3 E 16
1.0 E 17	8.5 E 15	1.8 E 16	2.8 E 16
2.0 E 17	9.2 E 15	1.8 E 16	3.1 E 16
3.0 E 17	9.3 E 15	1.8 E 16	3.1 E 16
5.0 E 17			3.1 E 16
1.0 E 18			3.1 E 16

Reference:

G. Staudenmaier et al., J. Nucl. Mater. 84, 149 (1979).

Accuracy: Unknown

Note: (1) For a definition of trapping see note 2b at the beginning of this section.

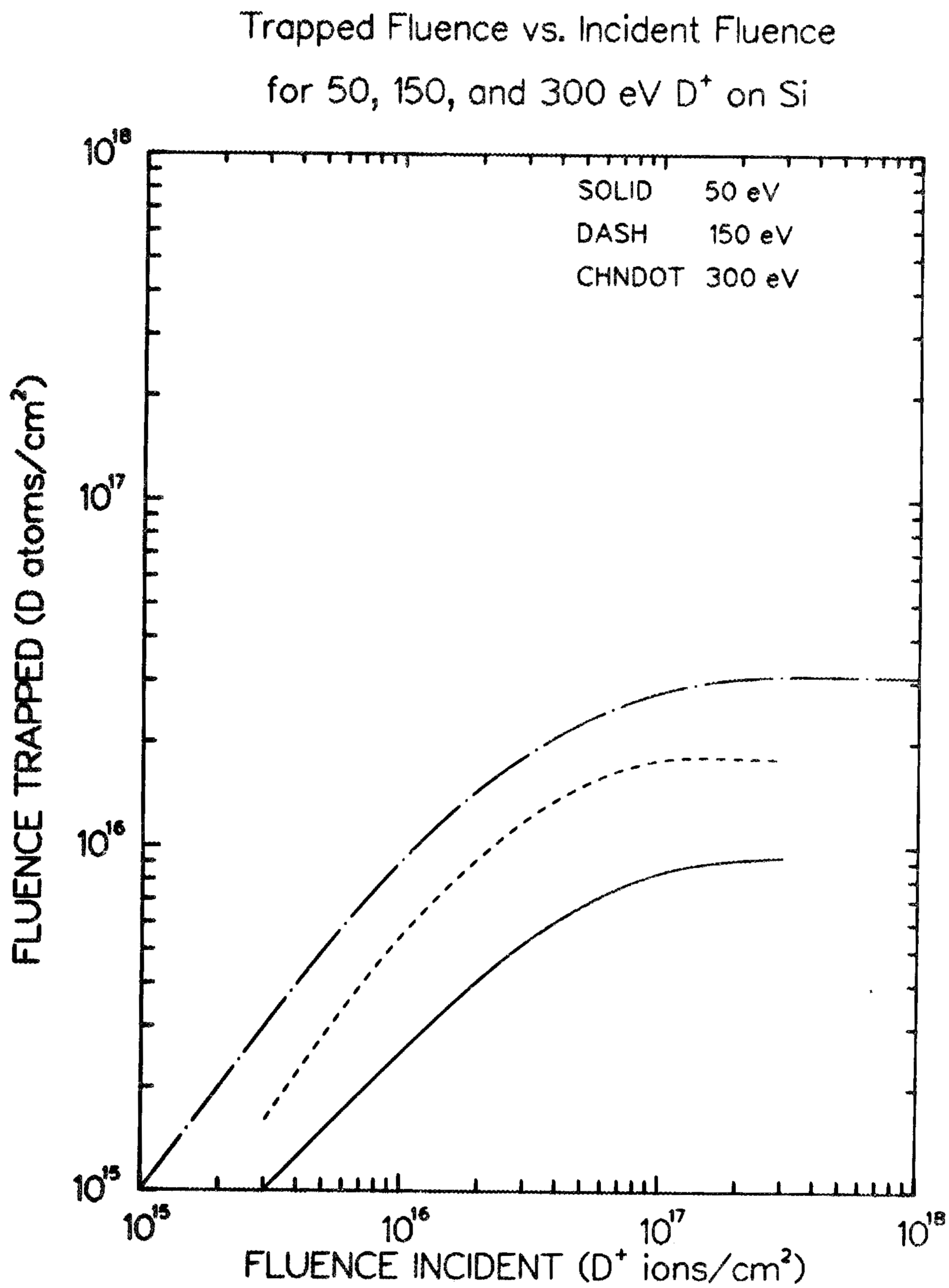
Trapped Fluence vs. Incident Fluence
for 50, 150, and 300 eV D+ on Si
SOLID 50 eV
DASH 150 eV
CHNDOT 300 eV
FLUENCE TRAPPED (D atoms/cm2)
10^18
10^17
10^16
10^15
10^15
10^16
10^17
10^18
FLUENCE INCIDENT (D+ ions/cm2)

Trapped Fluence at 500 eV, 700 eV, and 1 keV

as a Function of Incident Fluence for D^+ on Si

(normal incidence, room temperature, single crystal)

Fluence Incident (D^+ ions/cm^2)	Fluence Trapped (D atoms/cm^2)		
	500 eV	700 eV	1 keV
1.0 E 15	1.0 E 15	1.0 E 15	1.0 E 15
2.0 E 15	2.0 E 15	2.0 E 15	2.0 E 15
3.0 E 15	3.0 E 15	3.0 E 15	3.0 E 15
5.0 E 15	5.0 E 15	5.0 E 15	5.0 E 15
1.0 E 16	1.0 E 16	1.0 E 16	1.0 E 16
2.0 E 16	2.0 E 16	2.0 E 16	2.0 E 16
3.0 E 16	2.8 E 16	3.0 E 16	3.0 E 16
5.0 E 16	4.0 E 16	4.5 E 16	5.0 E 16
1.0 E 17	4.9 E 16	5.8 E 16	7.2 E 16
2.0 E 17	5.1 E 16	6.7 E 16	8.0 E 16
3.0 E 17	5.3 E 16	7.0 E 16	8.3 E 16
5.0 E 17	5.4 E 16	7.0 E 16	8.5 E 16
1.0 E 18	5.4 E 16	7.0 E 16	8.5 E 16

Reference:

G. Staudenmaier et al., J. Nucl. Mater. 84, 149 (1979).

Accuracy: Unknown

Note: (1) For a definition of trapping see note 2b at the beginning of this section.

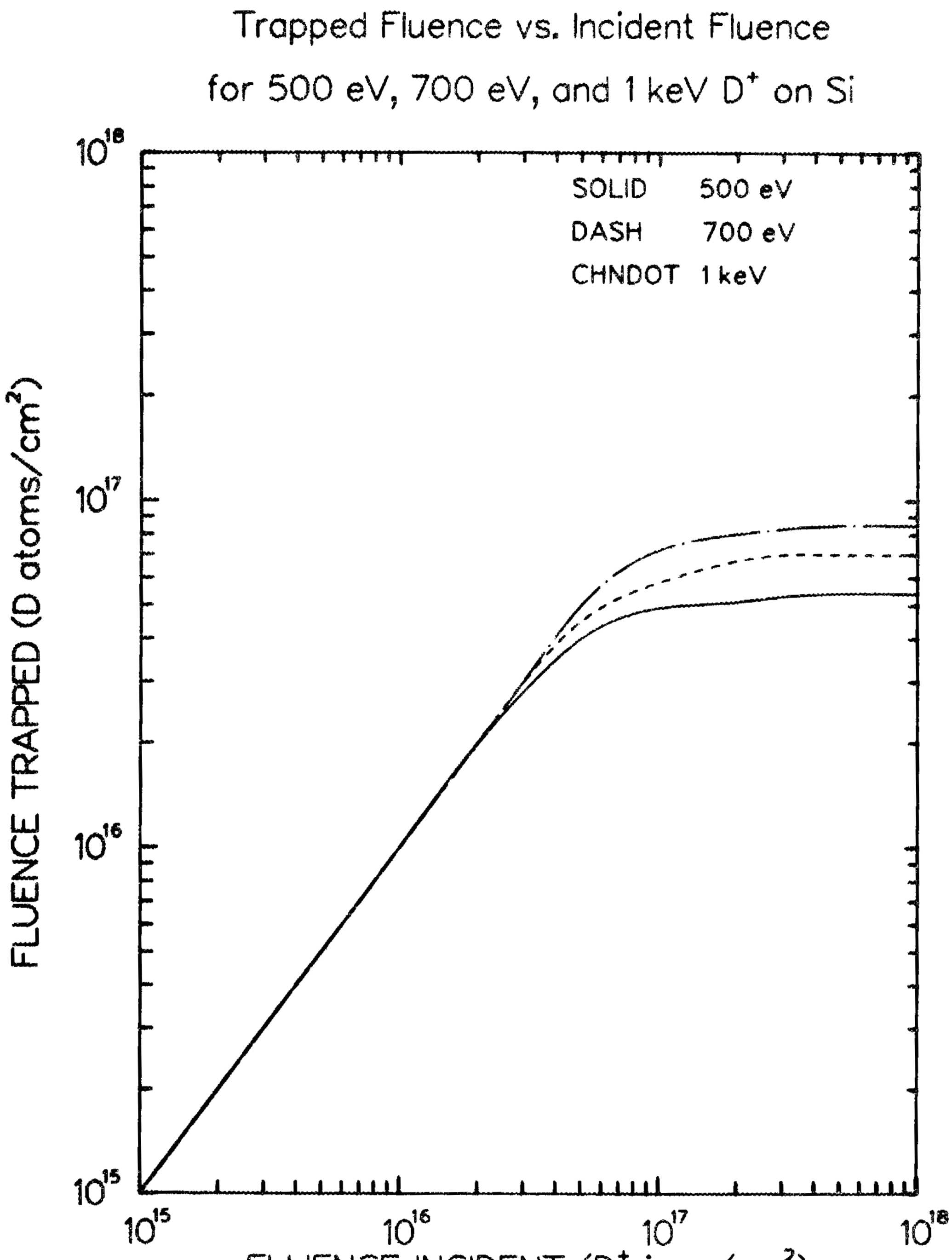
Trapped Fluence vs. Incident Fluence
for 500 eV, 700 eV, and 1 keV D+ on Si
SOLID 500 eV
DASH 700 eV
CHNDOT 1 keV
FLUENCE TRAPPED (D atoms/cm2)
FLUENCE INCIDENT (D+ ions/cm2)
10^15
10^16
10^17
10^18

Fluence of Deuterium Trapped at Saturation

for D^+ on Si

(normal incidence, room temperature, polycrystalline target)

Energy (keV)	Fluence Trapped at Saturation (D atoms/cm^2)
5.0 E-02	8.0 E 15
7.0 E-02	1.1 E 16
1.0 E-01	1.4 E 16
2.0 E-01	2.5 E 16
3.0 E-01	3.5 E 16
5.0 E-01	5.4 E 16
7.0 E-01	7.0 E 16
1.0 E 00	9.2 E 16

Reference:

G. Staudenmaier et al., J. Nucl. Mater. 84, 149 (1979).

Accuracy: ±10%

Note: (1) For a definition of trapped fluence and its relationship to reemission, see note 2b at the beginning of this section.

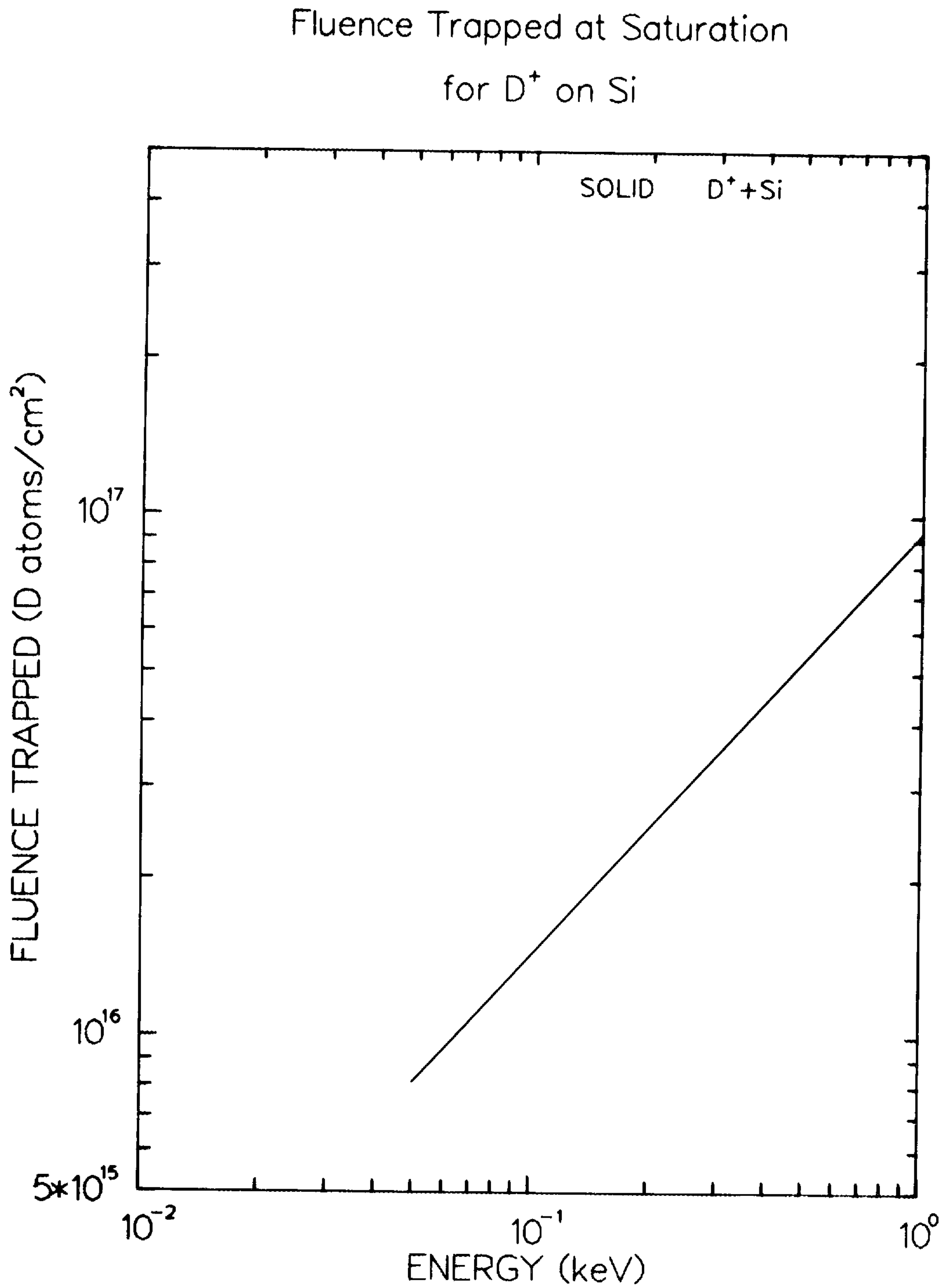
Fluence Trapped at Saturation
for D+ on Si
SOLID D+ + Si
FLUENCE TRAPPED (D atoms/cm2)
10^17
10^16
5*10^15
10^-2
10^-1
10^0
ENERGY (keV)

Reemission of Deuterium at Various Temperatures

for 20-keV D^+ on SiC

(normal incidence, various temperatures, 20-keV energy, polycrystalline target)

Fluence Incident (D^+ ions/cm^2)	Reemission Rate (%)			
	293 K	773 K	973 K	1273 K
0.0 E 00	0.0 E 00	0.0 E 00	0.0 E 00	1.6 E 01
2.0 E 16	2.0 E 00	3.0 E 00	6.0 E 00	2.0 E 01
4.0 E 16	2.0 E 00	4.0 E 00	7.0 E 00	2.3 E 01
6.0 E 16	3.0 E 00	4.0 E 00	8.0 E 00	2.5 E 01
8.0 E 16	3.0 E 00	5.0 E 00	9.0 E 00	2.9 E 01
1.0 E 17	3.0 E 00	5.0 E 00	1.0 E 01	3.6 E 01
2.0 E 17	3.0 E 00	6.0 E 00	1.6 E 01	6.8 E 01
4.0 E 17	4.0 E 00	1.1 E 01	4.1 E 01	8.6 E 01
6.0 E 17	6.0 E 00	2.0 E 01	5.7 E 01	9.3 E 01
8.0 E 17	8.0 E 00	3.1 E 01	6.5 E 01	9.5 E 01
1.0 E 18	1.1 E 01	3.9 E 01	7.3 E 01	9.6 E 01
1.2 E 18	1.6 E 01	4.6 E 01	7.7 E 01	9.7 E 01
1.4 E 18	2.3 E 01	5.3 E 01	8.2 E 01	9.7 E 01
1.6 E 18	3.0 E 01	5.8 E 01	8.5 E 01	9.7 E 01
1.8 E 18	3.7 E 01	6.2 E 01	8.9 E 01	9.7 E 01
2.0 E 18	4.3 E 01	6.5 E 01	9.0 E 01	9.7 E 01

Reference:

S. K. Erents, Inst. Phys. Conf. Ser. 28, 318 (1976).

Accuracy: Unknown

Note: (1) For a definition of reemission and how it relates to trapping, see note 2a at the beginning of this section.

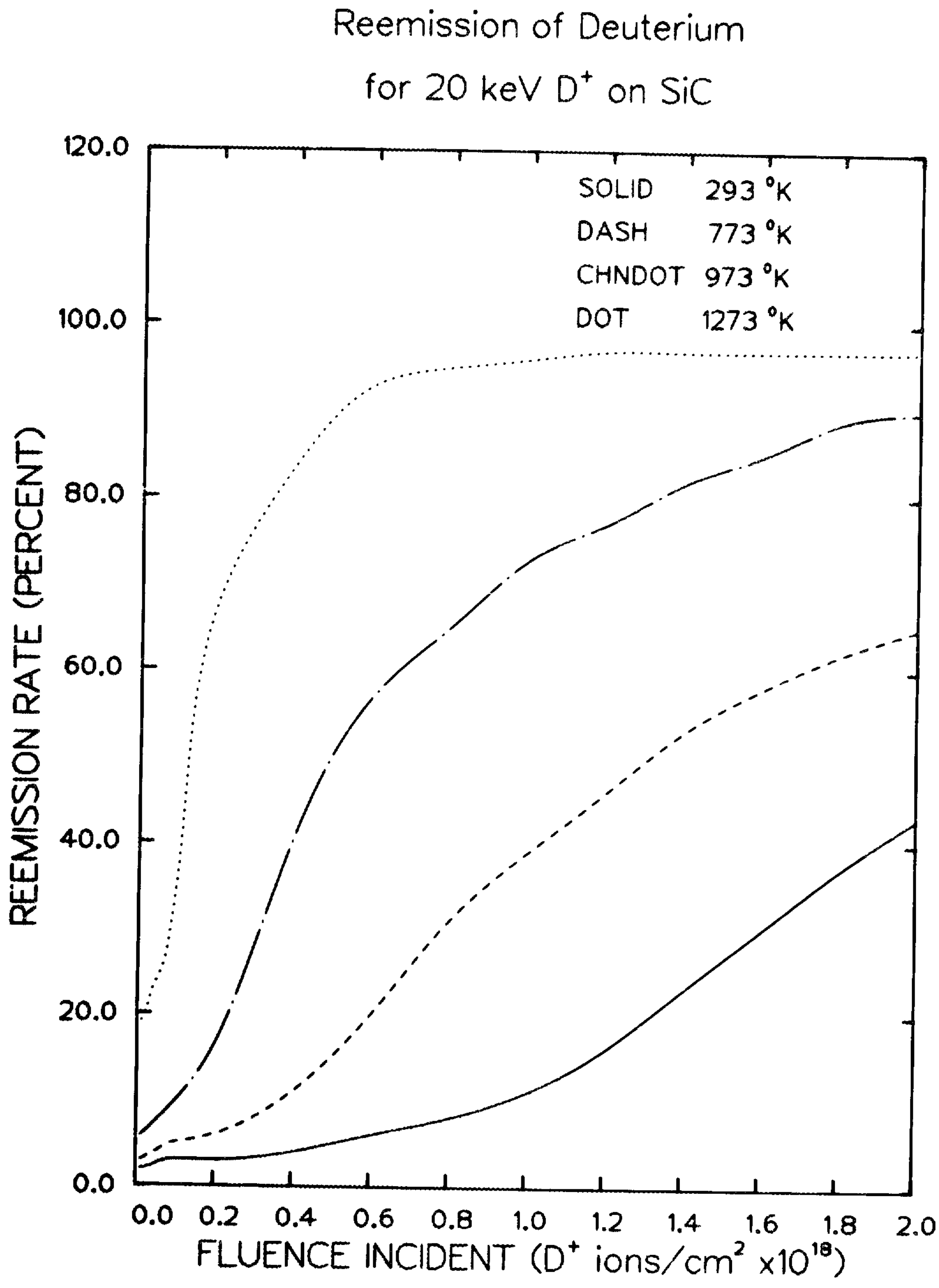
Reemission of Deuterium
for 20 keV D+ on SiC
SOLID 293 °K
DASH 773 °K
CHNDOT 973 °K
DOT 1273 °K
120.0
100.0
80.0
60.0
40.0
20.0
0.0
REEMISSION RATE (PERCENT)
0.0 0.2 0.4 0.6 0.8 1.0 1.2 1.4 1.6 1.8 2.0
FLUENCE INCIDENT (D+ ions/cm2 x10^18)

Trapping Coefficient as a Function of

Dose for 18-keV D^+ Impact on Ti

(normal incidence, various temperatures, 18-keV energy, polycrystalline target)

Fluence Incident (D^+ ions/cm^2)	Trapping Coefficient			
	477 K	531 K	699 K	728 K
8.0 E 16			8.7 E-01	8.3 E-01
1.0 E 17			8.6 E-01	7.8 E-01
2.0 E 17			6.8 E-01	4.7 E-01
3.0 E 17	9.4 E-01	9.2 E-01	5.0 E-01	3.4 E-01
5.0 E 17	9.3 E-01	8.9 E-01	3.9 E-01	2.3 E-01
7.0 E 17	9.2 E-01	8.6 E-01	3.5 E-01	2.0 E-01
1.0 E 18	9.0 E-01	8.3 E-01	3.1 E-01	1.7 E-01
2.0 E 18	8.8 E-01	7.7 E-01	2.6 E-01	1.4 E-01
3.0 E 18	8.6 E-01	7.3 E-01	2.4 E-01	1.3 E-01
5.0 E 18	8.3 E-01	6.8 E-01	2.2 E-01	1.2 E-01

Reference:

E. S. Hotston and G. M. McCracken, J. Nucl. Mater. 68, 277 (1977).

Accuracy: Unknown

Notes: (1) For a definition of trapping coefficient see note 2d at the beginning of this section.

(2) At low dose the coefficient should tend asymptotically to 0.97 because 3% of the beam is backscattered.

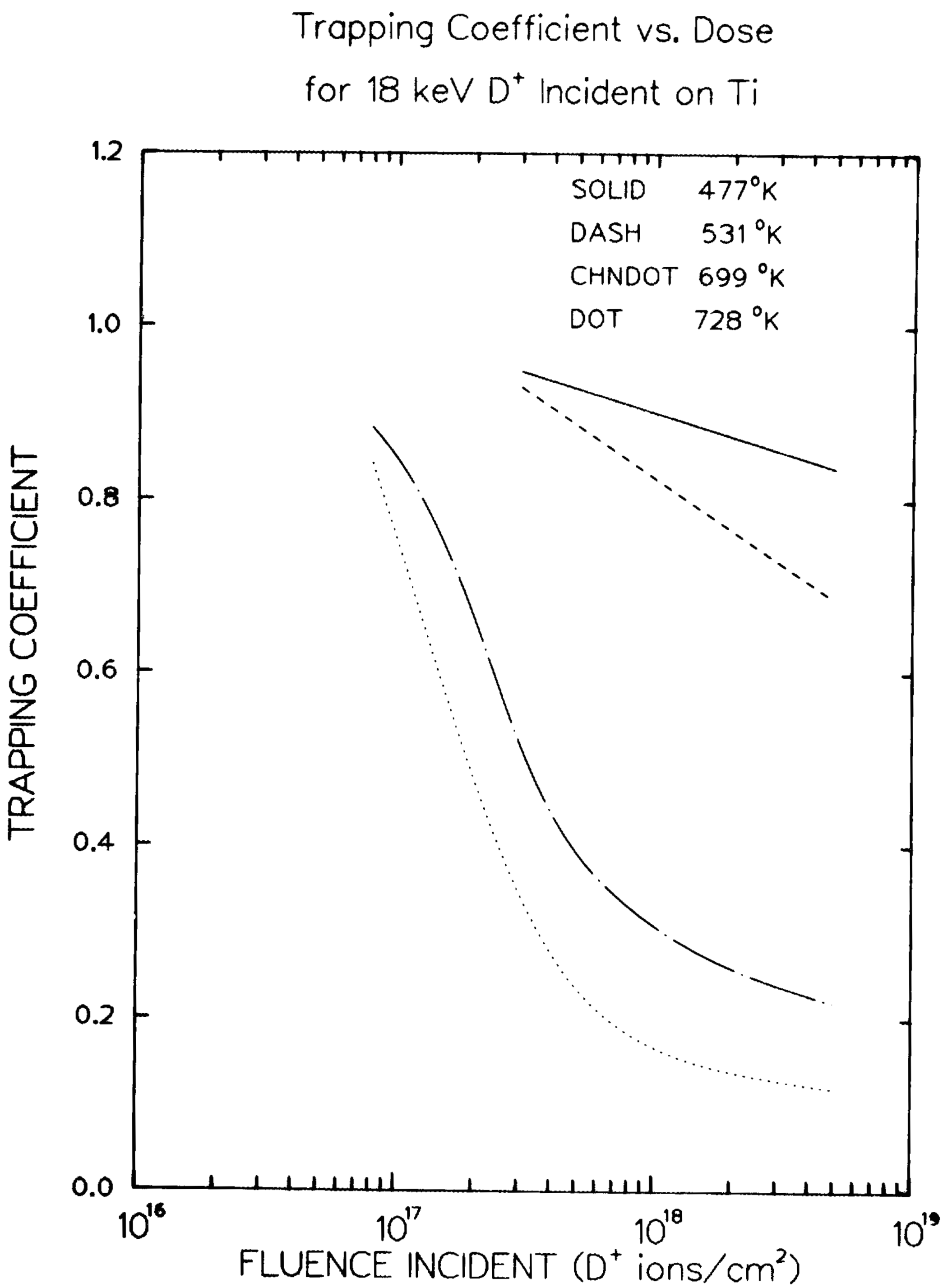
Trapping Coefficient vs. Dose
for 18 keV D+ Incident on Ti
SOLID 477°K
DASH 531°K
CHNDOT 699°K
DOT 728°K
TRAPPING COEFFICIENT
1.2
1.0
0.8
0.6
0.4
0.2
0.0
10^16
10^17
10^18
10^19
FLUENCE INCIDENT (D+ ions/cm2)

Trapping Coefficient as a Function of Temperature

at a Fixed Fluence (or Dose) for 18-keV D^+ Incident on Ti

(normal incidence; various temperatures; fixed fluence, or dose, of 5×10^{18} ions cm^{-2}; energy of 18 keV; polycrystalline target)

Temperature (K)	Trapping Coefficient
1.0 E 02	1.3 E-01
2.0 E 02	8.0 E-01
3.0 E 02	9.6 E-01
4.0 E 02	9.6 E-01
5.0 E 02	8.8 E-01
6.0 E 02	4.4 E-01
7.0 E 02	1.7 E-01
8.0 E 02	5.0 E-02
9.0 E 02	3.0 E-02

Reference:

G. M. McCracken et al., Proc. 4th Int. Vacuum Congress, Inst. Phys. Conf. Ser. 5, 149 (1968).

Accuracy: Unknown. The random scatter of the data points about the line given here is approximately ±10%.

Notes: (1) For a definition of trapping coefficient see note 2d at the beginning of this section.

(2) The data are for a fixed incident fluence (or dose) of 5×10^{18} D^+ ions cm^{-2}. For information on how trapping coefficient varies with incident fluence, see adjacent figures.

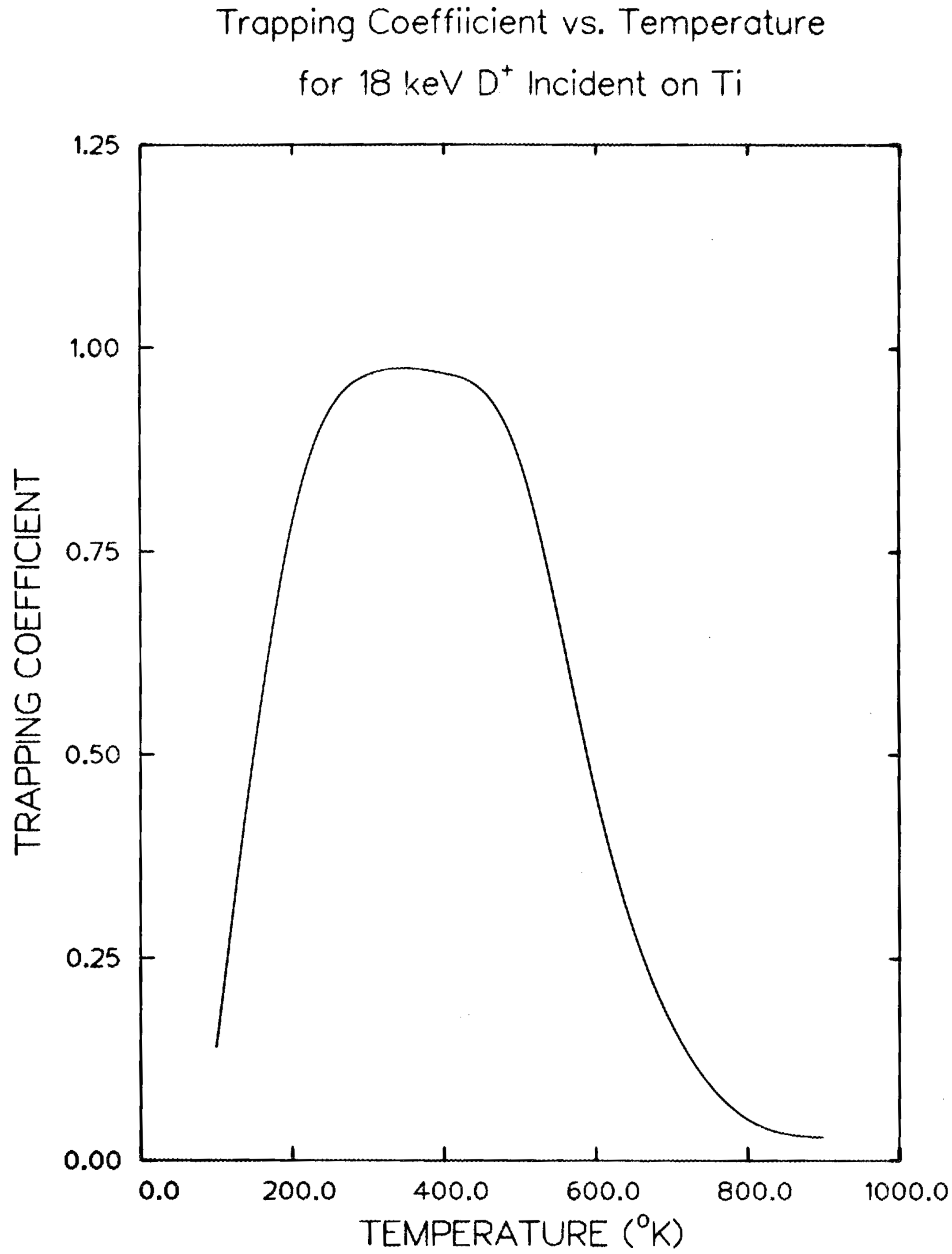
Trapping Coeffiicient vs. Temperature
for 18 keV D+ Incident on Ti
TRAPPING COEFFICIENT
1.25
1.00
0.75
0.50
0.25
0.00
0.0
200.0
400.0
600.0
800.0
1000.0
TEMPERATURE (°K)

Trapping Coefficient as a Function of Energy

at a Fixed Dose for H^+ Incident on Ti

(normal incidence, temperature in the region 403 to 503 K)

Energy (keV)	Trapping Coefficient
3.0 E-01	1.7 E-01
5.0 E-01	4.5 E-01
1.0 E 00	7.8 E-01
2.0 E 00	8.2 E-01
3.0 E 00	9.0 E-01
4.0 E 00	9.4 E-01
5.0 E 00	9.7 E-01
6.0 E 00	9.5 E-01

Reference:

J. Bohdansky et al., J. Nucl. Mater. 63, 115 (1976).

Accuracy: See below.

Notes: (1) For a definition of trapping coefficient see note 2d at the beginning of this section.

(2) Below 1 keV the data are believed to represent not Ti, but rather titanium oxide, which exists as a film on the sample. Thus, below 1 keV the accuracy of the data (insofar as they refer to Ti) are suspect.

(3) Fluence or dose used in the bombardment was between 3×10^{19} and 5×10^{20} ions cm^{-2}.

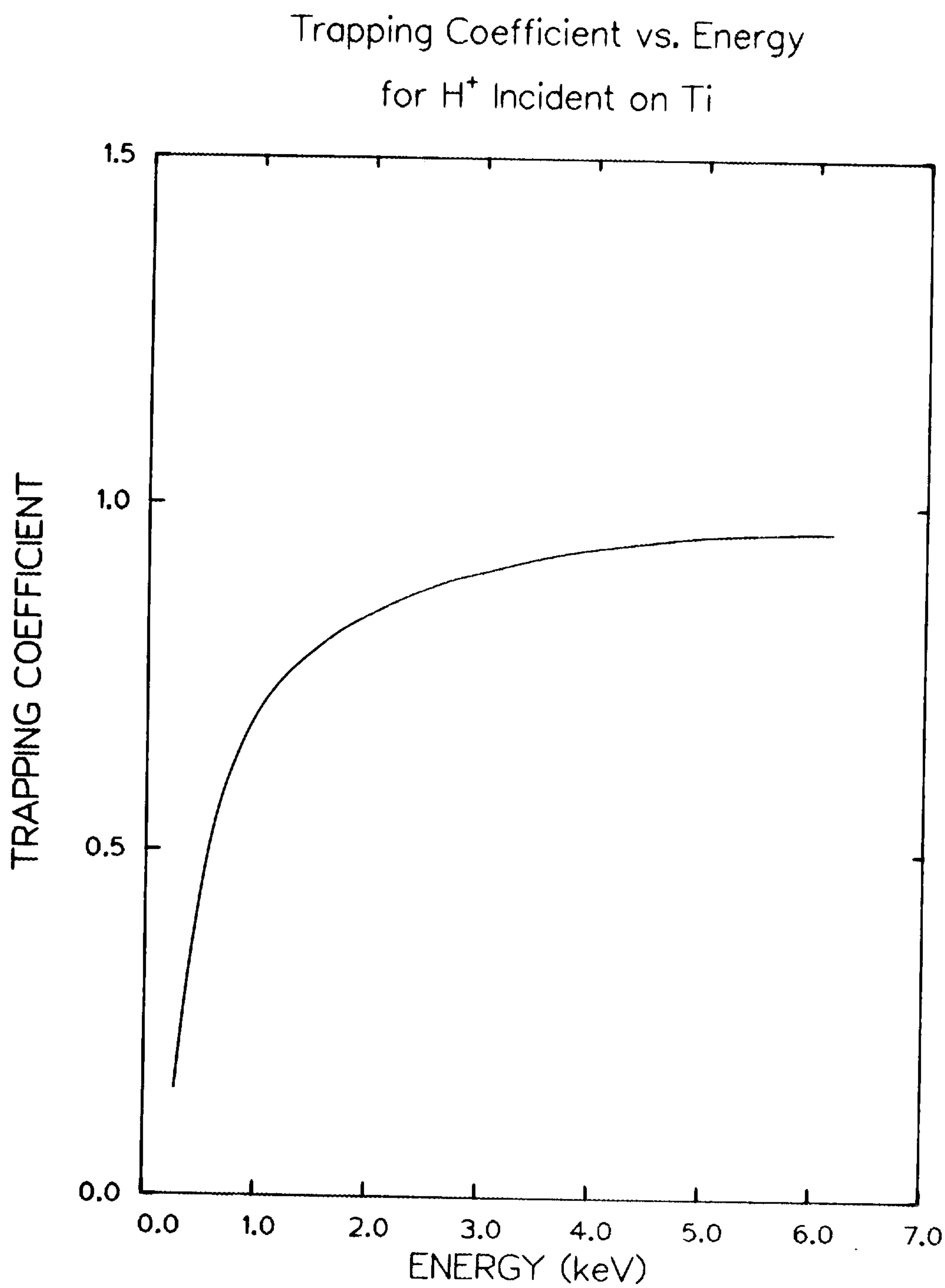
Trapping Coefficient vs. Energy
for H+ Incident on Ti
TRAPPING COEFFICIENT
1.5
1.0
0.5
0.0
0.0
1.0
2.0
3.0
4.0
5.0
6.0
7.0
ENERGY (keV)

Fluence Trapped at Saturation

for D^+ on Stainless Steel

(normal incidence, 90 K or 150 K temperature)

Energy (keV)	Fluence Trapped at Saturation (D atoms/cm^2)
1.25 E-01	2.4 E 16
2.0 E-01	3.6 E 16
3.0 E-01	5.3 E 16
5.0 E-01	8.8 E 16
7.0 E-01	1.2 E 17
1.0 E 00	1.7 E 17
2.0 E 00	3.4 E 17
3.0 E 00	5.0 E 17
5.0 E 00	8.1 E 17
7.0 E 00	1.0 E 18
1.0 E 01	1.3 E 18
1.5 E 01	1.6 E 18

References:

E. W. Thomas, J. Appl. Phys. 51, 1176 (1980).
R. S. Blewer et al., J. Nucl. Mater. 76 and 77, 305 (1978).

Accuracy: ±10%

Notes: (1) For a definition of trapped fluence and its relationship to reemission, see note 2b at the beginning of this section.

(2) Data up to 1 keV are by Thomas and are for a temperature of 90 K. Data at 1 keV and above are by Blewer et al., at a temperature of 150 K. The two data sets are in agreement at 1 keV.

(3) The work by Thomas uses type 304 stainless steel; the work by Blewer uses type 321.

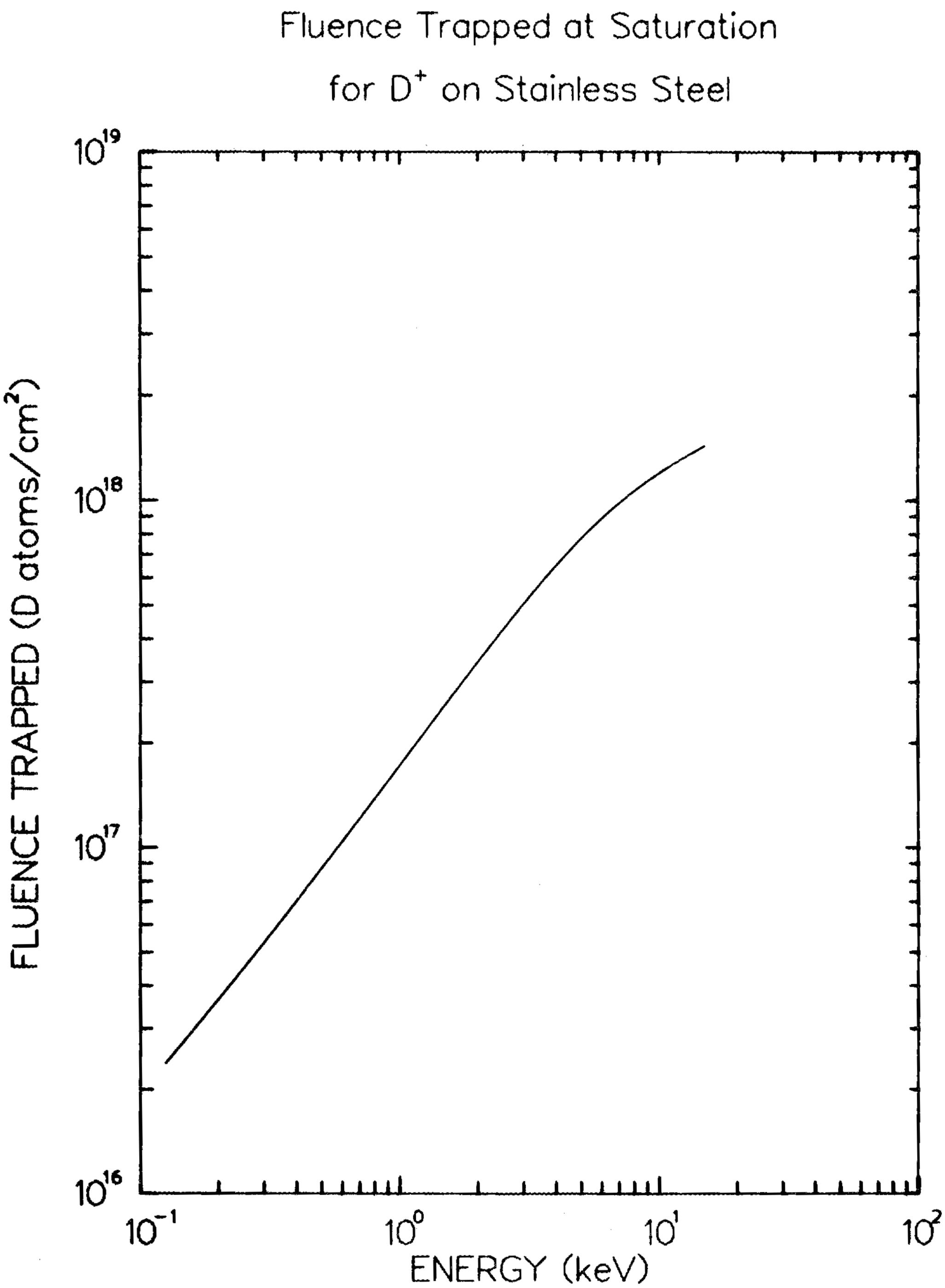
Fluence Trapped at Saturation
for D+ on Stainless Steel
FLUENCE TRAPPED (D atoms/cm2)
10^19
10^18
10^17
10^16
10^-1
10^0
10^1
10^2
ENERGY (keV)

Reemission of Deuterium Due to D^+ Impact on

Stainless Steel (Type 304) at Low Temperature

(normal incidence, 90 K temperature)

Fluence Incident (D^+ ions/cm^2)	Reemission Rate (%)			
	D^+(125 eV)	D^+(250 eV)	D^+(500 eV)	D^+(750 eV)
0.0 E 00	5.0 E 01	4.0 E 01	4.0 E 01	3.5 E 01
2.0 E 16	5.0 E 01	4.0 E 01	4.0 E 01	3.5 E 01
4.0 E 16	5.5 E 01	4.6 E 01	4.0 E 01	3.5 E 01
5.0 E 16	8.5 E 01	5.2 E 01	4.0 E 01	3.5 E 01
6.0 E 16	9.5 E 01	5.9 E 01	4.0 E 01	3.5 E 01
8.0 E 16	1.0 E 02	7.2 E 01	4.0 E 01	3.5 E 01
1.0 E 17	1.0 E 02	8.5 E 01	4.0 E 01	3.5 E 01
1.2 E 17		9.7 E 01	5.1 E 01	3.5 E 01
1.4 E 17		1.0 E 02	7.6 E 01	3.5 E 01
1.6 E 17		1.0 E 02	9.6 E 01	3.8 E 01
1.8 E 17			9.9 E 01	5.2 E 01
2.0 E 17			1.0 E 02	6.3 E 01
2.5 E 17			1.0 E 02	8.8 E 01
3.0 E 17				9.8 E 01
3.5 E 17				1.0 E 02
4.0 E 17				1.0 E 02

Reference:

E. W. Thomas, J. Appl. Phys. 51, 1176 (1980).

Accuracy: ±10%

Notes: (1) For a definition of reemission rate and how it relates to trapping, see note 2b at the beginning of this section.

(2) Further data for higher D^+ energies are to be found in the following table.

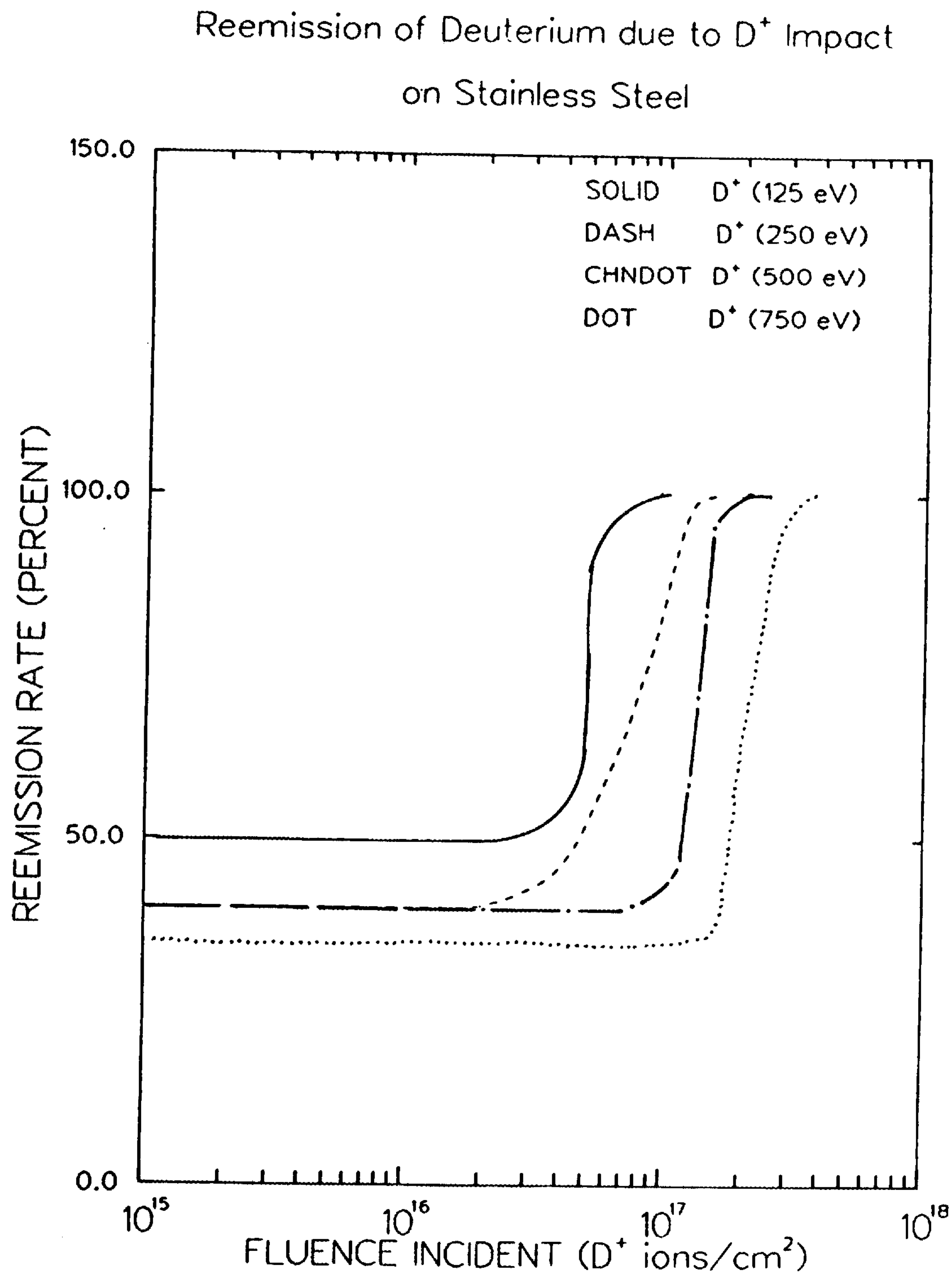

Reemission of Deuterium due to D+ Impact
on Stainless Steel
SOLID D+ (125 eV)
DASH D+ (250 eV)
CHNDOT D+ (500 eV)
DOT D+ (750 eV)
REEMISSION RATE (PERCENT)
150.0
100.0
50.0
0.0
10^15
10^16
10^17
10^18
FLUENCE INCIDENT (D+ ions/cm^2)

Reemission of Deuterium Due to D^+ Impact on Stainless Steel (Types 304 and 321) at Low Temperature

(normal incidence, 90 to 120 K temperature)

Fluence Incident (D^+ ions/cm^2)	Reemission Rate (%)			
	D^+ (1 keV)	D^+ (4 keV)	D^+ (7 keV)	D^+ (14 keV)
0.0 E 00	3.0 E 01	1.6 E 01	1.3 E 01	4.0 E 00
1.0 E 17	3.0 E 01	1.6 E 01	1.3 E 01	4.0 E 00
2.0 E 17	4.4 E 01	1.6 E 01	1.3 E 01	4.0 E 00
3.0 E 17	7.3 E 01	1.6 E 01	1.3 E 01	4.0 E 00
4.0 E 17	8.4 E 01	1.8 E 01	1.4 E 01	4.0 E 00
6.0 E 17	9.8 E 01	2.3 E 01	1.6 E 01	5.0 E 00
8.0 E 17	1.0 E 02	4.3 E 01	1.8 E 01	6.0 E 00
1.0 E 18	1.0 E 02	6.8 E 01	3.2 E 01	7.0 E 00
1.2 E 18		9.0 E 01	5.4 E 01	1.6 E 01
1.5 E 18		1.0 E 02	8.8 E 01	3.0 E 01
2.0 E 18		1.0 E 02	9.7 E 01	5.0 E 01
2.5 E 18			1.0 E 02	7.0 E 01
3.0 E 18			1.0 E 02	9.0 E 01
3.5 E 18				9.7 E 01
4.0 E 18				1.0 E 02

References:

R. S. Blewer et al., J. Nucl. Mater. 76 and 77, 305 (1978) (data for 4, 7, and 14 keV at 120 K temperature; E. W. Thomas, Georgia Institute of Technology, J. Appl. Phys. 51, 1176 (1980).

Accuracy: ±10%

Notes: (1) For a definition of reemission rate and how it relates to trapping, see note 2a at the beginning of this section.

(2) Further data for lower D^+ energies are to be found in the preceding table.

(3) Type 304 stainless steel was used for the 1-keV data, type 321 for the remainder.

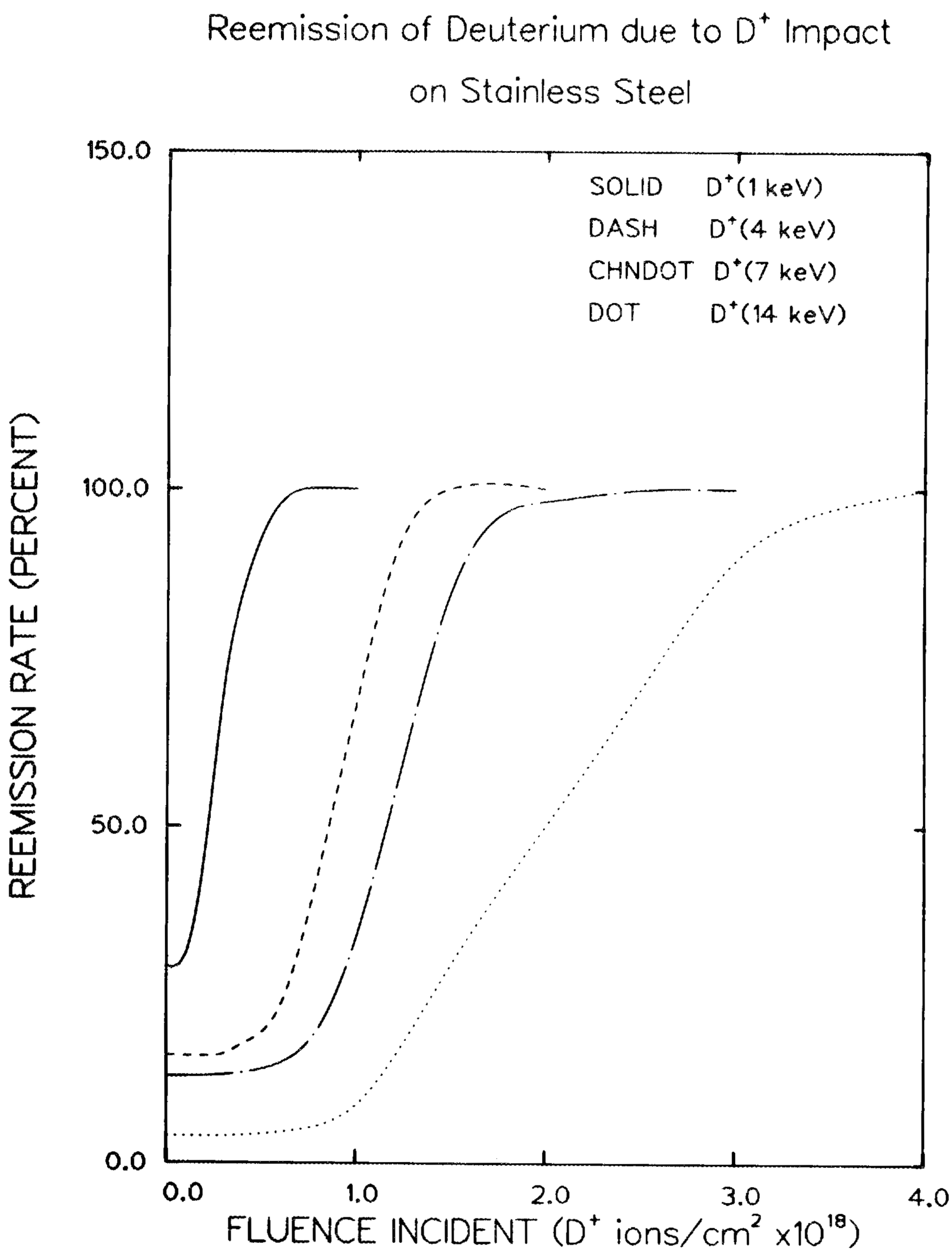
Reemission of Deuterium due to D+ Impact
on Stainless Steel
SOLID D+(1 keV)
DASH D+(4 keV)
CHNDOT D+(7 keV)
DOT D+(14 keV)
150.0
100.0
50.0
0.0
REEMISSION RATE (PERCENT)
0.0
1.0
2.0
3.0
4.0
FLUENCE INCIDENT (D+ ions/cm2 x10^18)

Reemission of Deuterium Due to D^+ Impact on Stainless

Steel at Room Temperature and Above

(normal incidence; data are for room temperature, but 500 K data are identical)

Fluence Incident (D^+ ions/cm^2)	Reemission rate (%)		
	D^+ (500 eV)	D^+ (750 eV)	D^+ (1000 eV)
0.0 E 00	4.0 E 01	3.5 E 01	3.0 E 01
1.0 E 16	7.8 E 01	5.5 E 01	4.2 E 01
2.0 E 16	9.2 E 01	7.2 E 01	5.3 E 01
4.0 E 16	1.0 E 02	8.7 E 01	6.7 E 01
6.0 E 16	1.0 E 02	9.4 E 01	7.5 E 01
8.0 E 16		9.8 E 01	8.1 E 01
1.0 E 17		1.0 E 02	8.5 E 01
1.2 E 17		1.0 E 02	8.9 E 01
1.4 E 17		1.0 E 02	9.1 E 01
1.6 E 17			9.3 E 01
1.8 E 17			9.4 E 01
2.0 E 17			9.6 E 01
2.2 E 17			9.7 E 01
2.4 E 17			9.8 E 01

Reference:

E. W. Thomas, J. Appl. Phys. 51, 1176 (1980).

Accuracy: ±10%

Notes: (1) For a definition of reemission rate and how it relates to trapping, see note 2a at the beginning of this section.

(2) Type 304 stainless steel was used.

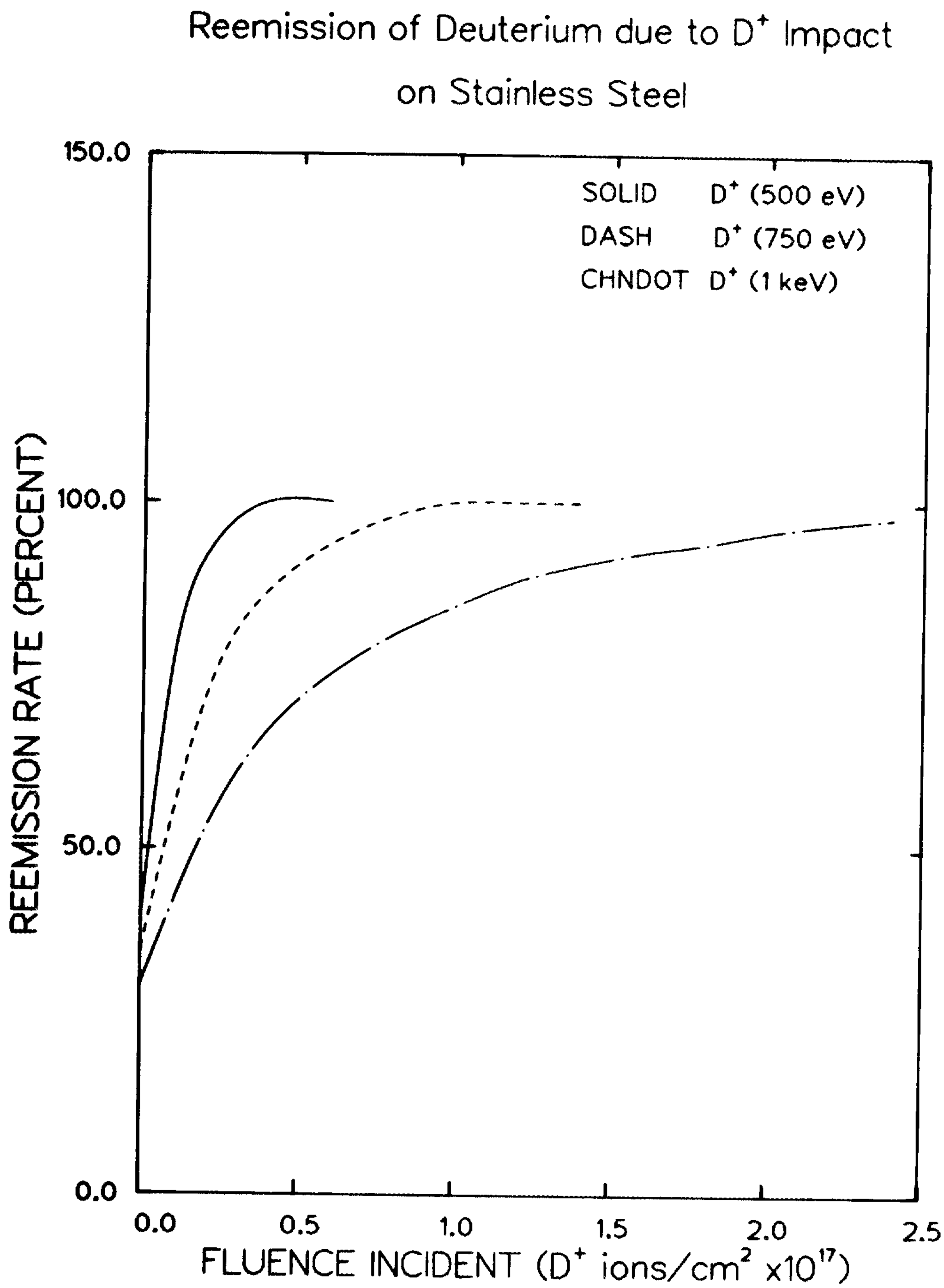
Reemission of Deuterium due to D+ Impact
on Stainless Steel
SOLID D+ (500 eV)
DASH D+ (750 eV)
CHNDOT D+ (1 keV)
150.0
100.0
50.0
0.0
REEMISSION RATE (PERCENT)
0.0
0.5
1.0
1.5
2.0
2.5
FLUENCE INCIDENT (D+ ions/cm2 x10^17)

Replacement Efficiency of D in Stainless Steel

by Subsequent H Impact

(normal incidence, temperature 150 K)

The data for for 1-, 4-, 7-, and 14-keV D replaced, respectively, by 1-, 4-, 7-, and 14-keV H; the result is independent of energy.

Fluence Relative to Saturation (n_H/n_{sat})	Replacement Efficiency Deuterium Released per Incident Proton dn_D/dn_H
0.0 E 00	1.0 E 00
5.0 E-01	5.4 E-01
1.0 E 00	2.8 E-01
1.5 E 00	1.6 E-01
2.0 E 00	1.1 E-01
2.5 E 00	1.0 E-01
3.0 E 00	8.0 E-02
3.5 E 00	6.0 E-02

Reference:

R. S. Blewer et al., J. Nucl. Mater. 76 and 77, 305 (1978).

Accuracy: ±10%

Notes: (1) For explanation of this parameter see note 2g at the beginning of this section.

(2) Type 321 stainless steel was used.

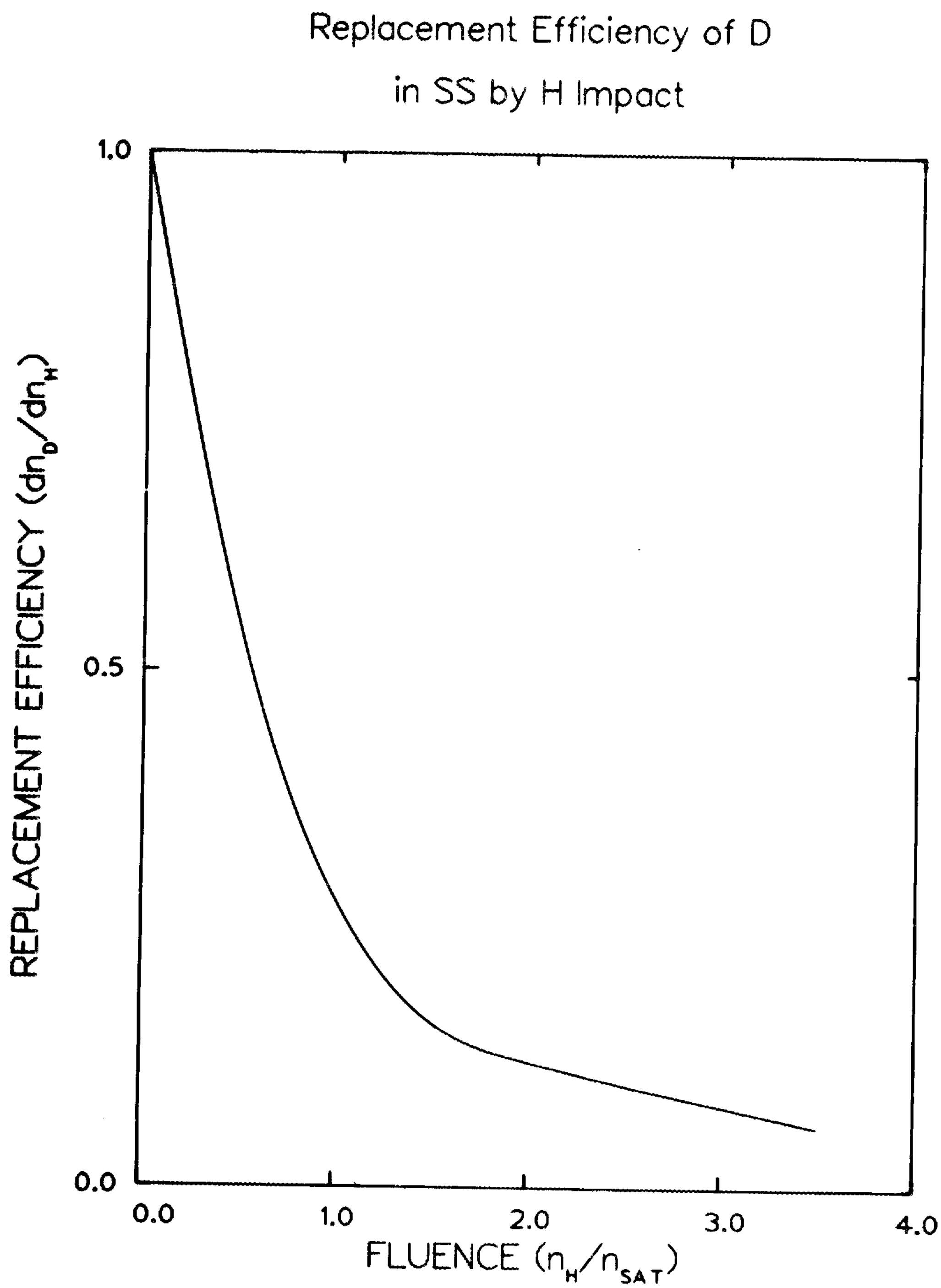
Replacement Efficiency of D
in SS by H Impact
1.0
0.5
0.0
REPLACEMENT EFFICIENCY (dn_D/dn_H)
0.0
1.0
2.0
3.0
4.0
FLUENCE (n_H/n_SAT)

Reemission of Deuterium Due to D^+ Impact on Ni

at Various Temperatures

(normal incidence, various temperatures, 18-keV energy)

Fluence Incident (D^+ ions/cm^2)	Reemission Rate (%)		
	208 K	273 K	323 K
0.0 E 00	0.0 E 00	0.0 E 00	0.0 E 00
1.0 E 16	3.0 E 00	5.0 E 00	4.9 E 01
2.0 E 16	6.0 E 00	9.0 E 00	6.3 E 01
3.0 E 16	7.0 E 00	1.2 E 01	6.8 E 01
4.0 E 16	8.0 E 00	1.5 E 01	7.1 E 01
5.0 E 16	8.0 E 00	1.8 E 01	7.3 E 01
7.0 E 16	8.0 E 00	2.4 E 01	7.4 E 01
1.0 E 17	8.0 E 00	3.3 E 01	7.4 E 01
1.5 E 17	9.0 E 00	4.3 E 01	
2.0 E 17	1.8 E 01	4.8 E 01	
2.5 E 17		5.3 E 01	

Reference:

K. Erents and G. M. McCracken, Br. J. Appl. Phys. (J. Phys. D) Ser. 2, 2, 1397 (1969).

Accuracy: Unknown

Notes: (1) For a definition of reemission and how it relates to trapping, see note 2a at the beginning of this section.

(2) A measurement at lower temperature (77 K) is given by K. Erents and G. M. McCracken, Radiat. Eff., 3, 123 (1970).

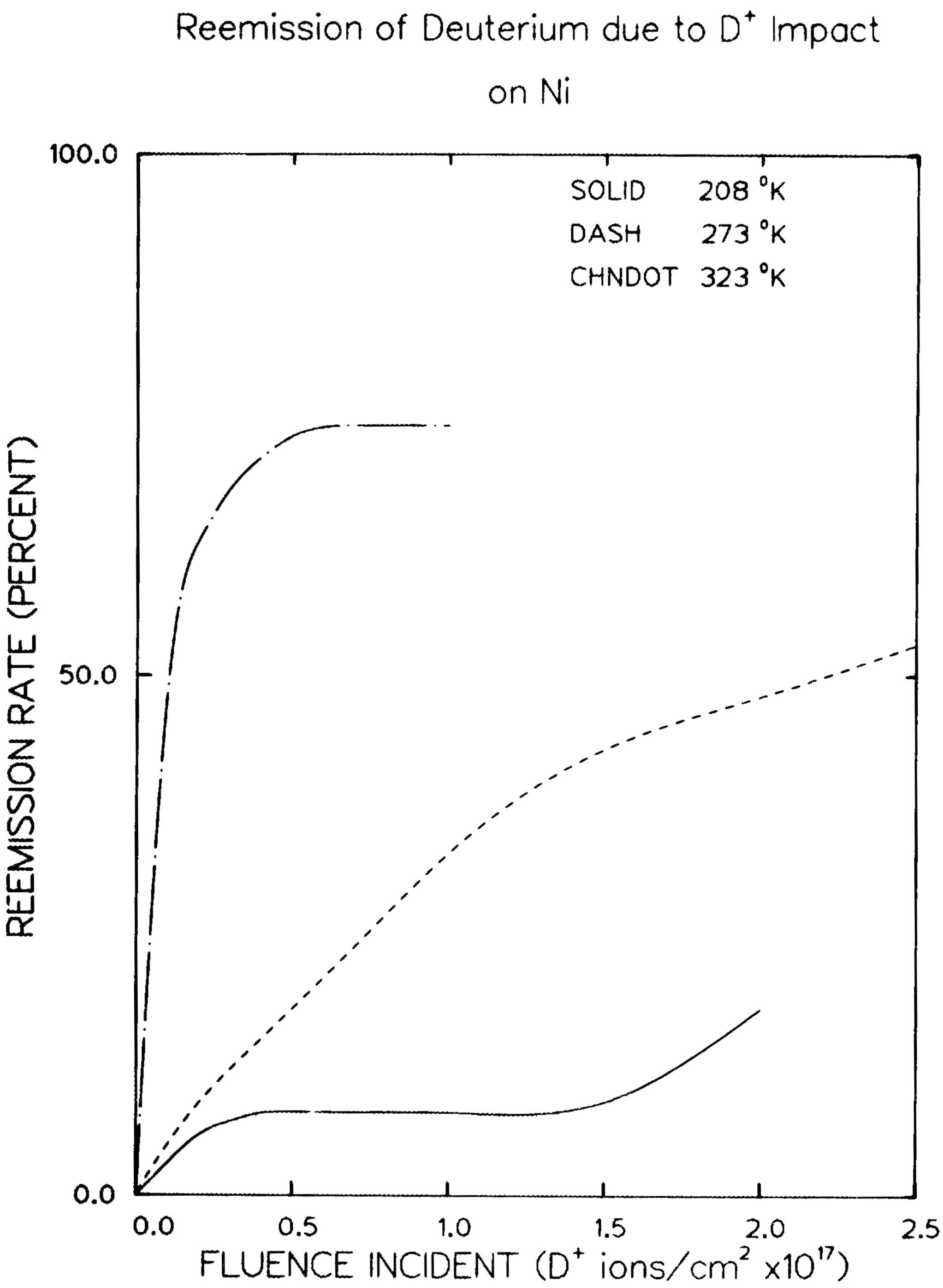

Reemission of Deuterium due to D+ Impact
on Ni
SOLID 208 °K
DASH 273 °K
CHNDOT 323 °K
REEMISSION RATE (PERCENT)
100.0
50.0
0.0
0.0
0.5
1.0
1.5
2.0
2.5
FLUENCE INCIDENT (D+ ions/cm2 x1017)

Trapped Fluence as a Function of Incident Fluence for D^+ on Mo with Various Predamage Conditions

(normal incidence; room temperature; 8-keV D^+ energy; predamage by 11-keV He^+ to the fluences shown; single crystal target)

Fluence Incident (D^+ ions/cm^2)	Fluence Trapped (D atoms/cm^2)			
	No Predamage	Predamage $6x10^{14}$ He/cm^2	Predamage $3x10^{15}$ He/cm^2	Predamage 10^{16} He/cm^2
0.0 E 00	0.0 E 00	0.0 E 00	0.0 E 00	0.0 E 00
1.0 E 16	2.5 E 15	7.0 E 15	7.0 E 15	7.0 E 15
2.0 E 16	5.5 E 15	1.1 E 16	1.3 E 16	1.3 E 16
3.0 E 16	8.0 E 15	1.3 E 16	2.0 E 16	2.0 E 16
4.0 E 16	1.0 E 16	1.5 E 16	2.3 E 16	2.7 E 16
5.0 E 16	1.1 E 16	1.7 E 16	2.5 E 16	3.3 E 16
6.0 E 16	1.2 E 16	1.8 E 16	2.7 E 16	3.6 E 16
7.0 E 16	1.3 E 16	2.0 E 16	2.8 E 16	3.8 E 16
8.0 E 16	1.4 E 16	2.2 E 16	3.0 E 16	4.0 E 16
9.0 E 16	1.5 E 16	2.3 E 16	3.2 E 16	4.3 E 16
1.0 E 17	1.6 E 16	2.5 E 16	3.4 E 16	4.5 E 16

Reference:

J. Bottinger et al., J. Appl. Phys. 48, 920 (1977).

Accuracy: Unknown

Notes: (1) For a definition of trapping see note 2b at the beginning of this section.

(2) "Predamage" is created by a preliminary bombardment with 11-keV He^+ to the dose indicated; no quantitative measure of the damage was made.

(3) The cited reference includes additional data for predamage with other projectiles (Ne^+, Bi^+).

(4) The data are for an aligned signel crystal of Mo. Limited studies on polycrystalline Mo show similar behavior [see S. T. Picraux et al., J. Nucl. Mater. 63, 110 (1976)].

(5) Additional data are to be found in work by G. M. McCracken and S. K. Erents, in Applications of Ion Beams to Metals, ed. by S. T. Picraux et al. (Plenum Publ. Corp., New York, 1974), p. 585.

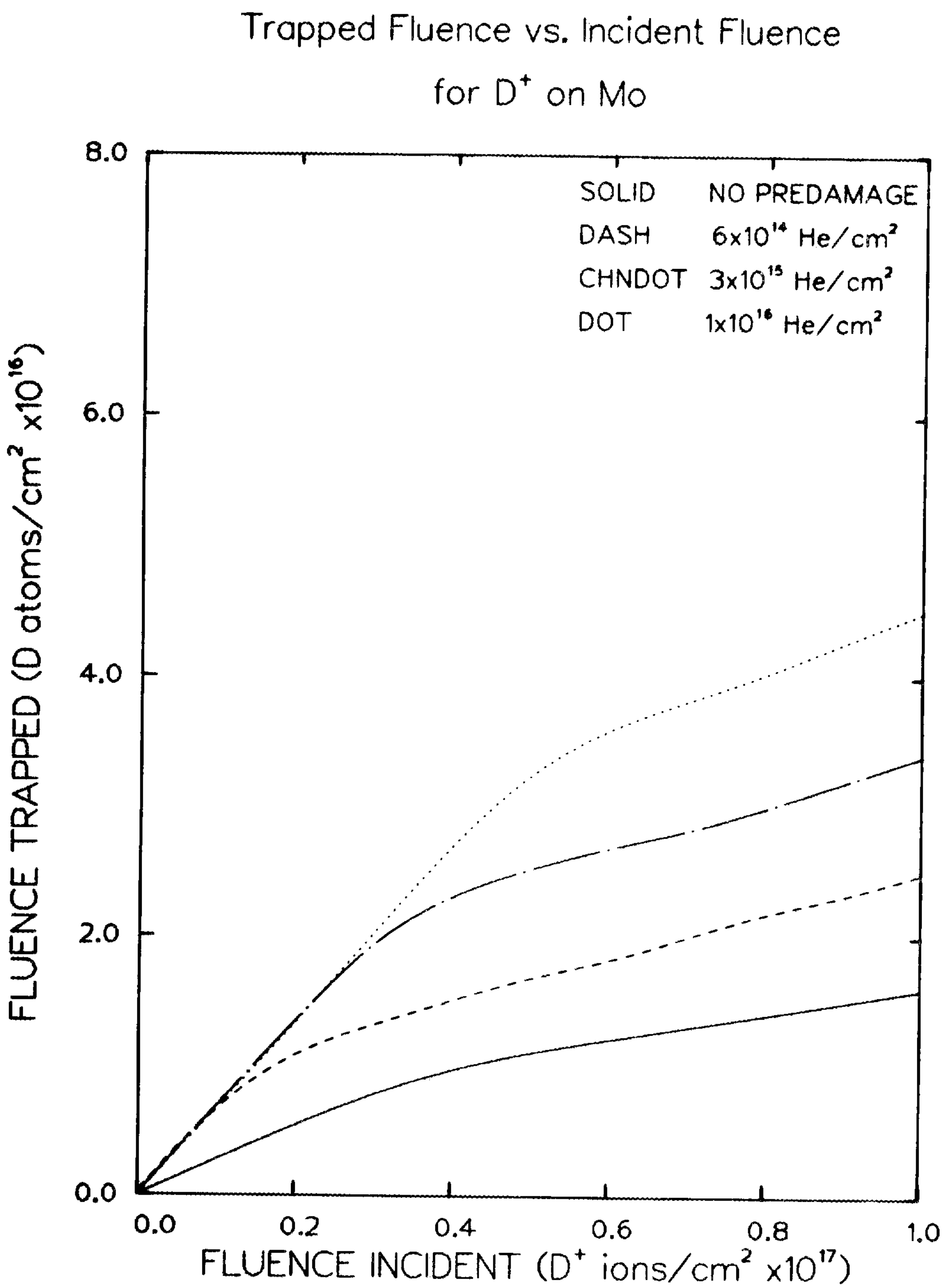
Trapped Fluence vs. Incident Fluence
for D+ on Mo
SOLID NO PREDAMAGE
DASH 6x10^14 He/cm^2
CHNDOT 3x10^15 He/cm^2
DOT 1x10^16 He/cm^2
FLUENCE TRAPPED (D atoms/cm^2 x10^16)
FLUENCE INCIDENT (D+ ions/cm^2 x10^17)
0.0
2.0
4.0
6.0
8.0
0.0
0.2
0.4
0.6
0.8
1.0

INDEX

INTERNAL DISTRIBUTION

1-25. C. F. Barnett
26. L. A. Berry
27. R. E. Clausing
28. R. J. Colchin
29. O. H. Crawford
30. S. Datz
31. R. A. Dory
32. J. L. Dunlap
33. C. A. Foster
34. D. C. Gregory
35. P. M. Griffin
36. H. H. Haselton
37. C. C. Havener
38. S. Hiroe
39. H. Howe
40. H. T. Hunter
41. R. C. Isler
42-66. M. I. Kirkpatrick
67. H. F. Krause
68. R. A. Langley
69. F. W. Meyer
70. G. Michaels
71-95. R. A. Phaneuf
96. J. A. Rome
97. P. Ryan
98. I. A. Sellin
99. W. L. Stirling
100. C. E. Thomas
101. C. C. Tsai
102. J. H. Whealton
103. W. White
104. J. B. Wilgen
105. Central Research Library
106. Document Reference Section
107-108. Laboratory Records
109. Laboratory Records, RC
110. ORNL Patent Section
111. Fusion Energy Div. Library
112. Fusion Engineering Design Center

EXTERNAL DISTRIBUTION

113. Office of Assistant Manager, Energy Research and Development, DOE-ORO
114. Dr. V. A. Abramov, Institute Atommoi Energii, I. V. Kurchatova, 46 Ulitsa Kurchatova, Moscow D-182, U.S.S.R.
115. Dr. I. Alexeff, Dept. Electrical Engineering, Ferris Hall, University of Tennessee, Knoxville, TN 37996-2100
116. Dr. M. A. Ali, Chemistry Department, Howard University, Washington, DC 20059
117. Dr. P. Allison, Los Alamos National Laboratory, P. O. Box 1663, MS H-818, Los Alamos, NM 87545
118. Dr. R. C. Amme, Department of Physics, University of Denver, Denver, CO 80208
119. Dr. N. O. Andersen, Institute of Physics, University of Aarhus, Dk-8000 Aarhus C, Denmark
120. Dr. L. W. Anderson, Department of Physics, University of Wisconsin, Madison, WI 53706
121. Dr. K. Ando, Atomic Process Laboratory, Rikagaku Kenkyusho, The Institute of Phys. & Chem. Res., Wako-Shi, Saitama, 351, Japan
122. Dr. D. Armstrong, Los Alamos National Laboratory, P. O. Box 1663, MS H-821, Los Alamos, NM 87544
123. Dr. M. Bacal, Laboratoire P.M.I., Ecole Polytechnique, 91128 Palaiseau Cedex, France

124. Mr. T. Banno, University of Tokyo, Faculty of Engineering, Department of Applied Phys., Bunkyo-Ku Tokyo, Japan
125. Dr. A. Barany, Inst. of Theoretical Physics, Uppsala University, Thunbergsv. 3, S-752 38 Uppsala, Sweden
126. Dr. M. Barat, LCAM Bat 351, Universite Paris-Sud, 91405-Orsay Cedex, France
127. Dr. W. Bauer, Sandia Laboratories, Dept. 8340, Livermore, CA 94550
128. Dr. J. F. Baur, GA Technologies Inc., P. O. Box 85608, San Diego, CA 92138
129. Dr. H. Behrens, Fachinformationszentrum, Energie Physik Mathematick Gmbh, 7514 Eggenstein-Leopoldshafen 2, Federal Republic Germany
130. Dr. K. Behringer, Jet Joint Undertaking, Culham Laboratory, Abingdon, Oxon. OX14 3DB, England
131. Dr. R. Behrisch, Max-Planck-Institut für Plasmaphysik, Boltzmannstr. 2, D-8046 Garching Bei Munchen, West Germany
132. Prof. G. Bekefi, Department of Physics, Room 36-213, Massachusetts Inst. of Techn., Cambridge, MA 02139
133. Dr. R. D. Bengtson, Department of Physics, University of Texas, Austin, TX 78712
134. Dr. D. Berenyi, Inst. of Nuclear Research of The Hungarian Academy of Sci., H-4001 Debrecen Pf. 51,, 18/C Bem Ter, Hungary
135. Dr. K. H. Berkner, Bldg. 50, Rm. 149, 1 Cyclotron Road, Lawrence Berkeley Laboratory, Berkeley, CA 94720
136. Prof. R. S. Berry, Department of Chemistry, The University of Chicago, 5735 South Ellis Avenue, Chicago, IL 60637
137. Dr. P. J. Bertoncini, Argonne National Laboratory, 9700 South Cass Avenue, Argonne, IL 60439
138. Biblioteca - Att. Clelia De Palo, Enea-Centro Ricerche, C.P. 65, 00044 Frascati, Roma, Italy
139. Dr. R. S. Blewer, Sandia Laboratories, Org. 2147, P. O. Box 5800, Alburquerque, NM 87185
140. Dr. S. L. Bliman, Centre D'etudes Nucleaires, De Grenoble, 85 X Avenue Des Martyrs, F-38041 Grenoble, Cedex, France
141. Prof. Dr. A. L. Boers, Kernfysisch Versneller, Instituut Der Rijksuniversiteit, Universiteitscomplex Paddepoel, 9747 AA Groningen, The Netherlands
142. Dr. R. Boxman, School of Engineering, Tel-Aviv University, Ramat-Aviv, Tel-Aviv 69978, Israel
143. Dr. Manuel Braun, Forskningsinstitutet for Atomfysik, Frescativagen 24, S-104 05 Stockholm, Sweden
144. Dr. F. Bresnock, 36 Milltown Road, New Fairfield, CT 06810
145. Dr. F. Brouillard, Institut De Physique, Chemin Du Cyclotron. 2, Universite De Louvain, B 1348 Louvain-La-Neuve, Belgium
146. Dr. K. H. Burrell, GA Technologies Inc., P. O. Box 85608, San Diego, CA 92138
147. Dr. V. A. Burtsev, D. V. Efremov Scientific Res., Inst. of Electrophys. Apparatus, 188631, Leningrad, U.S.S.R.
148. Dr. J. Callaway, Dept. of Phys. and Astronomy, Louisiana State University, Baton Rouge, LA 70803

149. Dr. J. D. Callen, Nuclear Engineering Dept., ERB, 1500 Johnson Drive, University of Wisconsin, Madison, WI 053706
150. Dr. S. Chakrabarti, Space Sciences Laboratory, Univ. California-Berkeley, Berkeley, CA 94720
151. Dr. F. Chang, Astronaut Office/Code CB, NASA Johnson Space Center, Houston, TX 77058
152. Dr. C. L. Chen, Westinghouse Research and Development Center, 1310 Beulah Road, Pittsburgh, PA 15235
153. Dr. C. K. Choi, School of Nuclear Engineering, Purdue University, West Lafayette, IN 47907
154. Dr. Y. P. Chong, Lawrence Livermore National Lab., P. O. Box 808, MS L-626, Livermore, CA 94550
155. Prof. S. Chu, Department of Chemistry, University of Kansas, Lawrence, KS 66045
156. Dr. D. A. Church, Physics Dept., Texas A&M University, College Station, TX 77843
157. Dr. A. Chutjian, Jet Propulsion Laboratory, Mail Stop 183-601, California Inst. of Techn., 4800 Oak Grove Drive, Pasadena, CA 91109
158. Dr. E. J. Clothiaux, Department of Physics, Auburn University, Auburn, AL 36849-3501
159. Dr. F. H. Coensgen, Radiation Laboratory, Lawrence Livermore National Lab., P.O. Box 808, Livermore, CA 94550
160. Dr. M. J. Coggiola, Molecular Physics Lab., SRI International, 333 Ravenswood Avenue, Menlo Park, CA 94025
161. Dr. S. A. Cohen, Plasma Physics Laboratory, Forrestal Campus, Princeton University, Princeton, NJ 08544
162. Prof. R. W. Conn, UCLA, 6291 Boelter Hall, Los Angeles, CA 90024
163. Dr. K. Connor, ECSE Department, Rensselaer Polytechnic Institute, Troy, NY 12181
164. Dr. D. L. Cook, Organization 1260, Sandia Laboratories, P. O. Box 5800, Albuquerque, NM 87185
165. Dr. J. L. Cook, AAEC Research Establishment, Physics Division, AAEC - Lucas Heights, Sutherland 2232, N.S.W., Australia
166. Dr. J.N.L. Coonor, Department of Chemistry, University of Manchester, Manchester M13 9PL, England
167. Dr. D. H. Crandall, ER-542, G-215 GTN, Office of Fusion Energy, U.S. Dept. of Energy, Washington, DC 20545
168. Dr. R. A. Dandl, Applied Microwave Plasma Concepts, 2210 Encinitas Blvd., Suite P, Encinitas, CA 92024
169. Dr. R. Danford, Intl. Research & Evaluation, Attn: Input Processing Director, 21098 IRE Control Center, Eagan, MM 55121
170. Dr. H. Davis, LANL, P. O. Box 1663, MS E-526, Los Alamos, NM 87545
171. Dr. F. J. De Heer, FOM-Institute for Atomic and Molecular Physics, Kruislaan 407, 1098 SJ Amsterdam, The Netherlands
172. Prof. J. L. Delcroix, Lab. Physique Des Plasmas, Faculte Des Sci. D'Orsay, Batiment 212, F-91400 Orsay, France
173. Prof. K. T. Dolder, Dept. of Atomic Physics, School of Physics, Univ. of Newcastle Upon Tyne, Newcastle-On-Tyne NE1 7RU, England

174. Dr. J. J. Dorning, Department of NEEP, Reactor Facility, University of Virginia, Charlottesville, VA 22901
175. Dr. L. D. Doverspike, Department of Physics, College of William & Mary, Williamsburg, VA 23185
176. Dr. J. R. Drake, Royal Institute of Technology, Division Plasma Physics, Teknikringen 31, S-100 44, Stockholm 70, Sweden
177. Dr. H. W. Drawin, Centre D'etudes Nucleaires, De Fontenay-Aux-Roses, DRFC - SCP, B. P. No 6, F-92260 Fontenay-Aux-Roses, France
178. Dr. R. Dubois, Battelle-Pacific Northwest Labs, P. O. Box 999, Richland, WA 99352
179. Dr. P. D. Dumont, Universite De Liege, Faculte Des Sciences, Inst. De Phys. Nucl. Experiment., Sart Tilman B - 4000 Liege 1, Belgium
180. Dr. G. H. Dunn, JILA, Campus Box 440, University of Colorado, Boulder, CO 80309
181. Dr. H. F. Dylla, Princeton Plasma Physics Lab., Princeton University, P. O. Box 451, Princeton, NJ 08544
182. Dr. W. Eckstein, Max-Planck-Institut für Plasmaphysik, 8046 Garching, Bei Muchen, West Germany
183. EG&G Idaho, Inc., Attn: Inel Techn. Library-I.F., P.O. Box 1625, Idaho Falls, ID 83415
184. Dr. R. C. Elton, Code 4733, Naval Research Lab., Washington, DC 20375
185. Dr. B. Feinberg, Lawrence Berkeley Laboratory, University of California, MS 71259, Berkeley, CA 94720
186. Dr. C. R. Finfgeld, Office of Fusion Energy, Office of Energy Research, Mail Station G-256, U.S. Department of Energy, Washington, DC 20545
187. Dr. J. H. Fink, 4023 East Avenue, Hayward, CA 04542
188. Dr. M. Fink, RLM Bldg. 10.202, Department of Physics, University of Texas, Austin, TX 78712
189. Dr. R. K. Fisher, GA Technologies, Inc., P. O. Box 85608, L-338, San Diego, CA 92138
190. Dr. D. L. Flamm, Room 6E216, Bell Laboratories, 600 Mountain Avenue, Murray Hill, NJ 07974
191. Dr. H. H. Fleischmann, Department of Applied Physics, Clark Hall, Cornell University, Ithaca, NY 14853
192. Dr. R. F. Fleming, 19167 Stedwick Drive, Gaithersburgh, MD 20879
193. Dr. R. J. Fonck, Plasma Physics Laboratory, Princeton University, P. O. Box 451, Princeton, NJ 08544
194. Dr. T. K. Fowler, Lawrence Livermore Laboratory, P. O. Box 5511, Mail Code L-640, Livermore, CA 94550
195. Dr. R. S. Freund, Bell AT&T Labs., Rm. 1D-256, Murray Hill, NJ 07974
196. Dr. A. Fukuda, Quantumtechnology Division, Electrotechnical Laboratory, 1-1-4, Umezono, Sakura-Mura, Niihari-Gun, Ibaraki, Japan
197. Dr. G. Fussmann, Max-Planck Institut fuer Plasmaphysik (IPP), 8046 Garching, Bei Munchen, Germany Abtl. E3

198. Dr. A. Futch, MS L-437, Lawrence Livermore National Lab., P.O. Box 808, Livermore, CA 94550
199. Dr. J. Gallagher, JILA, University of Colorado, Boulder, CO 80309
200. Dr. A. Garscadden, Aero Propulsion Laboratory, AFWAL-POOC-3, Building 450, Wright-Patterson AFB, Dayton, OH 45433
201. Mrs. B. Garton, Department of Physics, Imperial College of Science & Technology, London S.W. 7, England
202. Dr. W. B. Gauster, Division 6248, Sandia National Laboratories, Albuquerque, NM 87185
203. Dr. K. W. Gentle, Department of Physics, University of Texas, Austin, TX 78712
204. Prof. H. B. Gilbody, Department of Pure & Applied Phys., The Queen's University of Belfast, Belfast BT 7, 1NN, Northern Ireland
205. Dr. H. Goldberg, Rockwell Hanford Operations, 622-G Bldg., 600-W Area, Richland, WA 99352
206. Dr. L. B. Golden, Department of Physics, The Worthington Scranton Campus, Pennsylvania State Univ., 120 Ridge View Drive, Dunmore, PA 18512
207. Dr. S. Goldsmith, Department of Physics, Tel-Aviv University, Tel-Aviv, Israel
208. Dr. I. N. Golovin, I. V. Kurchatov Institute, Atomic Energy, Ulitsa Kurchatova 46, Moscow 123182, U.S.S.R.
209. Dr. R. W. Gould, MS 128-95, Dept. of Applied Physics, California Institute of Techn., Pasadena, CA 91109
210. Dr. W. G. Graham, Physics Department, New University of Ulster, Coleraine BT52 1SA, Northern Ireland
211. Dr. T. A. Green, Division 1151, Sandia National Laboratories, Albuquerque, NM 87185
212. Dr. E. Greenspan, Atomic Energy Commission, Nuclear Research Centre-Negev, P. O. Box 9001, Beersheva, 84190, Israel
213. Dr. R. J. Groebner, Doublet III Program, 13/463, GA Technologies Inc., P. O. Box 85608, San Diego, CA 92138
214. Dr. R. A. Gross, Department of Applied Physics & Nuclear Engineering, Columbia University, New York, NY 10027
215. Dr. D. Gruen, Chemistry Division, Argonne National Laboratory, 9700 S. Cass Avenue, Argonne, IL 60439
216. Dr. G. E. Guest, Applied Microwave Plasma Concepts, 2210 Encinitas Blvd., Suite P, Encinitas, CA 92024
217. Dr. A. Haasz, Univ. of Toronto, Inst. for Aerospace Studies, 4925 Dufferin Street, Downsview, Ontario, Canada M3H 5T6
218. Dr. L. Hage, Library Adm. Department, Technische Hogeschool, Bibliotheek, 2120.41233, Postbus 513, 5600-MB Eindhoven, The Netherlands
219. Dr. S. Hagmann, Department of Physics, Kansas State University, Manhattan, KS 66506
220. Dr. S. M. Hamberger, Plasma Research Laboratory, Australian National University, G. P. O. Box 4, Canberra, ACT, 2601, Australia

221. Dr. S. P. Hatchett II, L-477, Lawrence Livermore National Lab., Livermore, CA 94550
222. Dr. H. C. Hayden, Department of Physics, U-46, University of Connecticut, Storrs, CT 06268
223. Dr. F. A. Herrero, Code 960, NASA Goddard, Greenbelt, MD 20771
224. Dr. R. A. Hess, Laboratory for Plasma and Fusion Energy Studies, University of Maryland, College Park, MD 20742
225. Dr. R. L. Hickok, Jr., ECSE Dept. JEC 6003, Rensselaer Polytechnic Inst., Troy, NY 12180-3590
226. Dr. K. W. Hill, Plasma Physics Laboratory, Princeton University, P. O. Box 451, Princeton, NJ 08544
227. Dr. G. Himmel, Ruhr-Universitat Bochum, Experimentalphysik, Lehrstuhl II, Universitatsstr. 150, Postfach 102148, 4630 Bochum 1, West Germany
228. Dr. J. R. Hiskes, L-630, Lawrence Livermore National Lab., P.O. Box 5511, Livermore, CA 94550
229. Dr. B. Hodge, Fusion Research Center, RLM 11.222, University of Texas, Austin, TX 78712
230. Dr. S.-P. Hong, Bell Laboratories, 555 Union Boulevard, Allentown, PA 18103
231. Dr. E. B. Hooper, Jr., Neutral Beam Group, Lawrence Livermore National Lab., P. O. Box 5511, L-537, Livermore, CA 94550
232. Dr. J. W. Hooper, 5260 Northside Drive, N.W., Atlanta, GA 30327
233. Dr. G. R. Hopkins, GA Technologies Inc., P. O. Box 85608, San Diego, CA 92138
234. Dr. W. F. Huebner, Group T-4, MS 212, Los Alamos National Laboratory, P. O. Box 1663, Los Alamos, NM 87545
235. Dr. J. G. Hughes, International Atomic Energy Agency, Wagramerstrasse 5, P. O. Box 100, A-1400 Vienna, Austria
236. Dr. A. Hunt, Lawrence Livermore National Lab., P. O. Box 5511, L-637, Livermore, CA 94550
237. International Research & Evaluation, Attn: IRE-ITTD Input Processing Dir., 21098 Ire Control Ctr., Eagan, MN 55121
238. Dr. Y. Itikawa, Institute of Space and Astronautical Science, 6-1, Komaba 4-Chome, Meguro-Ku, Tokyo 153, Japan
239. Dr. F. C. Jahoda, CTR Division, Los Alamos National Laboratory, P.O. Box 1663, MS F-639, Los Alamos, NM 87545
240. Dr. A. K. Jain, Government of India, Bhabha Atomic Research Centre, Nuclear Physics Division, Trombay Bombay 400 085, India
241. Dr. B. C. Johnson, Harvard College Observatory, Cambridge, MA 02138
242. Dr. P. B. Johnson, Department of Physics, Victoria University of Weelington, Private Bag Wellington, New Zealand
243. Dr. R. E. Johnson, Dept. of Nuclear Engineering and Engineering Physics, Thornton Hall, University of Virginia, Charlottesville, VA 22901
244. Dr. E. G. Jones, Systems Research Lab., Inc., 2800 Indian Ripple Road, Dayton, OH 45440
245. Dr. E. M. Jones, Jet Joint Undertaking, Data Acquisitions Group, Codas Division J2, Abingdon, Oxfordshire OX14 3EA, England

246. Dr. K. W. Jones, Brookhaven National Laboratory, Bldg. 901-A, Upton, NY 11973
247. Dr. W. D. Jones, Department of Physics, University of South Florida, Tampa, FL 33620
248. Dr. R. A. Jong, Lawrence Livermore Laboratory, P. O. Box 5511, L-637, Livermore, CA 94550
249. Dr. B. R. Junker, Code 412, Office of Naval Research, 800 North Quincy Street, Arlington, VA 22217
250. Dr. T. Kammash, Dept. of Nuclear Engineering, University of Michigan, Ann Arbor, MI 48104
251. Dr. T. Kato, Research Information Center, Institute of Plasma Physics, Nagoya University, Nagoya 464, Japan
252. Dr. K. Katsonis, Lab. Physique Des Plasmas, Faculte Des Sci. D'Orsay, Batiment 212, F-91400 Orsay, France
253. Dr. J. J. Kaufman, Department of Chemistry, Johns Hopkins University, Baltimore, MD 21218
254. Dr. R. A. Kenefick, Dept. of Physics, Texas A&M University, College Station, TX 77843
255. Kernforschungszentrum Karlsruhe GMBH, Literaturabteilung, Postfach 3640, D-7500 Karlsruhe, Federal Republic of Germany
256. Dr. Y.-K. Kim, Bldg. 221, Rm A-267, National Bureau of Standards, Gaithersburg, MD 20899
257. KMS Fusion, Inc., Library, 3621 S. State Road, P. O. Box 1567, Ann Arbor, MI 48106
258. Dr. H. Knudsen, Institute of Physics, University of Aarhus, DK-8000, Aarhus C, Denmark
259. Dr. K. Kondo, Plasma Physics Laboratory, Kyoto University, Gokashyo Uji, Kyoto, Japan
260. Dr. G. Kulcinski, Dept. of Nuclear Engineering, University of Wisconsin, Madison, WI 53706
261. Dr. H. J. Kunze, Institut fuer Exp.-Physics, Ruhr Universitaet, 4630 Bochum, West Germany
262. Dr. Neal F. Lane, University of Colorado, P. O. Box 7150, Colorado Springs, CO 80933-7150
263. Dr. B. Laskowski, Analatom Inc., 253 Humboldt Court, Sunnyvale, CA 94086
264. Lawrence Livermore National Lab., Attention: Tech. Infor. Dept., P. O. Box 5500, Livermore, CA 94550
265. Dr. N. H. Lazar, Bldg. R1, Defense and Space Systems Group of TRW Inc., One Space Park, Redondo Beach, CA 90278
266. Prof. B. Lehnert, The Royal Institute of Techn., Div. of Plasma Phys. Fusion Res., Stockholm, 70, Sweden
267. Dr. W. N. Lennard, Solid State Science, Chemistry & Materials Division, Atomic Energy of Canada Limited, Nuclear Laboratories, Chalk River, Ontario, Canada KOJ 1JO
268. Dr. G. W. Leppelmeier, Magnetic Fusion Energy Division, Lawrence Livermore National Lab., P. O. Box 5511, L-637, Livermore, CA 94550
269. Dr. K. N. Leung, Bldg. 4, Lawrence Berkeley Laboratory, Berkeley, CA 94720

270. Dr. K. Leung, Fusion Engineering, 6291 Boelter Hall, UCLA, Los Angeles, CA 90024
271, Dr. M. A. Levine, Lawrence Berkeley Laboratory, University of California, Bldg. 9, MS 41230, Berkeley, CA 94720
272. Prof. D. Lichtman, Department of Physics, Univ. of Wisconsin-Milwaukee, Milwaukee, WI 53201
273. Dr. A. Lietzke, Lawrence Berkeley Laboratory, 1 Cyclotron Road, Bldg. 4, Berkeley, CA 94720
274. Dr. C. C. Lin, Department of Physics, University of Wisconsin, Madison, MI 53706
275. Dr. F. Linder, Department of Physics, Univ. of Kaiserslautern, D-675 Kaiserslautern, West Germany
276. Dr. A. E. Livingston, Department of Physics, University of Notre Dame, Notre Dame, IN 46556
277. Dr. G. J. Lockwood, Division 1234, Sandia National Laboratories, P. O. Box 5800, Albuquerque, NM 87185
278. Dr. D. C. Lorents, Chemical Physic Laboratory, SRI International, 333 Ravenwood Avenue, Menlo Park, CA 94025
279. Dr. A. Lorenz, Deputy Head, Nuclear Data Section, International Atomic Energy Agency, Wagramerstrasse 5, P. O. Box 100, A-1400 Vienna, Austria
280. Prof. M. Los, FOM-Institute of Atomic and Molecular Physics, Kruislaan 407, Amsterdam/watergraafsmeer, The Netherlands
281. Los Alamos National Laboratory, Attention: Librarian, MS P362, P. O. Box 1663, Los Alamos, NM 87545
282. Ms. H. W. Lovitts, Sci. Information Service, Inc., 7 Woodland Avenue, Larchmont, NY 10538
283. Dr. M. W. Lucas, University of Sussex, School of Mathematical and Physical Sciences, Falmer, Brighton BN1 9QH, United Kingdom
284. Dr. S. R. Lundeen, Department of Physics, University of Notre Dame, Nieuwland Science Hall, Notre Dame, IN 46556
285. Dr. D. M. Manos, Plasma Physics Laboratory, Princeton University, P. O. Box 451, Princeton, NJ 08544
286. Dr. S. T. Manson, Department of Physics, Georgia State University, Atlanta, GA 30303
287. Dr. E. S. Marmar, Massachusetts Institute of Techn., NW 16-280, Cambridge, MA 02139
288. Dr. J. V. Martinez, Division of Chemical Sciences, Off. of Basic Energy Sci., J-309, U.S. Department of Energy, Washington, DC 20545
289. Dr. S. Matsuda, Fusion Research Center, Japan Atomic Energy Res. Inst., Mukaiyama, Naka-Machi, Naka-Gen, Ibaraki-Ken, T 311-02 Japan
290. Dr. M. Mattioli, Association Euratom-CEA Sur La Fusion, DPH - PFC - B.P. 6, F 92260 Fontenay-Aux-Roses, France
291. Dr. H. M. Mayer, Max-Planck-Institut fuer Plasmaphys., 8046 Garching, West Germany
292. Max-Planck-Inst. fuer Plasmaphys., Mrs. A. Hohaus, Librarian, 8046 Garching Bei Muenchen, West Germany

293. Dr. J. W. McConkey, Department of Physics, University of Windsor, Windsor, Ontario N9B 3P4, Canada
294. Dr. G. M. McCracken, Culham Laboratory, Abingdon Oxfordshire OX14 3DB, England
295. Prof. E. W. McDaniel, School of Physics, Georgia Institute of Technology, Atlanta, GA 30332
296. Dr. R. McFarland, Department of Physics, University of Missouri-Rolla, Rolla, MO 65401
297. Dr. W. Meckbach, Centro Atomico Bariloche, 8400 San Carlos De Bariloche, Argentina
298. Dr. B. B. Meckel, Deposition Technology, Inc., 8963 Carroll Way, San Diego, CA 92121
299. Dr. D. R. Mikkelsen, Plasma Physics Laboratory, Princeton University, P. O. Box 451, Princeton, NJ 08544
300. Dr. G. H. Miley, University of Illinois, 216 Nuclear Engineering Lab., 103 S. Goodwin Avenue, Urbana, IL 61801
301. Dr. S. V. Mirnov, I. V. Kurchatov Institute of Atomic Energy, Ulitsa Kurchatova, 46, Moscow 123182, U.S.S.R.
302. Mirror Fusion Experimental Group, Lawrence Livermore National Laboratory, P. O. Box 808, Livermore, CA 94550
303. Dr. A. A. Mondelli, Science Applications, Inc., 8400 Westpark Drive, McLean, Virginia 22102
304. Dr. H. W. Moos, Physics Department, Johns Hopkins University, Baltimore, MD 21218
305. Dr. T. J. Morgan, Department of Physics, Wesleyan University, Middletown, CT 06457
306. Dr. W. L. Morgan, L-18, Lawrence Livermore National Lab., University of California, P. O. Box 808, Livermore, CA 94550
307. Dr. K. Mori, 1-508 Shakujii-Koen Danchi, 1-127 Kamishakujii, Nerima-Ku, Tokyo 177, Japan
308. Dr. K. Moses, JAYCOR, Plasma Technology Division, 2908 Oregon Court, Bldg. I-7, Torrance, CA 90503
309. Dr. Y. Nakai, Department of Physics, Japan Atomic Energy Res. Inst., Tokai Research Establishment, Tokai-Mura, Naka-Gun, Ibaraki-Ken, Japan
310. Dr. S. Nakazaki, Department of Applied Physics, Faculty of Engineering, Miyazaki University, Miyazaki 880, Japan
311. Dr. F. Nehring, Rt. 3, Box 57A, Clinton, TN 37716
312. Dr. D. W. Norcross, JILA, Campus Box 440, University of Colorado, Boulder, CO 80309
313. Dr. K. W. Ogilvie, Code 692, Goddard Space Flight Center, Greenbelt, MD 20771
314. Dr. T. Ohkawa, GA Technologies, Inc., P. O. Box 85608, San Diego, CA 92138
315. Dr. S. Ohtani, Institute of Plasma Physics, Nagoya University, Nagoya 464, Japan
316. Dr. J. E. Osher, Lawrence Livermore National Lab., University of California, P. O. Box 808, L-637, Livermore, CA 94550
317. Dr. A. Osman, Theoretical Nuclear Physics, Department of Physics, Faculty of Science, Cairo University, Cairo, Egypt

318. Dr. M. Otsuka, Institute of Plasma Physics, Nagoya University, Nagoya, Japan
319. Dr. W. Ott, Max-Planck-Institut fuer Plasmaphysik, 8046 Garching Bei Muenchen, West Germany
320. Dr. H. G. Paretzke, GSF, D-8042 Neuherberg, West Germany
321. Dr. E. S. Parilis, Institute of Electronics, Tashkent, U.S.S.R.
322. Dr. J. T. Park, Vice Chancellor, Physics Department, 102 Physics, University of Missouri-Rolla, Rolla, MO 65401
323. Dr. N. J. Peacock, Culham Laboratory, Ukaea Research Group, Abingdon Oxfordshire OX 14 3DB, England
324. Dr. D. C. Pease, Delco Systems Operations, 6767 Hollister, Goleta, CA 93117
325. Dr. P. J. Persiani, Argonne National Laboraory, 9700 South Cass Avenue, Bldg. 208, Argonne, IL 60439
326. Dr. J. R. Peterson, SRI International, Menlo Park, CA 94025
327. Prof. E. Pfender, Dept. of Mechanical Engineering, University of Minnesota, 125 Mechanical Engineering Bldg., Minneapolis, MN 55455
328. Dr. L. G. Phadke, Physics Department, Northeastern State University, Tahlequah, OK 74464
329. Dr. A. V. Phelps, JILA, University of Colorado, Boulder, CO 80309
330. Physics and Applied Maths Library, College Park, The Queen's University of Belfast, Belfast BT 7 1NN, Northern Ireland
331. Physics/Optics/Astron. Library, 374 Bausch & Lomb Building, University of Rochester, Rochester, NY 14627
332. Plasma Fusion Center Library, Massachusetts Inst. of Technology, NW 16-153, Cambridge, MA 02139
333. Dr. R. S. Post, Massachusetts Institute of Techn., Plasma Fusion Center, 190 Albany Street, Cambridge, MA 02139
334. Dr. K. Prelec, Accelerator Department, Building 911B, Brookhaven National Laboratory, Upton, NY 11973
335. Dr. F. Prevot, Centre D'etudes Nucleaires de Fontenay-AuxRoses, Drfc, B. P. No 6, 92260 Fontenay-Aux-Roses, France
336. Princeton University, Attention: C-Site Library, Plasma Physics Laboratory, P.O. Box 451, Princeton, NJ 08544
337. Dr. G. Proulx, Pulse Sciences, Inc., 14796 Wicks Blvd., San Leandro, CA 94577
338. Dr. R. V. Pyle, Bldg. 4-230, Lawrence Berkeley Laboratory, Berkeley, CA 94720
339. Dr. B. H. Quon, JAYCOR, Plasma Technology Div., 2908 Oregon Ct., Bldg. I-7, Torrance, CA 90503
340. Dr. D. Register, Phillips Petroleum Co., MS-118-AL, PRC, Bartlesville, OK 74004
341. Dr. D. J. Rej, Los Alamos National Laboratory, Ctr. 3, MS 638, P. O. Box 1663, Los Alamos, NM 87545
342. Dr. J. Reece Roth, University of Tennessee, Dept. of Electrical Engineering, Rm. 316, Ferris Hall, Knoxville, TN 37916
343. Dr. H. Rohr, Max-Planck-Inst. fuer Plasmaphys., Boltzmann Str. 3, D-8046 Garching Bei Munchen, West Germany
344. Dr. W. L. Rowan, Fusion Research Center, University of Texas, Austin, TX 78712

345. Dr. M. E. Rudd, Dept. Physics and Astronomy, University of Nabraska, Lincoln, NE 68588-0111
346. Dr. J. R. Rumble, Physics Building A323, National Bureau of Standards, Washington, DC 20234
347. Rutherford Appleton Laboratory, Mrs. E. Marsh, Librarian, Chilton, Didcot, Oxfordshire OX11 0QX, England
348. Dr. G. Schilling, Plasma Physics Laboratory, Princeton University, P. O. Box 451, Princeton, NJ 08544
349. Dr. A. S. Schlachter, Lawrence Berkeley Laboratory, University of California, Berkeley, CA 94720
350. Dr. J. J. Schmidt, Nuclear Data Section, International Atomic Energy Agency, Wagramerstrasse 5, P. O. Box 100, A-1400 Vienna, Austria
351. Dr. M. Seidl, Stevens Inst. Techn., Dept. of Physics, Hoboken, NJ 07030
352. Dr. V. S. Senashenko, Institute of Nuclear Physics, M. V. Lomonosov Moscow State Univ., Moscow 119899, U.S.S.R.
353. Dr. A. Surjalal Sharma, Plasma Physics Programme, Physical Research Laboratory, Navrangpura, Ahmedabad-380-009., India
354. Dr. V. B. Sheorey, 461 Physical Research Laboratory, Navrangpura, Ahmedabad-380-009, India
355. Dr. J. Sherman, AT-2, MS 818, Los Alamos National Laboratory, Los Alamos, NM 87545
356. Dr. M. Shimada, Plasma Physics Laboratory, Princeton University, P. O. Box 451, Princeton, NJ 08544
357. Dr. T. Shirai, Japan Atomic Energy Research Inst., Tokai-Mura, Naka-Gun, Ibaraki-Ken, Japan
358. Dr. R. Shuker, Department of Physics, Ben-Gurion University of the Negev, P. O. Box 653, Beer Sheva 84105, Israel
359. Dr. P. Sigmund, Institut Physics, Campusvej 55, Odense University, 5230 Odense, Denmark
360. Dr. C. H. Skinner, Plasma Physics Laboratory, Princeton University, James Forrestal Campus, Princeton, NJ 08544
361. Dr. J. N. Smith, Mail Stop L-520, General Atomic Company, P.O. Box 81608, San Diego, CA 92138
362. Dr. L. D. Smullin, Massachusetts Institute of Techn., Dept. of Electrical Engineering and Computer Science, Cambridge, MA 02139
363. Dr. E. Speth, Department of Technology, Max-Planck-Institut fuer Plasmaphysik, 8046 Garching Bei Munchen, West Germany
364. Prof. J. C. Sprott, Department of Physics, Univ. of Wisconsin, Madison, 1150 University Avenue, Madison, WI 53706
365. Dr. K. R. Stalder, 515 King Street, Redwood, CA 94062
366. Prof. B. Stansfield, Universite de Quebec, Institut National De La Recherche Scientifique, Case Postale 1020, Varennes, Quebec, Canada
367. Dr. J. W. Stearns, MS 5-119, Lawrence Berkeley Laboratory, 1 Cyclotron Road, Berkeley, CA 94720
368. Dr. R. F. Stebbings, Dept. Space Phys. & Astron., Rice University, Houston, TX 77001

369. Dr. D. Steiner, Dept. Nuclear Engineering, Rensselaer Polytechnic Institute, Troy, NY 12181
370. Dr. W. C. Stwalley, Department of Chemistry, University of Iowa, Iowa City, IA 52242
371. Dr. H. Sugiyama, Electrotechnical Laboratory, 1-1-4 Umezone, Sakura-Mura, Niihari-Gun, Ibaraki-Ken, Japan
372. Dr. A. Surjalal Sharma, Plasma Physics Programme, Physical Research Laboratory, Navrangpura, Ahmedabad-380-009., India
373. Dr. D. R. Sweetman, U.K.A.E.A., Culham Laboratory, Bldg. E-5, Abingdon, Oxfordshire OX14 3DB, United Kingdom
374. Dr. H. Takahashi, Brookhaven National Laboratory, Upton, Long Island, NY 11973
375. Prof. K. Takayanagi, Inst. of Space & Astron. Sci., Komaba 4-6-1, Meguro-Ku, Tokyo 153, Japan
376. Dr. H. Tawara, Institute of Plasma Physics, Nagoya University, Nagoya 464, Japan
377. Technical Information Center, Stone & Webster Engineering Corp., 3 Executive Campus, P. O. Box 5200, Cherry Hill, NJ 08034
378. Dr. D. M. Thomas, L-334, GA Technologies, Inc., P. O. Box 85608, San Diego, CA 92138
379. Dr. E. W. Thomas, School of Physics, Georgia Institute of Technology, Atlanta, GA 30332
380. Dr. L. H. Toburen, Battelle Pacific Northwest Labs, 300 Area 3745-B, P. O. Box 999, Richland, WA 99352
381. U.K.A.E.A. Culham Laboratory, Attn: Mrs. S. Smith, Library Reading Room, Abingdon, Oxfordshire OX14 3DB, United Kingdom
382. Dr. M. C. Undersood, Reservoir Technology Branch, B. P. Research Centre, Chertsey Road, Sunbury-Di-Thames, Middlesex, England
383. Dr. J. Valerio, General Dynamics Corp., Covair Division, P. O. Box 80847, MS 42-6210, San Diego, CA 92138
384. Dr. E. Veje, Physics Laboratory II, University of Copenhagen, H. C. Orsted Institute, Universitetsparken 5, DK 2100 Copenhagen, Denmark
385. Dr. H. Vernickel, Max-Planck-Institut fuer Plasmaphys., 8046 Garching Bei Munchen, West Germany
386. Prof. G. C. Vlases, Aerospace and Energetics, Research Program, FL-10, University of Washington, Seattle, WA 98195
387. Dr. S. E. Von Goeler, Plasma Physics Laboratory, Princeton University, P. O. Box 451, Princeton, NJ 08544
388. Dr. F. Waelbroeck, Institut fuer Plasmaphysik, Kernforschungsanlage, 517 Juelich, Federal Republic of Germany
389. Dr. F. Wagner, Max-Planck-Inst. fuer Plasmaphys., D-8046 Garching, West Germany
390. Prof. K. Wiesemann, Ruehr-Universitaet, Inst. Exp. Phys. Agii, Postfach 102148, D-4630 Bochum 1, West Germany
391. Dr. J. F. Williams, Department of Physics, The University of Western Australia, Nedlands, Western Australia 6009
392. Dr. H. Winter, Institut Fuer Allgemeine Physik, Technische Universitaet Wien, Karlsplatz 13, A-1040 Wien, Austria

393. John G. Wolbach Library, Attention: Librarian, Harvard College Observatory, 60 Garden Street, Cambridge, MA 02138

394. Dr. J. T. Woo, Interscience, Inc., One Washington Avenue, Suite 1, Schenectady, NY 12305

395. Dr. R.L.C. Wu, Brehm Laboratory, Wright State University, Dayton, OH 45435

396. Dr. C. E. Young, Chm 200, Argonne National Lab., 9700 South Cass Avenue, Argonne, IL 60439

397-423. Technical Information Center, Department of Energy, Oak Ridge, Tennessee 37831

424-500. Controlled Fusion Atomic Data Center, Bldg. 6003, ORNL